Cohesion failure and Mitosis:

From Molecular Mechanisms to Organismal Consequences

Mihailo Mirkovic

Dissertation presented to obtain the PhD degree in Molecular Biology

Instituto de Tecnologia Química e Biológica António Xavier | Universidade Nova de Lisboa

Research work coordinated by: Instituto Gulbenkian de Ciencia

Oeiras, May 2018

Table of Contents

Declaration

I declare that this dissertation and the data presented are the result of my own work, developed between 2014 and 2018 in the laboratory of Dr. Raquel Oliveira at the Instituto Gulbenkian de Ciência in Oeiras, Portugal. Specific author contributions are indicated in each chapter, in the Acknowledgements section.

Financial support was granted by Fundação para a Ciência e a Tecnologia, doctoral fellowship PD/BD/52438/2013 and ERC Starting Grant (StG), LS3, ERC-2014-STG-638917, Marie Curie Career Integration Grant (MCCIG321883/CCC) and an EMBO Installation Grant (IG2778).

Declaração

Declaro que esta dissertação de doutoramento e os dados nela apresentados são o resultado do meu trabalho, desenvolvido entre 2014 e 2018 no laboratório do Dr.Raquel Oliveria no Instituto Gulbenkian de Ciência em Oeiras, Portugal. As contribuições de cada autor são indicadas em cada capítulo na secção dos Agradecimentos/Acknowledgements.

O apoio financeiro foi concedido pela Fundação para a Ciência e Tecnologia, através da bolsa de doutorame nto PD/BD/52438/2013e porfundos do Conselho Europeu de Investigação ERC Starting Grant (StG), LS3, ERC-2014-STG-638917, Marie Curie Career Integration Grant (MCCIG321883/CCC), EMBO Installation Grant (IG2778).

Summary

Mitosis is a dynamic culmination of the cell cycle, resulting in generation of two daughter cells from one mother. In order for this to happen, the cell must package its DNA into chromosomes and divide it equally amongst progeny. To ensure this process happens accurately, the cell glues identical chromosomes together so it can segregate them in symmetrical fashion during anaphase. The glue holding chromosomes together is a molecule called cohesin, which encompasses replicated DNA fibers via topological entrapment. The aim of this thesis was to study the immediate mitotic response to premature cohesion loss, as well as the long term consequences of such perturbed mitosis for the cell and the whole organism. In order to study cohesion loss in mitosis, we utilized an established acute system for cohesin depletion, via the use of TEV protease, which cleaves TEV sites inserted into cohesin within hours after heat shock induction, or minutes after injection. To study cohesion loss in the entire organism, we modified the existing TEV tool in *D.melanogaster* to include a cohesin rescue step, generating a transient cohesin loss, which would impair mitosis in a window time, while minimizing chronic damage to the organism.

The **Chapter I** of the thesis focuses on the interplay between cohesin loss and mechanisms protecting mitotic fidelity. It has previously been demonstrated that premature cohesion loss triggers the activation of the Spindle Assembly Checkpoint (SAC), a system for mitotic delay generated by unattached chromosomes, whose main role is to provide more time for Aurora B, the main error correction protagonist, do destabilize erroneously attached chromosomes and allow for biorientation. However, cells escape

SAC surveillance upon cohesion loss relatively fast, resulting in aneuploidy. Our work provided additional insight on why cohesin loss is not robustly detected by the SAC. We have demonstrated that upon premature cohesion loss, chromosomes undergo cycles of attachment and detachment to the mitotic spindle, which are Aurora B dependent. However these cycles of detachment and consecutive SAC generation decline during the arrest and result in aberrant mitotic exit. The likely reason behind this is the fact that Aurora B, as well as SAC are dependent on the activity of Cdk1-Cyclin B complex. On the other hand, the stability of Cyclin B is SAC dependent, as SAC abolishment leads to Cyclin B degradation. To add an additional layer of complexity, Aurora B activity, which leads to SAC generation, is also Cyclin B dependent.

This places the entire system in a positive feedback state, where the activity decline in any of the three main modules (SAC, Aurora B and Cyclin B) results in a mitotic exit, despite the dire consequences for the cell.

In the **Chapter II** of the thesis, we examined situations that alleviate mitotic defects caused by premature loss of cohesin. An interesting modulator screen of our collaborators, in the *Drosophila* wing disc, revealed that cohesion defects can be suppressed if the SAC is downregulated. This is a very counterintuitive result, as the SAC is one of the main guardians of mitotic fidelity. However, we demonstrate that the prolonged mitosis due to SAC activation in the absence of cohesin is actually detrimental to the symmetry of genome segregation, when compared to mitosis without cohesion where SAC is not active. The culprit behind this aggravated

asymmetry when mitosis is prolonged is the error correction and Aurora B activation, which results in continuous cycles of chromosome shuffling, attachment and detachment. Live imaging and the quantification of centromere segregation at the anaphase in the embryo, as well as the wing disc, demonstrated that mitotic fidelity can be enhanced in the absence of cohesin in two major ways. The first is the SAC inhibition, which shortens mitosis and allows for mitotic exit without excessive chromosome shuffling and motion. The second is the inhibition of Aurora B, which results in a similar rescue of symmetry, as it prevents chromosome spindle disengagement and inhibits SAC in the process. Surprisingly, even in the complete absence of cohesin, the initial chromosome-microtubule capture is quite accurate, and additional rounds of trying to correct an unfixable error only make the situation worse.

The **Chapter III** of the thesis examines the consequences of mitosis without cohesin at the level of a developing organism. Since cohesin has numerous interphase roles, we developed a system in which the initial cleavage of cohesin is followed by a rescue with a TEV-resistant, wild type variant. This tool was adapted to use in the entire developing *Drosophila melanogaster,* and when used to generate cohesin loss and subsequent genome imbalance, it resulted in eclosion of adult flies with severe motion defects and an extremely short lifespan. We traced the fate of aneuploid cells in two tissues, the epithelial wing disc, and the stem cell of the nervous system, the Neuroblast. We demonstrate, as previously published, that aneuploidy in the wing results in cell death and compensatory proliferation. However, the brain stem cells, Neuroblasts, display a high tolerance for aneuploidy,

undergoing multiple aneuploid cell cycles, accumulating chromosomes, and showing a delayed appearance of aneuploid stress response. These cells displayed chromosomal instability just hours after becoming aneuploid, further contributing to their karyotype diversity. We then utilized drosophila genetics to examine organ sufficiency when faced with developmental aneuploidy. We did so by protecting only the brain from developmental aneuploidy with the use of Neuroblast-specific drivers to express the non-cleavable version of cohesin constitutively. Protecting only the brain, but not the rest of the developing organism from aneuploidy induction completely rescues the motion defects and the lifespan of adults. This result points to the brain as a limiting tissue in metazoan aneuploid development.

Resumo

A mitose é o culminar dinâmico do ciclo celular, que resulta na geração de duas células filhas a partir de uma mãe. Para que isso aconteça, a célula deve empacotar o DNA em cromossomas e dividi-lo igualmente entre as células descendentes. De forma a garantir que este processo aconteça com precisão, a célula "cola" os cromossomas idênticos um ao outro para assim os segregar simetricamente durante a anafase. A cola que mantém os cromossomas juntos é uma molécula chamada coesina, que engloba as fibras de DNA vizinhas, prendendo-as topologicamente. O principal objetivo desta tese foi estudar a resposta mitótica imediata à perda prematura dessa coesão, bem como as consequências a longo prazo de uma mitose perturbada por tal, para a célula e para o organismo como um todo. Para estudar a perda da coesão na mitose, este trabalho baseou-se num sistema de perturbação agudo, estabelecido para depleção da coesina, através do uso da protease TEV. Esta cliva sequências TEV inseridas na coesina, horas após a indução de choque térmico ou minutos após a injeção. Para estudar a perda de coesão em todo o organismo, modificamos a ferramenta TEV existente em *D. melanogaster* para incluir uma etapa de resgate da coesina, gerando uma perda transitória desta, que prejudicaria a mitose numa janela de tempo limitada, minimizando os danos crónicos no organismo.

O **Capítulo I** deste trabalho foca na interação entre a perda de coesina e o mecanismo que protege a fidelidade mitótica. Foi demonstrado anteriormente que a perda prematura de coesão

desencadeia a ativação do ponto de controlo mitótico (SAC), um sistema de atraso mitótico gerado por cromossomas não ligados, cujo principal papel é o de fornecer mais tempo para a Aurora B, principal protetora de correção de erros, fixar cromossomas erroneamente ligados. No entanto, após perda de coesão, as células escapam à vigilância do SAC relativamente rápido, levando a células aneuploides. O nosso trabalho forneceu informações adicionais sobre como a perda de coesina não é detetada de forma robusta pelo SAC. Nós demonstramos que, após a perda prematura da coesão, os cromossomas sofrem ciclos de fixação e desprendimento do fuso mitótico, que são dependentes da Aurora B. No entanto, esses ciclos de desprendimento e ativação consecutiva do SAC diminuem durante o bloqueio e resultam numa saída mitótica aberrante. A razão provável por trás disso é o fato de que a Aurora B, bem como SAC, são dependentes da atividade do complexo Cdk1-Ciclina B. Por outro lado, a estabilidade da Ciclina B é dependente do SAC, uma vez que a supressão do SAC leva à degradação da Ciclina B. Para adicionar uma camada adicional de complexidade, a atividade da Aurora B, que leva à ativação do SAC, também é dependente da Ciclina B.

Tal coloca o sistema num estado de *feedback* positivo, onde o declínio em qualquer um dos três módulos principais (SAC, Aurora B e Ciclina B) resulta numa saída mitótica, apesar das terríveis consequências para a célula.

No **Capítulo II** desta tese, examinamos situações que aliviam defeitos mitóticos causados pela perda prematura da coesina. Um *screen* fenotípico interessante a partir do disco imaginal da asa de

Drosophila revelou que os defeitos de coesão podem ser suprimidos se o SAC for regulado negativamente. Este é um resultado muito contra-intuitivo, uma vez que o SAC é um dos principais guardiões da fidelidade mitótica. No entanto, demonstramos que a mitose prolongada devido à ativação do SAC na ausência de coesina é realmente prejudicial à simetria da segregação do genoma, quando comparado à mitose sem coesão onde o SAC não está ativo. O culpado por trás dessa assimetria agravada quando a mitose é prolongada é a correção de erros e a ativação da Aurora B, que resulta em ciclos contínuos de reordenação, fixação e desprendimento dos cromossomas. Através de *live imaging* e da quantificação da segregação do centrómero na anafase no embrião, bem como no disco imaginal da asa, demonstraram que a fidelidade mitótica pode ser aumentada na ausência de coesina de duas formas principais. A primeira é através da inibição do SAC, que encurta a mitose e permite a saída mitótica sem o excessivo embaralhamento e movimento dos cromossomas. A segunda é através da inibição da Aurora B, que resulta num resgate semelhante de simetria, já que impede o desprender dos cromossomas do fuso mitótico, inibindo o SAC no processo. Surpreendentemente, mesmo na ausência completa de coesina, parece que a captura inicial dos cromossomas e microtúbulos é bastante precisa, e tentativas adicionais de corrigir um erro não-remediável só pioram a situação.

O **Capítulo III** desta tese examina as consequências da mitose sem coesina ao nível do organismo em desenvolvimento. Uma vez que coesina tem numerosos papéis interfásicos, desenvolvemos um sistema no qual a clivagem inicial da coesina é seguida por um resgate com uma variante de tipo *wild-type* resistente a TEV. Esta

ferramenta foi adaptada de forma a poder ser usada durante todo o desenvolvimento da *Drosophila melanogaster*. Quando usada para gerar perda da coesina e subsequente desequilíbrio do genoma, resultou na eclosão de moscas adultas com defeitos de movimento severos e um tempo de vida extremamente curto. Traçamos o destino das células aneuploides em dois tecidos, o disco epitelial da asa e a célula estaminal do sistema nervoso, o neuroblasto. Demonstramos, como publicado anteriormente, que a aneuploidia na asa resulta em morte celular. No entanto, as células estaminais cerebrais, os neuroblastos, apresentaram uma alta tolerância à aneuploidia, sofrendo múltiplos ciclos celulares aneuplóides, acumulando cromossomas e apresentando um atraso no aparecimento das respostas dos sinalizadores de *stress*. Essas células apresentaram instabilidade cromossômica apenas algumas horas após se tornarem aneuploides, contribuindo ainda mais para a diversidade cariotípica. Utilizamos então a genética da *Drosophila* para examinar a suficiência de cada órgão quando confrontados com a aneuploidia ao nível do desenvolvimento. Fizemos isso protegendo apenas o cérebro da aneuploidia no desenvolvimento, fazendo com que a versão não-clivável da coesina fosse expressa constitutivamente e especificamente em neuroblastos. Proteger apenas o cérebro, mas não o resto do organismo em desenvolvimento da indução de aneuploidia, resgata completamente os defeitos de movimento e o tempo de vida dos adultos. Este resultado aponta para que o cérebro seja um tecido limitante no desenvolvimento aneuplóide metazoário.

Acknowledgments

I was told that this is the most difficult part of Thesis writing, and I was told correctly. The section is way too short to properly thank everyone who influenced me and my work during this five year period.

To Raquel, I joined your lab after being unceremoniously kicked out from another, and I cannot thank you enough for everything. As a founding member of the lab, your (infinite) patience, insane work ethic and scientific rigor, made me feel I really have someone to look up to as a model scientist. Trough endless microscope sessions, discussions, cigarette and coffee breaks, quarrels about what is the “right” experiment, I have never felt my opinion, however naïve it may have been, was not listened to, or my curiosity unanswered. This truly motivated me to grow, and as a supervisor, there is no greater gift you can give to a novice scientist; Apart from teaching them not to do a western blot on a piece of cardboard. Thank you, I could not have asked for a better supervisor.

To Ana, these five PhD years were full of doubt for me. Without your support, nothing would be possible, nor worth it, as your endless kindness and love kept me afloat and sane trough many difficult times. I can only hope that one day I can give back for all the good things you gave to me through these intense years.

Hvala ti duso!

To the members of the CHR lab, past and present, Pedro, Ewa, Xana, Sara, Mariana, Lina, Cintia, Catarina, Margarida, and the endless stream of interns and summer students, thank you for

putting up with me for all these years and beer hours, I know it was quite a task. Among such a large group of people, there was not a single bad apple, and every day the lab felt like a comfortable place to work. I know that wherever I go, I will likely work in a place with an atmosphere far more somber than the one we have created as a group.

To Gaston, thank you for teaching me to view science as an art form, and to always embrace crazy experiments and unexpected outcomes.

To Lars and the entire Epilab, thank you for “adopting” me when I was a lone student in CHR group, thank you for all the beautiful moments in and outside the IGC. Joao, thank you for all the fishing trips!

To Monica, Elio, Florence, Alekos, thank you for the scientific and non-scientific discussions and guidance. And to Alekos, thanks for all the tzatziki!

To the staff of the IGC Microscopy Facility (especially Nuno Martins) and the Fly room (Lilliana Vieira), thank you for your fine work which made mine possible.

Finally, to my Mother and Father, Varja and Zarko, to my brothers and sister, Jakov, Luka, Olga, and the entire family, thank you for the continuous support in my somewhat peculiar interests and endeavors.

Hvala vam za sve, Volim vas!

List of Publications (6), in chronological Order:

1) Centromere-Independent Accumulation of Cohesin at Ectopic Heterochromatin Sites Induces Chromosome Stretching during Anaphase

Raquel A. Oliveira , Shaila Kotadia , Alexandra Tavares, Mihailo Mirkovic, Katherine Bowlin, Christian S. Eichinger, Kim Nasmyth, William Sullivan .

Published: October7, 2014, PLOS Biology

2) Premature Sister Chromatid Separation Is Poorly Detected by the Spindle Assembly Checkpoint as a Result of System-Level Feedback

Mihailo Mirkovic, Lukas H. Hutter, Béla Novák, Raquel A.

Cell Reports, Volume 13, Issue 3, p469–478, 20 October 2015

3) Centromeric Cohesin: Molecular Glue and Much More.

Mirkovic M, Oliveira RA.

Progress in Molecular and Subcellular Biology. 2017;56:485-513.

4) Absence of the Spindle Assembly Checkpoint restores mitotic fidelity upon loss of sister chromatid cohesion

Rui D. Silva*, Mihailo Mirkovic*, Leonardo G. Guilgur, Om S. Rathore, Rui Gonçalo Martinho, Raquel A. Oliveira

**Equal Contribution*

Current Biology, 2018 *Continued on next page…*

5) Neuronal development restricts organism recovery upon reversible loss of cohesin and consequent aneuploidy

Mihailo Mirkovic*****, Leonardo G. Guilgur*, Diogo Santos , Raquel A. Oliveira (Submitted)

**Equal Contribution*

6) A quantitative view on cohesin decay in mitotic fidelity

Sara Carvalhal, Alexandra J. Tavares, Mariana B. Santos, Mihailo Mirkovic, and Raquel A. Oliveira JCB 2018

1.0 General Introduction

Mitosis as the culmination of the cell cycle

Cell division is a fundamental process of life. It allows the transmission of information, encoded in the genome or the cytosol, from one generation to another, while simultaneously providing the capacity for rejuvenation. As such, this process is repeated numerous times during the lifetime of unicellular organisms, and billions of times during the development and growth of metazoans. Just the sheer numerical scale of this process requires extreme accuracy as errors in cell division can lead to cell death, decline of cell fitness or the rise of a disease.

Cell division is the last stage of the process known as the cell cycle. Cell cycle consists of the G1 stage, mainly characterized by rapid growth and cell volume increase, S phase, where DNA is replicated and the cell is already committed to division. After replication takes place, G2 stage represents a time when the cell undergoes large scale biosynthesis in order to prepare for mitosis. Each of these stages and their transitions are highly regulated events, with multiple checkpoints. The G1 to S transition is mainly dependent on cell growth, allowing the cell to measure its own size before committing to DNA replication and consequent division. S phase is marked by replication of genomic loci, and has a checkpoint of its own, as errors during DNA replication can recruit the DNA damage and repair machinery. G2 to Mitosis transition is regulated by the tug of war between Cyclin B-Cdk1 accumulation and activation, and its inhibitors, such as the Wee phosphatase. Once the cell commits to mitotic entry, there is no going back.

Mitosis in its self is a fascinating process. To put on a bit of a personal twist on this introduction, after the first time of observing mitosis at the microscope, I had no qualms about studying this process during my PhD. I knew nothing about it (and still know very little), but I knew I wanted to study it. The sheer speed and magnificent orchestration of this process is the reason why every microscopist remembers his first live encounter with a dividing cell.

Cell division happens on the timescale from minutes to up to an hour in metazoans, and is by far the shortest stage of the cell cycle. However, in that time, the changes in the cell architecture are both rapid and profound. In metazoans, the nuclear envelope, the great barrier between the cytosol and the DNA is destroyed by the activity of Cdk1-Cyclin B mitotic complex. At the same time, the migration of duplicated centrosomes, coupled with the polymerization of tubulin give rise to the mitotic spindle, which fills the space vacated by the nuclear envelope. This mitotic spindle aims to make contact with the DNA, which itself undergoes rapid and profound changes.

The DNA undergoes a poorly understood process known as condensation, in which the entire genome is compacted into distinct units, called chromosomes. This takes place by extensive and dynamic DNA looping and reorganizing, chaperoned by the activity of Mitotic kinases and numerous molecules regulating chromatin structure. Among the key structural molecules involved in chromosome organization and architecture are cohesin and condensin. One ensures that the chromosomes which are identical are linked, while another ensures their discrete existence as compact units, structurally independent from each other.

All these rapid changes result in a classical mitotic image which is present in any elementary school textbook; Metaphase, a stage where condensed chromosomes are bioriented on the mitotic spindle, in the middle of the cytosol.

The end of mitosis is carefully orchestrated and rapid. Simultaneously, Cohesin is destroyed, allowing the spindle to pull the chromosomes to the poles, and at the same time, Cyclin B-Cdk1 activity is downregulated, unleashing the activity of phosphatases and allowing for cytokinesis and mitotic exit to take place. This is followed by the reformation of the nuclear envelope, which results in two daughter cells arising from a common mother.

Introduction 1.1- Cohesin and its role in the cell cycle

This chapter is adapted from:

Centromeric Cohesin: Molecular Glue and Much More.

Mirkovic M, Oliveira RA.

Progress in Molecular and Subcellular Biology. 2017;56:485-513.

ABSTRACT

Sister chromatid cohesion, mediated by the cohesin complex, is a pre-requisite for faithful chromosome segregation during mitosis. Premature release of sister chromatid cohesion leads to random segregation of the genetic material and consequent aneuploidy. Multiple regulatory mechanisms ensure proper timing for cohesion establishment, concomitant with DNA replication, and cohesion release during the subsequent mitosis. Here we summarize the most important phases of the cohesin cycle and the coordination of cohesion release with the progression through mitosis. We further discuss recent evidence that has revealed additional functions for centromeric localization of cohesin in the fidelity of mitosis in metazoans. Beyond its well-established role as “molecular glue”, centromeric cohesin complexes are now emerging as a scaffold for multiple fundamental processes during mitosis, including the formation of correct chromosome and kinetochore architecture, force balance with the mitotic spindle, and the association with key molecules that regulate mitotic fidelity, particularly at the chromosomal inner-centromere. Centromeric chromatin may be thus seen as a dynamic place where cohesin ensures mitotic fidelity by multiple means.

1.1.1 The importance of gluing DNA molecules

Mitosis is the most dynamic period in the life of the cell. In a short period of time, the cell condenses its DNA into discrete chromosomes, aligns them on the metaphase plane, and finally, destroys the forces that hold equal-DNA molecules together, creating two identical daughter nuclei in the process. The fidelity of this process relies on cells' ability to keep the two identical sister chromatids together from the moment of DNA replication until the later stages of mitosis, once (and only when) the conditions for their separation are met.

Sister chromatid cohesion provides cells with the ability to determine chromosome identity, as cohesed sister chromatids are identical and therefore need to be pulled to opposite poles. Moreover, sister chromatid cohesion provides the counterforce that resist the pulling force of the spindle, thus preventing premature sister chromatid separation (Oliveira et al., 2010; Tanaka et al., 2000), and random chromosome segregation. Cohesin is also essential for the correct geometry of the kinetochore region which promotes effective, stable capture of the kinetochores by the mitotic spindle, leading to the biorientation of chromosomes during metaphase (Ng et al., 2009; Sakuno et al., 2009; Stephens et al., 2013).

Therefore, to align chromosomes at the metaphase plane and segregate them symmetrically, chromosomal cohesive state must be maintained until anaphase at all cost. Premature separation of chromosomes renders the cell unable to align chromosomes correctly, causing random segregation of the genetic material and

consequent aneuploidy (Figure 1), which is usually lethal and a common cause of human pathological conditions (**Box 1**).

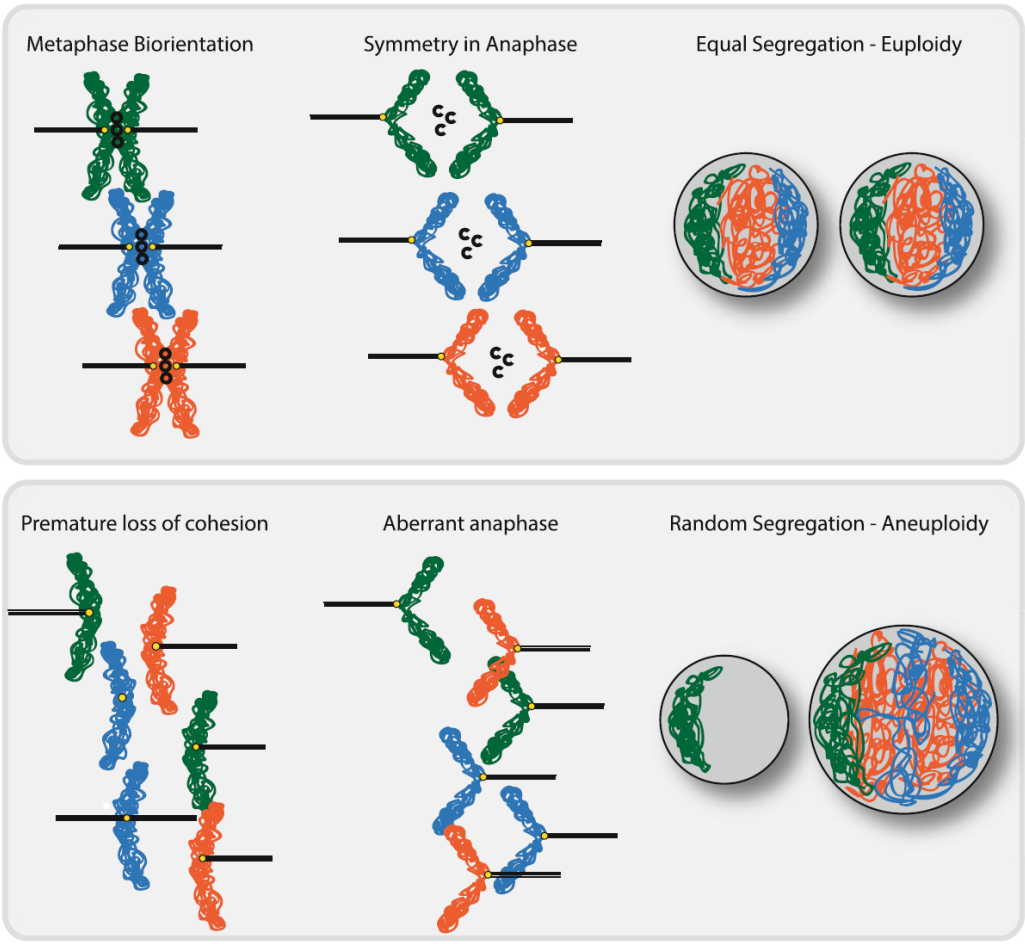

Fig. 1 Sister chromatid cohesion during mitosis. *Cohesin is essential for biorientation of chromosomes on the metaphase plane and the symmetry of subsequent anaphase. Defects in sister chromatid cohesion result in premature separation of sister chromatids, resulting in random chromosome segregation and aneuploidy*

Box 1 – Sister Chromatid cohesion defects and human disease

Proteins involved in keeping the two sister DNAs together have been linked to several human-health and reproduction conditions. Defects in cohesion and mechanisms regulating cohesin are common amongst **cancer** cells (De Koninck and Losada, 2016; Losada, 2014). Cancer cells display Chromosomal Instability (CIN) characterized by frequent gain or loss of chromosomes (Holland and Cleveland, 2009). CIN enhances the speed at which the cancer cells can evolve, by gaining or losing whole chromosomes, making them highly adaptable to any possible treatment. Interestingly, recent studies have been able to reverse the chromosomal instability of multiple cancer-derived cells lines by reinstating the network associated with protection of cohesin (Tanno et al., 2015).

Age-related **female infertility** has also been proposed to relate with cohesion decay, giving rise to genetic abnormalities such as Down's syndrome (Reviewed in (Webster and Schuh, 2016). "Cohesion fatigue", evidenced by decreased levels of cohesion is followed by segregation defects and decreased fertility in oocytes (Patel et al., 2015; Zielinska et al., 2015). It is currently thought that the meiotic cohesin variant is loaded into an oocyte only during the germ-line development (pre-meiotic S-phase) without significant turn-over (Burkhardt et al., 2016; Tachibana-Konwalski et al., 2013). This would mean that oocytes solely rely on cohesion established during their creation, and maintain it throughout the entire reproductive life cycle of the female, which lasts for decades in humans. Studies in human oocytes have shown that cohesin deficiency, present in older females, contributes to the increased

distance between bivalents in meiosis and leads to aberrant kinetochore attachments and segregation errors, resulting in the increased frequency of aneuploidy (Patel et al., 2015; Zielinska et al., 2015).

Other rare developmental disorders have also been linked to the cohesion process and are now known as "***Cohesinopathies****"* *(*reviewed in references (Dorsett, 2007; Liu and Krantz, 2008; Remeseiro et al., 2013)). Most of these diseases are linked to the non-mitotic roles of the cohesion apparatus (e.g. regulation of transcription and genome architecture). However, a certain number of Cohesinopathies, such as the Roberts or Warsaw breakage syndromes exhibit cohesion defects between replicated chromatids during mitosis, resulting in aneuploidy and mitotic defects (Tomkins et al., 1979; van der Lelij et al., 2010).

In order to understand how defects in chromosome cohesion take place, it is fundamental to understand the molecular structure of the cohesin complex, as well as the principle mechanisms underlying its loading, establishment and release during the cell cycle. Here we summarize our current knowledge on the regulation of sister chromatid cohesion. We further highlight the importance of such dynamic regulation for the efficiency of mitosis, in mechanisms that go far beyond cohesin's primary role in sister chromatid cohesion.

Cohesin: the molecular glue that holds chromosomes together

The molecule responsible for the pairing of replicated chromosomes is called cohesin (Guacci et al., 1997; Michaelis et

al., 1997) (Figure 2). Cohesin is a tripartite ring complex, which topologically entraps replicated DNA molecules keeping them together until the onset of anaphase (Haering et al., 2008; Ivanov and Nasmyth, 2005). The core of this ring complex is composed out of three molecules: SMC 1 and SMC 3 (belonging to the Structural Maintenance of Chromosomes protein family) and the kleisin subunit Scc1, which connects them (Nasmyth and Haering, 2009; Peters et al., 2008). (Figure2). Additional proteins directly associate with the cohesin complex (Scc3/SA, Pds5, WAPL, Sororin) and are thought to have critical roles in cohesin dynamics, and consequently mitotic fidelity (summarized in Box 2).

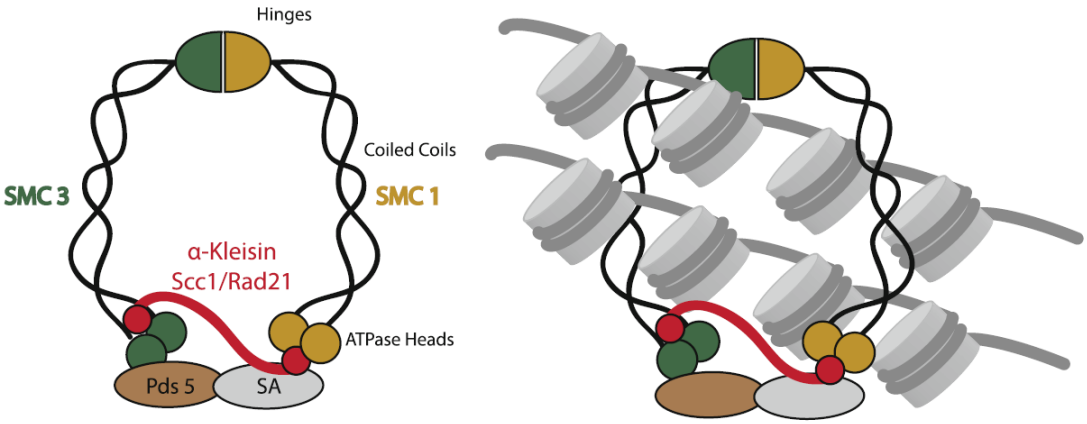

Figure. 2 The cohesin complex. *Cohesin complex forms a ring-shaped molecule that topologically embraces sister DNA molecules inside its ring*

Cohesin and its regulators

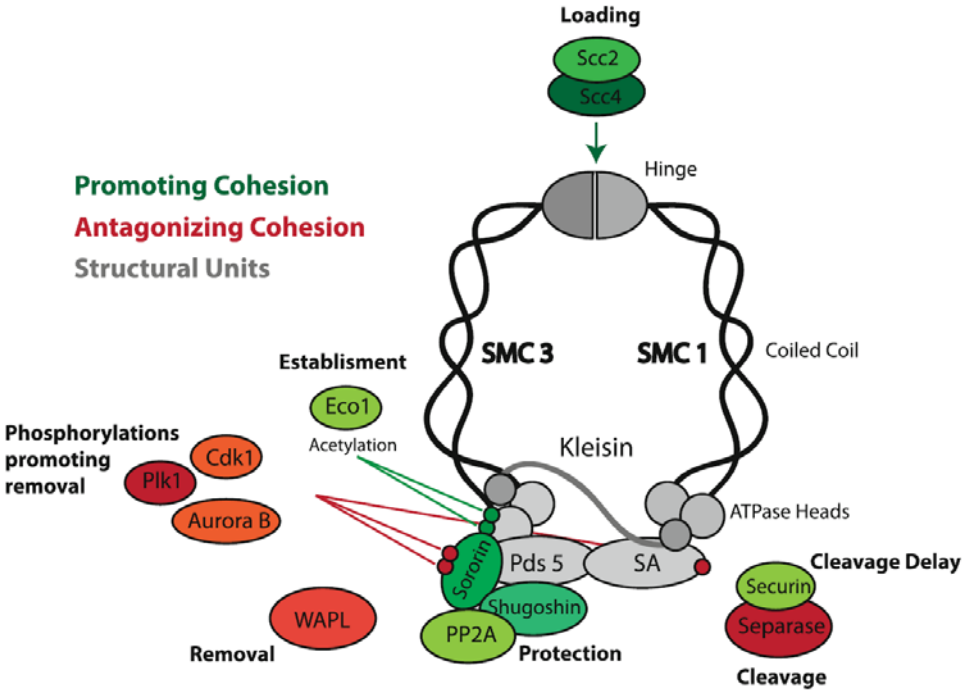

Figure 3: *Cohesin and associated molecules. The cohesin complex and the different associated molecules that modulate cohesin's function. Molecules are color-coded according to their influence on the stability of cohesin's association with chromatin (molecules that promote cohesion are in green; cohesion antagonists in red and proteins with dual effect in orange)*

Table 1 Cohesin and its regulators

Name	Function	Mode of operation
SMC1	Structural/ATP binding and hydrolysis	Part of the ring; interacts with SMC3 through the hinge and the α-kleisin through the ATPase heads; binds and hydrolysis ATP
SMC3	Structural/ATP binding and hydrolysis	Part of the ring; interacts with SMC1 through the hinge and the α-kleisin through its coiled-coil; binds and hydrolysis ATP
α-kleisin/Rad21/Scc1	Structural/scaffold	Closes the ring by bridging the heads of SMC1/3; serves as a scaffold to other regulatory proteins
Pds5	Structural/scaffold	Connects the ring with various other molecules: (e.g. Sororin and WAPL)
SA/Scc3	Structural/scaffold	Essential for the ring structure; phosphorylated by Plk1 during prophase pathway
Scc2/NIPB/NIPBL	Loading	Required for cohesin loading; possibly opens SMC1/3 hinges
Scc4/Mau-2	Loading	Required for cohesin loading; possibly opens SMC1/3 hinges
Eco1/ESCO1	Establishment	Acetylates SMC3 heads, promoting sororin recruitment
WAPL	Removal	Interacts with Pds5 and disrupts the SMC3/kleisin interface, opening the ring
Sororin	Protection	Blocks WAPL interaction with Pds5
Cdk1/CycB	Removal/protection/cleavage inhibitor	Removes sororin; promotes shugoshin localization; inhibits separase
Aurora B	Removal/protection	Removes sororin; promotes shugoshin localization
Plk1	Removal/cleavage	Promotes cohesin release through SA phosphorylation; enhances Rad21/Scc1 cleavage by separase
Shugoshin	Protection	Recruits PP2A to the cohesin complex
PP2A	Protection	Dephosphorylates sororin
Securin	Cleavage inhibitor	Inhibits separase activation
Separase	Cleavage	Cleaves the Rad21/Scc1 subunit and opens the ring

The most popular, and soundly tested cohesin ring model postulates that cohesin keeps sister chromatids together by entrapping sister DNA fibers within the same cohesin ring (Haering et al., 2008). EM-studies support that cohesin rings are about 40 nm in diameter (Haering et al., 2002) thus providing sufficient space for enclosing two 11 nm fibers. Other models have been proposed, such as the “handcuff” model, in which cohesion is mediated by two interlinked cohesin complexes, each entrapping its own DNA fiber (Diaz-Martinez et al., 2008; Guacci, 2007). In either case, solid evidence supports that cohesin’s interaction with DNA is of a topological nature (Haering et al., 2008; Ivanov and Nasmyth, 2005), emphasizing that regulation of cohesin binding and function relies on the opening and closing the interphases between the core components (discussed below).

Besides its role in sister chromatid cohesion, cohesin also regulates transcription, contributes to the DNA repair mechanisms, and participates it the organization of the genome in mitotic and post-mitotic tissues (Nasmyth and Haering, 2009; Peters et al., 2008)

The distribution and presence of cohesin on chromatin during the cell cycle coincides with its multiple roles. Cohesin is loaded onto chromatin during G1 phase in budding yeast (Guacci et al., 1997) , and already in telophase in vertebrates (Losada et al., 1998). During G1 phase, Fluorescence Recovery After Photo-bleaching (FRAP) studies have shown that cohesin is dynamically interacting with the DNA (Gerlich et al., 2006). Similar dynamics was observed in cells that are not undergoing mitotic divisions, for example, endocycling Drosophila Salivary glands (Eichinger et al., 2013). This highly dynamic nature of cohesin-DNA interaction in non-dividing or non-replicated cells is believed to relate to

cohesin's role in transcription regulation and interphase genome architecture.

Following the onset of S phase, a fraction of cohesin molecules establishes cohesion between newly replicated sister chromatids. Specific changes on the cohesin complex (discussed below) ensure the post-replicative stabilization of cohesin-DNA interaction concomitantly or right after replication fork passage. This cohesive state is then maintained until the subsequent mitosis.

In early mitosis, the majority of the cohesin complexes are released from chromosome arms. By the time cells reach metaphase, cohesion is solely maintained by a small pool of cohesin molecules retained at the centromeric and pericentromeric regions (Losada et al., 1998; Waizenegger et al., 2000; Warren et al., 2000).

At the onset of anaphase, remaining centromeric cohesin is destroyed in a rapid and acute manner by a cysteine protease named Separase, allowing the segregation of sister chromatids by the spindle (Uhlmann et al., 1999). This enzyme cleaves the kleisin subunit Rad21/Scc1 releasing sister chromatids from topological entrapment. The destruction of cohesin during anaphase marks the point of no return for the mitotic cell: once cohesin is cleaved, separation of the chromatids is rapid and irreversible. Consequently, release of cohesin from mitotic chromosomes is a highly regulated affair. The key surveillance mechanism governing cohesin release is the Spindle Assembly Checkpoint(SAC) (Reviewed in (Musacchio and Salmon, 2007). The SAC regulates cohesin cleavage by delaying the onset of anaphase until all the chromosomes are bioriented on the metaphase plane. SAC mediates this delay by directly inhibiting the Anaphase Promoting

Complex/Cyclosome (APC/C), whose activity is needed for anaphase events. APC/C mediates cohesin cleavage trough indirect activation of Separase, the protease responsible for proteolytic opening of the cohesin ring.

Loss of cohesin or cohesin-regulators in virtually all organisms results in premature separation of sister chromatids (Guacci et al., 1997; Losada et al., 1998; Michaelis et al., 1997; Mirkovic et al., 2015; Sumara et al., 2000; Vagnarelli et al., 2004), arguing that cohesin is the most significant force that counteracts spindle forces. Nevertheless, it is conceivable that other forces may additionally play a role in chromosome cohesion. In particular, DNA-DNA intertwines (catenation) have long been argued to contribute to cohesion during mitosis (Reviewed in (Diaz-Martinez et al., 2008; Guacci, 2007; Liu et al., 2009b). Due to the helical nature of the DNA molecule, the replication fork passage creates tangles between replicated DNA molecules. These catenations need to be resolved before the onset of anaphase; otherwise, the entanglements will cause chromosome bridges and breakages in the DNA molecule. Topoisomerase II is the molecule responsible for de-catenation of these linkages and inhibition of this enzyme leads to accumulation of catenations, which are sufficient to confer cohesion even in the absence of cohesin proteins (Toyoda and Yanagida, 2006; Vagnarelli et al., 2004).

How much residual catenation contributes to cohesion during normal mitosis is a matter of debate. Although residual catenation has been observed even in anaphase segregating chromatids (Baumann et al., 2007), inhibition of topoisomerase specifically during metaphase has only a small effect on the efficiency of chromosome segregation (Oliveira et al., 2010). This suggests that

residual catenation may contribute to chromosome cohesion; yet, it is insufficient to resist the drastic spindle forces affecting chromosomes during mitosis. More importantly, unlike cohesin's destruction, which requires SAC silencing and APC/C activation, there is little to no evidence that removal of residual catenation is delayed by cell cycle progression checkpoints which control mitosis. SUMOylation of topoisomerase II has been proposed to restrict centromeric de-catenation during mitosis (Bachant et al., 2002; Dawlaty et al., 2008; Ryu et al., 2010), but there is no evidence that this reaction is under surveillance of the SAC. Thus, regulation of the cohesive state of chromosomes is mechanistically linked to the control of cohesin's association with chromatin throughout the cell cycle, which will be discussed below.

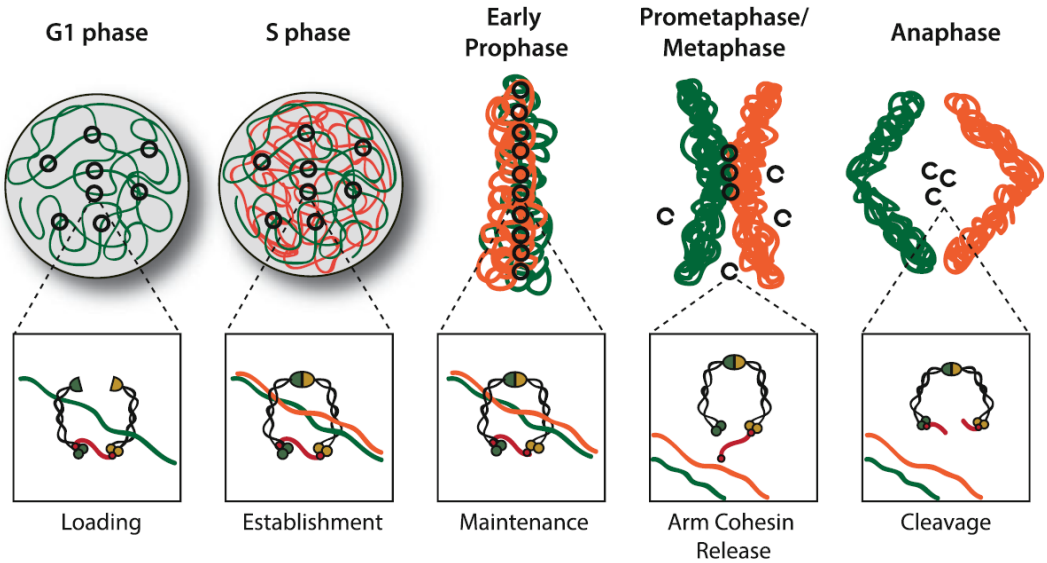

Fig. 4 Overview of the cohesin cycle*. Cohesin is loaded in telophase or G1, and is dynamically associated with chromatin. Upon replication, cohesion is established, connecting two replicated strands. Non-centromeric cohesin is removed from chromosome arms during prophase in metazoans, resulting in X-shaped chromosomes in metaphase. Finally, cohesin is cleaved during anaphase, allowing for the separation of sister chromatids.*

1.1.2 The Cohesin Cycle

A) The cohesin cycle : Chromatin Loading

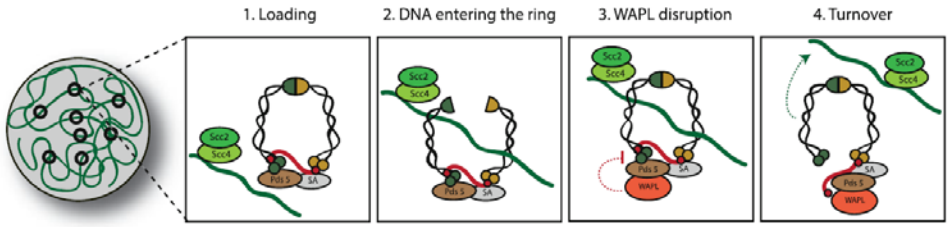

Fig. 5 Cohesin loading and turnover*. Cohesin loading onto DNA depends on the Scc2/4complex. DNA loading involves opening of the SMC1/3 interface, the hinge. Before replication, this interaction is dynamic, as loaded cohesin can be destabilized by WAPL, which opens the SMC3/Kleisin interface and releases cohesin from the chromatin.*

Cohesin loading onto chromatin is dependent on a two-protein complex known as Scc2/4 , also known as NIPB (Nipped-B) in *D.melanogaster*, or NIPBL (NIPB-Like) complex in humans (Ocampo-Hafalla and Uhlmann, 2011). The Scc2/Scc4 loading complex is essential for sister chromatid cohesion during G1/S phase, but not during G2 (Ciosk et al., 2000; Uhlmann and Nasmyth, 1998). This would entail that the Scc2/Scc4 has a primary function of loading cohesin onto the chromatin, but not in its stabilization or maintenance.

Given the ring-like architecture of cohesin, its loading onto chromatin requires opening of the ring. Elegant experiments with fusion of interfaces between different cohesin components support that the entry gate for cohesin loading resides at the interface of the SMC1 and SMC3 hinge domains, in an ATP-dependent process (Arumugam et al., 2003; Gruber et al., 2006; Weitzer et al.,

2003). Nevertheless, the molecular mechanism by which Scc2/4 promote cohesin's loading remains unknown.

Sites of cohesin loading do not necessarily coincide with cohesin's accumulation. This is mostly due to the fact that once loaded, cohesin complexes can slide on the DNA molecule (Hu et al., 2011; Lengronne et al., 2004; Ocampo-Hafalla et al., 2016; Stigler et al., 2016). Additionally, before DNA replication, the cohesin molecules display a highly dynamic association with DNA (Gerlich et al., 2006). Dissociation of cohesin from un-replicated DNA molecules is mediated by Wings-apart like protein (WAPL) (Gandhi et al., 2006; Kueng et al., 2006; Verni et al., 2000). Upon binding to the cohesin complex, WAPL removes cohesin from chromatin by disrupting the interface between SMC3 and Rad21/Scc1 subunits (Buheitel and Stemmann, 2013; Eichinger et al., 2013).

Cohesin loading is not a uniform event across the chromatin landscape and is found to be enriched at the centromeric/pericentromeric regions in most species studied so far (Blat and Kleckner, 1999; Glynn et al., 2004; Oliveira et al., 2014). Studies in budding yeast support that cohesin enrichment at the centromere is dependent on centromeric DNA sequences as well as proteins involved in kinetochore assembly (Megee and Koshland, 1999; Tanaka et al., 1999; Weber et al., 2004). However, species with longer centromeric sequences, such as fission yeast, rely on heterochromatin rather than centromeric sequences for cohesin enrichment (Bernard et al., 2001; Nonaka et al., 2002). In accordance, recent studies in *D. melanogaster* showed that cohesin enrichment at ectopic regions of pericentromeric heterochromatin occurs in the absence of a proximal centromere, most likely due to preferential binding of the

cohesin loading factor Scc2/Scc4 (Nipped B) (Oliveira et al., 2014). The preferential activity of Nipped B at the centromeric region is thought to be due to the specific state of pericentromeric heterochromatin, mainly H4K20 and H3K9 methylations and the presence of HP1 protein, tough clear links have been controversial (Hahn et al., 2013; Koch et al., 2008).

B) The cohesin cycle II: Cohesion establishment

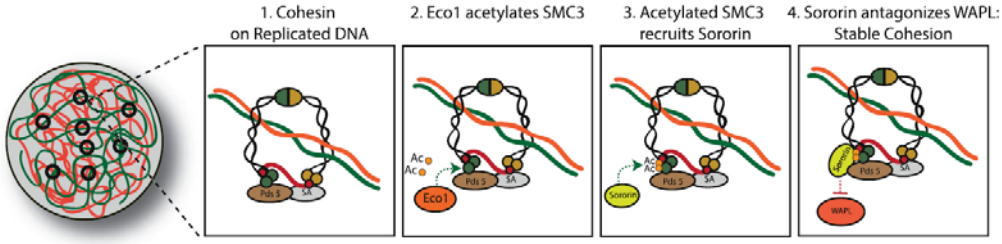

***Fig. 6 Cohesion establishment during S phase**. Upon DNA replication, a fraction of cohesin becomes stable on the chromatin. This happens due to SMC3 acetylation by Eco1 and recruitment of Sororin, protecting the cohesin complex from WAPL removal. This stable fraction of cohesin is considered "cohesive" cohesin, stably binding sister chromatids until the end of mitosis*

Cohesin establishment occurs during replication, at the time the newly replicated DNA molecule is being formed. Disruption of cohesin loading during G1 results in sister chromatid defects, while disruption during G2 does not. This means that the "effective" cohesion is established during S phase, during DNA replication (Uhlmann and Nasmyth, 1998). At the onset of replication, the dynamic properties of cohesin turnover change and a new pool of

stable, “cohesive” cohesin can be identified by FRAP (Gerlich et al., 2006).

Stabilization of cohesin complexes upon replication depends on the Eco1 acetyl transferase (Skibbens et al., 1999; Tanaka et al., 2000; Toth et al., 1999). This enzyme acetylates cohesin associated with replicated DNA at specific lysine residues on SMC3 and failure to acetylate leads to cohesion defects and cell death. The mechanism by which SMC3 lysine acetylation prevents cohesin de-association once it is bound to chromatin is contentious (reviewed in (Rudra and Skibbens, 2013)). Some studies propose models in which the acetylation locks the SMC3/kleisin interface, effectively closing the ring; however, these findings are inconsistent with the fact that SMC3 can be acetylated before replication (Rudra and Skibbens, 2013). SMC3 acetylation during the S phase has also been shown to confer cohesin protection by aiding the recruitment of Sororin, which favors cohesion establishment by protecting acetylated cohesin complexes from WAPL-mediated removal (Nishiyama et al., 2010).

These stably associated cohesin molecules (~30% of total chromatin bound cohesin (Gerlich et al., 2006)) are responsible for sustaining cohesion from the time of DNA replication until the subsequent mitosis.

C) The cohesin cycle: Cohesin's Prophase Release and retention at the centromere

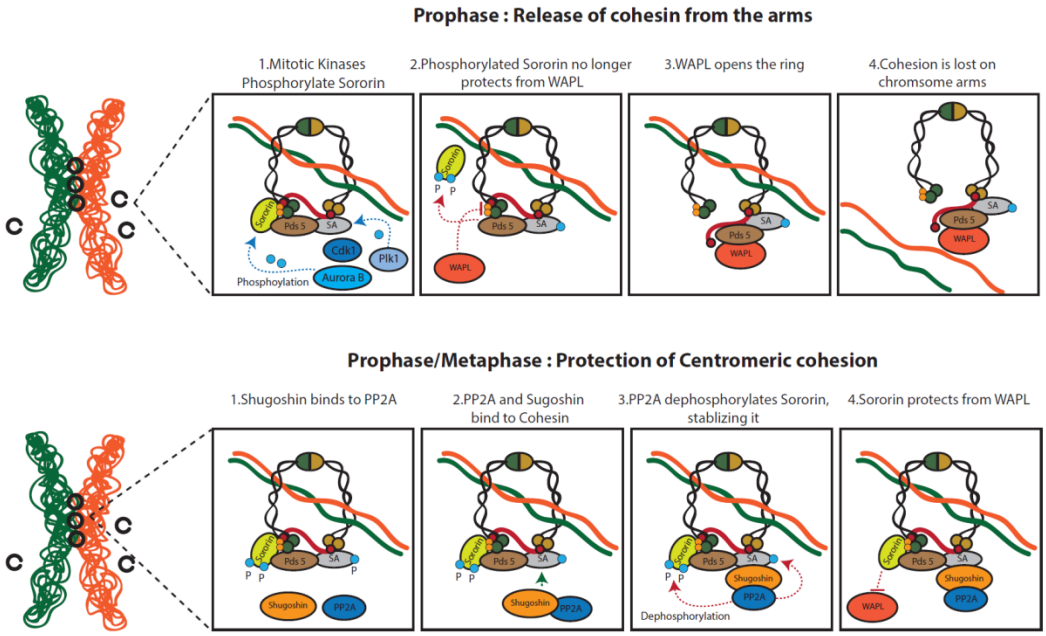

Fig. 7 Cohesin release during early mitosis and centromeric protection*. In metazoans, cohesin is removed from the arms by the prophase pathway. Mitotic kinases phosphorylate Sororin and SA. Phosphorylation induces Sororin displacement, which allows WAPL to destabilize cohesin. Centromeric cohesin complex are protected from this removal process as Shugoshin/PP2A complex protects centromeric cohesion from WAPL-mediated removal*

Once the cell enters mitosis, profound changes in the distribution of cohesin begin to take place. Cohesin at the chromosome arms is removed while centromeric cohesion is retained (Losada et al., 1998; Waizenegger et al., 2000; Warren et al., 2000). The loss of arm cohesion, coupled with centromeric retention gives the characteristic "X" shape to the metaphase chromosomes. The removal of cohesin from the arms in early mitosis is a consequence

of the “prophase pathway” which mainly relies on action of WAPL protein (Gandhi et al., 2006; Kueng et al., 2006).

WAPL imposes opening of the cohesin ring by disrupting the interface between SMC3 and Rad21/Scc1 subunits (Buheitel and Stemmann, 2013; Eichinger et al., 2013). Consequently, WAPL mutations or knockdown leads to the loss of the characteristic X shape of chromosomes, with cohesin remaining all over chromosome arms (Gandhi et al., 2006; Haarhuis et al., 2013; Kueng et al., 2006).

Several mitotic kinases contribute to the process of cohesin removal, by phosphorylating key proteins involved in the cohesin cycle. Aurora B and Cyclin Dependent Kinase 1 (Cdk1) were shown to antagonize Sororin by phosphorylation, resulting in its dissociation from chromosome arms during prophase (Dreier et al., 2011; Nishiyama et al., 2013). WAPL and Sororin directly compete for the binding to the cohesin-associated protein Pds5 (Nishiyama et al., 2010). The removal of Sororin from chromosome arms during prophase favors WAPL binding, and consequently the removal of cohesin complexes from chromosome arms. In addition to antagonizing Sororin, Aurora B seems to participate in WAPL activation, thus directly promoting cohesin removal (Nishiyama et al., 2013)

Polo Like kinase (Plk) is another key mitotic kinase participating in the cohesin cycle. The phosphorylation activity of Plk1 is crucial for the release of cohesin during the prophase pathway by phosphorylation of SA (Hauf et al., 2005; Lenart et al., 2007; Sumara et al., 2002). The net result of these changes in the

cohesin complex results in the removal of most of cohesin from chromosome arms but not from the centromeric region.

How are centromeric complexes protected from prophase pathway removal?

A key molecule in the protection of centromeric cohesion is called Shugoshin, meaning “Guardian Spirit” in Japanese (also known as MEI-S332 in D. melanogaster). Shugoshin confers protection of cohesin specifically at the centromere of both mitotic and meiotic cells (Kerrebrock et al., 1992; Kitajima et al., 2004; McGuinness et al., 2005).

Shugoshin is moved to the centromeric chromatin in complex with the PP2A phosphatase at the onset of mitosis (Kitajima et al., 2006; Liu et al., 2013b). Sugoshin-PP2A complex protects centromeric cohesin from WAPL-mediated removal by several means:

It antagonizes the Aurora B/Cdk1 mediated phosphorylation of Sororin and thereby favors Sororin interaction with Pds5, shifting the WAPL/Sororin competition for cohesin binding towards Sororin, preventing WAPL-mediated removal (Dreier et al., 2011; Liu et al., 2013b; Nishiyama et al., 2013). Aurora B and Cdk1 also phosphorylate and aid in the centromeric localization and activation of Shugoshin (Kitajima et al., 2006; Liu et al., 2013b; Tanno et al., 2010). This means that Cdk1 and Aurora B have conflicting roles in cohesin maintenance. They destabilize Sororin and thereby promote cohesin dissociation along chromosome arms, while at the same time localize and activate Shugoshin at the centromere, allowing for cohesin protection. Shugoshin-PP2A also protects cohesion by counteracting Plk1-mediated phosphorylation of SA

(Hauf et al., 2005; Kitajima et al., 2006; McGuinness et al., 2005) and by directly competing with WAPL for the binding to cohesin (Hara et al., 2014).

This protection mechanism is of outmost importance as centromeric cohesin complexes are the only ones that suffice cohesion maintenance during prometaphase and metaphase, while chromosomes are under drastic pulling and pushing forces exerted by the mitotic spindle to accomplish chromosome alignment.

D) The cohesin cycle: The final cut

Mitosis is a process of trial and error, with a few decisive breakpoints. Mitotic events of chromosome attachment, substrate phosphorylation, and biorientation are mostly redundantly regulated, and reversible. This allows for ample error correction in an otherwise error prone process. However, once the metaphase is formed, and chromosomes are bioriented, the cell reaches the point of no return: cohesin cleavage.

The cleavage of cohesin at the metaphase-to-anaphase transition is conducted by a large cysteine protease called Separase, which cleaves the kleisin subunit, distancing the heads of SMC1 and SMC3 subunits (Lin et al., 2016; Uhlmann et al., 2000). This opens the cohesin ring, releasing sister DNA molecules from the proteinaceous cage.

Once the forces that hold chromosomes together are released, there is no going back: therefore, centromeric cohesin cleavage must occur only after multiple safeguard mechanisms have been satisfied. Separase activity is tightly regulated and inhibited through multiple mechanisms until the onset of anaphase.

Firstly, Separase is inhibited by the binding of Securin, whose degradation is a prerequisite for sister chromatid separation (Ciosk et al., 1998; Hirano et al., 1986; Zou et al., 1999). Securin inhibits Separase by binding to its active site and abolishing its interaction with other substrates (Hornig et al., 2002; Lin et al., 2016). However, mutants for Securin in several organisms do not suffer from premature loss of cohesion, evidencing that other mechanisms of Separase inhibition must be in place (Alexandru et al., 2001; Hellmuth et al., 2015) (see below). Furthermore, Securin has been proposed to work as a Separase chaperone by binding to bind to the nascent Separase and aiding in its proper folding and activity (Jallepalli et al., 2001). Consequently, Securin was shown to be required for sister chromatid separation in fission yeast and D*. melanogaster* (Funabiki et al., 1996; Stratmann and Lehner, 1996).

The second layer of Separase inhibition is mediated by the Cdk1-Cyclin B complex. Cyclin B-Cdk1 phosphorylates Separase and this phosphorylation promotes Cdk1-CycB-separase binding, preventing Separase activation until the onset of anaphase (Gorr et al., 2005; Stemmann et al., 2001). The dual inhibition of Separase by CycB-Cdk1/Securin is lifted by the APC/C, an E3 ubiquitin ligase, which is the main effector of anaphase (reviewed in (Primorac and Musacchio, 2013; Sullivan and Morgan, 2007)). The APC/C ubiquitinates both Securin and Cyclin B, targeting them for the degradation by the proteasome, releasing the Separase from its double leash. This, in turn, leads to cohesin cleavage and the onset of anaphase (Oliveira and Nasmyth, 2010).

Given the importance of this transition, the APC/C itself is tightly regulated during mitosis by a surveillance mechanism known as

the Spindle Assembly Checkpoint (SAC) (Musacchio and Salmon, 2007; Sullivan and Morgan, 2007). The key effector of this mechanism is the Mitotic Checkpoint Complex (MCC). Unattached kinetochores catalyze the formation of this inhibitory complex, which sequesters Cdc20, a key activator required for APC/C activity (Musacchio and Salmon, 2007; Sullivan and Morgan, 2007). The MCC complex is composed of Mad2, BubR1, Bub3 and Cdc20, and that form a complex that actively binds and inactivates the APC/C (Primorac and Musacchio, 2013). As long as the SAC is active and the MCC is being produced at unattached kinetochores, the APC/C will not be activated by cdc20, Cyclin B and Securin will remain intact, Separase inactive, and cohesin will not be cleaved.

This equilibrium changes once metaphase is achieved and chromosomes are bioriented. Stable chromosome attachments result in SAC satisfaction and the release of Cdc20 from the inhibitory MCC complex (Primorac and Musacchio, 2013; Sullivan and Morgan, 2007). Once this happens, APC/C binds Cdc20 becoming active to ubiquitinate Cyclin B and Securin. Ubiquitination promotes the proteasome-mediated degradation of these targets and consequently the release of Separase from its inhibition. Anaphase is imminent.

Since chromosome biorientation and microtubule attachment are highly dynamic processes, once all the chromosomes are bioriented, the decision to commit to anaphase must be rapid and the execution swift. Indeed, live imaging analysis revealed that separase-mediated cohesin cleavage happens within a few minutes during the metaphase-to-anaphase transition (Gerlich et al., 2006; Oliveira et al., 2014; Yaakov et al., 2012).

In order to achieve this sharp metaphase to anaphase transition and rapid cohesin cleavage, multiple positive feedback mechanisms are needed to create a molecular switch. Firstly, Separase has autocatalytic activity, and once released from its Cyclin B-Cdk/Securin inhibition, it is able to cleave itself, and convert to an even more enzymatically potent form (Waizenegger et al., 2002). Furthermore, APC/C is constantly ubiquitinating the MCC and trying to pry away the Cdc20 subunit away from it, weakening the SAC signal in the process (He et al., 2011; Uzunova et al., 2012). In this way APC, accelerates its own release from SAC inhibition during anaphase.

In addition (or in parallel) to separase-mediated cleavage, the cohesin protection machinery is also released from centromeres at the metaphase to anaphase transition, which may accelerate cohesin release. Release of Shugoshin/PP2A from the centromeres may additionally promote the Plk1-mediated phosphorylation of Rad21/Scc1 (Plk1-mediated), which enhances its cleavage by the Separase (Alexandru et al., 2001; Hornig and Uhlmann, 2004).

Moreover, both Shugoshin and Sororin, two key molecules involved in cohesin protection, are directly targeted for degradation by the APC/C (Karamysheva et al., 2009; Rankin et al., 2005). Whether or not removal of the mechanisms involved in cohesin protection actively contribute to the sharp cohesion release process remains to be determined.

As discussed above, cohesin cleavage is only initiated once chromosome biorientation is achieved. Thus, given that chromosomes at this stage are being pulled by mitotic spindle,

release of cohesin is on its own sufficient to trigger pole-ward chromosome movement (Oliveira et al., 2010; Uhlmann et al., 2000). This, however, is insufficient for efficient anaphase chromosome movement. Sister chromatid separation, when triggered alone, results in ~1/3 slower movements, and concomitant re-activation of the SAC and error-correction mechanisms (Mirchenko and Uhlmann, 2010; Oliveira et al., 2010) . Uncoupling cohesin cleavage from Cyclin B destruction leads to similar failures in chromosome segregation (Parry et al., 2003; Vazquez-Novelle and Petronczki, 2010; Vazquez-Novelle et al., 2014). Successful anaphase onset thus relies not only on a sharp anaphase transition but also on a synchrony between sister chromatid cohesion release and cell cycle progression. The fact that cohesin cleavage is regulated by the APC/C, which cleaves both securin (cohesin release) and Cyclin B (cohesin release + cell cycle transition) should in principle provide this synchrony. Additional feedbacks, however, further ensure that sister chromatid separation occurs in synchrony with inactivation of Cdk1 (reviewed in (Kamenz and Hauf, 2016)).

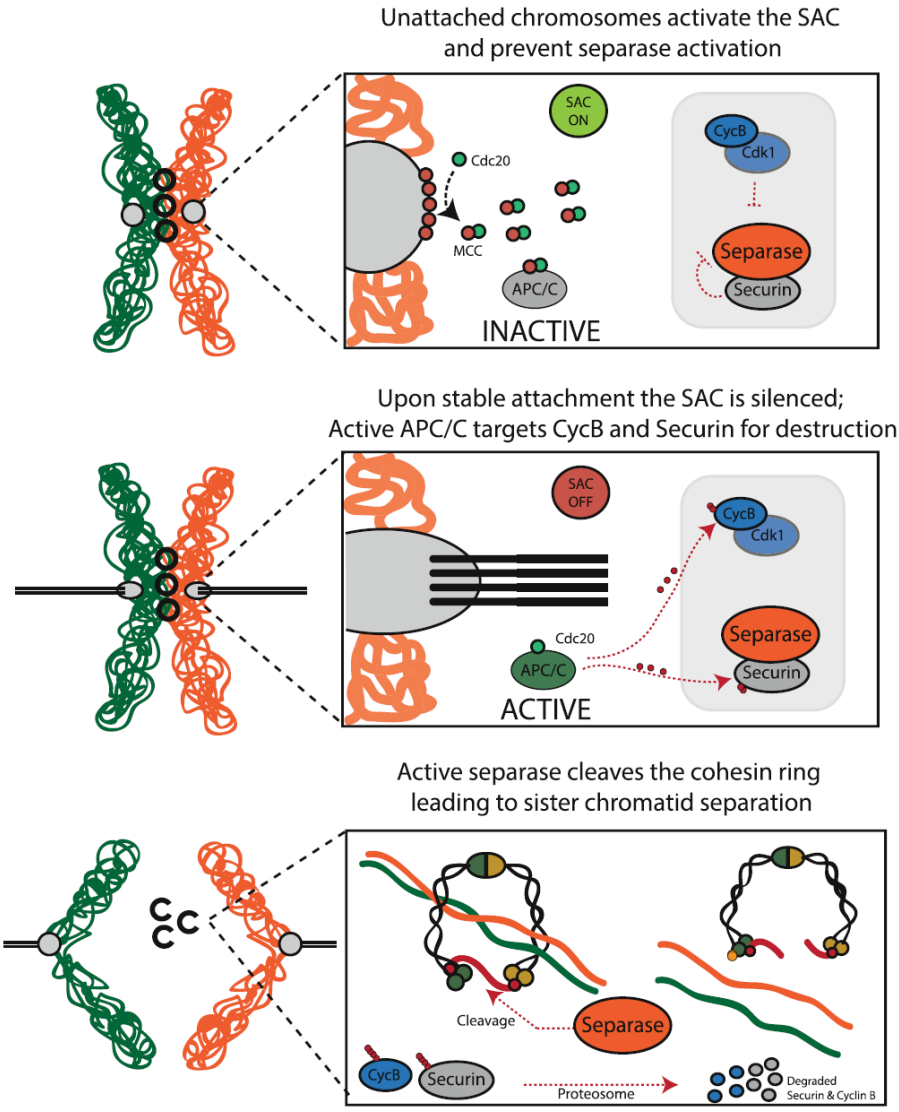

Fig. 8 Cohesin cleavage at the metaphase-to-anaphase transition

In the presence of unattached kinetochores, the spindle assembly checkpoint is activated and generates the formation of the mitotic checkpoint complex (MCC) that prevents anaphase promoting complex/cyclosome activation. Separase is kept inactive by securin and Cdk1/CyclinB binding. b Upon bipolar attachment, the SAC signal is extinguished and the APC/C is activated. Active APC/C ubiquitinates securin and Cyclin B and targets them for degradation. c Active separase cleaves the Rad21/Scc1 subunit and causes ring opening. This opening allows the spindle to drag sister chromatids to opposite poles

1.1.3 Functional implications for a multiple-step cohesin removal

Cohesin binding and release is a dynamic and multi-step process whose mechanisms are mostly conserved across species. Exception goes for the dual-step removal for cohesin during mitosis. In budding yeast, unlike in metazoans, arm cohesion is not removed at the onset of mitosis and the entire cohesin pool is removed at the metaphase to anaphase transition by Separase. The question does arise as to why do metazoans have a two-step removal of cohesin? Does accumulation and retention of cohesin specifically at the centromeric region play any specific function in metazoans? When considering the biological significance of multiple steps for cohesion removal present during mitosis, one must have interphase functions of cohesin in mind. During prophase removal of cohesin, the Scc1 subunit is not cleaved, but disengaged from SMC3 (see above), leaving intact cohesin complexes in the cytoplasm. This cohesin is not reloaded during mitosis, possibly due to the dissociation of the Scc2/4 loading complex from chromosomes (Watrin et al., 2006; Woodman et al., 2014). However, this cohesin can load freely during the impending telophase/G1 and preform roles in transcription regulation and interphase genome architecture early in the subsequent cell cycle. Thus, the prophase pathway may be seen as a recycling mechanism, protecting the majority of cohesin from cleavage during anaphase. It is nevertheless becoming more and more evident, however, that the concentration of cohesin specifically around the centromere fulfills important functions for the efficiency of mitosis, as outlined below.

1.1.4 Sister Chromatid Resolution

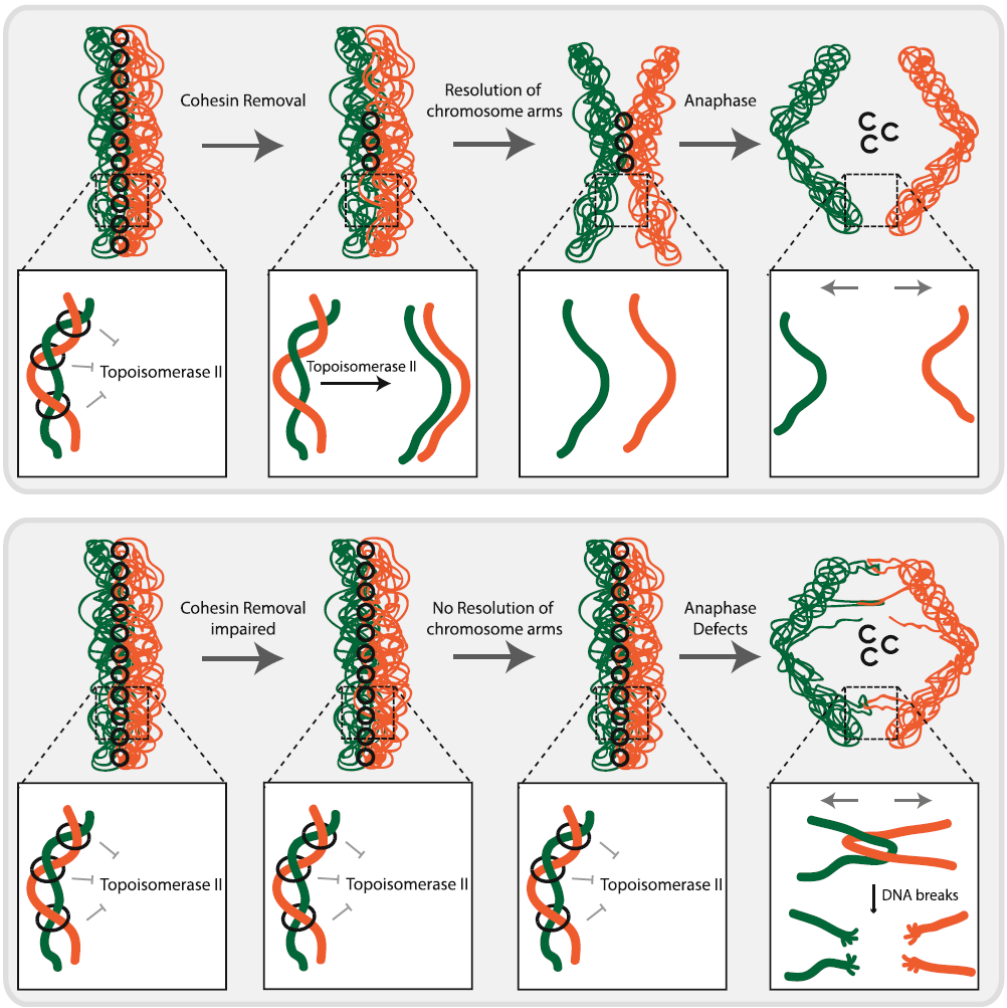

Fig. 9 Cohesin and sister chromatid resolution*. Cohesin entrapment prevents efficient decatenation by topoisomerase II. Cohesin removal from chromosome arms ensures proper sister chromatid resolution. Abnormal retention of cohesin on the arms results in residual entanglements and consequently mitotic defects*

During replication, sister DNA molecules become heavily intertwined as a consequence of the unwinding of parental DNA strands and/or colliding replication forks. In order to segregate these tangled sister molecules into two daughter cells, their catenations must be resolved. Failure to resolve such DNA intertwines by topoisomerase II leads to breaks in the DNA molecules during anaphase, when chromosomes are pulled to the poles by the spindle. Cohesin was shown to block the action of Topoisomerase II (Farcas et al., 2011; Sen et al., 2016), possibly by keeping the two sisters in such close proximity that disfavors their efficient decatenation. Thus, cohesin removal from chromosome arms during prophase is believed to aid sister chromatid resolution along chromosome arms, providing Topoisomerase II with enough space to resolve catenations.

The degree to which sister chromatid resolution can occur in the presence of chromosome-bound cohesin has been hard to estimate. A recent study has elegantly shown that in the absence of WAPL, when cohesin is retained all over chromosome arms, most of sister chromatid resolution can be observed, at least at the limit of the cytological method applied to differentially label individual sister chromatids (Nagasaka et al., 2016). Thus, although cohesin may impair efficient decatenation, the degree of chromosome intertwines even in the presence of cohesin must be residual.

These residual levels of chromosome intertwines are nevertheless sufficient to impair efficient chromosome segregation. When cohesin is not removed from chromosome arms in a timely manner, which happens if WAPL is down-regulated and the prophase pathway inhibited, chromosomes lose their characteristic “X-shape”

and cells undergo an erroneous anaphase, marked by detectable chromosome bridges during anaphase (Haarhuis et al., 2013; Tedeschi et al., 2013). Similar results were observed in cells expressing a modified version of Sororin that lacks its Cdk1-phosphorylation site. This version is not removed from chromosomes arms at the onset of mitosis leading to over-cohesion of metaphase chromosome arms and lagging chromosomes during anaphase (Nishiyama et al., 2013). Moreover, chromosome rearrangements that misplace pericentromeric heterochromatin away from the centromere were shown to abnormally accumulate non-centromeric cohesin (Oliveira et al., 2014). These chromosomes also exhibit chromatin stretching during anaphase, specifically at ectopic cohesin-retention sites. Thus, the spatial and temporal positioning of cohesin on the mitotic chromosome is crucial for timely chromosome resolution. Any disturbance, such as prolonged retention or enrichment of cohesin along chromosome arms leads to incomplete sister chromatid separation, followed by mitotic errors.

1.1.5 Inner-centromere defining platform:

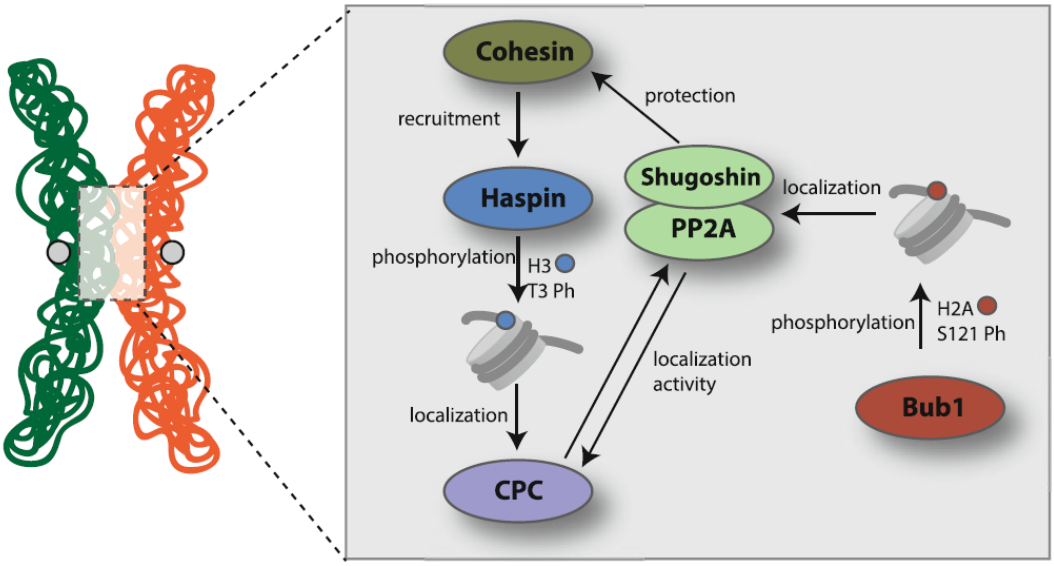

***Fig. 10 The inner centromere network**. Cohesin sets the blueprint for the inner centromere network, regulating chromosome architecture and microtubule attachment. Cohesin is needed for the recruitment of Haspin kinase, which triggers the cascade resulting in recruitment of CPC and Shugoshin to the pericentromeric region*

Centromeric cohesin has recently emerged as a core component of the inner centromeric network and thereby influences the localization of important machinery that regulates mitotic fidelity.

Kinetochore microtubule attachments are regulated by the actions of Aurora B, a key mitotic kinase that destabilizes erroneous kinetochore-microtubule attachments. It is well established that Aurora B destabilizes attachments that are not under tension through the phosphorylation of key kinetochore substrates (Biggins and Murray, 2001). This phosphorylation results in microtubule

detachment and the creation of unattached kinetochores that can trigger SAC signaling. Aurora B, together with its regulatory partners INCENP, Borealin and Survivin, forms the Chromosome Passenger Complex (CPC). This complex decorates the entire chromosome length during early mitotic stages but dynamically shifts its localization towards prometaphase/metaphase, becoming highly enriched at the inner centromeric region (Reviewed in (Carmena et al., 2012).

Cohesin's importance for CPC localization has been documented in several studies (Carretero et al., 2013; Haarhuis et al., 2013; Kenney and Heald, 2006; Mirkovic et al., 2015; Sonoda et al., 2001; Vass et al., 2003) but only recently the mechanistic details for this interaction are being elucidated. CPC localization to the inner centromere was shown to depend on two histone marks: Histone H3 phosphorylation on Threonine 3 (H3pT3) and histone 2A-serine 121 (H2A-S121) phosphorylation (Yamagishi et al., 2010). The cohesin subunit PDS5A interacts with the Haspin Kinase, which is the kinase responsible for H3T3 phosphorylation (Yamagishi et al., 2010). Depletion of Pds5 or Cohesin subunits result in delocalized Aurora B and possibly impaired error correction (Carretero et al., 2013; Mirkovic et al., 2015; Yamagishi et al., 2010). Interestingly enough, "too much" cohesin produces a similar phenotype, as WAPL depleted cells also exhibit delocalized Aurora B signals and defective error-correction capacity (Haarhuis et al., 2013).

In addition to CPC localization, cohesin also plays a role in the localization of another key inner centromere component: Shugoshin. Shugoshin interacts directly with cohesin and requires this interaction for its activity (Liu et al., 2013a; Liu et al., 2013b). In

this way, cohesin enhances its own centromeric protection but also contributes to other events that are governed by Sgo1 at the centromeres, namely biorientation of sister chromatids, localization of the CPC and SAC silencing (reviewed in (Marston, 2015)).

Thus, while enhancing its own protection, cohesin plays a pivotal role in the establishment of the inner centromere network.

1.1.6 Force Balance

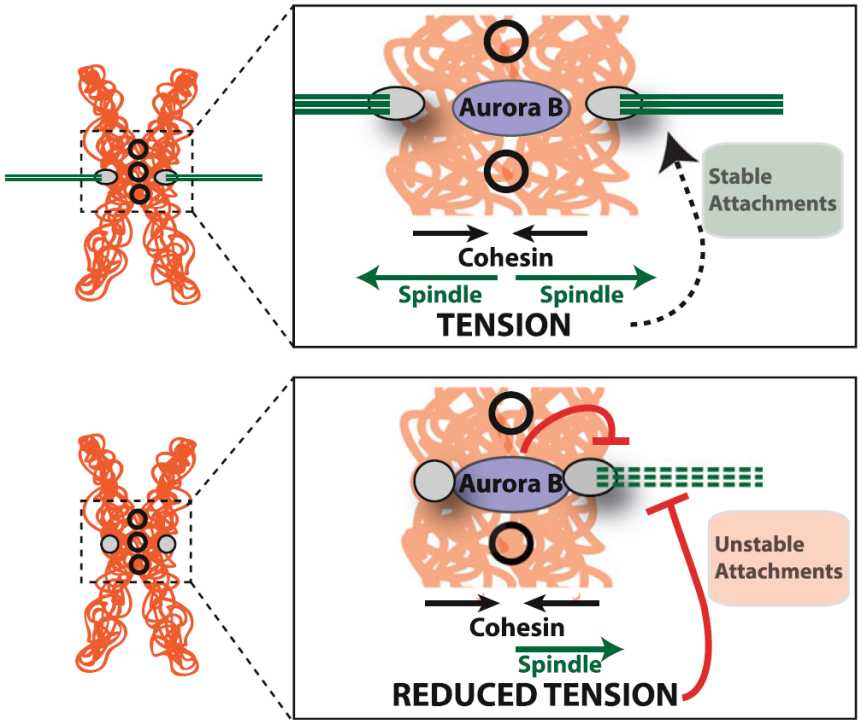

***Fig. 11 Force balance**. Cohesin is the major force resisting the mitotic spindle during metaphase. The antagonism between cohesin and the spindle results in sufficient tension that is required to stabilize the attachments of microtubules to the kinetochore. Erroneous attachments (e.g. mono-oriented chromosomes or chromosome with the two kinetochores bound to the same pole)are not under sufficient tension. This reduced tension leads to destabilization of these interactions by Aurora B kinase*

Centromeric retention of cohesin has profound roles in mitotic fidelity, as it is the condition for biorientation of chromosomes and symmetrical segregation of the genome. The binding and stability of microtubule attachments to the kinetochore is enhanced by the tension between the spindle and the kinetochore, both in vivo and in vitro (reviewed in (Biggins, 2015)). Tension-dependent stabilization of kinetochore-microtubule interactions depends on an intrinsic stabilization ability of the mechanical force exerted by the microtubule pulling forces (Akiyoshi et al., 2010), as well as on biochemical changes that promote the stabilization of kinetochore-microtubule interactions. The latter are regulated by Aurora B kinase, responsible for the correction of erroneous microtubule-kinetochore interactions through the phosphorylation of key kinetochore substrates. Upon bipolar attachment, i.e. maximal tension, the increase in the distance between the inner-centromeric Aurora B and the kinetochore is believed to displace Aurora-B away from its targets thus reverting Aurora-B mediated destabilization of microtubule attachments (Liu et al., 2009a).

How chromosome tension is established, sensed and ultimately regulates kinetochore- microtubule interactions has been widely investigated. Bipolar attachment increases tension across the entire pericentromeric domain (inter-kinetochore tension), but also within each individual kinetochore, marked by the increase in the distance between the proteins of inner and outer kinetochore (reviewed in (Maresca and Salmon, 2010). Both intra- and inter-kinetochore stretch require a counterforce to the spindle to generate stable microtubule attachment and tension. The cohesin ring presents the only force at the centromere that is able to resist the pulling forces of the spindle. Thus, centromeric cohesion

contributes to the generation of tension needed for stable chromosome biorientation on the metaphase plane (Figure X). It provides the counterforce necessary to maintain a force-equilibrium between with the mitotic spindle, which can generate forces of up to hundreds of piconewtons (Nicklas et al., 1995; Ye et al., 2016). In agreement with cohesin's major role in the establishment of both inter and intra-kinetochore tension, loss of cohesin prior to or during metaphase leads to extensive chromosome shuffling along the spindle, as attachments to isolated single sisters are highly unstable (Drpic et al., 2015; Mirkovic et al., 2015; Oliveira et al., 2010).

Whether or not cohesin could also contribute to tension sensing has also been speculated. Upon bipolar attachment, tension across sister chromatids will influence the entire pericentromeric domain and evidence suggests that this alone can lead to removal of centromeric cohesin complexes (Eckert et al., 2007; Ocampo-Hafalla et al., 2007). More distal pericentromeric domains would then provide the necessary antagonistic force to the spindle. This dynamic change on the cohesive forces could alone provide a clue to sense bipolar attachment. In agreement, cohesin-associated molecules, particularly Shugoshin, have been proposed to contribute to tension sensing and SAC silencing at the metaphase to anaphase transition (reviewed in (Marston, 2015)).

However, inter-kinetochore stretch does not seem to be necessary for tension sensing as chromosomes in which two neighboring kinetochores were artificially tethered, preventing the inter-kinetochore stretch, still resulted in normal metaphase attachment. These experiments imply that mechanical tension exerted on the single kinetochore might be more important than the stretching

between kinetochore pairs itself to stabilize chromosome attachments (Nannas and Murray, 2014).

Regardless of the exact location that senses chromosome tension, the structure of the pericentromeric domain will likely play a major influence on the force provided by the chromosomes (Stephens et al., 2013). Does this force balance require a specific amount of cohesin at chromosomes and does centromeric accumulation play a role? It is conceivable that reaching the right spindle counter-force requires a fine-tuning of cohesin levels at chromosome. This has been difficult to tackle experimentally as manipulating cohesin levels is not a trivial task. Metazoan chromosomes with artificial high levels of cohesin (e.g. WAPL knock-down) do display defects in chromosome attachment. Although these have been largely attributed to defects in the localization of the machinery that regulates microtubule-kinetochore attachments (see above), it remains to be determined the consequences of too much cohesion on tension establishment and sensing, independently of Aurora B localization.

1.1.7 Anaphase sharpness

Cohesin destruction marks the onset of anaphase, a point of no return for every dividing cell. As discussed above, several feedback loops operate at this stage to ensure efficient cohesin cleavage at this crucial transition. Restricting cohesin to centromeric region may be an additional mechanism to ensure fast anaphase onset and promote synchrony of anaphase movements, particularly in organisms containing variable chromosome sizes. Separase is functionally active along the entire chromosome, as evidenced by complete cohesin cleavage in WAPL mutants, in which cohesin is

now all over chromosome arms, or in cells expressing Separase sensors targeted to the entire chromosomes (Haarhuis et al., 2013; Oliveira et al., 2014; Shindo et al., 2012; Yaakov et al., 2012).

Whether or not the efficiency of cohesin cleavage is the same all over the chromatin mass has been quite controversial. Direct measurements of Separase activity using engineered sensors at different chromosome loci in budding yeast, failed to detect any delay of cleaving telomeric vs centromeric sites (Yaakov et al., 2012). In contrast, other studies support that removal of cohesin at regions distal to the centromere is less efficient than at centromere-proximal ones (Oliveira et al., 2014; Renshaw et al., 2010). These studies thus suggest that although Separase is capable of cleaving cohesin all over chromosome arms, coupling residual cohesion to the centromere may be an efficient way to accelerate cohesin degradation. This could be due to the pulling force of the spindle that could aid in cohesin release, or enhanced Separase activity at the centromeric region.

1.1.8 Concluding remarks

In the cell biology field, centromeric cohesin is mostly viewed as an architectural molecule, a molecular glue linking sister chromatids and preventing random chromosome segregation. However, it is crucial to shift such a viewpoint in order to encompass all the diverse functions of cohesin during nuclear division. Restricting cohesion to the centromeric region during mitosis is of paramount importance for efficient chromosome resolution and segregation. Cohesin itself provides the main elastic force necessary to resist the metaphase spindle and establish biorientation of the chromosomes during metaphase. Cohesin is also crucial for the

establishment of an inner-centromere network thus contributing to the localization and function of proteins involved in the regulation of chromosome attachments and spindle assembly checkpoint. As such, mitotic cohesin is way more than a pure “architectural” molecule and should be viewed as a dynamic scaffold for multiple mitotic processes, rather than a hinge keeping chromosomes together.

References

Akiyoshi, B., Sarangapani, K.K., Powers, A.F., Nelson, C.R., Reichow, S.L., Arellano-Santoyo, H., Gonen, T., Ranish, J.A., Asbury, C.L., and Biggins, S. (2010). Tension directly stabilizes reconstituted kinetochore-microtubule attachments. Nature *468*, 576-579.

Alexandru, G., Uhlmann, F., Mechtler, K., Poupart, M.A., and Nasmyth, K. (2001). Phosphorylation of the cohesin subunit Scc1 by Polo/Cdc5 kinase regulates sister chromatid separation in yeast. Cell *105*, 459-472.

Arumugam, P., Gruber, S., Tanaka, K., Haering, C.H., Mechtler, K., and Nasmyth, K. (2003). ATP hydrolysis is required for cohesin's association with chromosomes. Curr Biol *13*, 1941-1953.

Bachant, J., Alcasabas, A., Blat, Y., Kleckner, N., and Elledge, S.J. (2002). The SUMO-1 isopeptidase Smt4 is linked to centromeric cohesion through SUMO-1 modification of DNA topoisomerase II. Mol Cell *9*, 1169-1182.

Baumann, C., Korner, R., Hofmann, K., and Nigg, E.A. (2007). PICH, a centromere-associated SNF2 family ATPase, is regulated by Plk1 and required for the spindle checkpoint. Cell *128*, 101-114.

Bernard, P., Maure, J.F., Partridge, J.F., Genier, S., Javerzat, J.P., and Allshire, R.C. (2001). Requirement of heterochromatin for cohesion at centromeres. Science *294*, 2539-2542.

Biggins, S. (2015). Under Tension: Kinetochores and Basic Research. Genetics *200*, 681-682.

Biggins, S., and Murray, A.W. (2001). The budding yeast protein kinase Ipl1/Aurora allows the absence of tension to activate the spindle checkpoint. Genes Dev *15*, 3118-3129.

Blat, Y., and Kleckner, N. (1999). Cohesins bind to preferential sites along yeast chromosome III, with differential regulation along arms versus the centric region. Cell *98*, 249-259.

Buheitel, J., and Stemmann, O. (2013). Prophase pathway-dependent removal of cohesin from human chromosomes requires opening of the Smc3-Scc1 gate. EMBO J *32*, 666-676.

Burkhardt, S., Borsos, M., Szydlowska, A., Godwin, J., Williams, S.A., Cohen, P.E., Hirota, T., Saitou, M., and Tachibana-Konwalski, K. (2016). Chromosome Cohesion Established by Rec8-Cohesin in Fetal Oocytes Is Maintained without Detectable Turnover in Oocytes Arrested for Months in Mice. Curr Biol *26*, 678-685.

Carmena, M., Wheelock, M., Funabiki, H., and Earnshaw, W.C. (2012). The chromosomal passenger complex (CPC): from easy rider to the godfather of mitosis. Nat Rev Mol Cell Biol *13*, 789-803.

Carretero, M., Ruiz-Torres, M., Rodriguez-Corsino, M., Barthelemy, I., and Losada, A. (2013). Pds5B is required for cohesion establishment and Aurora B accumulation at centromeres. EMBO J *32*, 2938-2949.
Ciosk, R., Shirayama, M., Shevchenko, A., Tanaka, T., Toth, A., Shevchenko, A., and Nasmyth, K. (2000). Cohesin's binding to chromosomes depends on a separate complex consisting of Scc2 and Scc4 proteins. Mol Cell *5*, 243-254.
Ciosk, R., Zachariae, W., Michaelis, C., Shevchenko, A., Mann, M., and Nasmyth, K. (1998). An ESP1/PDS1 complex regulates loss of sister chromatid cohesion at the metaphase to anaphase transition in yeast. Cell *93*, 1067-1076.
Dawlaty, M.M., Malureanu, L., Jeganathan, K.B., Kao, E., Sustmann, C., Tahk, S., Shuai, K., Grosschedl, R., and van Deursen, J.M. (2008). Resolution of sister centromeres requires RanBP2-mediated SUMOylation of topoisomerase IIalpha. Cell *133*, 103-115.
De Koninck, M., and Losada, A. (2016). Cohesin Mutations in Cancer. Cold Spring Harb Perspect Med.
Diaz-Martinez, L.A., Gimenez-Abian, J.F., and Clarke, D.J. (2008). Chromosome cohesion - rings, knots, orcs and fellowship. J Cell Sci *121*, 2107-2114.
Dorsett, D. (2007). Roles of the sister chromatid cohesion apparatus in gene expression, development, and human syndromes. Chromosoma *116*, 1-13.
Dreier, M.R., Bekier, M.E., 2nd, and Taylor, W.R. (2011). Regulation of sororin by Cdk1-mediated phosphorylation. J Cell Sci *124*, 2976-2987.
Drpic, D., Pereira, A.J., Barisic, M., Maresca, T.J., and Maiato, H. (2015). Polar Ejection Forces Promote the Conversion from Lateral to End-on Kinetochore-Microtubule Attachments on Mono-oriented Chromosomes. Cell Rep *13*, 460-469.
Eckert, C.A., Gravdahl, D.J., and Megee, P.C. (2007). The enhancement of pericentromeric cohesin association by conserved kinetochore components promotes high-fidelity chromosome segregation and is sensitive to microtubule-based tension. Genes Dev *21*, 278-291.
Eichinger, C.S., Kurze, A., Oliveira, R.A., and Nasmyth, K. (2013). Disengaging the Smc3/kleisin interface releases cohesin from Drosophila chromosomes during interphase and mitosis. EMBO J *32*, 656-665.
Farcas, A.M., Uluocak, P., Helmhart, W., and Nasmyth, K. (2011). Cohesin's concatenation of sister DNAs maintains their intertwining. Mol Cell *44*, 97-107.
Funabiki, H., Kumada, K., and Yanagida, M. (1996). Fission yeast Cut1 and Cut2 are essential for sister chromatid separation, concentrate along the metaphase spindle and form large complexes. EMBO J *15*, 6617-6628.

Gandhi, R., Gillespie, P.J., and Hirano, T. (2006). Human Wapl is a cohesin-binding protein that promotes sister-chromatid resolution in mitotic prophase. Curr Biol *16*, 2406-2417.
Gerlich, D., Koch, B., Dupeux, F., Peters, J.M., and Ellenberg, J. (2006). Live-cell imaging reveals a stable cohesin-chromatin interaction after but not before DNA replication. Curr Biol *16*, 1571-1578.
Glynn, E.F., Megee, P.C., Yu, H.G., Mistrot, C., Unal, E., Koshland, D.E., DeRisi, J.L., and Gerton, J.L. (2004). Genome-wide mapping of the cohesin complex in the yeast Saccharomyces cerevisiae. PLoS Biol *2*, E259.
Gorr, I.H., Boos, D., and Stemmann, O. (2005). Mutual inhibition of separase and Cdk1 by two-step complex formation. Mol Cell *19*, 135-141.
Gruber, S., Arumugam, P., Katou, Y., Kuglitsch, D., Helmhart, W., Shirahige, K., and Nasmyth, K. (2006). Evidence that loading of cohesin onto chromosomes involves opening of its SMC hinge. Cell *127*, 523-537.
Guacci, V. (2007). Sister chromatid cohesion: the cohesin cleavage model does not ring true. Genes Cells *12*, 693-708.
Guacci, V., Koshland, D., and Strunnikov, A. (1997). A direct link between sister chromatid cohesion and chromosome condensation revealed through the analysis of MCD1 in S. cerevisiae. Cell *91*, 47-57.
Haarhuis, J.H., Elbatsh, A.M., van den Broek, B., Camps, D., Erkan, H., Jalink, K., Medema, R.H., and Rowland, B.D. (2013). WAPL-mediated removal of cohesin protects against segregation errors and aneuploidy. Curr Biol *23*, 2071-2077.
Haering, C.H., Farcas, A.M., Arumugam, P., Metson, J., and Nasmyth, K. (2008). The cohesin ring concatenates sister DNA molecules. Nature *454*, 297-301.
Haering, C.H., Lowe, J., Hochwagen, A., and Nasmyth, K. (2002). Molecular architecture of SMC proteins and the yeast cohesin complex. Mol Cell *9*, 773-788.
Hahn, M., Dambacher, S., Dulev, S., Kuznetsova, A.Y., Eck, S., Worz, S., Sadic, D., Schulte, M., Mallm, J.P., Maiser, A.*, et al.* (2013). Suv4-20h2 mediates chromatin compaction and is important for cohesin recruitment to heterochromatin. Genes Dev *27*, 859-872.
Hara, K., Zheng, G., Qu, Q., Liu, H., Ouyang, Z., Chen, Z., Tomchick, D.R., and Yu, H. (2014). Structure of cohesin subcomplex pinpoints direct shugoshin-Wapl antagonism in centromeric cohesion. Nat Struct Mol Biol *21*, 864-870.
Hauf, S., Roitinger, E., Koch, B., Dittrich, C.M., Mechtler, K., and Peters, J.M. (2005). Dissociation of cohesin from chromosome arms and loss of arm cohesion during early mitosis depends on phosphorylation of SA2. PLoS Biol *3*, e69.

He, E., Kapuy, O., Oliveira, R.A., Uhlmann, F., Tyson, J.J., and Novak, B. (2011). System-level feedbacks make the anaphase switch irreversible. Proc Natl Acad Sci U S A *108*, 10016-10021.
Hellmuth, S., Pohlmann, C., Brown, A., Bottger, F., Sprinzl, M., and Stemmann, O. (2015). Positive and negative regulation of vertebrate separase by Cdk1-cyclin B1 may explain why securin is dispensable. J Biol Chem *290*, 8002-8010.
Hirano, T., Funahashi, S., Uemura, T., and Yanagida, M. (1986). Isolation and characterization of Schizosaccharomyces pombe cutmutants that block nuclear division but not cytokinesis. EMBO J *5*, 2973-2979.
Holland, A.J., and Cleveland, D.W. (2009). Boveri revisited: chromosomal instability, aneuploidy and tumorigenesis. Nat Rev Mol Cell Biol *10*, 478-487.
Hornig, N.C., Knowles, P.P., McDonald, N.Q., and Uhlmann, F. (2002). The dual mechanism of separase regulation by securin. Curr Biol *12*, 973-982.
Hornig, N.C., and Uhlmann, F. (2004). Preferential cleavage of chromatin-bound cohesin after targeted phosphorylation by Polo-like kinase. EMBO J *23*, 3144-3153.
Hu, B., Itoh, T., Mishra, A., Katoh, Y., Chan, K.L., Upcher, W., Godlee, C., Roig, M.B., Shirahige, K., and Nasmyth, K. (2011). ATP hydrolysis is required for relocating cohesin from sites occupied by its Scc2/4 loading complex. Curr Biol *21*, 12-24.
Ivanov, D., and Nasmyth, K. (2005). A topological interaction between cohesin rings and a circular minichromosome. Cell *122*, 849-860.
Jallepalli, P.V., Waizenegger, I.C., Bunz, F., Langer, S., Speicher, M.R., Peters, J.M., Kinzler, K.W., Vogelstein, B., and Lengauer, C. (2001). Securin is required for chromosomal stability in human cells. Cell *105*, 445-457.
Kamenz, J., and Hauf, S. (2016). Time To Split Up: Dynamics of Chromosome Separation. Trends Cell Biol.
Karamysheva, Z., Diaz-Martinez, L.A., Crow, S.E., Li, B., and Yu, H. (2009). Multiple anaphase-promoting complex/cyclosome degrons mediate the degradation of human Sgo1. J Biol Chem *284*, 1772-1780.
Kenney, R.D., and Heald, R. (2006). Essential roles for cohesin in kinetochore and spindle function in Xenopus egg extracts. J Cell Sci *119*, 5057-5066.
Kerrebrock, A.W., Miyazaki, W.Y., Birnby, D., and Orr-Weaver, T.L. (1992). The Drosophila mei-S332 gene promotes sister-chromatid cohesion in meiosis following kinetochore differentiation. Genetics *130*, 827-841.
Kitajima, T.S., Kawashima, S.A., and Watanabe, Y. (2004). The conserved kinetochore protein shugoshin protects centromeric cohesion during meiosis. Nature *427*, 510-517.

Kitajima, T.S., Sakuno, T., Ishiguro, K., Iemura, S., Natsume, T., Kawashima, S.A., and Watanabe, Y. (2006). Shugoshin collaborates with protein phosphatase 2A to protect cohesin. Nature *441*, 46-52.
Koch, B., Kueng, S., Ruckenbauer, C., Wendt, K.S., and Peters, J.M. (2008). The Suv39h-HP1 histone methylation pathway is dispensable for enrichment and protection of cohesin at centromeres in mammalian cells. Chromosoma *117*, 199-210.
Kueng, S., Hegemann, B., Peters, B.H., Lipp, J.J., Schleiffer, A., Mechtler, K., and Peters, J.M. (2006). Wapl controls the dynamic association of cohesin with chromatin. Cell *127*, 955-967.
Lenart, P., Petronczki, M., Steegmaier, M., Di Fiore, B., Lipp, J.J., Hoffmann, M., Rettig, W.J., Kraut, N., and Peters, J.M. (2007). The small-molecule inhibitor BI 2536 reveals novel insights into mitotic roles of polo-like kinase 1. Curr Biol *17*, 304-315.
Lengronne, A., Katou, Y., Mori, S., Yokobayashi, S., Kelly, G.P., Itoh, T., Watanabe, Y., Shirahige, K., and Uhlmann, F. (2004). Cohesin relocation from sites of chromosomal loading to places of convergent transcription. Nature *430*, 573-578.
Lin, Z., Luo, X., and Yu, H. (2016). Structural basis of cohesin cleavage by separase. Nature *532*, 131-134.
Liu, D., Vader, G., Vromans, M.J., Lampson, M.A., and Lens, S.M. (2009a). Sensing chromosome bi-orientation by spatial separation of aurora B kinase from kinetochore substrates. Science *323*, 1350-1353.
Liu, H., Jia, L., and Yu, H. (2013a). Phospho-H2A and cohesin specify distinct tension-regulated Sgo1 pools at kinetochores and inner centromeres. Curr Biol *23*, 1927-1933.
Liu, H., Rankin, S., and Yu, H. (2013b). Phosphorylation-enabled binding of SGO1-PP2A to cohesin protects sororin and centromeric cohesion during mitosis. Nat Cell Biol *15*, 40-49.
Liu, J., and Krantz, I.D. (2008). Cohesin and human disease. Annu Rev Genomics Hum Genet *9*, 303-320.
Liu, Z., Deibler, R.W., Chan, H.S., and Zechiedrich, L. (2009b). The why and how of DNA unlinking. Nucleic Acids Res *37*, 661-671.
Losada, A. (2014). Cohesin in cancer: chromosome segregation and beyond. Nat Rev Cancer *14*, 389-393.
Losada, A., Hirano, M., and Hirano, T. (1998). Identification of Xenopus SMC protein complexes required for sister chromatid cohesion. Genes Dev *12*, 1986-1997.
Maresca, T.J., and Salmon, E.D. (2010). Welcome to a new kind of tension: translating kinetochore mechanics into a wait-anaphase signal. J Cell Sci *123*, 825-835.

Marston, A.L. (2015). Shugoshins: tension-sensitive pericentromeric adaptors safeguarding chromosome segregation. Mol Cell Biol *35*, 634-648.
McGuinness, B.E., Hirota, T., Kudo, N.R., Peters, J.M., and Nasmyth, K. (2005). Shugoshin prevents dissociation of cohesin from centromeres during mitosis in vertebrate cells. PLoS Biol *3*, e86.
Megee, P.C., and Koshland, D. (1999). A functional assay for centromere-associated sister chromatid cohesion. Science *285*, 254-257.
Michaelis, C., Ciosk, R., and Nasmyth, K. (1997). Cohesins: chromosomal proteins that prevent premature separation of sister chromatids. Cell *91*, 35-45.
Mirchenko, L., and Uhlmann, F. (2010). Sli15(INCENP) dephosphorylation prevents mitotic checkpoint reengagement due to loss of tension at anaphase onset. Curr Biol *20*, 1396-1401.
Mirkovic, M., Hutter, L.H., Novak, B., and Oliveira, R.A. (2015). Premature Sister Chromatid Separation Is Poorly Detected by the Spindle Assembly Checkpoint as a Result of System-Level Feedback. Cell Rep *13*, 470-478.
Musacchio, A., and Salmon, E.D. (2007). The spindle-assembly checkpoint in space and time. Nat Rev Mol Cell Biol *8*, 379-393.
Nagasaka, K., Hossain, M.J., Roberti, M.J., Ellenberg, J., and Hirota, T. (2016). Sister chromatid resolution is an intrinsic part of chromosome organization in prophase. Nat Cell Biol *18*, 692-699.
Nannas, N.J., and Murray, A.W. (2014). Tethering sister centromeres to each other suggests the spindle checkpoint detects stretch within the kinetochore. PLoS Genet *10*, e1004492.
Nasmyth, K., and Haering, C.H. (2009). Cohesin: its roles and mechanisms. Annu Rev Genet *43*, 525-558.
Ng, T.M., Waples, W.G., Lavoie, B.D., and Biggins, S. (2009). Pericentromeric sister chromatid cohesion promotes kinetochore biorientation. Mol Biol Cell *20*, 3818-3827.
Nicklas, R.B., Ward, S.C., and Gorbsky, G.J. (1995). Kinetochore chemistry is sensitive to tension and may link mitotic forces to a cell cycle checkpoint. J Cell Biol *130*, 929-939.
Nishiyama, T., Ladurner, R., Schmitz, J., Kreidl, E., Schleiffer, A., Bhaskara, V., Bando, M., Shirahige, K., Hyman, A.A., Mechtler, K.*, et al.* (2010). Sororin mediates sister chromatid cohesion by antagonizing Wapl. Cell *143*, 737-749.
Nishiyama, T., Sykora, M.M., Huis in 't Veld, P.J., Mechtler, K., and Peters, J.M. (2013). Aurora B and Cdk1 mediate Wapl activation and release of acetylated cohesin from chromosomes by phosphorylating Sororin. Proc Natl Acad Sci U S A *110*, 13404-13409.

Nonaka, N., Kitajima, T., Yokobayashi, S., Xiao, G., Yamamoto, M., Grewal, S.I., and Watanabe, Y. (2002). Recruitment of cohesin to heterochromatic regions by Swi6/HP1 in fission yeast. Nat Cell Biol *4*, 89-93.
Ocampo-Hafalla, M., Munoz, S., Samora, C.P., and Uhlmann, F. (2016). Evidence for cohesin sliding along budding yeast chromosomes. Open Biol *6*.
Ocampo-Hafalla, M.T., Katou, Y., Shirahige, K., and Uhlmann, F. (2007). Displacement and re-accumulation of centromeric cohesin during transient pre-anaphase centromere splitting. Chromosoma *116*, 531-544.
Ocampo-Hafalla, M.T., and Uhlmann, F. (2011). Cohesin loading and sliding. J Cell Sci *124*, 685-691.
Oliveira, R.A., Hamilton, R.S., Pauli, A., Davis, I., and Nasmyth, K. (2010). Cohesin cleavage and Cdk inhibition trigger formation of daughter nuclei. Nat Cell Biol *12*, 185-192.
Oliveira, R.A., Kotadia, S., Tavares, A., Mirkovic, M., Bowlin, K., Eichinger, C.S., Nasmyth, K., and Sullivan, W. (2014). Centromere-independent accumulation of cohesin at ectopic heterochromatin sites induces chromosome stretching during anaphase. PLoS Biol *12*, e1001962.
Oliveira, R.A., and Nasmyth, K. (2010). Getting through anaphase: splitting the sisters and beyond. Biochem Soc Trans *38*, 1639-1644.
Parry, D.H., Hickson, G.R., and O'Farrell, P.H. (2003). Cyclin B destruction triggers changes in kinetochore behavior essential for successful anaphase. Curr Biol *13*, 647-653.
Patel, J., Tan, S.L., Hartshorne, G.M., and McAinsh, A.D. (2015). Unique geometry of sister kinetochores in human oocytes during meiosis I may explain maternal age-associated increases in chromosomal abnormalities. Biol Open *5*, 178-184.
Peters, J.M., Tedeschi, A., and Schmitz, J. (2008). The cohesin complex and its roles in chromosome biology. Genes Dev *22*, 3089-3114.
Primorac, I., and Musacchio, A. (2013). Panta rhei: the APC/C at steady state. J Cell Biol *201*, 177-189.
Rankin, S., Ayad, N.G., and Kirschner, M.W. (2005). Sororin, a substrate of the anaphase-promoting complex, is required for sister chromatid cohesion in vertebrates. Mol Cell *18*, 185-200.
Remeseiro, S., Cuadrado, A., and Losada, A. (2013). Cohesin in development and disease. Development *140*, 3715-3718.
Renshaw, M.J., Ward, J.J., Kanemaki, M., Natsume, K., Nedelec, F.J., and Tanaka, T.U. (2010). Condensins promote chromosome recoiling during early anaphase to complete sister chromatid separation. Dev Cell *19*, 232-244.

Rudra, S., and Skibbens, R.V. (2013). Cohesin codes - interpreting chromatin architecture and the many facets of cohesin function. J Cell Sci *126*, 31-41.
Ryu, H., Furuta, M., Kirkpatrick, D., Gygi, S.P., and Azuma, Y. (2010). PIASy-dependent SUMOylation regulates DNA topoisomerase IIalpha activity. J Cell Biol *191*, 783-794.
Sakuno, T., Tada, K., and Watanabe, Y. (2009). Kinetochore geometry defined by cohesion within the centromere. Nature *458*, 852-858.
Sen, N., Leonard, J., Torres, R., Garcia-Luis, J., Palou-Marin, G., and Aragon, L. (2016). Physical Proximity of Sister Chromatids Promotes Top2-Dependent Intertwining. Mol Cell *64*, 134-147.
Shindo, N., Kumada, K., and Hirota, T. (2012). Separase sensor reveals dual roles for separase coordinating cohesin cleavage and cdk1 inhibition. Dev Cell *23*, 112-123.
Skibbens, R.V., Corson, L.B., Koshland, D., and Hieter, P. (1999). Ctf7p is essential for sister chromatid cohesion and links mitotic chromosome structure to the DNA replication machinery. Genes Dev *13*, 307-319.
Sonoda, E., Matsusaka, T., Morrison, C., Vagnarelli, P., Hoshi, O., Ushiki, T., Nojima, K., Fukagawa, T., Waizenegger, I.C., Peters, J.M*., et al.* (2001). Scc1/Rad21/Mcd1 is required for sister chromatid cohesion and kinetochore function in vertebrate cells. Dev Cell *1*, 759-770.
Stemmann, O., Zou, H., Gerber, S.A., Gygi, S.P., and Kirschner, M.W. (2001). Dual inhibition of sister chromatid separation at metaphase. Cell *107*, 715-726.
Stephens, A.D., Quammen, C.W., Chang, B., Haase, J., Taylor, R.M., 2nd, and Bloom, K. (2013). The spatial segregation of pericentric cohesin and condensin in the mitotic spindle. Mol Biol Cell *24*, 3909-3919.
Stigler, J., Camdere, G.O., Koshland, D.E., and Greene, E.C. (2016). Single-Molecule Imaging Reveals a Collapsed Conformational State for DNA-Bound Cohesin. Cell Rep *15*, 988-998.
Stratmann, R., and Lehner, C.F. (1996). Separation of sister chromatids in mitosis requires the Drosophila pimples product, a protein degraded after the metaphase/anaphase transition. Cell *84*, 25-35.
Sullivan, M., and Morgan, D.O. (2007). Finishing mitosis, one step at a time. Nat Rev Mol Cell Biol *8*, 894-903.
Sumara, I., Vorlaufer, E., Gieffers, C., Peters, B.H., and Peters, J.M. (2000). Characterization of vertebrate cohesin complexes and their regulation in prophase. J Cell Biol *151*, 749-762.
Sumara, I., Vorlaufer, E., Stukenberg, P.T., Kelm, O., Redemann, N., Nigg, E.A., and Peters, J.M. (2002). The dissociation of cohesin from chromosomes in prophase is regulated by Polo-like kinase. Mol Cell *9*, 515-525.

Tachibana-Konwalski, K., Godwin, J., Borsos, M., Rattani, A., Adams, D.J., and Nasmyth, K. (2013). Spindle assembly checkpoint of oocytes depends on a kinetochore structure determined by cohesin in meiosis I. Curr Biol *23*, 2534-2539.
Tanaka, T., Cosma, M.P., Wirth, K., and Nasmyth, K. (1999). Identification of cohesin association sites at centromeres and along chromosome arms. Cell *98*, 847-858.
Tanaka, T., Fuchs, J., Loidl, J., and Nasmyth, K. (2000). Cohesin ensures bipolar attachment of microtubules to sister centromeres and resists their precocious separation. Nat Cell Biol *2*, 492-499.
Tanno, Y., Kitajima, T.S., Honda, T., Ando, Y., Ishiguro, K., and Watanabe, Y. (2010). Phosphorylation of mammalian Sgo2 by Aurora B recruits PP2A and MCAK to centromeres. Genes Dev *24*, 2169-2179.
Tanno, Y., Susumu, H., Kawamura, M., Sugimura, H., Honda, T., and Watanabe, Y. (2015). The inner centromere-shugoshin network prevents chromosomal instability. Science *349*, 1237-1240.
Tedeschi, A., Wutz, G., Huet, S., Jaritz, M., Wuensche, A., Schirghuber, E., Davidson, I.F., Tang, W., Cisneros, D.A., Bhaskara, V*., et al.* (2013). Wapl is an essential regulator of chromatin structure and chromosome segregation. Nature *501*, 564-568.
Tomkins, D., Hunter, A., and Roberts, M. (1979). Cytogenetic findings in Roberts-SC phocomelia syndrome(s). Am J Med Genet *4*, 17-26.
Toth, A., Ciosk, R., Uhlmann, F., Galova, M., Schleiffer, A., and Nasmyth, K. (1999). Yeast cohesin complex requires a conserved protein, Eco1p(Ctf7), to establish cohesion between sister chromatids during DNA replication. Genes Dev *13*, 320-333.
Toyoda, Y., and Yanagida, M. (2006). Coordinated requirements of human topo II and cohesin for metaphase centromere alignment under Mad2-dependent spindle checkpoint surveillance. Mol Biol Cell *17*, 2287-2302.
Uhlmann, F., Lottspeich, F., and Nasmyth, K. (1999). Sister-chromatid separation at anaphase onset is promoted by cleavage of the cohesin subunit Scc1. Nature *400*, 37-42.
Uhlmann, F., and Nasmyth, K. (1998). Cohesion between sister chromatids must be established during DNA replication. Curr Biol *8*, 1095-1101.
Uhlmann, F., Wernic, D., Poupart, M.A., Koonin, E.V., and Nasmyth, K. (2000). Cleavage of cohesin by the CD clan protease separin triggers anaphase in yeast. Cell *103*, 375-386.
Uzunova, K., Dye, B.T., Schutz, H., Ladurner, R., Petzold, G., Toyoda, Y., Jarvis, M.A., Brown, N.G., Poser, I., Novatchkova, M*., et al.* (2012). APC15

mediates CDC20 autoubiquitylation by APC/C(MCC) and disassembly of the mitotic checkpoint complex. Nat Struct Mol Biol *19*, 1116-1123.
Vagnarelli, P., Morrison, C., Dodson, H., Sonoda, E., Takeda, S., and Earnshaw, W.C. (2004). Analysis of Scc1-deficient cells defines a key metaphase role of vertebrate cohesin in linking sister kinetochores. EMBO Rep *5*, 167-171.
van der Lelij, P., Chrzanowska, K.H., Godthelp, B.C., Rooimans, M.A., Oostra, A.B., Stumm, M., Zdzienicka, M.Z., Joenje, H., and de Winter, J.P. (2010). Warsaw breakage syndrome, a cohesinopathy associated with mutations in the XPD helicase family member DDX11/ChlR1. Am J Hum Genet *86*, 262-266.
Vass, S., Cotterill, S., Valdeolmillos, A.M., Barbero, J.L., Lin, E., Warren, W.D., and Heck, M.M. (2003). Depletion of Drad21/Scc1 in Drosophila cells leads to instability of the cohesin complex and disruption of mitotic progression. Curr Biol *13*, 208-218.
Vazquez-Novelle, M.D., and Petronczki, M. (2010). Relocation of the chromosomal passenger complex prevents mitotic checkpoint engagement at anaphase. Curr Biol *20*, 1402-1407.
Vazquez-Novelle, M.D., Sansregret, L., Dick, A.E., Smith, C.A., McAinsh, A.D., Gerlich, D.W., and Petronczki, M. (2014). Cdk1 inactivation terminates mitotic checkpoint surveillance and stabilizes kinetochore attachments in anaphase. Curr Biol *24*, 638-645.
Verni, F., Gandhi, R., Goldberg, M.L., and Gatti, M. (2000). Genetic and molecular analysis of wings apart-like (wapl), a gene controlling heterochromatin organization in Drosophila melanogaster. Genetics *154*, 1693-1710.
Waizenegger, I., Gimenez-Abian, J.F., Wernic, D., and Peters, J.M. (2002). Regulation of human separase by securin binding and autocleavage. Curr Biol *12*, 1368-1378.
Waizenegger, I.C., Hauf, S., Meinke, A., and Peters, J.M. (2000). Two distinct pathways remove mammalian cohesin from chromosome arms in prophase and from centromeres in anaphase. Cell *103*, 399-410.
Warren, W.D., Steffensen, S., Lin, E., Coelho, P., Loupart, M., Cobbe, N., Lee, J.Y., McKay, M.J., Orr-Weaver, T., Heck, M.M.*, et al.* (2000). The Drosophila RAD21 cohesin persists at the centromere region in mitosis. Curr Biol *10*, 1463-1466.
Watrin, E., Schleiffer, A., Tanaka, K., Eisenhaber, F., Nasmyth, K., and Peters, J.M. (2006). Human Scc4 is required for cohesin binding to chromatin, sister-chromatid cohesion, and mitotic progression. Curr Biol *16*, 863-874.

Weber, S.A., Gerton, J.L., Polancic, J.E., DeRisi, J.L., Koshland, D., and Megee, P.C. (2004). The kinetochore is an enhancer of pericentric cohesin binding. PLoS Biol *2*, E260.
Webster, A., and Schuh, M. (2016). Mechanisms of Aneuploidy in Human Eggs. Trends Cell Biol.
Weitzer, S., Lehane, C., and Uhlmann, F. (2003). A model for ATP hydrolysis-dependent binding of cohesin to DNA. Curr Biol *13*, 1930-1940.
Woodman, J., Fara, T., Dzieciatkowska, M., Trejo, M., Luong, N., Hansen, K.C., and Megee, P.C. (2014). Cell cycle-specific cleavage of Scc2 regulates its cohesin deposition activity. Proc Natl Acad Sci U S A *111*, 7060-7065.
Yaakov, G., Thorn, K., and Morgan, D.O. (2012). Separase biosensor reveals that cohesin cleavage timing depends on phosphatase PP2A(Cdc55) regulation. Dev Cell *23*, 124-136.
Yamagishi, Y., Honda, T., Tanno, Y., and Watanabe, Y. (2010). Two histone marks establish the inner centromere and chromosome bi-orientation. Science *330*, 239-243.
Ye, A.A., Cane, S., and Maresca, T.J. (2016). Chromosome biorientation produces hundreds of piconewtons at a metazoan kinetochore. Nat Commun *7*, 13221.
Zielinska, A.P., Holubcova, Z., Blayney, M., Elder, K., and Schuh, M. (2015). Sister kinetochore splitting and precocious disintegration of bivalents could explain the maternal age effect. Elife *4*, e11389.
Zou, H., McGarry, T.J., Bernal, T., and Kirschner, M.W. (1999). Identification of a vertebrate sister-chromatid separation inhibitor involved in transformation and tumorigenesis. Science *285*, 418-422.

Introduction 1.2

Guardians of Mitotic Symmetry

The symmetry of genome segregation is fundamental for successful mitosis. Disturbance of mitotic symmetry leads to aneuploidy, a phenomenon where the genome is unequal in two daughter cells. Aneuploidy is a hallmark of cancer and multiple developmental disorders, with a high fitness cost for the cell, often resulting in cell death. Aneuploidy and its consequences will be reviewed in the section 1.3 of the introduction.

A dividing cell has multiple ways of monitoring that symmetrical genome segregation takes place. There are intricate mechanisms ensuring that cohesin cleavage and anaphase separation of chromatids can happen only when chromosomes are correctly aligned and bioriented on the metaphase plane. For this to happen, the two main processes of chromosome congression and separation need to be placed in a chronologically conditional relationship. First, chromosomal congression must take place, a process of chromosome transport to the spindle mid-zone, and their capture by the spindle from each pole, in a symmetric, bioriented manner. Following this process is chromosome separation, marked by cohesin cleavage and movement of single chromatids to the poles, finalized by mitotic exit and nuclear envelope reformation. Correct chromosome congression and alignment must precede separation and mitotic exit; otherwise, mitotic errors are imminent.

Different biological systems have different ways of giving the cell enough time to properly align its chromosomes in order to guarantee mitotic fidelity. Across most metazoans, the Spindle

Assembly Checkpoint (SAC) plays a fundamental role in regulating mitotic timing and allowing for proper chromosome congression and biorientation. The SAC is a complex mechanism which effectively acts as a mitotic break, halting the onset of anaphase until everything is ready.

The first experiments which postulated that there is some kind of mechanism that delays mitotic progression when chromosome-spindle interactions are perturbed were done almost fifty years ago (Nicklas and Koch, 1969; Zirkle, 1970).

The Spindle Assembly checkpoint was further characterized in budding yeast screens for spindle poisons, where it was observed that yeast cells in which the spindle was depolymerized would delay cell cycle progression an accumulate in mitosis (Li and Murray, 1991; Rieder and Palazzo, 1992). Further genetic screens identified the genes responsible for the mitotic arrest in the absence of the spindle in vertebrates (Li and Benezra, 1996).

Since then, the Spindle Assembly checkpoint has been intensely studied for decades, and most of its molecular framework is characterized and somewhat defined (Reviewed in Lara-Gonzalez et al., 2012; Musacchio and Salmon, 2007). What we know today is that the “Spindle Assembly Checkpoint”, is a misnomer, as the checkpoint does not sense “spindle assembly”, but reacts to the presence of unattached chromosomes during mitosis.

The main source of active SAC signaling is the unattached kinetochore. The kinetochore is a complex molecular machinery consisting of hundreds of proteins, which serves as the point of interaction between the mitotic spindle and the chromosome. Centromere is the basis for the formation of the kinetochore.

Centromeres are marked by CENP-A deposition, which is epigenetically inherited from one generation to another(Black and Cleveland, 2011). At the unattached kinetochore, a cascade of molecular events is needed in order to mount the SAC response. The core components participating in the SAC initiation are the kinases: Bub, BubR1 and Mps 1. The exact chronology of steps by which the initial SAC response is mounted is not completely understood.

The initial activities of Bub and Mps1 kinases result in Mad1 recruitment and phosphorylation (London and Biggins, 2014). Phosphorylated Mad1 serves as a scaffold for recruitment of Mad2 and enables conversion of MAD2 from an open (O-Mad2), to an active, closed protein form: C-Mad2 (De Antoni et al., 2005; Luo et al., 2002). Alongside C-Mad2, three other factors are recruited to the kinetochore: BUBR1, Bub3 and CDC20. Together, they are assembled into a diffusible complex made called the MCC (Mitotic Checkpoint Complex), which is the effector of the Spindle Assembly Checkpoint (Chao et al., 2012).

The formation of MCC at the kinetochore is a quick and dynamic process, and was thought to be amazingly efficient. Early studies in which laser ablation was used to detach a single chromosome during mitosis postulated that only one unattached kinetochore can generate enough SAC signaling to delay an entire cell in mitosis for a long period of time (Rieder et al., 1995) Together with the discovery of the kinetochore's ability to catalyze O-Mad2 to C-Mad2 conversion, this lead to an "all or nothing" model of the SAC, where a single unaligned chromosome was thought to act as a "red light" for mitotic progression (Rieder et al., 1995).

Only within last five years, conclusive studies demonstrated that one signaling kinetochore is not SAC “saturating”, and that the efficiency of MCC production is directly proportional to the number of unattached kinetochores in SAC-arrested cells (Collin et al., 2013; Dick and Gerlich, 2013).

After being assembled at the unattached kinetochore, the MCC diffuses through the mitotic cytosol where it acts as an inhibitor of the Anaphase Promoting Complex (APC/C), previously discussed in the Introduction 1.1 and reviewed in (Sivakumar and Gorbsky, 2015). The APC/C is an E3 ubiquitin ligase, whose ubiquitination activity is strictly regulated during mitosis. The MCC acts as an inhibitor of APC/C in a twofold manner. Firstly, the MCC binds and sequesters Cdc20, which is the key factor needed for the ubiquitination activity of the APC, secondly, the MCC complex itself docks on the APC and inhibits free Cdc20 binding(Izawa and Pines, 2015).

The possible reason to why the inhibition of APC/C is so tightly regulated is because APC/C activation marks the onset of anaphase, which results in cohesin cleavage and mitotic exit, representing the point of no return for the dividing cell.

When APC/C is coupled to Cdc20 it has the ability to ubiquitinate Securin and target it for degradation by the proteasome. This releases Separase from inhibition (Reviewed in 1.1), resulting in the cleavage of the kleisin subunit of Cohesin, allowing for chromosome separation to take place.

On the other hand, APC/C-Cdc20 has the ability to directly target Cyclin B for ubiquitination and degradation(Hershko, 1996). Without the functional Cyclin B subunit, the Cdk1-Cyclin B complex

is rendered inactive, allowing for the phosphatases to revert mitotic phosphorylation invoked by this complex, resulting in mitotic exit (Visconti et al., 2013).

The exact mechanism by which the SAC is generated at the kinetochore and its very nature has been a topic of debate for decades.

The very first experiments of Nicklas (Nicklas and Koch, 1969), where performed by mechanical tweezers, used to misalign chromosomes during grasshopper spermatocyte meiosis. This resulted in a mitotic delay. Many following studies noted that disruptions of microtubule-kinetochore interactions by the loss of proper spindle rigidity and tension also caused a mitotic delay. Therefore, a big question in the field became if the SAC senses the lack of chromosome attachment, or a perturbed tension state on the chromosomes?

This conundrum arose from the studies where the spindle was perturbed in a manner that would influence the tension between the chromosomes and the spindle, but supposedly, not the attachment state at the kinetochore (Biggins and Murray, 2001; Hardwick et al., 1996)

Today we know that this debate was framed in a wrong manner, mostly akin to the “Which came first, the chicken or the egg?” type of debate. The SAC itself is a downstream process, a direct result of the absence of chromosome-microtubule interactions, which are regulated by other mechanisms; and although these mechanisms *technically* do not belong to the “SAC”, are functionally and fundamentally inseparable from it.

Such are the error correction mechanisms of the mitotic cell, whose principal effector is the Chromosomal Passenger Complex (CPC) consisting of Survivin, Borealin, INCENP and Aurora B (Reviewed in (Carmena et al., 2012) The main active component of the CPC is the Aurora B kinase, a kinase with the breath of effect similar to the one of Cdk1-Cyclin B during mitosis. Aurora B is involved in many processes, including chromosome condensation, error correction, checkpoint function, cytokinesis, through the phosphorylation of numerous mitotic substrates. The main function of Aurora B that will be discussed here is the one related to the SAC generation and error correction activity at the kinetochore(Biggins et al., 1999).

Aurora B is required for the SAC response if the tension between the chromosome and the spindle is impaired (Biggins and Murray, 2001). One of these tension-impaired states is the premature loss of cohesin (Mirkovic et al., 2015). Studies where Aurora B function was impaired by RNAi identified it as a tension sensor at the kinetochore which allows for metaphase formation (Adams et al., 2001) Aurora B plays the role of error correction by sensing incorrect chromosome attachments which do not result in chromosome bi-orientation; such is the case with merotelic and syntelic attachments. Error correction of aberrant attachments is done through the phosphorylation of outer kinetochore proteins by Aurora B (Reviewed in (Lampson and Cheeseman, 2011). Aurora B has the ability to phosphorylate Ndc80/Hec1 and KNL1, key kinetochore components for microtubule attachment stability. Once phosphorylated, these kinetochore components change microtubule binding affinity, resulting in a catastrophe of the

adjacent microtubule fiber. This in return liberates the kinetochore from attachment and allows for SAC signal generation.

The way in which Aurora B activity senses tension seems to be dependent on the distance between Aurora and its kinetochore substrate (Liu et al., 2009). The bulk of Aurora B is localized at the inner centromere during mitosis. Aurora B localization is dependent on two phosphorylation marks and their intersection at the inner chromatin, deposited by two kinases: Haspin and Bub (Yamagishi et al., 2010). Haspin is a cohesin associated kinase, which phosphorylates the H3TH histone mark. Bub kinase, on the other hand, phosphorylates HS120. Studies demonstrate that the CPC complex is localized to the inner centromere at the intersection of these two marks in human cells. The relationship between cohesion and the inner centromere, as well as cohesin and Aurora B recruitment is described in more detail in *Introduction 1.1- Cohesin and the inner centromere network.*

The positioning of Aurora B in between the two kinetochores is critical in our understanding of tension sensing. It is thought that during metaphase, when the centromeres are being pulled to the opposite poles while still being bound by cohesin, the stretching provided is enough to distance Aurora B away from its substrate (Liu et al., 2009)This physical model assumes that the destabilizing activity of Aurora B is conveyed by the pool located in between the two centromeres. Therefore, the “tension” sensed would be the distance between the inner centromere Aurora B pool and the outer kinetochore substrates. This leads us to another conundrum present in the field.

What is the location and nature of tension that is being sensed by the error correction machinery? The canonical model implies inter-kinetochore tension, which is the consequence of centromeric chromatin stretching under the forces exerted by the metaphase spindle(Shelby et al., 1996). This is an interesting model, but not quite in tune with the kinetochore “breathing”, a phenomenon of oscillatory motion of kinetochores observed in the metaphase cells (Jaqaman et al., 2010). Interestingly, during metaphase, chromatin acts like an elastic spring, implying that maintaining stable attachments in these oscillating conditions would be a difficult task, if the inter-centromere tension was the only readout. Furthermore, what is clearly evident from live imaging is that not only that the distance between the centromeres is increased during the biorientation, but the very architecture attached kinetochore changes and stretches. This Intrakinetochore stretch was implicated in SAC silencing during metaphase (Maresca and Salmon, 2009; Uchida et al., 2009)

The Intrakinetochore stretch measurements are done by taking advantage of the kinetochore size, and differentially labeling molecules that are closer to the attachment site (outer kinetochore), and ones anchoring the kinetochore to the chromatin (inner kinetochore). These studies clearly displayed that the distance between inner and outer kinetochore increases during metaphase biorientation. This lead to the classification of a new kind of tension called the Intrakinetochore tension(Maresca and Salmon, 2010). Therefore it is important to understand which kind of tension satisfies Aurora B, and results in SAC silencing: “inter” or “intra” kinetochore tension? (Reviewed in (Khodjakov and Pines, 2010)

Reinforcing the intra-kinetochore stretch argument , experiments in which the kinetochores from the same chromosome were tethered to each other, and unable to stretch during the metaphase displayed normal mitotic progression (Nannas and Murray, 2014), showing that the error correction can be satisfied without the increase of the distance between the centromere pair. However, the interpretation of these experiments is somewhat ambiguous, as tethering still creates a rigid force connecting the two opposing kinetochores, and the Intrakinetochore stretch might me directly dependent on the interkinetochore rigidity and tension.

On the opposite end of the spectrum, studies in which kinetochores are separated and inter-kinetochore tension is completely eliminated via cohesin cleavage or replication inhibition provided different conclusions. If kinetochore pairs are separated, the spindle still interacts with isolated single kinetochores, but these interactions are unstable, and highly erroneous to say the least. The only way to stabilize interactions is tough the inhibition or decay of normal error correction activity (Drpic et al., 2015; Mirkovic et al., 2015; O'Connell et al., 2008).

In addition, experiments with Eg5 inhibitors like Monastrol, where cells form monopolar spindles, and chromosomes can only from syntelic attachments, result in robust SAC activation. This further validates that not any kind of kinetochore-spindle interaction can satisfy the SAC , bipolarity is required (Brito et al., 2008)

Therefore, both *intra* and *inter* kinetochore tension are able to satisfy the error correction to a certain degree, but not in complete absence of one another. As is usually the case, the answer to the conundrum goes far beyond the simple “either/or” question.

Aurora B and the CPC activity are far from being the only mechanisms regulating kinetochore-microtubule stability. The polymerization and dynamics of microtubules themselves change under tension and during mitosis. In vitro essays in which the extending microtubules were allowed to bind to a “kinetochore” attached to a substrate, therefore generating tension, decreased their rate of de-polymerization and catastrophe(Akiyoshi et al., 2010). Furthermore, the activity of mitotic Cyclins A and B are implicated in microtubule dynamics and stability (Kabeche and Compton, 2013; Ookata et al., 1995).

Therefore, tension sensing at the kinetochore is regulated in a complex and intricate manner, probably depending on intra kinetochore architecture changes, as well as elastic stretching of the inter kinetochore chromatin.

Now, after having described how error correction senses tension defects and contributes to their de-stabilization of erroneous attachments, we can go back to the original question of whether the SAC on its own can sense tension defects.

The most likely answer is no. Recent elegant studies put a nail in the coffin to the tension-SAC model, by utilizing Hec1 (NDC 80) alanine mutants that are resistant to Aurora B mediated phosphorylation, and therefore, CPC-mediated error correction. The authors of these studies then incubated the Hec1 alanine mutants in Monastrol, a drug resulting formation of monopolar mitotic spindles. This leads to accumulation of aberrant, yet stable kinetochore-microtubule attachments, which cannot generate normal tension. No additional SAC signal was generated in this situation, proving that attachment is enough to prevent SAC

signaling in the absence of proper tension (Etemad et al., 2015; Tauchman et al., 2015).

However, in the context of physiological mitosis, the SAC and the error correction mechanisms are inseparable. The unattached kinetochore is the generator of the SAC signal, but in the presence of the spindle, the only way to generate the unattached kinetochore is through the action of the error correction. Microtubule dynamics are measured in milliseconds, while an average metazoan mitosis lasts for tens of minutes. As such, the only physiological way of generating a “wait for anaphase” signal in the presence of an active spindle is trough constitutive action of the error correction machinery.

In summary, the error correction and the SAC are the two main guardians of mitotic symmetry. They are fundamental for congression, biorientation and timely anaphase onset, and as such represent the two pillars of accurate genome segregation.

Therefore, it would seem completely unimaginable that any dividing organism could function without a SAC. However, SAC mutants are viable in *S.cerevisiae, D.melanogaster* and *C.elegans* (Buffin et al., 2007; Kitagawa and Rose, 1999; Li and Murray, 1991). This does not mean that the checkpoint is redundant, but rather replaceable in “ideal” conditions, such are the ones in the laboratory. Perturbing these conditions resulted in lower fitness and aneuploidy in organisms without the SAC (Buffin et al., 2007).

This draws a very interesting distinction mentioned at the beginning of this introduction. Most metazoans require SAC to buy time for proper chromosome capture, but some can obviously do quite fine without it. Why is this case? It seems that the distinction might lie in

the kinetics of Cyclin B degradation in mitosis. In vertebrates, if SAC is inhibited, mitotic exit takes place far before normal anaphase timing (Liu et al., 2003; Meraldi et al., 2004), resulting in miss-segregation and aneuploidy. In *Drosophila* however, this difference is quite mild, as mutants for SAC in the Neuroblast undergo mitosis about one minute faster than the control (Buffin et al., 2007). Therefore, the efficiency of mitosis in *D.melanogaster*, and *C.elegans* which contain four and six chromosomes respectively might not require additional time, and SAC might be relegated to a "seat belt" function: present in all situations, but useful only in the case of the crash.

Recently, new studies have started to shed the light on other mitotic "breaks" that might work independently of the SAC. For instance, hipomorphic Aurora A mutants in *Drosophila* Neuroblasts undergo a mitotic delay even when placed in a Mad2 mutant background (Caous et al., 2015). In fission yeast, Shugoshin seems to be implicated in generating a mitotic delay that is SAC independent (Meadows et al., 2017). And while most of the SAC community is investing immense power of *in vitro* approaches, coupled to finest structural biology and large scale "-omics" to sort out the finest kinks of conventional SAC mechanisms, more interesting things might be hiding in plain sight

References

Adams, R.R., Maiato, H., Earnshaw, W.C., and Carmena, M. (2001). Essential roles of Drosophila inner centromere protein (INCENP) and aurora B in histone H3 phosphorylation, metaphase chromosome alignment, kinetochore disjunction, and chromosome segregation. J Cell Biol *153*, 865-880.

Akiyoshi, B., Sarangapani, K.K., Powers, A.F., Nelson, C.R., Reichow, S.L., Arellano-Santoyo, H., Gonen, T., Ranish, J.A., Asbury, C.L., and Biggins, S. (2010). Tension directly stabilizes reconstituted kinetochore-microtubule attachments. Nature *468*, 576-579.

Biggins, S., and Murray, A.W. (2001). The budding yeast protein kinase Ipl1/Aurora allows the absence of tension to activate the spindle checkpoint. Genes Dev *15*, 3118-3129.

Biggins, S., Severin, F.F., Bhalla, N., Sassoon, I., Hyman, A.A., and Murray, A.W. (1999). The conserved protein kinase Ipl1 regulates microtubule binding to kinetochores in budding yeast. Genes Dev *13*, 532-544.

Black, B.E., and Cleveland, D.W. (2011). Epigenetic centromere propagation and the nature of CENP-a nucleosomes. Cell *144*, 471-479.

Brito, D.A., Yang, Z., and Rieder, C.L. (2008). Microtubules do not promote mitotic slippage when the spindle assembly checkpoint cannot be satisfied. J Cell Biol *182*, 623-629.

Buffin, E., Emre, D., and Karess, R.E. (2007). Flies without a spindle checkpoint. Nat Cell Biol *9*, 565-572.

Caous, R., Pascal, A., Rome, P., Richard-Parpaillon, L., Karess, R., and Giet, R. (2015). Spindle assembly checkpoint inactivation fails to suppress neuroblast tumour formation in aurA mutant Drosophila. Nat Commun *6*, 8879.

Carmena, M., Wheelock, M., Funabiki, H., and Earnshaw, W.C. (2012). The chromosomal passenger complex (CPC): from easy rider to the godfather of mitosis. Nat Rev Mol Cell Biol *13*, 789-803.

Chao, W.C., Kulkarni, K., Zhang, Z., Kong, E.H., and Barford, D. (2012). Structure of the mitotic checkpoint complex. Nature *484*, 208-213.

Collin, P., Nashchekina, O., Walker, R., and Pines, J. (2013). The spindle assembly checkpoint works like a rheostat rather than a toggle switch. Nat Cell Biol *15*, 1378-1385.

De Antoni, A., Pearson, C.G., Cimini, D., Canman, J.C., Sala, V., Nezi, L., Mapelli, M., Sironi, L., Faretta, M., Salmon, E.D*., et al.* (2005). The Mad1/Mad2 complex as a template for Mad2 activation in the spindle assembly checkpoint. Curr Biol *15*, 214-225.

Dick, A.E., and Gerlich, D.W. (2013). Kinetic framework of spindle assembly checkpoint signalling. Nat Cell Biol *15*, 1370-1377.
Drpic, D., Pereira, A.J., Barisic, M., Maresca, T.J., and Maiato, H. (2015). Polar Ejection Forces Promote the Conversion from Lateral to End-on Kinetochore-Microtubule Attachments on Mono-oriented Chromosomes. Cell Rep *13*, 460-469.
Etemad, B., Kuijt, T.E., and Kops, G.J. (2015). Kinetochore-microtubule attachment is sufficient to satisfy the human spindle assembly checkpoint. Nat Commun *6*, 8987.
Hardwick, K.G., Weiss, E., Luca, F.C., Winey, M., and Murray, A.W. (1996). Activation of the budding yeast spindle assembly checkpoint without mitotic spindle disruption. Science *273*, 953-956.
Hershko, A. (1996). Mechanisms and regulation of ubiquitin-mediated cyclin degradation. Adv Exp Med Biol *389*, 221-227.
Izawa, D., and Pines, J. (2015). The mitotic checkpoint complex binds a second CDC20 to inhibit active APC/C. Nature *517*, 631-634.
Jaqaman, K., King, E.M., Amaro, A.C., Winter, J.R., Dorn, J.F., Elliott, H.L., McHedlishvili, N., McClelland, S.E., Porter, I.M., Posch, M.*, et al.* (2010). Kinetochore alignment within the metaphase plate is regulated by centromere stiffness and microtubule depolymerases. J Cell Biol *188*, 665-679.
Kabeche, L., and Compton, D.A. (2013). Cyclin A regulates kinetochore microtubules to promote faithful chromosome segregation. Nature *502*, 110-113.
Khodjakov, A., and Pines, J. (2010). Centromere tension: a divisive issue. Nat Cell Biol *12*, 919-923.
Kitagawa, R., and Rose, A.M. (1999). Components of the spindle-assembly checkpoint are essential in Caenorhabditis elegans. Nat Cell Biol *1*, 514-521.
Lampson, M.A., and Cheeseman, I.M. (2011). Sensing centromere tension: Aurora B and the regulation of kinetochore function. Trends Cell Biol *21*, 133-140.
Lara-Gonzalez, P., Westhorpe, F.G., and Taylor, S.S. (2012). The spindle assembly checkpoint. Curr Biol *22*, R966-980.
Li, R., and Murray, A.W. (1991). Feedback control of mitosis in budding yeast. Cell *66*, 519-531.
Li, Y., and Benezra, R. (1996). Identification of a human mitotic checkpoint gene: hsMAD2. Science *274*, 246-248.
Liu, D., Vader, G., Vromans, M.J., Lampson, M.A., and Lens, S.M. (2009). Sensing chromosome bi-orientation by spatial separation of aurora B kinase from kinetochore substrates. Science *323*, 1350-1353.

Liu, S.T., Hittle, J.C., Jablonski, S.A., Campbell, M.S., Yoda, K., and Yen, T.J. (2003). Human CENP-I specifies localization of CENP-F, MAD1 and MAD2 to kinetochores and is essential for mitosis. Nat Cell Biol *5*, 341-345.
London, N., and Biggins, S. (2014). Mad1 kinetochore recruitment by Mps1-mediated phosphorylation of Bub1 signals the spindle checkpoint. Genes Dev *28*, 140-152.
Luo, X., Tang, Z., Rizo, J., and Yu, H. (2002). The Mad2 spindle checkpoint protein undergoes similar major conformational changes upon binding to either Mad1 or Cdc20. Mol Cell *9*, 59-71.
Maresca, T.J., and Salmon, E.D. (2009). Intrakinetochore stretch is associated with changes in kinetochore phosphorylation and spindle assembly checkpoint activity. J Cell Biol *184*, 373-381.
Maresca, T.J., and Salmon, E.D. (2010). Welcome to a new kind of tension: translating kinetochore mechanics into a wait-anaphase signal. J Cell Sci *123*, 825-835.
Meadows, J.C., Lancaster, T.C., Buttrick, G.J., Sochaj, A.M., Messin, L.J., Del Mar Mora-Santos, M., Hardwick, K.G., and Millar, J.B.A. (2017). Identification of a Sgo2-Dependent but Mad2-Independent Pathway Controlling Anaphase Onset in Fission Yeast. Cell Rep *18*, 1422-1433.
Meraldi, P., Draviam, V.M., and Sorger, P.K. (2004). Timing and checkpoints in the regulation of mitotic progression. Dev Cell *7*, 45-60.
Mirkovic, M., Hutter, L.H., Novak, B., and Oliveira, R.A. (2015). Premature Sister Chromatid Separation Is Poorly Detected by the Spindle Assembly Checkpoint as a Result of System-Level Feedback. Cell Rep *13*, 470-478.
Musacchio, A., and Salmon, E.D. (2007). The spindle-assembly checkpoint in space and time. Nat Rev Mol Cell Biol *8*, 379-393.
Nannas, N.J., and Murray, A.W. (2014). Tethering sister centromeres to each other suggests the spindle checkpoint detects stretch within the kinetochore. PLoS Genet *10*, e1004492.
Nicklas, R.B., and Koch, C.A. (1969). Chromosome micromanipulation. 3. Spindle fiber tension and the reorientation of mal-oriented chromosomes. J Cell Biol *43*, 40-50.
O'Connell, C.B., Loncarek, J., Hergert, P., Kourtidis, A., Conklin, D.S., and Khodjakov, A. (2008). The spindle assembly checkpoint is satisfied in the absence of interkinetochore tension during mitosis with unreplicated genomes. J Cell Biol *183*, 29-36.
Oliveira, R.A., Kotadia, S., Tavares, A., Mirkovic, M., Bowlin, K., Eichinger, C.S., Nasmyth, K., and Sullivan, W. (2014). Centromere-independent accumulation of cohesin at ectopic heterochromatin sites induces chromosome stretching during anaphase. PLoS Biol *12*, e1001962.
Ookata, K., Hisanaga, S., Bulinski, J.C., Murofushi, H., Aizawa, H., Itoh, T.J., Hotani, H., Okumura, E., Tachibana, K., and Kishimoto, T. (1995). Cyclin B

interaction with microtubule-associated protein 4 (MAP4) targets p34cdc2 kinase to microtubules and is a potential regulator of M-phase microtubule dynamics. J Cell Biol *128*, 849-862.
Rieder, C.L., Cole, R.W., Khodjakov, A., and Sluder, G. (1995). The checkpoint delaying anaphase in response to chromosome monoorientation is mediated by an inhibitory signal produced by unattached kinetochores. J Cell Biol *130*, 941-948.
Rieder, C.L., and Palazzo, R.E. (1992). Colcemid and the mitotic cycle. J Cell Sci *102 (Pt 3)*, 387-392.
Shelby, R.D., Hahn, K.M., and Sullivan, K.F. (1996). Dynamic elastic behavior of alpha-satellite DNA domains visualized in situ in living human cells. J Cell Biol *135*, 545-557.
Sivakumar, S., and Gorbsky, G.J. (2015). Spatiotemporal regulation of the anaphase-promoting complex in mitosis. Nat Rev Mol Cell Biol *16*, 82-94.
Tauchman, E.C., Boehm, F.J., and DeLuca, J.G. (2015). Stable kinetochore-microtubule attachment is sufficient to silence the spindle assembly checkpoint in human cells. Nat Commun *6*, 10036.
Uchida, K.S., Takagaki, K., Kumada, K., Hirayama, Y., Noda, T., and Hirota, T. (2009). Kinetochore stretching inactivates the spindle assembly checkpoint. J Cell Biol *184*, 383-390.
Visconti, R., Palazzo, L., Pepe, A., Della Monica, R., and Grieco, D. (2013). The end of mitosis from a phosphatase perspective. Cell Cycle *12*, 17-19.
Yamagishi, Y., Honda, T., Tanno, Y., and Watanabe, Y. (2010). Two histone marks establish the inner centromere and chromosome bi-orientation. Science *330*, 239-243.
Zirkle, R.E. (1970). Ultraviolet-microbeam irradiation of newt-cell cytoplasm: spindle destruction, false anaphase, and delay of true anaphase. Radiat Res *41*, 516-537.

1.3. Aneuploidy and its consequences

Aneuploidy is a state of chromosome imbalance in the cell, where chromosome number or composition is different from the canonical *2n,* haploid or polyploid karyotype. Aneuploidy can also be "segmental". This is the case when the cell contains an imbalance in certain chromosomal loci.

Aneuploidy has been observed over a century ago by Theodor Boveri in sea urchin embryos. The experiments he conducted included urchin eggs that were fertilized by two sperm simultaneously, resulting in the presence of multiple centrosomes and formation of multipolar spindles .This leads to mitotic errors and genome imbalance in the developing urchin embryo.

In the next few years, Boveri started hypothesizing about the origins of tumorigenesis which resulted in publication of his book "*Concerning the origin of malignant tumors"* in 1914 which postulated that the aneuploidy is a causative event for malignancy (Boveri, 2008; Hansford and Huntsman, 2014).

Today we know that aneuploidy is a hallmark of cancer and common in developmental disorders, frequently resulting in miscarriage (Hassold and Hunt, 2001; Santaguida and Amon, 2015). As such, it has been profusely studied for decades, through numerous different approaches. Unfortunately, studying aneuploidy is very akin to studying cancer. To quote Leo Tolstoy ""All happy families are alike; each unhappy family is unhappy in its own way." Same can be said for aneuploid cells. Every euploid cell is functional; each aneuploid cell is perturbed in its own way. For organisms that carry their genome over multiple chromosomes,

there can be thousands to billions of combinations of possible aneuploid karyotypes(Zhu et al., 2018).

Furthermore, contributing to this aneuploid “individuality” is the fact that chromosome imbalance causes disruption in hundreds if not thousands of genes simultaneously, causing complete havoc in multiple signaling networks and resulting in a general stress response. This large scale network disruption can lead to diverse phenotypic outcomes, even in aneuploid cells of the same karyotype (Beach et al., 2017).

The general stress responses associated with aneuploidy might be the only conclusive features arising from decades of studying it. There is general stress response to genome imbalance, independent of the aneuploid karyotype (Reviewed in (Santaguida and Amon, 2015; Zhu et al., 2018). This is due to the fact that chromosome numbers different than *2n* result in two of the following outcomes at the transcript, and then at the protein level: either the cell has too much of X, or the cell has too little of X.

The only way to compensate for genome imbalance would be some sort of chromosomal “buffering”, a phenomenon where copy number of a gene is perturbed, but the protein and transcript content stays relatively similar to the wild-type situation. This phenomenon is common in sex chromosomes, as organisms have evolved tools of compensating the for copy number difference between the sexes either by overexpression or inhibition; however, in autosomes, chromosomal buffering is controversial and has been a subject of much dispute (Gasch et al., 2016; Hose et al., 2015; Torres et al., 2016).

In the case of whole-chromosome aneuploidy, genetic imbalance inevitably results in protein imbalance and severe strain for the protein quality machinery of the cell (Donnelly and Storchova, 2015; Oromendia et al., 2012; Torres et al., 2010).

In this case, chromosome loss can either cause the loss or downregulation of proteins necessary for proper protein folding and quality control, or chromosome gain can cause protein overexpression and overload for the protein quality control machinery. Gene imbalance can disrupt multimeric protein complexes coded on different chromosomes, which need the product from both copies to be in a defined stoichiometry in order to function.

Yeast and mammalian aneuploid cells exhibit upregulation of heat shock proteins (Aivazidis et al., 2017; Torres et al., 2007). Heat shock proteins belong to the chaperone family, and aid in proper protein folding and maturation, as well as protection in the time of stress. Another important factor for protein homeostasis is the ubiquitin machinery required for protein targeting for degradation by the proteasome. Ubiquitination has been observed to be upregulated in cells isolated from Down's Syndrome patients (Engidawork and Lubec, 2001), also, aneuploid yeast mutants that exhibited improved ubiquitination capability had higher proliferation rates than other aneuploid counterparts (Torres et al., 2010).

Therefore, aneuploidy is associated with severe protein dosage imbalance and general stress for the protein quality control machinery, regardless of the exact karyotype of aneuploidy in question.

As a consequence of different gene copy number and protein imbalance, numerous other processes are affected. Aneuploid cells commonly exhibit metabolic stress response, DNA replication stress, impairment of autophagy, and other stress responses, extensively reviewed in (Santaguida and Amon, 2015; Zhu et al., 2018).

For the purpose of this PhD thesis, some of the more interesting consequences of aneuploidy are mitotic errors and aberrations arising from the aneuploid state. The imbalance in protein stoichiometry caused by aneuploidy likely translates onto mitotic proteins as well, resulting in errors and unpredictable outcomes in terms of genetic material distribution.

This phenomenon of mitotic uncertainty is known as “chromosomal instability”: the possibility of the cell to lose or gain chromosomes due to its impaired mitotic fidelity.

First observations of aneuploid cells undergoing aberrant divisions date from almost forty years ago, where trizomic budding yeast strains were shown to be prone to chromosome loss(Campbell et al., 1981).

Chromosomal instability of aneuploid cells leads to an interesting positive feedback loop: cells becoming chromosomally unbalanced, aneuploid, could generate even more imbalanced genomes in their progeny. This has profound implications on evolution and diversity of aneuploid karyotypes, which are associated with malignancy.

The link between aneuploidy and resulting chromosomal instability has been quite correlational until the last few years. Studies in colorectal tumors and aneuploid lymphocytes showed that these

cells undergo mitosis with a higher frequency of errors (Duesberg et al., 1998; Reish et al., 2006).

Recently, development of new approaches and the advance of live imaging microscopy have led to experimental layouts where aneuploidy is induced in a controlled manner, and its mitotic consequences are traced in real time. One of these studies used an assay in which a single mitotic chromosome was added to the dividing cell, resulting in chromosomal instability and miss-segregation (Passerini et al., 2016). Another study utilized the same approach to generate trizomic cell lines for multiple chromosomes only to find them evolve into complex karyotypes several days later (Sheltzer et al., 2017). Furthermore, another study from the same group in which transient inhibition of the SAC resulted in aneuploid cells has shown that even after the SAC inhibitor has been washed out, the newly aneuploid cells continue dividing in an aberrant manner resulting in segmental and whole chromosome aneuploidies (Santaguida et al., 2017).

These studies point to a self-perpetuating cycle of genome instability: once errors have been made, they can only become worse, resulting in even more genome instability.

We have shortly summarized various heavy stresses associated with aneuploidy, most of them likely stemming from a gene dosage imbalance. However, aneuploidy is often observed in the context of a malignant tumor, whose defining feature is high fitness and proliferative capacity of cells. Also, it has been thought for decades that aneuploidy is widely present in the human organism, ranging from liver cells to adult neurons and hepatocytes, where aneuploidy was thought to confer additional adaptive roles.

On the other hand, aneuploidy has a high fitness cost for the cell, and is associated with developmental disorders such as the Down syndrome and microcephaly, as well as miscarriage or embryonic lethality.

Therefore, it seems that aneuploidy and its effect could be highly dependent of the context and the aneuploid karyotype. Its presence in a certain stage of development, tissue, or a genomic background can lead to the death of a cell or an organism. In a different context, it can result in cell over-proliferation and cancer.

The correlational link between aneuploidy and cancer stems from a simple, undeniable observation: 90% of solid tumors are aneuploid (Weaver and Cleveland, 2006). However, we know today that most tumors also harbor mutations in apoptotic genes which make these transformed cells resistant to almost anything. So the real question is: Is aneuploidy a cause or a consequence that might confer selective advantage, or maybe even simply a side-product of cell immortality?

With the advancement of our knowledge about mitosis, some tools were in place to test these hypotheses. Characterization of the SAC genes, crucial for mitotic fidelity in vertebrates, led to studies in which SAC was impaired in mice to perturb mitosis (Baker et al., 2004; Dai et al., 2004; Michel et al., 2001). Impairment of BubR1 gene dosage led to chromosomal instability, premature ageing and aneuploidy, but not spontaneous cancer genesis (Baker et al., 2004).Another common way of generating aneuploidy in animals or tissue culture became overexpression of Plk4, a protein controlling centrosome amplification (Habedanck et al., 2005). When conducted in mice, Plk4 overexpression was not enough to

spontaneously induce tumorigenesis without being placed in a p53 mutant background (Vitre et al., 2015). However, the same perturbation, if done chronically, for months, was enough to elicit tumorigenesis in multiple affected mouse tissues, without p53 disruption (Levine et al., 2017). The flaw of these studies is that they do not distinguish aneuploidy from p53 loss trough chromosome miss-segregation. The origin of tumors in these experiments could be the clones which had lost apoptotic genes, bringing us back to square one.

Drosophila melanogaster can also be used as a model system for overgrowth/invasiveness; some would even call it a “cancer” model system (Basto et al., 2008; Januschke and Gonzalez, 2008). An interesting *Drosophila* overgrowth assay relies on transplantation of a tissue from a larva to the abdomen of an adult fly. In these assays, the transplant tissue is labeled with a fluorescent tag, enabling growth and invasiveness tracking in the following days (Rossi and Gonzalez, 2015).Although flawed, this system can be extremely useful, as it allows the usage of immense drosophila genetic tool base for the study of invasiveness and overgrowth. Screens combining mitotic perturbations that would induce aneuploidy would not cause overgrowth unless coupled to the inhibition of cell death(Gonzalez, 2013). These results demonstrate that aneuploidy, on its own, is not enough for malignancy; suppression of apoptosis is needed as well. Furthermore, tools that generated trizomic lines in mammalian cells, across multiple chromosomes, observed a large loss of cell fitness and proliferation in malignantly transformed aneuploid cells, when compared to diploid malignant counterparts (Sheltzer et al., 2017).

Therefore, aneuploidy can act as a tumor suppressor(Holland and Cleveland, 2009).

Thus, true adaptive power of aneuploidy likely lays in chromosomal instability which results in karyotype diversification, leading to the rise of malignant clones in certain circumstances.

Knowing the price of aneuploidy, it is interesting to examine if there is any aneuploidy occurring during normal animal development.

Non-metazoan organisms seem to exhibit higher tolerance to aneuploidy, as wild type yeast strains can be aneuploid and successful, and plants as well as some other fungi have a high aneuploidy tolerance (Hose et al., 2015; Zhu et al., 2018). A comparative study of 38 aneuploid yeast strains has shown that while aneuploid yeast grow slower than the diploids in normal conditions, under stress, certain aneuploidies provided a significant growth advantage (Pavelka et al., 2010).

However, in metazoan organisms, aneuploidy tolerance seems to be very low or nonexistent.

Fruit flies for instance, can be triploid and viable, albeit sterile (Bridges, 1921b). However, the loss of whole chromosome is not tolerated in the fruit fly, unless it is the 4^{th} chromosome, which contains a minimal number of genes (Bridges, 1921a). In humans, the only aneuploidy which is known to lead to adult viability is the trisomy of the 21^{st} chromosome, also known as the Down Syndrome, occurring in about 0.1% of live births (de Graaf et al., 2015). All other human aneuploidies result in embryo lethality (Hassold and Hunt, 2001). Therefore, at the level of the whole

metazoan organism, constitutive aneuploidy results in catastrophic outcomes.

However, metazoan organisms are composed of diverse tissues, each containing specific cell profiles and local tissue niches. Could these be conductive to aneuploidy tolerance, otherwise lethal at the level of the entire organism?

A recent comprehensive review on aneuploidy (Zhu et al., 2018), previously cited in this introduction, states : "*Various studies estimated 1-33% of human neurons to be aneuploid and 4-50% of human hepatocytes to be aneuploid"*. Notice the tenfold variance in the bottom and the top number for aneuploidy percentage in the two respective tissues. For decades, Fluorescence *In Situ* Hybridization (FISH) experiments have been used to asses aneuploidy in human tissues. This lead to a wide spread belief that human neurons are frequently aneuploid, some papers even postulating that this aneuploidy promotes neural plasticity (Muotri and Gage, 2006; Rehen et al., 2001). The same was the case with human liver, where FISH karyotyping lead to the conclusion that the liver is composed out of a large portion (50%) of aneuploid hepatocytes, conferring selective advantage (Duncan et al., 2012; Duncan et al., 2010). However, FISH karyotyping is very prone to error, especially in interphase cells, which in human and *drosophila*, tend to cluster homologous genetic loci onto a single location in the nucleus (Wu and Morris, 1999). Recent emergence of single cell sequencing allows for more accurate karyotyping of cell populations from distinct tissues. A study from the Amon lab examined mouse and human tissues by single cell sequencing and found extremely low rates of aneuploidy in the liver and the brain, comparable to the skin (below 1%) (Knouse et al., 2014).

Thus, the likely conclusion is that there is no organ specific niche that would compensate for the high physiological cost of aneuploidy.

The one thing that cannot be emphasized enough is that there is no such thing as an “aneuploidy”, only “aneuploidies”. The major caveat of studying aneuploidy is the fact that we rely on uncontrolled mitotic perturbation to generate it. By doing so, we are unable to “design” an aneuploid karyotype of choice, and rely on randomization of genetic material. Randomization infers individuality, and as previously stated, even aneuploid cells of the same karyotype can display different outcomes (Beach et al., 2017). Studying a random karyotype and hoping to elucidate anything beyond a general stress response is likely in vain. Another problem with the way we currently study aneuploidy is the lack of temporal resolution in tools used to induce aneuploidy in metazoans. As if the genome randomization alone is not enough to obstruct clear observation; a classical way of perturbing mitosis either in cell culture or in a metazoan organism is by chronic disturbance mitotic protein of interest, usually by RNAi or overexpression. This means that not only we are studying a random genome; we are also studying a random genome at a random point in time since it became randomized. What this approach clearly negates is aneuploid evolution and history. As mentioned before, aneuploidy results in accumulation of different stress responses, and complex karyotype evolution. Chronic approaches utilizing non-selective mitotic perturbation do not allow us to dissect the temporal order of each of these events.

Yet, recent advances open exciting new possibilities for the field. Both in yeast and human cells, new assays have been developed

to study aneuploidy of specific chromosomes. In yeast excision of the centromere of a specific chromosome leads to its miss-segregation (Beach et al., 2017). When coupled to a fluorescence marker, this allows for identification of loss of function or gain of function events, and sorting populations of the same aneuploid karyotype which can then can be traced trough time.

Another interesting addition to the field is, a new method of single chromosome introduction in vertebrate cells (Passerini et al., 2016; Sheltzer et al., 2017), which allows for specific chromosome gain of function analysis, in real time.

The next step would be designing inducible metazoan systems, preferably with controlled nature of the aneuploid karyotypes studied. Ideally, aneuploidy induction would also be tissue specific and acute, allowing for temporal resolution of aneuploid events, in a highly physiological context. Some of these efforts will be discussed in Chapter III.

References

Aivazidis, S., Coughlan, C.M., Rauniyar, A.K., Jiang, H., Liggett, L.A., Maclean, K.N., and Roede, J.R. (2017). The burden of trisomy 21 disrupts the proteostasis network in Down syndrome. PLoS One *12*, e0176307.
Baker, D.J., Jeganathan, K.B., Cameron, J.D., Thompson, M., Juneja, S., Kopecka, A., Kumar, R., Jenkins, R.B., de Groen, P.C., Roche, P.*, et al.* (2004). BubR1 insufficiency causes early onset of aging-associated phenotypes and infertility in mice. Nat Genet *36*, 744-749.
Basto, R., Brunk, K., Vinadogrova, T., Peel, N., Franz, A., Khodjakov, A., and Raff, J.W. (2008). Centrosome amplification can initiate tumorigenesis in flies. Cell *133*, 1032-1042.
Beach, R.R., Ricci-Tam, C., Brennan, C.M., Moomau, C.A., Hsu, P.H., Hua, B., Silberman, R.E., Springer, M., and Amon, A. (2017). Aneuploidy Causes Non-genetic Individuality. Cell *169*, 229-242 e221.

Boveri, T. (2008). Concerning the origin of malignant tumours by Theodor Boveri. Translated and annotated by Henry Harris. J Cell Sci *121 Suppl 1*, 1-84.
Bridges, C.B. (1921a). Proof of Non-Disjunction for the Fourth Chromosome of Drosophila Melanogaster. Science *53*, 308.
Bridges, C.B. (1921b). Triploid Intersexes in Drosophila Melanogaster. Science *54*, 252-254.
Campbell, D., Doctor, J.S., Feuersanger, J.H., and Doolittle, M.M. (1981). Differential mitotic stability of yeast disomes derived from triploid meiosis. Genetics *98*, 239-255.
Dai, W., Wang, Q., Liu, T., Swamy, M., Fang, Y., Xie, S., Mahmood, R., Yang, Y.M., Xu, M., and Rao, C.V. (2004). Slippage of mitotic arrest and enhanced tumor development in mice with BubR1 haploinsufficiency. Cancer Res *64*, 440-445.
de Graaf, G., Buckley, F., and Skotko, B.G. (2015). Estimates of the live births, natural losses, and elective terminations with Down syndrome in the United States. Am J Med Genet A *167A*, 756-767.
Donnelly, N., and Storchova, Z. (2015). Causes and consequences of protein folding stress in aneuploid cells. Cell Cycle *14*, 495-501.
Duesberg, P., Rausch, C., Rasnick, D., and Hehlmann, R. (1998). Genetic instability of cancer cells is proportional to their degree of aneuploidy. Proc Natl Acad Sci U S A *95*, 13692-13697.
Duncan, A.W., Hanlon Newell, A.E., Smith, L., Wilson, E.M., Olson, S.B., Thayer, M.J., Strom, S.C., and Grompe, M. (2012). Frequent aneuploidy among normal human hepatocytes. Gastroenterology *142*, 25-28.
Duncan, A.W., Taylor, M.H., Hickey, R.D., Hanlon Newell, A.E., Lenzi, M.L., Olson, S.B., Finegold, M.J., and Grompe, M. (2010). The ploidy conveyor of mature hepatocytes as a source of genetic variation. Nature *467*, 707-710.
Engidawork, E., and Lubec, G. (2001). Protein expression in Down syndrome brain. Amino Acids *21*, 331-361.
Gasch, A.P., Hose, J., Newton, M.A., Sardi, M., Yong, M., and Wang, Z. (2016). Further support for aneuploidy tolerance in wild yeast and effects of dosage compensation on gene copy-number evolution. Elife *5*, e14409.
Gonzalez, C. (2013). Drosophila melanogaster: a model and a tool to investigate malignancy and identify new therapeutics. Nat Rev Cancer *13*, 172-183.
Habedanck, R., Stierhof, Y.D., Wilkinson, C.J., and Nigg, E.A. (2005). The Polo kinase Plk4 functions in centriole duplication. Nat Cell Biol *7*, 1140-1146.

Hansford, S., and Huntsman, D.G. (2014). Boveri at 100: Theodor Boveri and genetic predisposition to cancer. J Pathol *234*, 142-145.
Hassold, T., and Hunt, P. (2001). To err (meiotically) is human: the genesis of human aneuploidy. Nat Rev Genet *2*, 280-291.
Holland, A.J., and Cleveland, D.W. (2009). Boveri revisited: chromosomal instability, aneuploidy and tumorigenesis. Nat Rev Mol Cell Biol *10*, 478-487.
Hose, J., Yong, C.M., Sardi, M., Wang, Z., Newton, M.A., and Gasch, A.P. (2015). Dosage compensation can buffer copy-number variation in wild yeast. Elife *4*.
Januschke, J., and Gonzalez, C. (2008). Drosophila asymmetric division, polarity and cancer. Oncogene *27*, 6994-7002.
Knouse, K.A., Wu, J., Whittaker, C.A., and Amon, A. (2014). Single cell sequencing reveals low levels of aneuploidy across mammalian tissues. Proc Natl Acad Sci U S A *111*, 13409-13414.
Levine, M.S., Bakker, B., Boeckx, B., Moyett, J., Lu, J., Vitre, B., Spierings, D.C., Lansdorp, P.M., Cleveland, D.W., Lambrechts, D*., et al.* (2017). Centrosome Amplification Is Sufficient to Promote Spontaneous Tumorigenesis in Mammals. Dev Cell *40*, 313-322 e315.
Michel, L.S., Liberal, V., Chatterjee, A., Kirchwegger, R., Pasche, B., Gerald, W., Dobles, M., Sorger, P.K., Murty, V.V., and Benezra, R. (2001). MAD2 haplo-insufficiency causes premature anaphase and chromosome instability in mammalian cells. Nature *409*, 355-359.
Muotri, A.R., and Gage, F.H. (2006). Generation of neuronal variability and complexity. Nature *441*, 1087-1093.
Oromendia, A.B., Dodgson, S.E., and Amon, A. (2012). Aneuploidy causes proteotoxic stress in yeast. Genes Dev *26*, 2696-2708.
Passerini, V., Ozeri-Galai, E., de Pagter, M.S., Donnelly, N., Schmalbrock, S., Kloosterman, W.P., Kerem, B., and Storchova, Z. (2016). The presence of extra chromosomes leads to genomic instability. Nat Commun *7*, 10754.
Pavelka, N., Rancati, G., Zhu, J., Bradford, W.D., Saraf, A., Florens, L., Sanderson, B.W., Hattem, G.L., and Li, R. (2010). Aneuploidy confers quantitative proteome changes and phenotypic variation in budding yeast. Nature *468*, 321-325.
Rehen, S.K., McConnell, M.J., Kaushal, D., Kingsbury, M.A., Yang, A.H., and Chun, J. (2001). Chromosomal variation in neurons of the developing and adult mammalian nervous system. Proc Natl Acad Sci U S A *98*, 13361-13366.
Reish, O., Brosh, N., Gobazov, R., Rosenblat, M., Libman, V., and Mashevich, M. (2006). Sporadic aneuploidy in PHA-stimulated

lymphocytes of Turner's syndrome patients. Chromosome Res *14*, 527-534.
Rossi, F., and Gonzalez, C. (2015). Studying tumor growth in Drosophila using the tissue allograft method. Nat Protoc *10*, 1525-1534.
Santaguida, S., and Amon, A. (2015). Short- and long-term effects of chromosome mis-segregation and aneuploidy. Nat Rev Mol Cell Biol *16*, 473-485.
Santaguida, S., Richardson, A., Iyer, D.R., M'Saad, O., Zasadil, L., Knouse, K.A., Wong, Y.L., Rhind, N., Desai, A., and Amon, A. (2017). Chromosome Mis-segregation Generates Cell-Cycle-Arrested Cells with Complex Karyotypes that Are Eliminated by the Immune System. Dev Cell *41*, 638-651 e635.
Sheltzer, J.M., Ko, J.H., Replogle, J.M., Habibe Burgos, N.C., Chung, E.S., Meehl, C.M., Sayles, N.M., Passerini, V., Storchova, Z., and Amon, A. (2017). Single-chromosome Gains Commonly Function as Tumor Suppressors. Cancer Cell *31*, 240-255.
Torres, E.M., Dephoure, N., Panneerselvam, A., Tucker, C.M., Whittaker, C.A., Gygi, S.P., Dunham, M.J., and Amon, A. (2010). Identification of aneuploidy-tolerating mutations. Cell *143*, 71-83.
Torres, E.M., Sokolsky, T., Tucker, C.M., Chan, L.Y., Boselli, M., Dunham, M.J., and Amon, A. (2007). Effects of aneuploidy on cellular physiology and cell division in haploid yeast. Science *317*, 916-924.
Torres, E.M., Springer, M., and Amon, A. (2016). No current evidence for widespread dosage compensation in S. cerevisiae. Elife *5*, e10996.
Vitre, B., Holland, A.J., Kulukian, A., Shoshani, O., Hirai, M., Wang, Y., Maldonado, M., Cho, T., Boubaker, J., Swing, D.A*., et al.* (2015). Chronic centrosome amplification without tumorigenesis. Proc Natl Acad Sci U S A *112*, E6321-6330.
Weaver, B.A., and Cleveland, D.W. (2006). Does aneuploidy cause cancer? Curr Opin Cell Biol *18*, 658-667.
Wu, C.T., and Morris, J.R. (1999). Transvection and other homology effects. Curr Opin Genet Dev *9*, 237-246.
Zhu, J., Tsai, H.J., Gordon, M.R., and Li, R. (2018). Cellular Stress Associated with Aneuploidy. Dev Cell *44*, 420-431.

Chapter I:

Premature loss of cohesin in Mitosis

Adapted from:

Premature sister chromatid separation is poorly detected by the spindle assembly checkpoint due to system-level feedbacks.

Mihailo Mirkovic, Lukas H. Hutter, Bela Novak and Raquel A. Oliveira *Cell Reports, Volume 13, Issue 3, p469–478, 20 October 2015*

Abstract

Sister chromatid cohesion, mediated by the cohesin complex, is essential for faithful mitosis. Nevertheless, evidence suggests that the surveillance mechanism that governs mitotic fidelity, the Spindle Assembly Checkpoint (SAC), is not robust enough to halt cell division when cohesion loss occurs prematurely. The mechanism behind this poor response is not properly understood. Using *Drosophila* developing brains, we show that full sister chromatid separation is insufficient for robust checkpoint response and cells abnormally exit mitosis after a short delay. Quantitative live cell imaging approaches, combined with mathematical modelling, indicate that frail SAC activation upon cohesion loss is caused by an intrinsic weak signalling capacity that is further potentiated by several feedback loops in the mitotic signalling network. We propose that upon premature loss of cohesion, multiple feedbacks involving Cyclin-dependent kinase 1 (Cdk1), gradually impair error-correction efficiency and accelerate mitotic exit. Our findings explain how cohesion defects may escape SAC surveillance.

Graphical Abstract

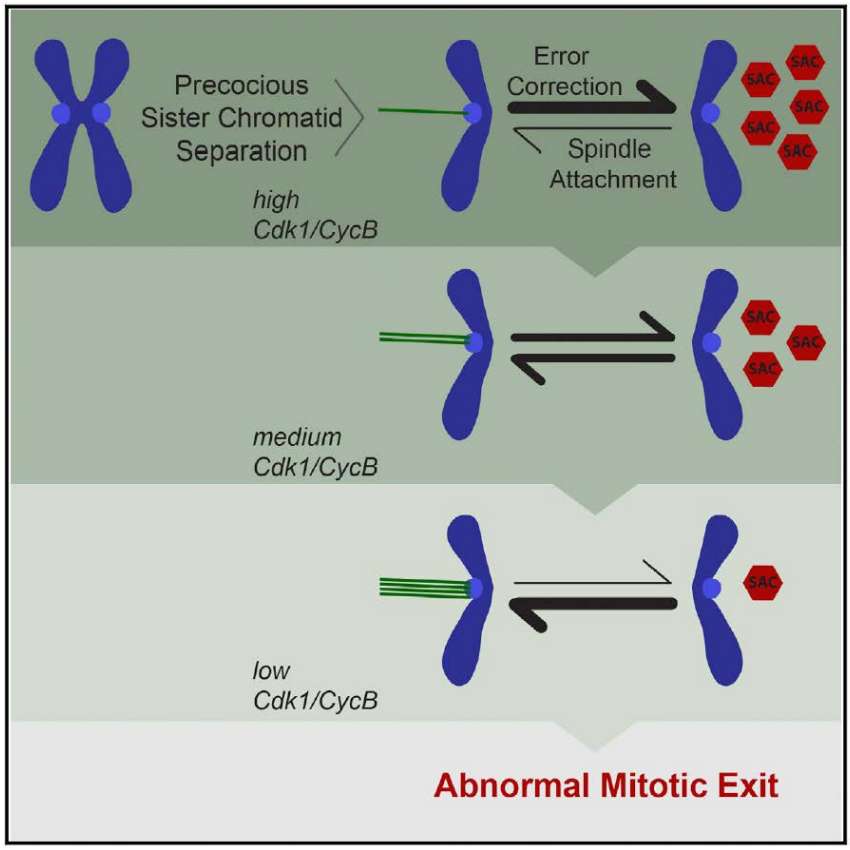

Highlights:

- Precocious sister chromatid separation does not elicit a robust SAC activation
- Error-correction efficiency declines gradually upon premature cohesion loss
- Mitotic exit upon cohesion loss is accelerated by multiple feedback loops
- Stability of microtubule-kinetochore attachments is ultrasensitive to Cdk1 inhibition

Introduction

Faithful chromosome segregation is governed by the Spindle Assembly Checkpoint (SAC), a surveillance mechanism that senses the state of spindle attachments and prevents progression through mitosis until all chromosomes are properly bi-oriented on the spindle (Musacchio, 2011; Nezi and Musacchio, 2009). This checkpoint operates by generating an inhibitory signal (Mitotic Checkpoint Complex, MCC) that inhibits the Anaphase-Promoting Complex/Cyclosome (APC/C) and thereby the onset of anaphase. Unattached kinetochores serve as a scaffold for the production of the MCC (Musacchio, 2011; Musacchio and Salmon, 2007) but it has long been debated whether or not tension across sister chromatids (and/or intra-kinetochore tension) can also be sensed by this checkpoint (Khodjakov and Pines, 2010; Maresca and Salmon, 2010; Pinsky and Biggins, 2005). Nevertheless, it is well accepted that tension plays a central role in the responsiveness of the SAC, even if indirectly, by modulating the stability of spindle attachments (Khodjakov and Pines, 2010; Maresca and Salmon, 2010; Nezi and Musacchio, 2009; Pinsky and Biggins, 2005). This regulation is achieved by the error-correction mechanisms, primarily mediated by Aurora B kinase, that destabilize kinetochore-microtubule interactions that are not under tension (Carmena et al., 2012; Liu et al., 2009).

Sister chromatid cohesion, mediated by the cohesin complex (Barbero, 2011; Losada, 2014), is a major contributor for tension establishment as it provides the counterforce that resists the opposite pulling forces of the microtubules upon spindle attachment (Oliveira et al., 2010; Tanaka et al., 2000). Cohesin is therefore essential for faithful mitosis, as it promotes biorientation and

thereby prevents random segregation of the genome. One would therefore expect that the SAC should be able to respond to cohesion defects and prevent mitotic exit upon premature cohesin loss. On the other hand, absence or mutations on cohesin subunits are associated with increased aneuploidy, including in some human disorders linked to cohesin malfunction (Barbero, 2011; Losada, 2014), implying that mitotic exit has taken place despite premature sister chromatid separation. Moreover, previous studies in budding yeast or mammalian cells have indicated that cells with unreplicated genomes or precociously separated sister chromatids, can eventually exit mitosis (Michaelis et al., 1997; O'Connell et al., 2008). This conundrum raises the possibility that despite the established role for sister chromatid cohesion as a major tension contributor, and consequently on the stability of spindle attachments, cohesion loss results in weak activation of the SAC. The molecular mechanisms behind this poor response, however, are not fully understood. Here we report a quantitative analysis on the robustness of the SAC activation during mitosis when sister chromatid separation occurs prematurely.

Results and Discussion

I.1 Premature Loss of Sister Chromatid Cohesion Does Not Elicit a Robust SAC Response

To determine the strength of the mitotic checkpoint response to premature loss of sister chromatid cohesion, we made use of a tool to induce acute removal of cohesin in living tissues, based on artificial cleavage of the cohesin protein Rad21 by an exogenous protease (Tobacco Etch Virus, TEV) (Oliveira et al., 2010; Pauli et al., 2008). We have focused our analysis on developing larval brain

Neuroblasts (NBs), stem cells that give rise to the central nervous system of the fly (Knoblich, 2008) and are known to have robust checkpoints. Accordingly, these cells arrest for many hours in mitosis when incubated with spindle poisons such as colchicine (Fig. 2 A, B). To induce cohesin cleavage, we used strains containing solely TEV-sensitive cohesin complexes and express TEV-protease under the heat-shock promoter (Pauli et al., 2008). Heat-shock delays mitotic entry (Maldonado-Codina et al., 1993) and nuclear division is resumed 148 ± 75 min (n=113 N=14) after heat-shock, enabling analysis of the consequences of cohesion loss within a single cell cycle (Fig. 1A).

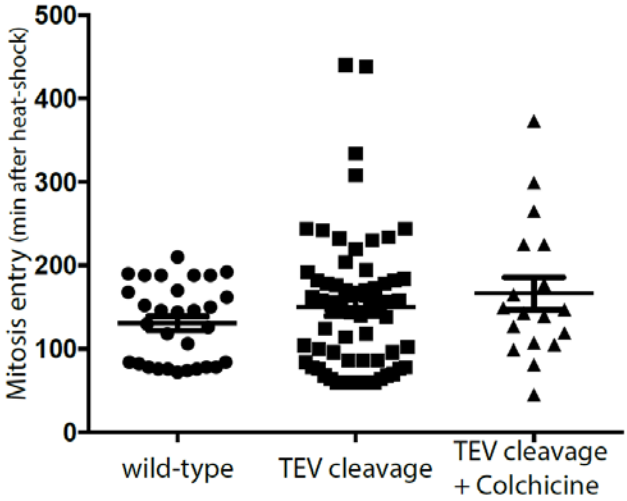

Figure *1A* – *Heat shock inhibits mitotic entry of Neuroblasts.*

To evaluate the robustness of the SAC in the presence of premature sister chromatid separation, we have quantified the time cells spend in mitosis (from Nuclear Envelope Breakdown (NEBD) to Nuclear envelope Formation (NEF).

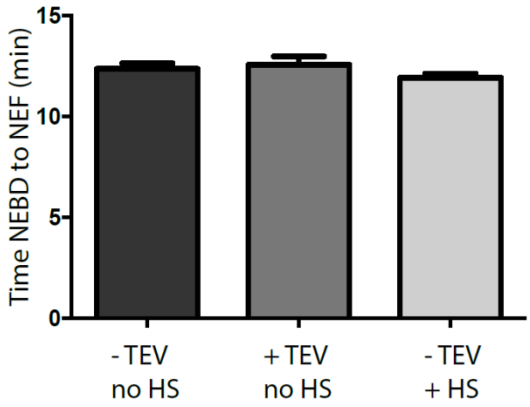

Figure 1B *– Heat shock and TEV expression do not perturb mitotic duration in Neuroblasts.*

While control cells spend around 12 minutes in mitosis (with or without heat shock), TEV-mediated cleavage of cohesin results in a mitotic delay (38.3 ± 13.1 min) (Fig. 2 and Movies S1 and S2). NBs from larvae not subjected to heat-shock do not show any mitotic delay implying that leaky TEV expression, if it exists, is unable to induce mitotic errors (Fig. 1B).

These results indicate that NBs elicit a SAC response that delays mitotic exit in response to prematurely separated sisters. However, this arrest is relatively modest when compared to colchicine-induced arrest (Fig 2B). A similar response was observed in Ganglion Mother Cells (GMCs), secondary precursor cells that derive from the NBs (1 C-D). Importantly, cohesin cleavage does not shorten the mitotic arrest in colchicine (Fig 2B); implying that cohesin depletion alone has no major effect on the SAC signalling capacity.

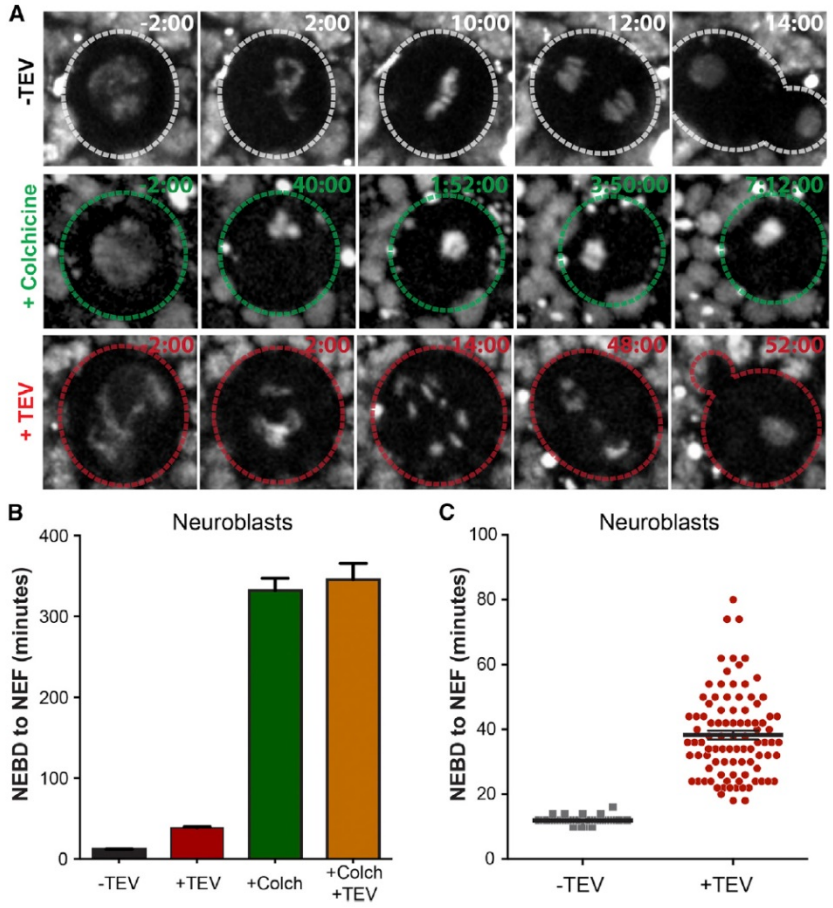

Figure 2- Premature loss of sister chromatid cohesion induces a short mitotic delay. A) *Images of dividing Drosophila Neuroblasts from heat-shocked wild-type strains (top), strains surviving solely on Rad21^{TEV} after heat-shocked induced TEV expression (middle) and wild-type brains incubated with 100 µM of colchicine (bottom). All strains express HisH2A-mRFP to follow chromosome dynamics and times (min:sec) are relative to nuclear envelope breakdown (NEBD); scale bar equals 5 µm and applies to all images;* ***B****) Average mitosis duration (NEBD to NEF) in heat-shocked control (n=41 N=4), TEV-mediated cohesin cleavage (n=93 N=8), colchicine treated (n=57 N=6) and colchicine treated after cohesin cleavage (n=15, N=2) larval Neuroblasts represented as mean ± SEM;* ***C)*** *Mitosis duration (NEBD to NEF) in wild-type (heat-shock control) and TEV-mediated cohesin cleavage larval Neuroblasts; See also Figure S1 and Movies S1 and S2*

I.2 Loss of Sister Chromatid Cohesion Activates EC Mechanisms during Early Mitosis

Drosophila neuronal cells are therefore highly SAC competent, yet fail to mount a robust response to cohesion loss if mitotic spindle is present. One would expect that even if transient spindle attachments take place in the absence of cohesin, these should become destabilized by the error-correction machinery, in response to lack of tension (Carmena et al., 2012; Liu et al., 2009). The resulting detached kinetochores should then provide a sufficiently strong SAC signal to prevent mitotic exit.

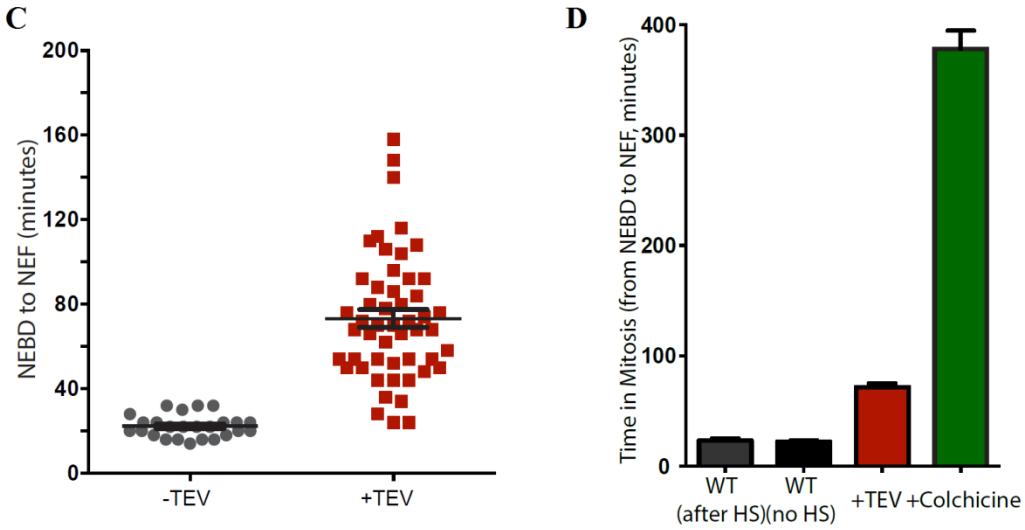

Figure 1 C-D.

C) *Ganglion Mother Cells (GMC) exibit a mild mitotic delay upon premature cohesion loss* ***D)*** *Colchicine incubation results in robust mitotic arrest.*

Our findings imply that the error correction machinery and the SAC show sub-optimal efficiency in detecting and arresting cell division in response to cohesion loss. Recent evidence suggests that Aurora B is not properly localized and shows reduced activity towards its known targets, upon depletion of cohesin subunits (Carretero et al., 2013; Kleyman et al., 2014; Yamagishi et al., 2010). In accordance, we confirmed that Aurora B is delocalized and specifically reduced in the centromere vicinity upon cohesin cleavage (Fig. 3A). A similar reduction was observed for one of the chromatin marks that mediate Aurora B accumulation, H3T3ph (Fig. 3B), thought to be regulated by the interaction of the responsible kinase (Haspin) with the cohesin subunit Pds5 (Yamagishi et al., 2010).

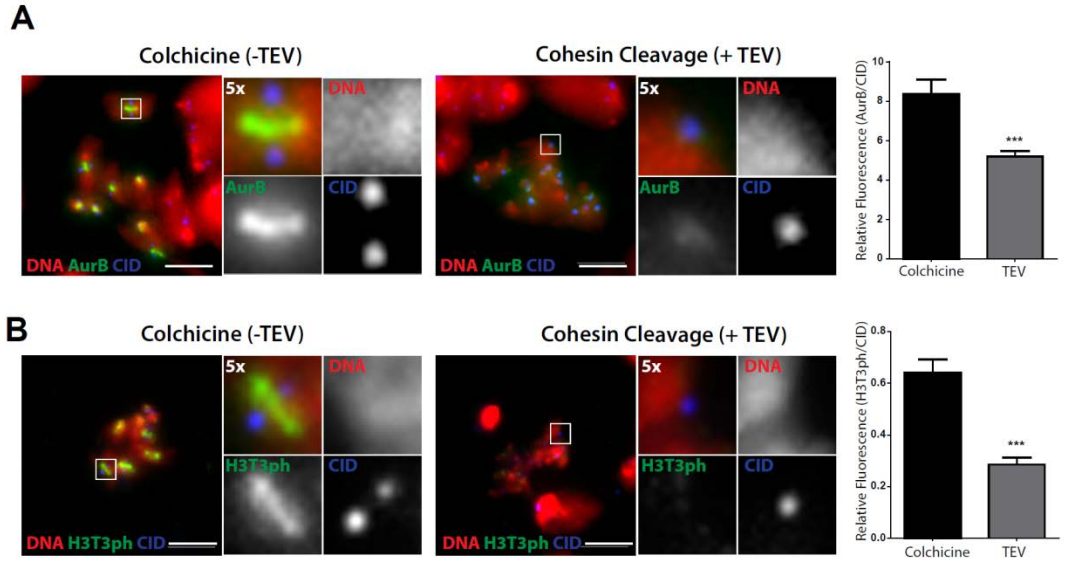

Figure 3 A-B.

A) *Cohesin depletion results in delocalization of Aurora B and decreased centromere intensity.* ***B)*** *Upon cohesin cleavage by TEV, the H3T3ph phosphorylation is decreased in mean intensity.*

Conversely, we also observe that engineered chromosomes containing ectopic heterochromatin sites, which are sufficient to recruit high levels of cohesin (Oliveira et al., 2014), are also able to accumulate significant levels of H3T3ph and Aurora B, despite not having a proximal centromere (Fig. 3 D, E). This result indicates that heterochromatin and cohesin accumulation are major drivers of Aurora B accumulation.

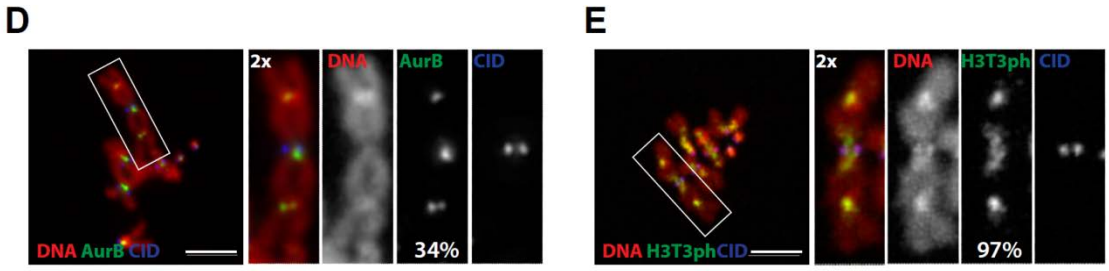

Figure 3 D-E.

Ectopic heterochromatin on C(2)En chromosome is sufficient to drive H3T3ph and Aurora B recruitment in the absence of centromere.

The observed correlation would support that weak SAC response in the presence of single sisters is related to defective Aurora B activity; however, two critical observations indicate that a malfunctioning error correction cannot fully explain the reduced SAC response. First, during initial stages of the arrest, we observe high levels of chromosome motion with oscillatory movements (Fig. 4 and Movies S2 and S3). After NEBD, single chromatids are initially pulled towards the poles, but remain highly mobile and soon start to shuffle between the poles. Quantitative analysis of

chromosome movement, estimated from the displacement of kinetochore positions in consecutive frames, reveals a high degree of chromatid motion, as evidenced by the high frequency of non-overlapping centromere positions between consecutive frames (Fig. 4 A, B and C). Such movements are likely the result of consecutive cycles of chromosome attachment, which are subsequently detached due to their tension-less nature, as previously suggested (Oliveira et al., 2010).

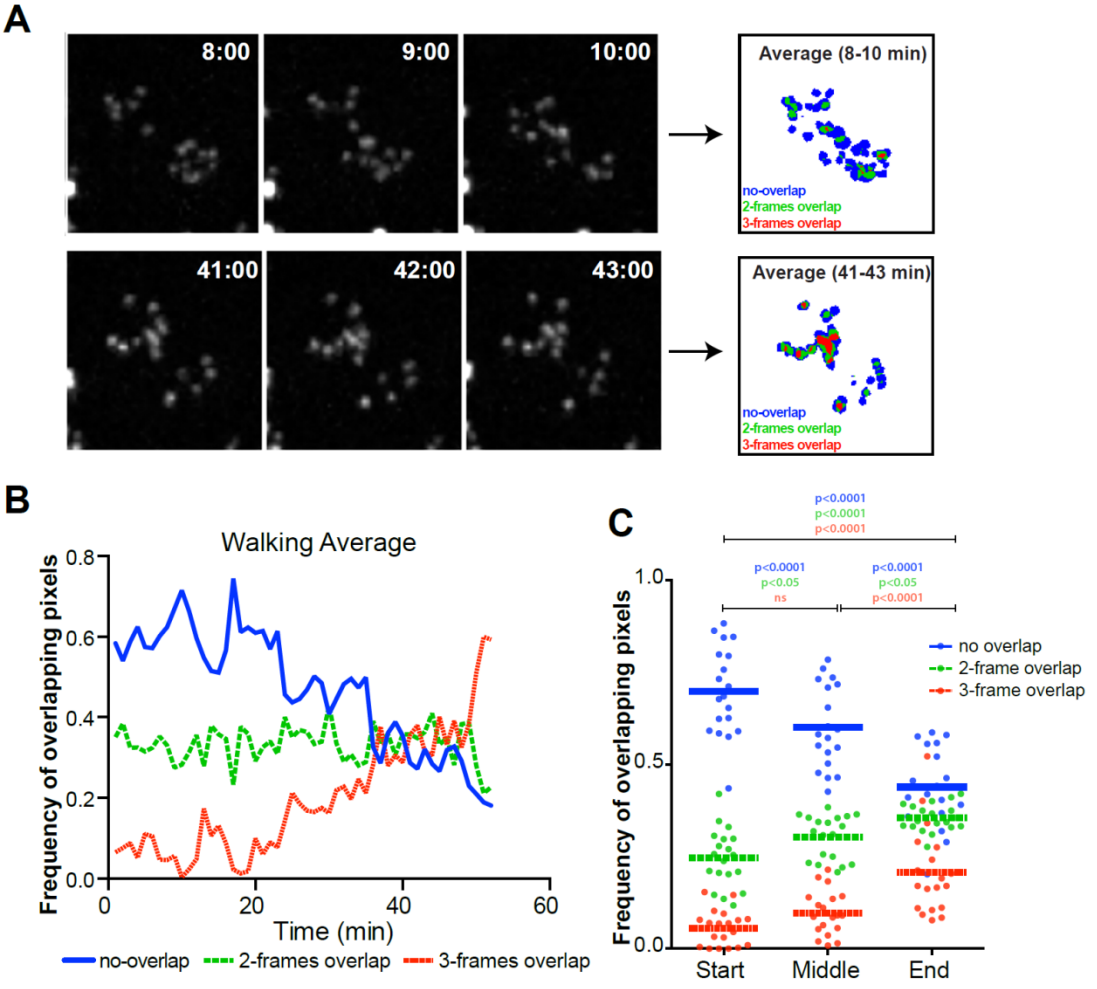

Figure 4- Single chromatids display a highly mobile behaviour that gradually declines during cohesin cleavage-induced mitotic delay.

A) *Stills from live cell imaging of CID-EGFP expressing neuroblasts upon cohesin cleavage at different time points (times are relative to NEBD). Left panel represents average of the binary images of 3 consecutive frames, used to estimate centromere displacements. Blue represents non-overlapping pixels, green represents pixels that overlap in 2 out of 3 frames and red represents pixels overlapping in the 3 frames.* ***B)*** *Centromere displacement during mitosis in the absence of cohesin (6 min post-NEBD to anaphase onset); graphs represent frequency of overlapping pixels from a walking average movies as illustrated in A.* ***C)*** *Centromere displacement at different times of arrest upon TEV-mediated cohesin cleavage: start: 6-10 min after NEBD; end: 6-10 min before anaphase onset; middle: 5 min at the midpoint of the arrest (n= 23 N=3); p represents the adjusted p-value by two-way ANOVA*

In accordance with this notion, movements are strongly reduced when Aurora B is inhibited by binucleine-2 (Smurnyy et al., 2010) (Fig. 4D). Secondly, the short but noticeable SAC response observed after cohesin cleavage, is dependent on Aurora B activity. Addition of binucleine-2 to cells that have just entered mitosis, and would therefore be expected to delay mitotic exit for additional 40 min, leads to abrupt mitotic exit in about 7,5 ± 0,5 min (Fig. 4E). This sharp mitotic exit could be attributed to the impairment of Aurora B activity in the destabilization of tensionless kinetochore-microtubule (KT-MT) attachments or, alternatively (or additionally), to the known role of this kinase in the SAC signalling (Hauf et al., 2003; Maldonado and Kapoor, 2011; Santaguida et al., 2011; Saurin et al., 2011). If Aurora B activity contributes primarily to SAC activity than one would expect inhibition of this kinase to

abrogate the SAC abruptly when the checkpoint is activated by the absence of spindle attachments. We therefore monitored the time of mitotic exit upon Binucleine-2 addition to colchicine-arrested cells. Our results show that upon Aurora B inhibition, colchicine-treated NBs eventually exit mitosis, but take a considerably longer time to do so, regardless whether cohesin has been cleaved or not (Fig. 4E). These results suggest that reversion of Aurora B mediated phosphorylation events required for SAC maintenance is kinetically slow. We therefore favour that the sudden mitotic exit observed upon Aurora B inhibition in TEV experiments, results primarily from the inhibition of the error correction activity rather than a direct inhibition on the SAC signalling capacity.

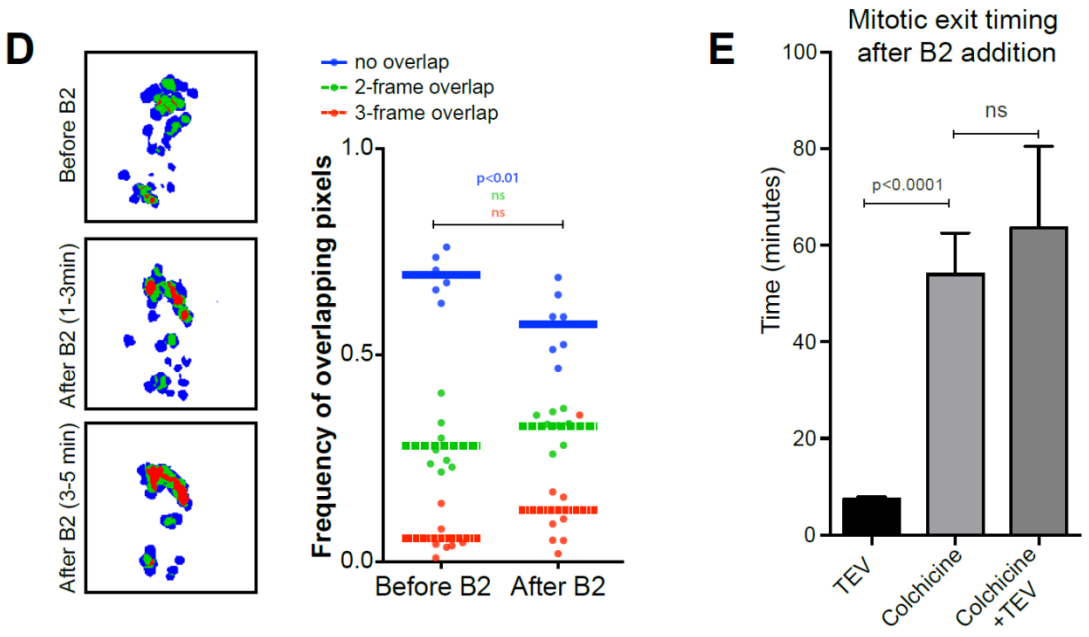

Figure 4 D-E: Mitotic delay and chromatid motion upon cohesin loss can be halted by Binucleine 2, an Aurora B inhibitor

D) *Centromere displacement before and after addition of an inhibitor that targets specifically Drosophila Aurora B (binucleine-2; final concentration: 25 μM); binuclein 2 was added 6-10 minutes after NEBD and centromere displacement was measured immediately after until anaphase onset (n=8 N=3); p represents the adjusted p-value by two-way ANOVA;* ***E)*** *Mitotic exit time after binuclein 2 addition in TEV-cleavage (n=33 N=3) and colchicine treatment (n=15 N=3) experiments represented as mean ± SEM. See also Figure S3 and Movies S2 and S3.*

I.3 Attachments of Single Chromatids to the Mitotic Spindle Are Progressively Stabilized

Taken together, these observations imply that Aurora B is at least partly functional in the absence of cohesin. If so, why is cohesion loss not sufficient to elicit a robust mitotic arrest? Given that the SAC response in the absence of cohesion depends on the ability to generate unattached kinetochores, we have monitored the state of KT-MT interactions throughout the entire duration of the arrest. We first monitored the degree of chromosome movement at different times of the arrest as mentioned above. While chromosomes are highly dynamic in the initial stages of the arrest, their movement becomes gradually reduced, suggesting that KT-MT interactions are progressively stabilized over time (Fig 4A, 4B). We envision three different possibilities that could account for KT-MT attachment stabilization in the presence of single sisters. First, stabilization of attachments could be caused by the accumulation of merotelic attachments, as previously reported in Mitosis with Unreplicated Genomes (MUGs) (O'Connell et al., 2008). Secondly, attachment could potentially be stabilized by tension in the absence of sister chromatid cohesion (for e.g. due to cytoplasmic drag). Lastly, attachments may be abnormally stabilized even in the

absence of maximal tension. To distinguish between these possibilities we have analysed the state of KT-MT attachments in more detail (Fig. 5A). This analysis revealed that the kinetochore occupancy is very high across the cells examined, and the most prevalent form of attachment displays kinetochores at the end of a well defined kinetochore bundle (end-on attachment). The high frequency of end-on attachments (66%) suggest that these are relatively stable (Fig. 5A). Importantly, we observed a low frequency of merotelic attachments (<15%, Fig. 5A), suggesting that accumulation of these abnormal attachments is unlikely to be the major cause for the observed decrease in motion. To confirm that this is also the case specifically at the time of mitotic exit, we have measured the positioning of centromeres at these later stages of mitosis. If abnormal mitotic exit were triggered by the accumulation of merotelic attachments one would expect centromeres to be preferentially placed in the middle of the segregation plane. In fact, in some cells we do find centromeres that lag behind the major chromatin mass (on average ~20%, Fig. 5B) and display obvious stretching once mitotic exit takes place, consistent with being bound to both poles. However, most kinetochores were found to be placed facing the poles, and do not stretch during poleward movement, supporting they are end-on attached (Fig. 5B). These results indicate that unlike the previous results in MUG cells (O'Connell et al., 2008), cohesion depletion leads to mitotic exit without major accumulation of merotelic attachments.

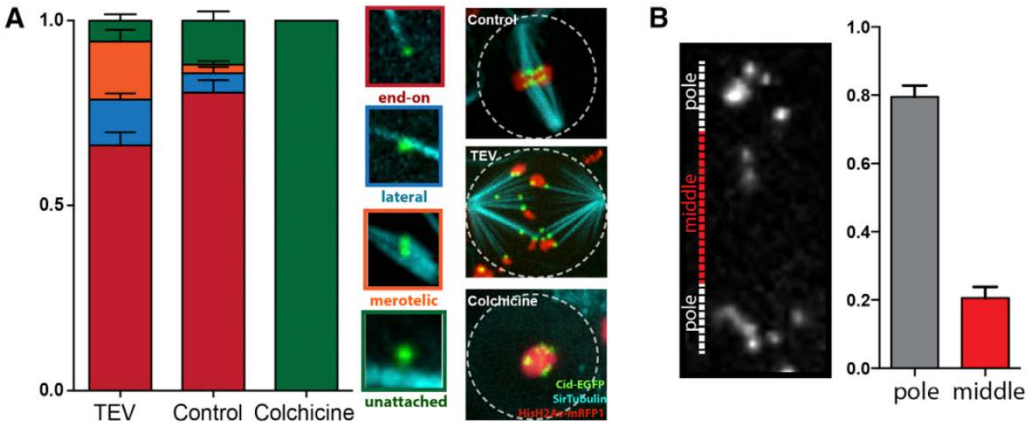

Figure 5 A-B – Cohesin loss results in High frequency of end-on attachments

A) *Frequency of kinetochore attachment observed upon after cohesin cleavage; brains expressing HisH2Av-mRFP1 (red) and Cid-EGDP (green) were shortly incubated with 100 nM Sir-Tub probes (Cyan) before brain squash; graph shows the profile of 30 NBs (N=3) at the random stage of mitotic delay highlighting that the most prevalent type of attachments are the end-on attachments;* ***B)*** *Quantifications of the centromere distribution at the time of mitotic exit; for each image, the segregation plane, determined based on the two most distal centromeres, was divided into two equally-sized regions as exemplified.*

To confirm that KT-MT attachments are indeed stabilized, we furthermore monitored the levels of Mad2-EGFP at kinetochore in live cells, throughout the duration of the arrest. Mad2 is a key component of the Mitotic Checkpoint Complex (MCC) that localizes to unattached kinetochores (Buffin et al., 2005; Musacchio, 2011; Musacchio and Salmon, 2007). We observe that upon cohesin cleavage, kinetochores show significant levels of Mad2 after NEBD

that fluctuate during the initial stages of the aberrant mitosis (Fig. 5C). Maximal amount is on average ⅓ the level observed in colchicine (data not shown). Importantly, at later stages the signals gradually decline. Cells exit mitosis once (and only when) all chromosomes are devoid of Mad2. These observations are further validated in fixed samples where we see significant asynchromy between different analysed cells but most lack high levels of Mad1 at kinetochores (Fig. 6B). Additionally, quantitative analysis of BubR1, a MCC component that leaves the kinetochores only when sisters are under tension (Buffin et al., 2005; Logarinho et al., 2004), reveals that its levels are reduced (⅓ of the levels in colchicine cells) but relatively constant throughout the arrest (Fig. 5D and data not shown).

Although there is a reduction during the arrest, the kinetics of BubR1 levels do not resemble the observed decrease in chromosome motion nor the dynamics of Mad2. Importantly, all kinetochores show similar levels of BubR1 across different cells analysed (Fig. 6C). We therefore favour that spindle attachments of single sisters, despite being mostly end-on, are progressively stabilized even without maximal tension.

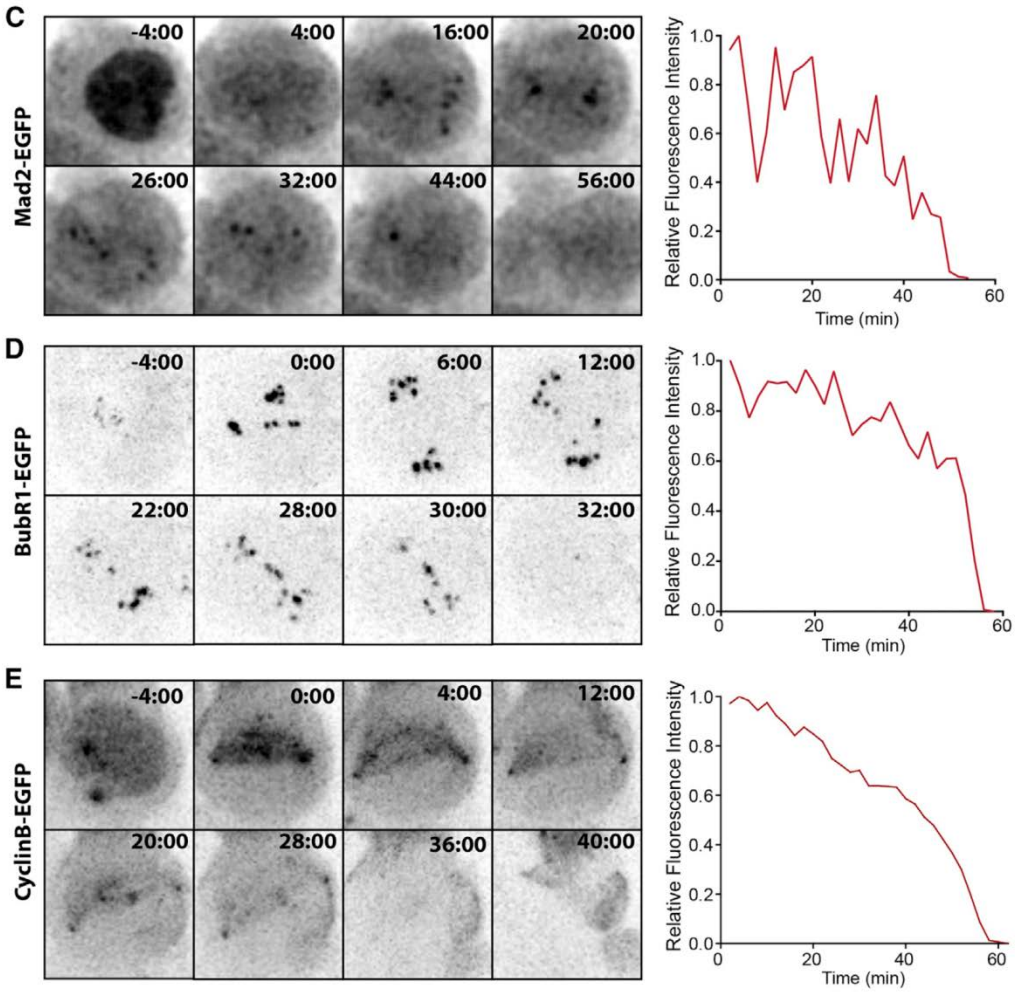

Figure 5 C-E: Cohesion loss leads to low production of MCC and premature decay of Cyclin B.

(C-E) *Stills from live-cell imaging of Mad2-GFP* ***(C)****, BubR1-GFP* ***(D)*** *and Cyclin B-GFP* ***(E)*** *during the mitotic delay induced by cohesin cleavage. Times are relative to NEBD; scale bar equals 5 µm and applies to all images; graphs represent the relative fluorescence intensity in cohesin cleavage and colchicine arrested cells, normalized to the maximum value within each dataset. See also Figure S4 and Movie S4.*

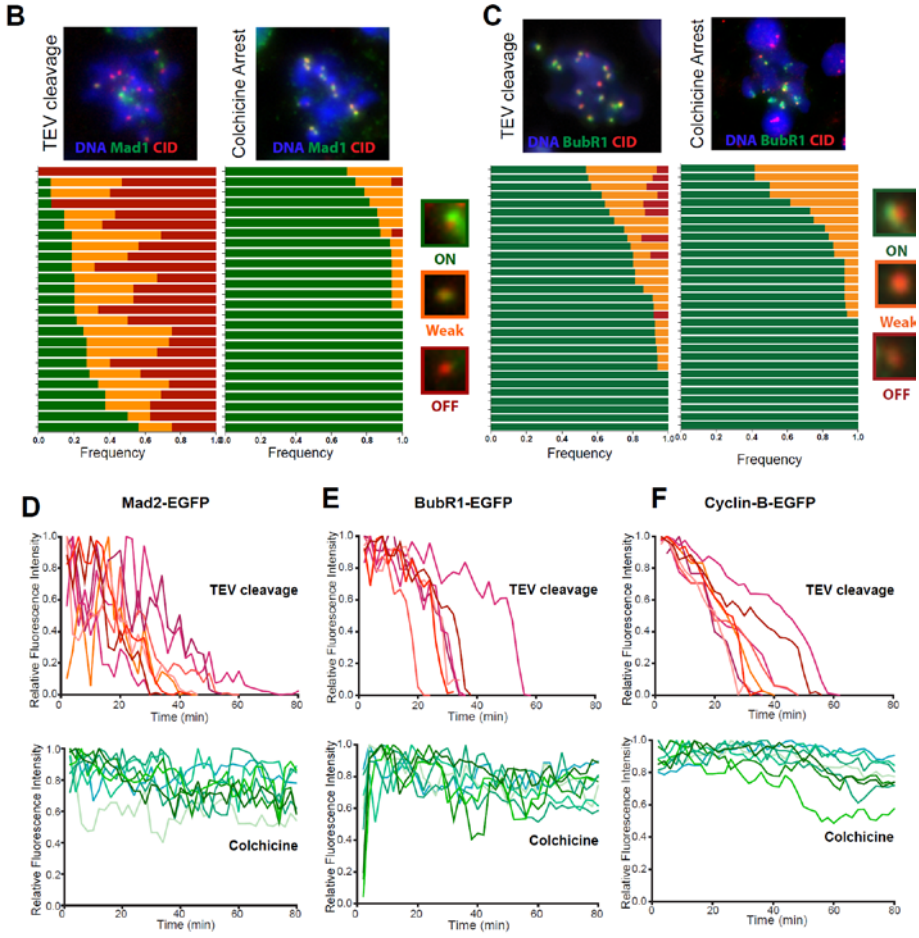

Figure 6 B-F B-C) *Immunofluorescence depicting single cell BubR1 and Mad1 Kinetochore occupancy upon premature Cohesin loss or Colchicine incubation.* ***D-F)*** *Live kinetics of BubR1, Mad2 and Cyclin B decay in individual Neuroblasts.*

I.4 Cyclin B Is Gradually Degraded during Cohesin Cleavage Mediated Mitotic Arrest

The results above suggest that throughout the mitotic delay there is a gradual transition between an initial phase, characterized by highly unstable KT-MT interactions resulting in a sufficiently strong SAC signal to prevent mitotic exit, to a later period with more stable attachments to the spindle and consequently decreased production of inhibitory signal. Given that cohesin depletion is an irreversible step, we assumed that this transition would be primarily governed by downstream consequences of a dynamic network.

In contrast to classical “all or nothing” view of the SAC (Rieder et al., 1995; Rieder et al., 1994), recent evidence supports graded SAC activity (Collin et al., 2013; Dick and Gerlich, 2013) arguing that its inhibitory activity is proportional to signal strength. It is therefore conceivable that an initial weak SAC signalling (caused by a high residence time of unstable attachments) leads to a partial activation of the APC/C and consequent partial Cyclin B degradation. To test this hypothesis we have monitored the levels of Cyc B-GFP in different experimental conditions. In the presence of spindle poisons such as colchicine, Cyc B levels remain high over the period of 1.5 hours (Fig. 6F; longer incubations cause a more pronounced decay in Cyc B levels, not shown). In contrast, mitosis in the presence of precocious sister chromatid separation leads to premature decay in Cyclin B levels. This is consistent with a graded SAC response (Collin et al., 2013; Dick and Gerlich, 2013) predicting that low levels of MCC would produce weak inactivation of the APC leading to significant Cyc B degradation (Fig. 5E).

I.5 Mathematical Modelling of Multiple Feedback across the Mitotic Network

Cdk1/Cyclin B activity is required for almost all aspects of mitosis; hence decay in Cyclin B levels is likely the major drive for mitotic exit. Nevertheless, several scenarios could serve as potential explanations for how Cyclin B decay can drive cells out of mitosis. To distinguish between different dynamic networks, we have adopted a mathematical modelling approach, which provides a quantitative framework for the description of accelerated mitotic exit observed upon premature sister-chromatid separation (Fig. 7). We have centred this analysis on the error correction (EC) module, characterized by the role of centromeric AuroraB complexes in destabilizing attached microtubule binding sites (MBS_a) at KTs (AurB —| MBS_a). Aurora B action is attenuated by KT stretching (Stretch —| AurB) which, in turn, is enhanced by sister chromatid cohesion during amphitelic attachment. We characterize KT tension by a “Stretch constant” (S), which is set to one during normal progression and to a small number when cohesin cleavage is induced. The choice for a small but larger than zero stretch value was based on recent findings that intra-kinetochore stretch contributes to SAC silencing (Maresca and Salmon, 2009, 2010; Nannas and Murray, 2014; Uchida et al., 2009) together with the fact that single sisters were often found attached to the spindle (Fig. 5A-B).

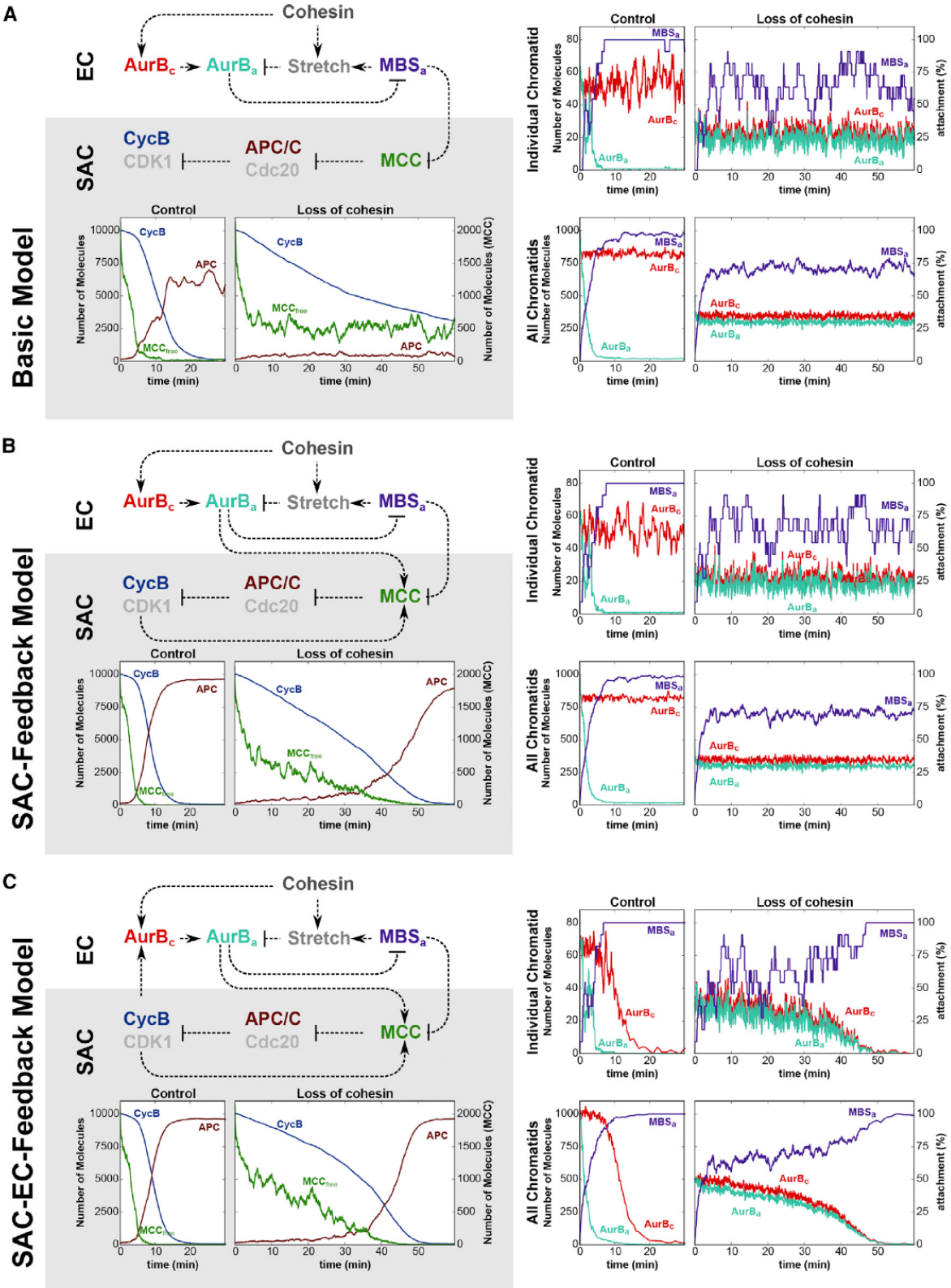
A
Basic Model
EC
SAC
Cohesin
AurBc
AurBa
Stretch
MBSa
CycB
CDK1
APC/C
Cdc20
MCC
Control
Loss of cohesin
Number of Molecules
Number of Molecules (MCC)
time (min)
APC
MCCfree
Individual Chromatid
All Chromatids
attachment (%)
B
SAC-Feedback Model
C
SAC-EC-Feedback Model

Figure 7 - Mathematical modelling of the interplay between error-correction (EC) and Spindle Assembly Checkpoint (SAC). *Comparison of three different scenarios for the interaction between the SAC and EC; Each panel shows a molecular influence diagram (top left), along with stochastic simulations for control cells and for the case of precocious loss of cohesin. The simulations show how these components change over time between nuclear envelope breakdown (t=0) and Cdk1 inactivation (mitotic exit). For clarity, time-courses for the SAC components (bottom left), and for EC components (right part) are shown separately in each panel. Simulations of the EC depict the behaviour of an individual chromatid (top) as well as the bulk behaviour of all chromatids (bottom).* ***A)*** *"Basic model". The EC module operating at centromeres-kinetochores uses Aurora B activity (AurBa) to destabilise MT-KT-attachments, and thereby converts attached microtubule-bindings sites (MBSa) into unattached bindings sites (MBSu). Attached MBS become stretched and thereby reduce the action of AurBa. This creates a double negative feedback loop. Both the activity of AurB, as well as the stretch depends on centromeric cohesins. MBSa act as input into the SAC module and suppress the formation of mitotic checkpoint complexes. MCC inhibition of APC/C-dependent CycB degradation regulates Cdk1 activity, which is the output of the SAC module.* ***B)*** *The "SAC-feedback model" is an extension of the "basic model": An additional internal positive feedback loop within the SAC module via Cdk1 and AurB promotes the production of MCC.* ***C)*** *The "SAC-EC-feedback model" is a further extension of the SAC-feedback model, where Cdk1 activity not only promotes MCC assembly, but additionally promotes AurB localisation. The mutual input-output relationship between ERC and SAC creates a positive feedback (amplification) loop (EC - SAC -EC).*

Cohesin plays a seemingly paradox role on the action and the level of Aur B at centromeres (see diagrams on Fig. 7 and Fig 8A). The

increased stretch caused by sister chromatid cohesion reduces AuroraB activity towards its targets (MBSa → Stretch —| AurB—| MBSa), creating a double negative feedback loop at the heart of the EC module. On the other hand, cohesion potentiates error-correction by stabilization of AurB molecules at centromeres (Fig. S2, (Carretero et al., 2013; Kleyman et al., 2014), which is captured by reduced dissociation constant of AurB in the model.

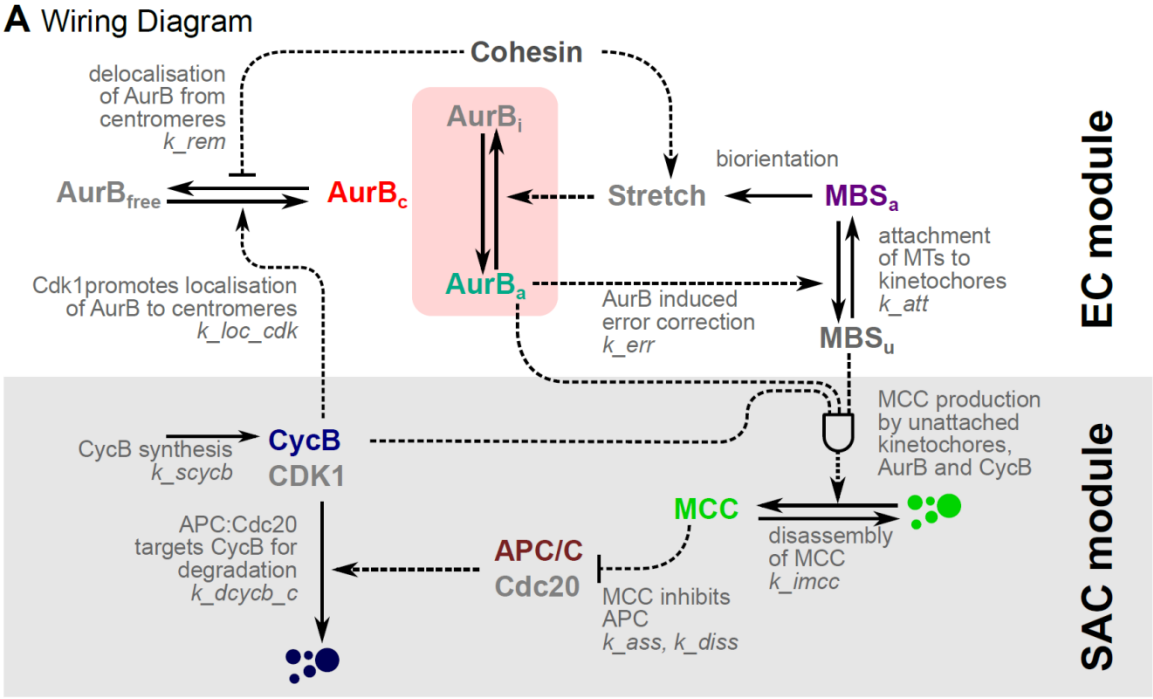

***Figure 8A**- Wiring Diagram of the Model*

The net products of the EC module are unattached kinetochores (MBS_u), which in turn, through the SAC module, catalyse the assembly of the inhibitory signal (MCC) that prevents mitotic exit by inhibiting APC/C-dependent Cyclin-B degradation (Fig 8A). All

these reactions are shared by the three models presented below in order to capture the dynamics of our experimental observations upon cohesin cleavage. For each model, the stochastic behaviour of single KT and the full complement KTs is presented, including the levels of centromeric Aurora B (its 'active' form as well as centromeric pool) and the number of MBS (11 per kinetochore (Maiato et al., 2006)). The behaviour of the SAC-module is illustrated by time-courses of CycB, APC/C and MCC.

In our "Basic model", SAC signalling is strictly downstream of the EC module by assuming a constitutive rate for the localization of AurB to the centromere (Fig. 7A). In the presence of cohesin, tension brings the effective activity of Aurora B sufficiently down in order to allow for attachments to stabilise. Our experimental observations in control cells are nicely recapitulated by carefully chosen set of parameters (see parameter description in Supplemental Experimental Procedures). However, the induced cohesin cleavage experiments cannot be captured with low levels of stretch constant, a likely scenario in the absence of cohesin (Fig. 8B provides an overview of the stretch parameter effect in all our models). The "basic model" predicts a mitotic arrest in the absence of sufficient tension because the EC module remains active and generates unattached kinetochores, which produce MCC and block mitotic exit (note persistent MCC levels and absence of APC activation on Fig. 7A). For these reasons, we assumed that additional feedback loops may be accelerating mitotic exit in the presence of single sisters.

In the “SAC-feedback model”, we have considered the role of Cdk1-CycB (D'Angiolella et al., 2003; Rattani et al., 2014; Vazquez-Novelle et al., 2014) and Aurora B (Hauf et al., 2003; Maldonado and Kapoor, 2011; Santaguida et al., 2011; Saurin et al., 2011) in MCC assembly (Fig. 7B). Introduction of these feedbacks accelerates mitotic exit allowing us to establish kinetic parameters that can fit the mitotic timings observed in both control and TEV-cleavage scenarios (Fig. 7B and 8). However, this model predicts persistent stochastic fluctuations for the microtubule attachment profile (Fig. 7B; note that MBSa do not increase over time), which is inconsistent with our experimental observations (Fig. 4 and 5). Additionally, this model postulates slowdown in Cyclin B degradation towards the later stages of the arrest (Fig. 7B). In contrast, we observe that CycB degradation occur in two stages: an initial linear decay followed sharp degradation at exit from mitosis (Fig. 3; see rates of CycB-degradation in Fig. 8C).

For these reasons, an additional feedback loop was introduced by a positive effect of Cdk1-CycB on the error correction machinery (“SAC-EC-feedback model”). Since Cdk1-CycB may affect error correction by several mechanisms (e.g. Aurora-B kinase activity/localization or microtubule dynamics), we simply described this effect by Cdk1-CycB dependence on centromeric localization, based on the fact that Cdk1 inactivation is known to remove centromeric Aurora-B at the metaphase-transition (Hummer and Mayer, 2009; Mirchenko and Uhlmann, 2010; Pereira and Schiebel, 2003; Tsukahara et al., 2010; Vazquez-Novelle and Petronczki, 2010). Other mechanisms, if in place, should have additive effects on the network. With the SAC-EC feedback in place, *in silico* simulations of the model faithfully matches the mitotic progression

upon cohesion loss of our experimental observations (Fig. 7C). In particular, inclusion of a positive feedback between SAC-EC makes the EC module sensitive to the levels of CycB. Consequently, simulations predict a gradual stabilization of KT-MT attachments (illustrated by the saturation of aMBS), as seen experimentally (Fig. 4). Additionally, this model also predicts that CycB degradation occurs slowly during early stages of the arrest, followed by higher degradation rates at the time of mitotic exit (Fig. 5E); see also CycB-degradation rates in Fig. 8C. This is consistent with a sharp activation of the APC/C, which is also predicted by the SAC-EC model (Fig. 7C, 8B)

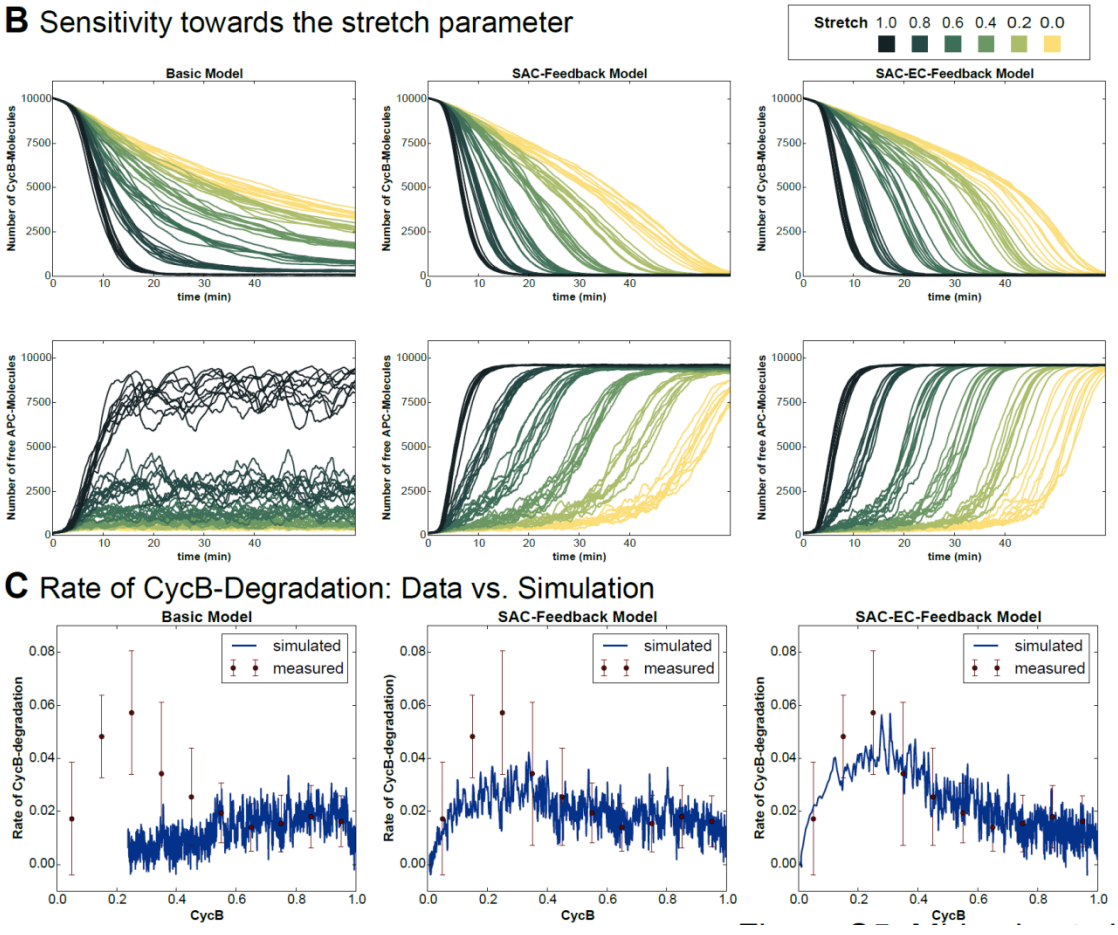

Figure 8 B-C: the three models.

B) *Differential sensitivity towards the stretch parameter in three models*

C) *Theoretical and experimental rates of Cyclin B degradation*

I.6 Cells with Premature Loss of Sister Chromatid Cohesion Are Ultrasensitive to Cdk1 Inhibition

Our experimental data is therefore best described by the “SAC-EC-feedback model”. Importantly, this model makes a critical testable prediction: mitosis duration upon cohesion depletion is ultrasensitive to mild Cdk inhibition (Fig 9A). In contrast to a linear sensitivity scenario, in which mitotic timing would be proportional to the level of residual Cdk activity, our model predicts that the multiple feedbacks will further accelerate mitotic entry and consequently mild Cdk inhibitions should have a strong effect on mitosis duration. Colchicine arrest is also predicted to display ultra-sensitivity although, in this case, to a lesser extent (note that in the absence of MT attachment there is only one feedback (SAC-feedback) potentiating Cdk inhibition sensitivity).

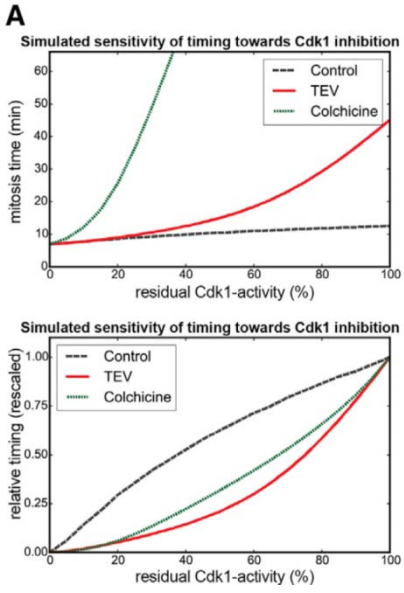

Figure 9A Mitosis with Precociously Separated Sister Chromatids Is Ultrasensitive to Cdk1 Inhibition

(A) *Predicted sensitivity of control, TEV-, and colchicine-treated cells to Cdk1-inhibition. Mitotic exit timing was determined by the time when theCycB level is reduced to 10% of its initial value. Bottom panel shows relative sensitivity of the different treatments; mitotic durations were rescaled between 0 (mitotic duration at 0% Cdk1- activity) and 1 (mitotic duration at 100% Cdk1activity).*

To test this prediction we have first investigated the efficiency of different doses of Cdk inhibitor Roscovitine in promoting mitotic exit in colchicine arrested cells (Fig 9B-C). While addition of 100 μM Roscovitine to Colchicine-arrested cells is sufficient to promote mitotic exit, 10 μM addition does not promote mitotic exit within the tested timeframe (2h). Importantly, control brains incubated with the same concentration prior to mitotic entry allow a significant number of control cells to enter and progress through mitosis with virtual no alteration in mitosis timing.

In contrast, such mild inhibition had a strong impact in the mitotic timing of cells undergoing mitosis with precocious sister chromatid separation (Fig 9 D) A further prediction of the model is that the shorter mitosis duration observed upon mild Cdk inhibition is caused by the inability of the error-correction to destabilize KN-MT attachments (Fig 9E). To test this, we have monitored the degree of chromosome motion in TEV-cleaved brains upon mild Cdk inhibition. Strikingly, these cells undergo mitosis with virtually no chromosome movement.

B

Roscovitine concentration (μM)	100	50	25	10
cells exiting mitosis/ cells analyzed	24/24	14/29	11/23	1/24
% mitotic exit	100%	48%	48%	4%

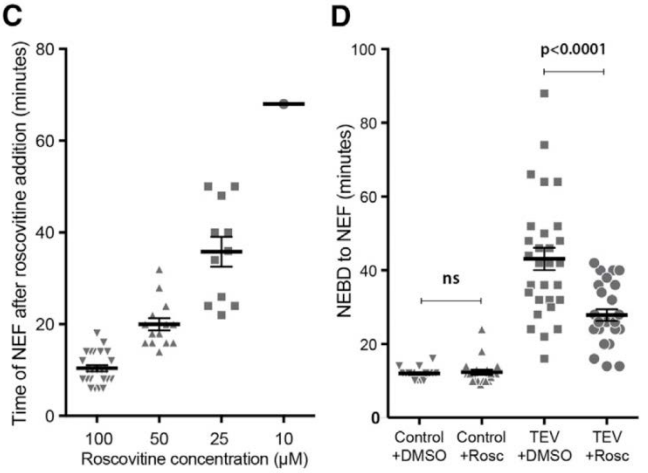

Figure 9 B-D Roscovitine effect on the Control, Colchicine incubated, and Cohesin cleaved Neuroblasts

B) *and* ***C)*** *Frequency (B) and time (C) of mitotic exit observed upon the addition of different doses of roscovitine to colchicine-arrested brains within 2 hr.(D) Mitosis duration in wild-type and TEV-mediated cohesin cleavage larval neuroblasts, with and without prior incubation with 10 mM roscovitine; adjusted p value by one-way ANOVA.*

Upon NEBD, sister centromeres separate and remain quite immobile throughout the duration of mitosis. To exclude that the observed low chromosome motion is an artefact of problems before mitotic entry, we have performed time-controlled addition of 10 μM Roscovitine to cohesin-cleaved cells minutes after NEBD, while high chromosome motion is maximal. Addition of 10 μM Roscovitine is sufficient to abolish chromosome movement almost instantly and trigger mitotic exit (Fig 9F). Altogether, these results suggest show that mild inhibition is Cdk is sufficient to impair error-correction. This suggests that amongst the many aspects of mitosis

controlled by Cdk1, regulation of the stability of KN-MT attachments is amongst the most sensitive ones.

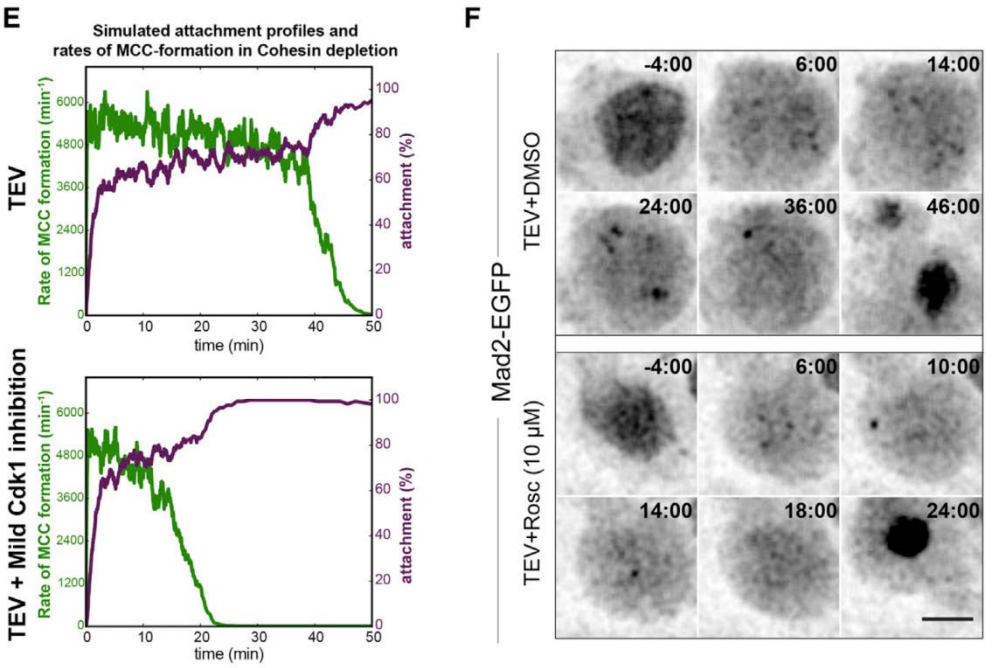

Figure 9 E-F Mild Cdk1 inhibition results in Mad2 signal abolishment upon cohesin removal.

(E) *Comparison of simulated attachment profiles and rates of MCC formation for cohesin cleaved cells with full Cdk1 activity (top) and subjected to 30% Cdk1 inhibition (bottom****).(F)*** *Stills from live-cell imaging of Mad2-GFP during the mitotic delay induced by TEV-mediated cohesin cleavage with and without incubation with10 mM roscovitine. Times are relative to NEBD; scale bar, 5 mm.*

I.7 Discussion

In summary, our analysis reveals that removal of a major tension contributor, such as sister chromatid cohesion, is insufficient for robust SAC activation. Such poor response can be attributed to two major findings: Firstly, single chromatids attach to the spindle with a high residence time, due an intrinsic slow kinetics of the error correction mechanisms or, more likely, to a sub-optimal efficiency of the error-correction machinery (Carretero et al., 2013; Kleyman et al., 2014; Yamagishi et al., 2010)). This, in turn, results in low MCC production.

Secondly, low MCC generation leads to partial CycB degradation, which feeds back on error-correction and MCC generation, promoting further stabilization of KT-MT attachments and reduction in MCC production. The feedbacks described in the "SAC-EC-feedbacks model" depict an amplification (positive feedback) loop between the error-correction and the SAC modules (ERC $\rightarrow$ SAC $\rightarrow$ERC) that in control cells stabilizes the high Cdk1 activity mitotic state until amphitelic attachment of all chromosomes is achieved. In response to cohesion loss, however, these feedbacks render premature cohesion almost insensitive to SAC surveillance. Additionally, the dependence on cohesin for efficient centromeric localization of Aurora B localization, together with the high sensitivity of error-correction to Cdk inhibition, may work as parallel mechanisms to ensure fast inactivation of the error correction mechanisms during anaphase, where cells have now to resist their tension-less state (Kops, 2014; Oliveira and Nasmyth, 2010). The caveat of such relationship is that it compromises how premature cohesion is sensed by the mitotic checkpoint.

Drosophila has a low number of chromosomes (8) making it more prone to silence the SAC, upon cohesin cleavage, within a testable time-frame. As such, loss of cohesion in mammalian cells may lead to a more prolonged SAC response, due to the higher number of signalling kinetochores (e.g. mouse embryos arrest for over 17 hours upon cohesin cleavage in mitosis (Tachibana-Konwalski et al., 2013)). Nevertheless, the regulatory networks described here are highly conserved across species predicting that mammalian cells with premature cohesion loss will likely eventually satisfy the SAC. Importantly, mild cohesion defects leading to partial levels of cohesion loss may be totally undetected by the SAC. This has important implications as known cases of mitotic cohesion problems associated with human disease (e.g. Cornelia de Lange, Roberts, Chronic Atrial and Intestinal Dysrhythmia (CIAD) Syndromes) are indeed characterized by relatively mild levels of sister chromatid separation (Chetaille et al., 2014; Jabs et al., 1991; Kaur et al., 2005; Vega et al., 2005).

I.8 Materials and Methods:

Drosophila strains

To destroy cohesin by TEV protease cleavage, *Drosophila* strains were used with TEV-cleavable Rad21 ($Rad21^{TEV}$) in a Rad21-null background ($Rad21^{ex15}$, $Rad21^{550\text{-}3TEV}$-myc) (Pauli et al., 2008). TEV expression was induced by heat-shocking 3rd instar larvae at 37ºC for 45 minutes. A complete list of used genotypes can be found in Sup.

Tissue Preparation for fixed and live-cell imaging

Third instar brains were dissected and prepared as previously described (Oliveira et al 2014). Further details can be found in SSS

Mathematical modelling

The model was simulated by Gillespie's Stochastic Simulation Algorithm (SSA) after converting the rate of elementary reactions into propensity functions. Details on model design, including equations and parameter can be found in Supp.

Acknowledgments

We would like to acknowledge Cellular Imaging Unit (IGC) for help with microscopy, Alexandra Tavares for excellent technical assistance, Claudio Sunkel and Mar Carmena for antibodies, Stefan Heidmann, Roger Karess, Jordan Raff, and the Bloomington Stock Center for fly strains, and Lars Janssen, Monica Bettencourt-Dias and Florence Janody for comments on the manuscript.

Funding:

MM is supported by a PhD scholarship awarded by the Fundação para a Ciência e Tecnologia (FCT), Portugal (SFRH/BD/52438/2013). LHH is a fellow of the Boehringer IngelheimPhD fellowship program and is partly funded by EPSRC. Work in the laboratory of R. Oliveira is supported by a Marie Curie Career Integration Grant (MCCIG321883/CCC) and an EMBO Installation Grant (IG2778). Work in the group of B. Novak is supported by the EC FP7 (MitoSys/241548) and BBSRC sLoLa (BB/MM00354X/1).

Author contributions: MM and RAO designed the experiments; MM carried out the experiments. LHH and BN performed the mathematical modelling. All authors wrote the paper

References:

Uncategorized References

Barbero, J.L. (2011). Sister chromatid cohesion control and aneuploidy. Cytogenetic and genome research *133*, 223-233.

Buffin, E., Lefebvre, C., Huang, J., Gagou, M.E., and Karess, R.E. (2005). Recruitment of Mad2 to the kinetochore requires the Rod/Zw10 complex. Curr Biol *15*, 856-861.

Carmena, M., Wheelock, M., Funabiki, H., and Earnshaw, W.C. (2012). The chromosomal passenger complex (CPC): from easy rider to the godfather of mitosis. Nature reviews Molecular cell biology *13*, 789-803.

Carretero, M., Ruiz-Torres, M., Rodriguez-Corsino, M., Barthelemy, I., and Losada, A. (2013). Pds5B is required for cohesion establishment and Aurora B accumulation at centromeres. The EMBO journal *32*, 2938-2949.

Chetaille, P., Preuss, C., Burkhard, S., Cote, J.M., Houde, C., Castilloux, J., Piche, J., Gosset, N., Leclerc, S., Wunnemann, F*., et al.* (2014). Mutations in SGOL1 cause a novel cohesinopathy affecting heart and gut rhythm. Nature genetics *46*, 1245-1249.

Collin, P., Nashchekina, O., Walker, R., and Pines, J. (2013). The spindle assembly checkpoint works like a rheostat rather than a toggle switch. Nat Cell Biol *15*, 1378-1385.

D'Angiolella, V., Mari, C., Nocera, D., Rametti, L., and Grieco, D. (2003). The spindle checkpoint requires cyclin-dependent kinase activity. Genes Dev *17*, 2520-2525.

Dick, A.E., and Gerlich, D.W. (2013). Kinetic framework of spindle assembly checkpoint signalling. Nat Cell Biol *15*, 1370-1377.

Hauf, S., Cole, R.W., LaTerra, S., Zimmer, C., Schnapp, G., Walter, R., Heckel, A., van Meel, J., Rieder, C.L., and Peters, J.M. (2003). The small molecule Hesperadin reveals a role for Aurora B in correcting kinetochore-microtubule attachment and in maintaining the spindle assembly checkpoint. The Journal of cell biology *161*, 281-294.

Hummer, S., and Mayer, T.U. (2009). Cdk1 negatively regulates midzone localization of the mitotic kinesin Mklp2 and the chromosomal passenger complex. Current biology : CB *19*, 607-612.

Jabs, E.W., Tuck-Muller, C.M., Cusano, R., and Rattner, J.B. (1991). Studies of mitotic and centromeric abnormalities in Roberts syndrome: implications for a defect in the mitotic mechanism. Chromosoma *100*, 251-261.

Kaur, M., DeScipio, C., McCallum, J., Yaeger, D., Devoto, M., Jackson, L.G., Spinner, N.B., and Krantz, I.D. (2005). Precocious sister chromatid separation (PSCS) in Cornelia de Lange syndrome. American journal of medical genetics Part A *138*, 27-31.

Khodjakov, A., and Pines, J. (2010). Centromere tension: a divisive issue. Nature cell biology *12*, 919-923.

Kleyman, M., Kabeche, L., and Compton, D.A. (2014). STAG2 promotes error correction in mitosis by regulating kinetochore-microtubule attachments. Journal of cell science *127*, 4225-4233.

Knoblich, J.A. (2008). Mechanisms of asymmetric stem cell division. Cell *132*, 583-597.

Kops, G.J. (2014). Cell division: SACing the anaphase problem. Current biology : CB *24*, R224-226.

Liu, D., Vader, G., Vromans, M.J., Lampson, M.A., and Lens, S.M. (2009). Sensing chromosome bi-orientation by spatial separation of aurora B kinase from kinetochore substrates. Science *323*, 1350-1353.

Logarinho, E., Bousbaa, H., Dias, J.M., Lopes, C., Amorim, I., Antunes-Martins, A., and Sunkel, C.E. (2004). Different spindle checkpoint proteins monitor microtubule attachment and tension at kinetochores in Drosophila cells. Journal of cell science *117*, 1757-1771.

Losada, A. (2014). Cohesin in cancer: chromosome segregation and beyond. Nat Rev Cancer *14*, 389-393.

Maiato, H., Hergert, P.J., Moutinho-Pereira, S., Dong, Y., Vandenbeldt, K.J., Rieder, C.L., and McEwen, B.F. (2006). The ultrastructure of the kinetochore and kinetochore fiber in Drosophila somatic cells. Chromosoma *115*, 469-480.

Maldonado-Codina, G., Llamazares, S., and Glover, D.M. (1993). Heat shock results in cell cycle delay and synchronisation of mitotic domains in cellularised Drosophila melanogaster embryos. Journal of cell science *105 (Pt 3)*, 711-720.

Maldonado, M., and Kapoor, T.M. (2011). Constitutive Mad1 targeting to kinetochores uncouples checkpoint signalling from chromosome biorientation. Nature cell biology *13*, 475-482.

Maresca, T.J., and Salmon, E.D. (2009). Intrakinetochore stretch is associated with changes in kinetochore phosphorylation and spindle assembly checkpoint activity. J Cell Biol *184*, 373-381.

Maresca, T.J., and Salmon, E.D. (2010). Welcome to a new kind of tension: translating kinetochore mechanics into a wait-anaphase signal. Journal of cell science *123*, 825-835.

Michaelis, C., Ciosk, R., and Nasmyth, K. (1997). Cohesins: chromosomal proteins that prevent premature separation of sister chromatids. Cell *91*, 35-45.

Mirchenko, L., and Uhlmann, F. (2010). Sli15(INCENP) dephosphorylation prevents mitotic checkpoint reengagement due to loss of tension at anaphase onset. Current biology : CB *20*, 1396-1401.

Musacchio, A. (2011). Spindle assembly checkpoint: the third decade. Philos Trans R Soc Lond B Biol Sci *366*, 3595-3604.

Musacchio, A., and Salmon, E.D. (2007). The spindle-assembly checkpoint in space and time. Nature reviews Molecular cell biology *8*, 379-393.

Nannas, N.J., and Murray, A.W. (2014). Tethering sister centromeres to each other suggests the spindle checkpoint detects stretch within the kinetochore. PLoS Genet *10*, e1004492.

Nezi, L., and Musacchio, A. (2009). Sister chromatid tension and the spindle assembly checkpoint. Curr Opin Cell Biol *21*, 785-795.

O'Connell, C.B., Loncarek, J., Hergert, P., Kourtidis, A., Conklin, D.S., and Khodjakov, A. (2008). The spindle assembly checkpoint is satisfied in the absence of interkinetochore tension during mitosis with unreplicated genomes. J Cell Biol *183*, 29-36.

Oliveira, R.A., Hamilton, R.S., Pauli, A., Davis, I., and Nasmyth, K. (2010). Cohesin cleavage and Cdk inhibition trigger formation of daughter nuclei. Nature cell biology *12*, 185-192.

Oliveira, R.A., Kotadia, S., Tavares, A., Mirkovic, M., Bowlin, K., Eichinger, C.S., Nasmyth, K., and Sullivan, W. (2014). Centromere-independent accumulation of cohesin at ectopic heterochromatin sites induces chromosome stretching during anaphase. PLoS biology *12*, e1001962.

Oliveira, R.A., and Nasmyth, K. (2010). Getting through anaphase: splitting the sisters and beyond. Biochem Soc Trans *38*, 1639-1644.

Pauli, A., Althoff, F., Oliveira, R.A., Heidmann, S., Schuldiner, O., Lehner, C.F., Dickson, B.J., and Nasmyth, K. (2008). Cell-type-specific TEV protease cleavage reveals cohesin functions in Drosophila neurons. Developmental cell *14*, 239-251.

Pereira, G., and Schiebel, E. (2003). Separase regulates INCENP-Aurora B anaphase spindle function through Cdc14. Science *302*, 2120-2124.

Pinsky, B.A., and Biggins, S. (2005). The spindle checkpoint: tension versus attachment. Trends Cell Biol *15*, 486-493.

Rattani, A., Vinod, P.K., Godwin, J., Tachibana-Konwalski, K., Wolna, M., Malumbres, M., Novak, B., and Nasmyth, K. (2014). Dependency of the spindle assembly checkpoint on Cdk1 renders the anaphase transition irreversible. Current biology : CB *24*, 630-637.

Rieder, C.L., Cole, R.W., Khodjakov, A., and Sluder, G. (1995). The checkpoint delaying anaphase in response to chromosome monoorientation is mediated by an inhibitory signal produced by unattached kinetochores. The Journal of cell biology *130*, 941-948.

Rieder, C.L., Schultz, A., Cole, R., and Sluder, G. (1994). Anaphase onset in vertebrate somatic cells is controlled by a checkpoint that monitors sister kinetochore attachment to the spindle. The Journal of cell biology *127*, 1301-1310.

Santaguida, S., Vernieri, C., Villa, F., Ciliberto, A., and Musacchio, A. (2011). Evidence that Aurora B is implicated in spindle checkpoint signalling independently of error correction. The EMBO journal *30*, 1508-1519.

Saurin, A.T., van der Waal, M.S., Medema, R.H., Lens, S.M., and Kops, G.J. (2011). Aurora B potentiates Mps1 activation to ensure rapid checkpoint establishment at the onset of mitosis. Nature communications *2*, 316.

Smurnyy, Y., Toms, A.V., Hickson, G.R., Eck, M.J., and Eggert, U.S. (2010). Binucleine 2, an isoform-specific inhibitor of Drosophila Aurora B kinase, provides insights into the mechanism of cytokinesis. ACS chemical biology *5*, 1015-1020.

Tachibana-Konwalski, K., Godwin, J., Borsos, M., Rattani, A., Adams, D.J., and Nasmyth, K. (2013). Spindle assembly checkpoint of oocytes depends on a kinetochore structure determined by cohesin in meiosis I. Current biology : CB *23*, 2534-2539.

Tanaka, T., Fuchs, J., Loidl, J., and Nasmyth, K. (2000). Cohesin ensures bipolar attachment of microtubules to sister centromeres and resists their precocious separation. Nature cell biology *2*, 492-499.

Tsukahara, T., Tanno, Y., and Watanabe, Y. (2010). Phosphorylation of the CPC by Cdk1 promotes chromosome bi-orientation. Nature *467*, 719-723.

Uchida, K.S., Takagaki, K., Kumada, K., Hirayama, Y., Noda, T., and Hirota, T. (2009). Kinetochore stretching inactivates the spindle assembly checkpoint. J Cell Biol *184*, 383-390.

Vazquez-Novelle, M.D., and Petronczki, M. (2010). Relocation of the chromosomal passenger complex prevents mitotic checkpoint engagement at anaphase. Curr Biol *20*, 1402-1407.

Vazquez-Novelle, M.D., Sansregret, L., Dick, A.E., Smith, C.A., McAinsh, A.D., Gerlich, D.W., and Petronczki, M. (2014). Cdk1 inactivation terminates mitotic checkpoint surveillance and stabilizes kinetochore attachments in anaphase. Curr Biol *24*, 638-645.

Vega, H., Waisfisz, Q., Gordillo, M., Sakai, N., Yanagihara, I., Yamada, M., van Gosliga, D., Kayserili, H., Xu, C., Ozono, K*., et al.* (2005). Roberts syndrome is caused by mutations in ESCO2, a human homolog of yeast ECO1 that is essential for the establishment of sister chromatid cohesion. Nature genetics *37*, 468-470.

Yamagishi, Y., Honda, T., Tanno, Y., and Watanabe, Y. (2010). Two histone marks establish the inner centromere and chromosome bi-orientation. Science *330*, 239-243.

Chapter II: Spindle Assembly Checkpoint aggravates Cohesin defects in Mitosis

Adapted from:

Absence of the Spindle Assembly Checkpoint restores mitotic fidelity upon loss of sister chromatid cohesion

Rui D. Silva*, Mihailo Mirkovic*, Leonardo G. Guilgur, Om S. Rathore, Rui Gonçalo Martinho and Raquel A. Oliveira

Current Biology 2018

** These authors contributed equally to the work*

Abstract

Sister chromatid cohesion is essential for faithful mitosis, as premature cohesion loss leads to random chromosome segregation and aneuploidy, resulting in abnormal development. To identify specific conditions capable of restoring defects associated with cohesion loss, we screened for genes whose depletion modulates *Drosophila* wing development when sister chromatid cohesion is impaired. Cohesion deficiency was induced by knock-down of the acetyltransferase Separation anxiety (San)/Naa50, a cohesin complex stabilizer. Several genes whose function impacts wing development upon cohesion loss were identified. Surprisingly, knockdown of key Spindle Assembly Checkpoint (SAC) proteins, Mad2 and Mps1, suppressed developmental defects associated with San depletion. SAC impairment upon cohesin removal, triggered by San depletion or artificial removal of the cohesin complex, prevented extensive genome shuffling, reduced segregation defects and restored cell survival. This counterintuitive phenotypic suppression was caused by an intrinsic bias for efficient

chromosome bi-orientation at mitotic entry, coupled with slow engagement of error-correction reactions. We conclude that mitotic timing determines the severity of defects associated with cohesion deficiency. Therefore, although divisions are still error-prone, SAC inactivation enhances cell survival and tissue homeostasis upon cohesion loss.

Results

The fidelity of mitosis depends on cohesive forces that keep sister chromatids together. Sister chromatid cohesion is mediated by cohesin, a tripartite ring complex that embraces sister chromatid fibres from the time of their replication until the subsequent mitosis [1-3]. Cleavage of cohesin by Separase, a cysteine protease, marks the anaphase onset, where single chromatids are dragged to the poles by the mitotic spindle after cohesive forces are destroyed [4-6]. Cohesin cleavage should only occur when all chromosomes are properly bio-oriented to ensure equal genome distribution. Unscheduled loss of sister chromatid cohesion is catastrophic for the cell as premature release of cohesive forces leads to random chromosome segregation.

Premature release of cohesive forces during mitosis is prevented by a safeguard mechanism known as the Spindle Assembly Checkpoint (SAC) (reviewed in [7, 8]). In the presence of unattached kinetochores, this safeguard mechanism prolongs mitosis by inhibiting the Anaphase Promoting Complex/Cyclosome (APC/C). SAC ensures that cohesin cleavage does not occur until all chromosomes are bioriented by blocking the APC/C, whose activation is needed for Separase activity. In contrast to its known role as a safeguard mechanism for mitotic fidelity, we describe the

unexpected observation that removal of the SAC alleviates mitotic errors when sister chromatid cohesion is compromised.

II.1 Drosophila wing modifier screen reveals that depletion of Mad2 and Mps1 suppresses the developmental defects associated with loss of cohesion.

Although the consequences of cohesin loss in unicellular organisms and cultured cells are well established, its impact on tissue proliferation and morphogenesis is poorly understood. To probe for conditions that would enhance or suppress cellular and tissue responses to cohesion defects, we performed a modifier screen in the adult *Drosophila* wing. We focused our analysis on the regulatory N-terminal acetyltransferase Separation anxiety (San) (also known as Naa50), required for establishment and/or maintenance of sister chromatid cohesion [9-12]. Our previous work proposed that San acetylates the N-terminus of Rad21 cohesin subunit and regulates the interaction between Rad21 and Smc3 [10]. Knock-down of this protein during development gives rise to an intermediate adult wing phenotype that is sensitive to phenotypic modulation (Figure 1A,B) and defects associated with San knock-down can be efficiently suppressed by several conditions that enhance cohesin stability on chromatin [10]. To search for modifiers (enhancers and suppressors) of the adult wing phenotype induced by San depletion, we co-expressed the *san* RNAi with 2955 RNAis, which theoretically deplete 2920 gene products (21% of all gene products annotated in Flybase vFB2017_06), specifically in larvae imaginal wing discs (using the Nubbin-Gal4 driver [13-15]) (Figure 1A).

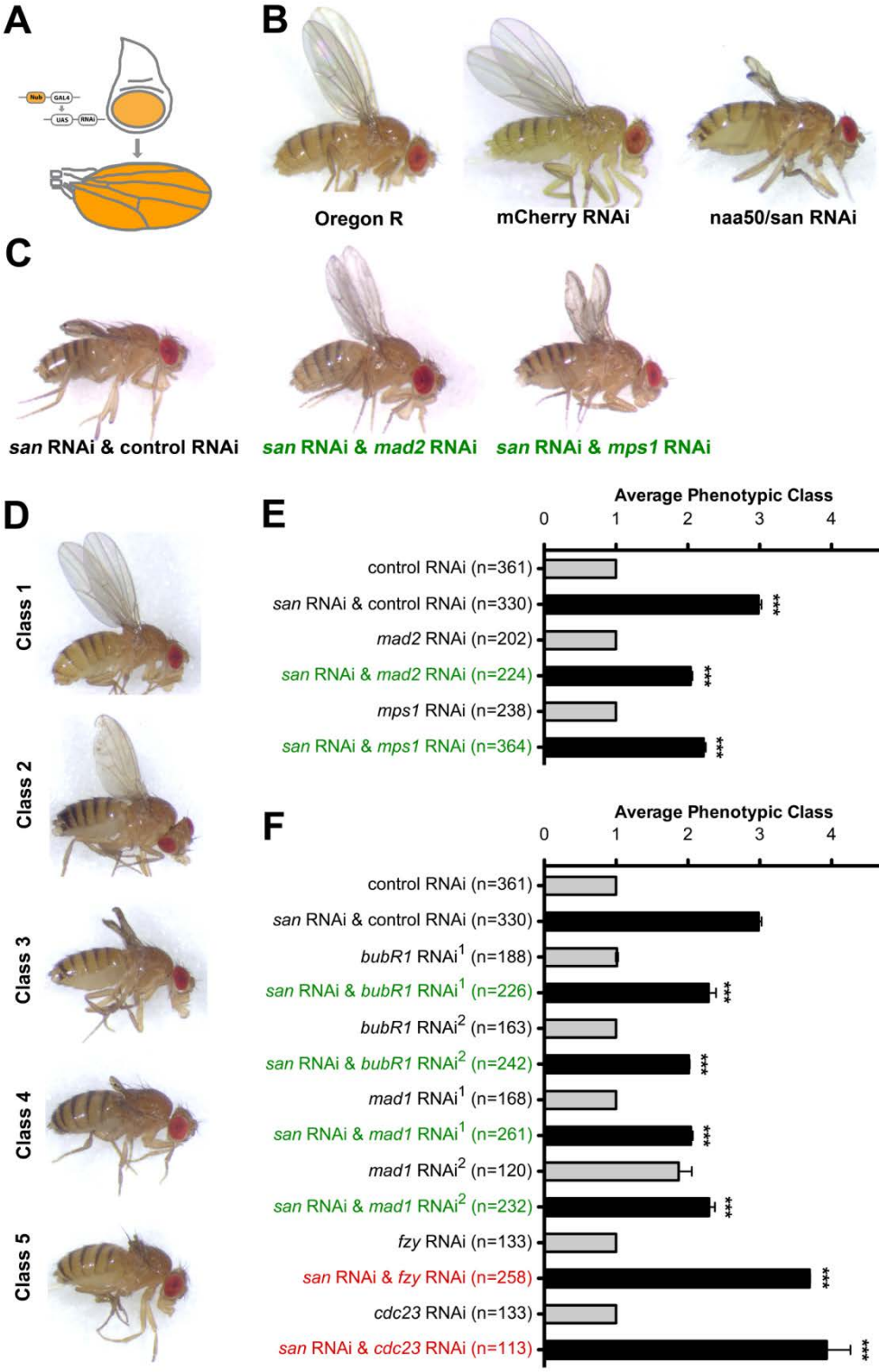
A
Nub
GAL4
UAS
RNAi
B
Oregon R
mCherry RNAi
naa50/san RNAi
C
san RNAi & control RNAi
san RNAi & mad2 RNAi
san RNAi & mps1 RNAi
D
Class 1
Class 2
Class 3
Class 4
Class 5
E
Average Phenotypic Class
0
1
2
3
4
5
control RNAi (n=361)
san RNAi & control RNAi (n=330)
mad2 RNAi (n=202)
san RNAi & mad2 RNAi (n=224)
mps1 RNAi (n=238)
san RNAi & mps1 RNAi (n=364)
***
F
Average Phenotypic Class
0
1
2
3
4
5
control RNAi (n=361)
san RNAi & control RNAi (n=330)
bubR1 RNAi1 (n=188)
san RNAi & bubR1 RNAi1 (n=226)
bubR1 RNAi2 (n=163)
san RNAi & bubR1 RNAi2 (n=242)
mad1 RNAi1 (n=168)
san RNAi & mad1 RNAi1 (n=261)
mad1 RNAi2 (n=120)
san RNAi & mad1 RNAi2 (n=232)
fzy RNAi (n=133)
san RNAi & fzy RNAi (n=258)
cdc23 RNAi (n=133)
san RNAi & cdc23 RNAi (n=113)
***

Figure1. SAC inhibition modifies san RNAi-induced adult wing developmental defects.

A) *Tissue-specific RNAi in the pouch of the larvae wing imaginal using the nubbin-Gal4 driver and the UAS/Gal4 system.* ***B)*** *Adult wings of wild type Drosophila (Oregon R), Drosophila expressing a control RNAi (mCherry RNAi) or expressing RNAi for san in the larvae wing imaginal discs.* ***C)*** *Representative adult Drosophila wing phenotypes co-expressing san RNAi with mCherry RNAi, mad2 RNAi or mps1 RNAi in the larvae wing imaginal discs.* ***D)*** *Adult wing phenotypic classes scored during the screen: class 1 (wild type wings); class 2 (weak wing developmental defects); class 3 (san RNAi-like wing phenotype); class 4 (highly abnormal wings); class 5 (absence or vestigial adult wings). Additional examples of the scored phenotypic classes are shown in [10].* ***E)*** *Quantification of Drosophila wing phenotypes expressing individual RNAi transgenes for control (mCherry), mad2 or mps1 (grey bars) or co-expressing san RNAi with control (mCherry) RNAi, mad2 RNAi or mps1 RNAi (black bars) in the larvae wing imaginal discs.* ***F)*** *Quantification of Drosophila wing phenotypes expressing individual RNAi transgenes for control (mCherry), bubR1, mad1, fzy and cdc23 (grey bars) or co-expressing san RNAi with control (mCherry) RNAi, bubR1 RNAis, mad1 RNAis, fzy RNAi and cdc23 RNAi (black bars) in the larvae wing imaginal discs. bubR1 RNAi^{1}, bubR1 RNAi^{2}, mad1 RNAi^{1} and mad1 RNAi^{2} were identified by a candidate gene analysis and correspond to the TRiP RNAis GL00236, GLV21065, GLV21088 and HMC03671, respectively. Phenotypic quantification of adult wings is mean ± SD of three independent experiments and is based on the classes described in (D) (***p < 0.0001, One-way ANOVA with Bonferroni's multiple comparison test; n represents the total number of scored flies).*

The resulting wings were scored in 5 categories, according to the severity of the phenotype (Figure 1D) [10]. Co-expression of *san* RNAi with a control RNAi transgene did not modify the adult wing

phenotype when compared to *san* RNAi transgene alone (Figure 1B and Figure 1C) [10]. Any isolated enhancer gene whose depletion alone resulted in adult wings phenotypes was discarded. All tested RNAi lines and scored wing phenotypes are shown in the Source Data file.

We identified 19 suppressors and 10 enhancers whose depletion specifically modified the *san* RNAi adult wing phenotype (Figure 2B). Given the increased regenerative capacity of wing discs [16-18] we expected to isolate genes involved in cohesin maintenance, in mitotic fidelity, and also in tissue response to mitotic damage.
As expected, the screen revealed components previously implicated in cohesin dynamics (*Mau2* and *eco*), validating its accuracy at isolating modifiers of cohesion state (Figure S1B) [10]. This approach also identified the cohesin component *vtd*/RAD21 RNAi as a modifier of *san* RNAi adult wing phenotype [10]. Most of the 29 genes identified in the screen, were already characterized in *Drosophila* and/or in other species (Table S1). About half of the identified genes were either related with mitosis (*Claspin*, *asp*, *Mps1*, *Eb1*, *eco*, *Mau2*, *γTub23C* and *mad2*) or with gene expression (CG5589, *JMJD7*, *Pabp2*, *His3* and *jumu*). Other identified genes were described to be important for maintaining apicobasal cell polarity and for actin cytoskeleton organization (*capu*, *cno* and *Cad99C*). We identified additional suppressors/enhancer genes related with different metabolic processes (*Sfxn1-3*, CG3842, *Dhap-at*, and *MFS18*), protein glycosylation (CG11388), synaptic adhesion (*Nlg4*), a paralogue of Naa20 N-terminal acetyltransferase (CG31730), and DNA repair/transcription (*Parp*).

B

Type of interaction	CG	Gene	TRiP number	Average wing phenotypic class (*n*)	
				Crossed with Nubbin-Gal4	*Crossed with Nubbin-Gal4 UAS-San RNAi*
Suppressors	CG31009	*Cad99C*	HMS01451	1.00 (240)	2.35 (353)
	CG3399	*capu*	HMS00712	1.00 (161)	2.40 (170)
	CG4625	*Dhap-at*	HMC03654	1.00 (189)	2.49 (211)
	CG3265	*Eb1*	HMS01568	1.00 (175)	2.44 (232)
	CG31613	*His3*	GL00255	2.56 (223)	2.48 (123)
	CG10133	*JMJD7*	HMS00578	1.00 (232)	2.50 (263)
	CG4029	*jumu*	HMS02839	1.00 (186)	2.44 (252)
	CG17498	*mad2*	GLC01381	1.08 (202)	2.04 (224)
	CG7643	*Mps1*	GL00184	1.00 (238)	2.22 (364)
	CG34139	*Nlg4*	HMS01710	1.04 (198)	2.50 (221)
	CG40411	*Parp*	GL00229	1.00 (92)	2.21 (109)
	CG11739	*Sfxn1-3*	HMS01674	1.00 (186)	2.58 (361)
	CG5589	-	HMS00325	2.04 (257)	2.70 (155)
	CG3842	-	HMC02378	1.03 (223)	2.05 (250)
	CG31730	-	HMS02540	1.68 (133)	2.24 (269)
	CG11388	-	HMS02633	1.00 (201)	2.37 (336)
	CG4766	-	HMC02404	1.91 (204)	2.36 (287)
	CG8746	-	HMS02863	1.95 (125)	2.34 (201)
	CG12592	-	GL00498	1.00 (183)	2.48 (382)
	CG7838	*BubR1* *	GL00236	1.01 (188)	2.29 (226)
	CG7838	*BubR1* *	GLV21065	1.00 (163)	2.01 (242)
	CG2072	*mad1* *	GLV21088	1.00 (168)	2.04 (261)
	CG2072	*mad1* *	HMC03671	1.87 (120)	2.29 (232)
Enhancers	CG6875	*asp*	GL00108	1.00 (262)	4.49 (216)
	CG42312	*cno*	HMS00239	1.04 (245)	3.81 (236)
	CG32251	*Claspin*	HMS00772	1.00 (168)	4.27 (182)
	CG8598	*eco*	GL00528	1.00 (191)	4.29 (181)
	GC4203	*Mau2*	HMS02374	1.00 (122)	3.72 (182)
	CG15438	*MFS18*	HMS00961	1.00 (102)	3.98 (164)
	CG2163	*Pabp2*	HMS00553	1.00 (153)	3.91 (206)
	CG3157	*γTub23C*	GL01171	1.05 (229)	3.54 (254)
	CG9773	-	HMS01044	1.11 (192)	4.12 (124)
	CG32243	-	GL00501	1.00 (244)	3.79 (254)
	CG4274	*fzy* *	HMS00964	1.00 (113)	3.69 (258)
	CG2508	*cdc23* *	HMJ23608	1.00 (133)	3.93 (113)

Figure 2B List of genetic modifiers of san RNAi wing phenotype. *The gene abbreviations used in this figure are from Flybase version FB2017_06. The RNAi GL00255 also theoretically depletes the histone H3 isoforms CG33833, CG33806, CG33839, CG33827, CG33854, CG33824, CG33818, CG33830, CG33863, CG33815, CG33866, CG33836, CG33803, CG33851, CG33809, CG33821, CG33845, CG33857, CG33848, CG33860, CG33842 and CG33812 and the RNAi HMJ23608 also theoretically depletes CG31687, a poorly expressed*

chimeric gene between cdc23 and CG31688. The gene CG5589 was classified as suppressor due to the strong adult wing phenotype of the correspondent RNAi when expressed in the wing imaginal discs with nubbin-Gal4 and the genetic interaction with eco and Mau2 has been previously described in [10]. The genetic interactions marked with an asterisk (*) were identified by a candidate gene approach. Results are mean of three independent crosses.

Surprisingly, two of the strongest suppressors were proteins that participate in the SAC, Mps1 and Mad2, and whose depletion specifically suppressed *san* RNAi adult wing phenotypes (Figure 1C,E). Given that both of these proteins belong to the same biological pathway, and both were isolated as suppressors of *san* RNAi, we hypothesized that impairment of SAC could rescue mitotic defects caused by cohesin deficiency. We tested this notion by a candidate gene approach and probed for genetic interactions with other SAC genes. Among the 4 additional SAC components probed (Bub3, Bub1, BubR1 and Mad1) (Source Data), RNAi for both Mad1 and BubR1 similarly suppressed the morphological defects associated with San depletion (Figure 1F and Figure 2B).

II.2 SAC inactivation rescues chromosome segregation defects associated with loss of cohesion.

To gain further insight on whether SAC inactivation could indeed rescue cohesion defects we sought out to evaluate mitotic fidelity in various experimental conditions. Live cell imaging analysis in the developing wing disc revealed, as expected by our previous work [10], that upon *san* RNAi, cells exhibited various degrees of sister chromatid cohesion defects. In control strains all cells underwent mitosis with normal metaphase morphology (Figure 3A, Figure 4

and Movie S1). Upon san RNAi only 13±10% displayed normal mitosis and most cells underwent partial or full sister chromatid separation (17±6 and 70±13%, respectively), resulting in SAC activation and extended mitosis (Figure 3A, B, Figure 4 and Movie S1).

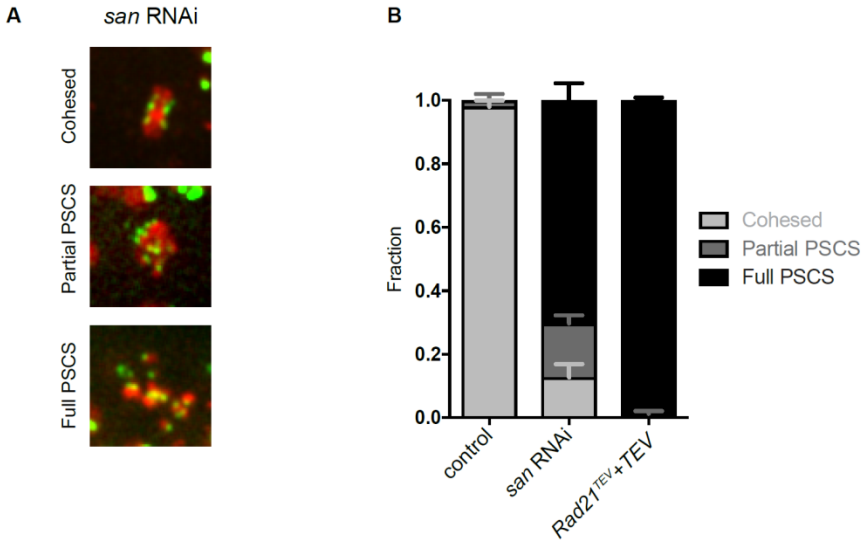

Figure 4 A-B SAN RNAi results in mitotic cohesion defects

A) *Stills from Live movies of wing disc cells dividing upon SAN RNAi expression. His-REF CID-EGFP B) Frequency of cohesion defects in the control, san RNAi expression, and hs-TEV induced cleavage of cohesin.*

More severe defects were obtained when cohesion loss was induced by acute artificial cleavage of cohesin Rad21 subunit, using a previously established TEV protease-mediated cleavage method [19]. In these experiments, wing imaginal discs were allowed to develop normally until 3rd instar larvae stage, when TEV protease was induced by heat-shock. After heat-shock Rad21 became quickly undetectable in cells expressing exclusively TEV-sensitive Rad21-EGFP (Figure 4C, D). TEV expression resulted in

full sister chromatid separation across all cells analysed (Figure 4B), leading to extended mitosis and chromatid shuffling between the poles (Figure 3C, D and Movie S2).

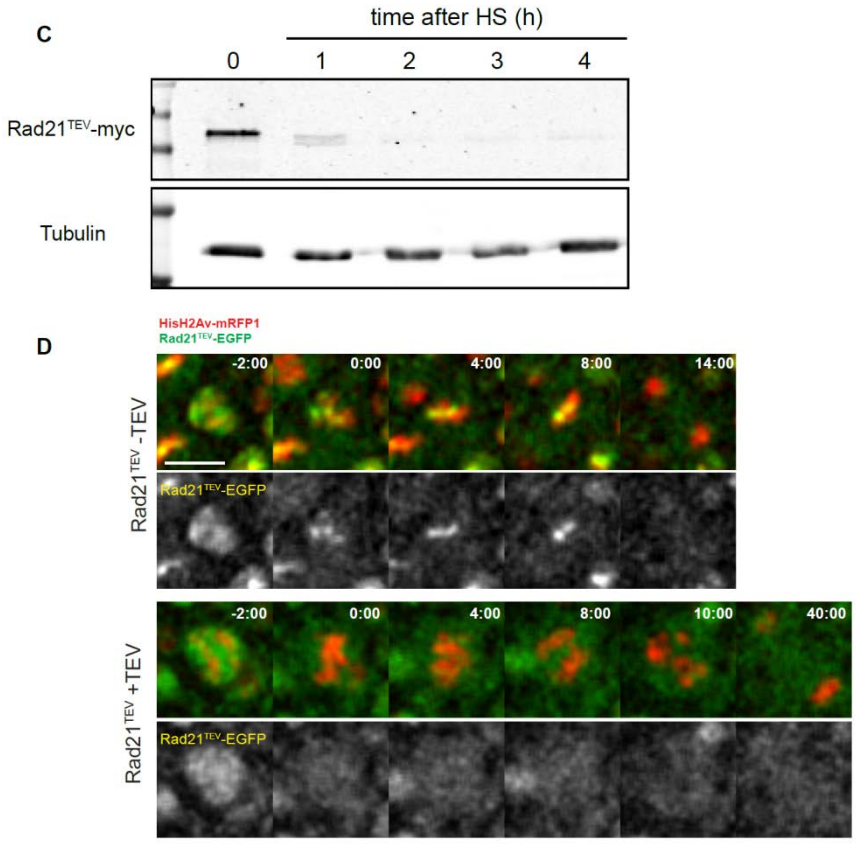

Figure 4 C-D. Premature sister chromatid separation upon TEV-mediated Rad21 cleavage C) *Western blot analysis of Rad21^{TEV}-EGFP levels before and after heat shock-induced TEV protease expression, probed with an anti-Rad21 antibody. Each lane corresponds to 10 dissected wing discs; anti-a-tubulin was used as loading control.* ***D)*** *Live-cell imaging analysis of strains surviving on Rad21^{TEV}-EGFP (green) without and with heat-shock induced TEV protease expression. Cells also express HisH2AvD-mRFP1. Times are relative to NEBD and scale bar is 5 µm and applies to all images.*

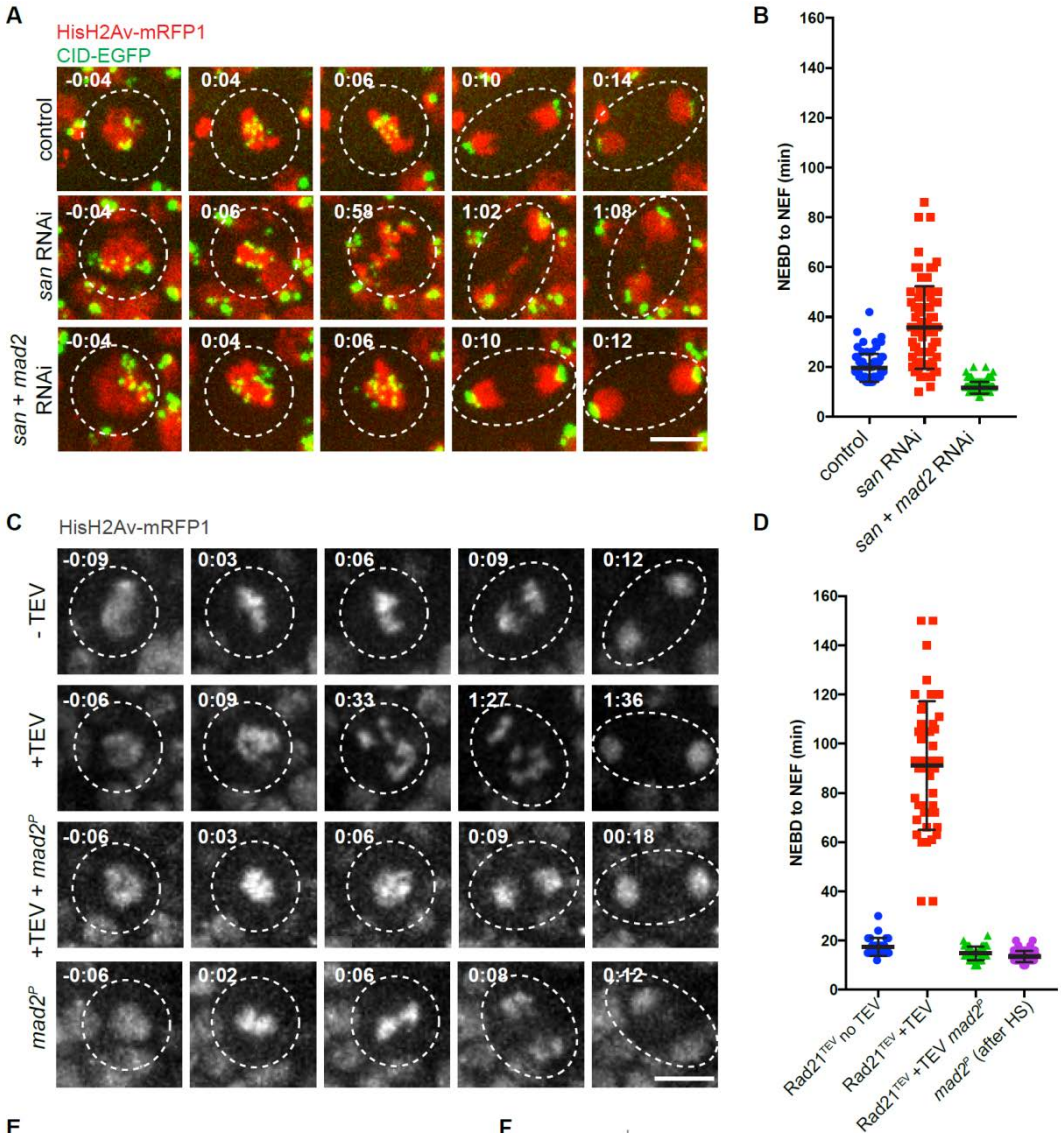

Figure 3 A-D Inhibition of SAC in wing imaginal discs abolishes the mitotic delay upon cohesin depletion

A) *Images from movies of the wing disc pouch in the control, san RNAi and san and mad2 RNAi strains. Strains contained HisH2Av-RFP (red) and CID-EGFP (green). Times are relative to NEDB. Scale bar is 5 µm.* ***B)*** *Quantification of mitotic duration in control, san RNAi, or san and mad2 RNAi strains. The duration of mitosis was measured from nuclear envelope breakdown (NEBD) to nuclear envelope formation (NEF) using H2Av-RFP channel. Images were taken every 2 minutes. Each dot*

represents an individual cell and lines represent mean ± SD (n= 71/5 for control, 77/5 for san RNAi and 124/5 for san+mad2 RNAi, n=number of cells/number of independent discs). ***C)*** *Images from movies of the wing disc from strains surviving solely on TEV-cleavable Rad21 (Rad21^{TEV}) with and without heat-shock induced TEV protease cleavage, in strains wild type or homozygous mutant for the mad2 gene. Strains also expressed HisH2Av-RFP (red) for visualization of mitotic duration and phenotype. Times are relative to NEDB. Scale bar is 5 µm* ***D)*** *Quantification of mitotic duration of the no heat shock control, upon TEV-protease mediated cleavage of Rad21^{TEV} and TEV-protease mediated cleavage of Rad21^{TEV} in a mad2 mutant background. The duration of mitosis was measured from nuclear envelope breakdown (NEBD) to nuclear envelope formation (NEF) using H2AvD-mRFP1. Images were taken every 2/3 minutes. Each dot represents an individual cell and lines represent mean ± SD (n= 27/4 for Rad21^{TEV} - TEV (no HS), 46/8 for Rad21^{TEV} + TEV, 46/4 for Rad21^{TEV}+TEV in a mad2^{P} background and 60/4 for mad2^{P} after heat-shock (HS), n=number of cells/number of independent discs).*

In order to inhibit the SAC, we focused on genetic conditions that remove Mad2, a key component of this checkpoint, as to date this protein is thought to be solely required for SAC response (in contrast to Mps1 that has been implicated in other mitotic functions [20]. Flies carrying null alleles for the *mad2* gene were previously shown to be viable [21] and its depletion in the larvae wing imaginal disc did not compromise wing development (Figure 1E). As expected, removal of Mad2 by RNAi or the *mad2^{P}* null allele abolished the mitotic delay in both experimental conditions for cohesion loss, *san* RNAi and TEV-mediated Rad21 cleavage (Figure 3A, B, C, D and Movies S1 and S2). More importantly, shortening of mitotic timing drastically reduced the frequency of

abnormal anaphase figures (Figure 3E). Whereas upon premature loss of cohesin mitotic exit often displays lagging chromatids or chromatin bridges, these segregation defects were significantly reduced when SAC was removed (Figure 3E).

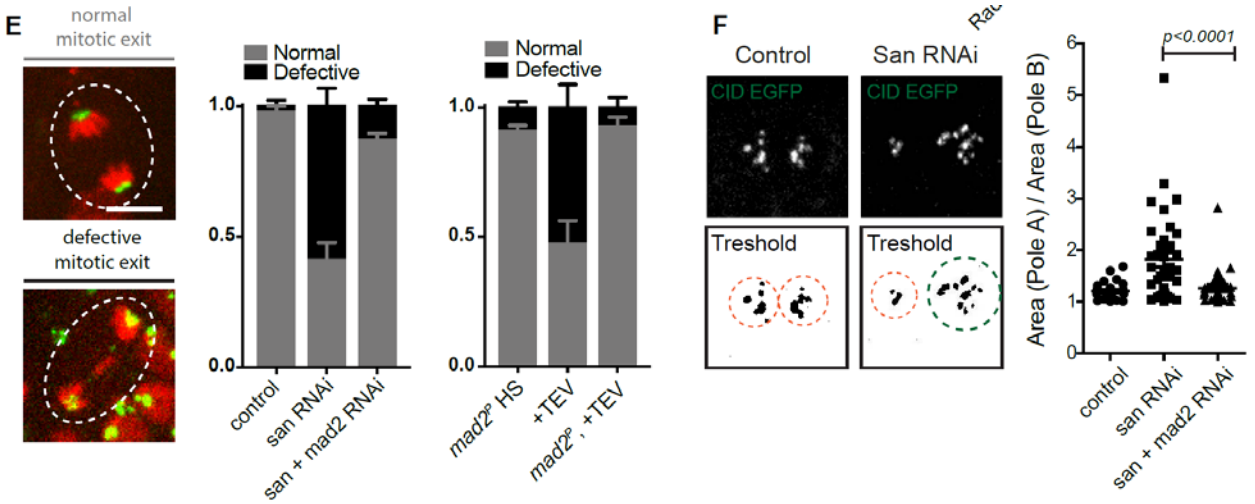

Figure 3E-F SAC removal enhances mitotic fidelity in cohesin absence

E) *Quantification of mitotic exit defects observed in the different experimental conditions; graph represents mean ± SEM of errors of individual discs* ***F)*** *Representative images of mitotic cells from San RNAi undergoing mitosis with normal and defective CID-EGFP distribution; Quantification of CID EGFP symmetry during mitotic exit.*

To further evaluate segregation defects we also estimated numerical errors in chromosome segregation. For this purpose, we measured the area occupied by centromeres in the vicinity of each pole during mitotic exit and segregation symmetry was calculated as the ratio between the areas occupied by each cluster of centromeres (Cid-EGFP) (Figure 3F). As expected, this value was close to one in control strains. San depletion caused a high degree of asymmetry between centromeric signals placed at the poles

(Figure 3F). Importantly, segregation symmetry was significantly restored when San was co-depleted with Mad2 (Figure 3F).

To test whether these results were restricted to larval wing discs, a parallel evaluation of chromosome segregation was performed in early syncytial blastoderm embryos. Cohesin cleavage in *Drosophila* syncytial embryos was induced by microinjection of TEV protease during interphase, as previously described [22]. This led to full separation of sister chromatids after NEBD and a short mitotic delay (Figure 5A, B, Movie S3). To test if such mitotic delay was SAC dependent, we performed similar experiments in a *mad2* mutant background. Mitotic duration under these conditions was indistinguishable from controls, implying that SAC surveillance is responsible for the delay in mitotic progression upon premature loss of sister chromatid cohesion (Figure 5A, B, Movie S3).

Analysis of chromosome distribution revealed strong asymmetry upon cohesin cleavage (Figure 5C). We additionally estimated the frequency of chromosomes that lag behind the segregation plane, ending up in the middle of the segregation plane during mitotic exit (most likely due to merotelic attachments) (Figure 5D).

Consistent with our previous results (Figure 3F), loss of SAC led to a significant reduction of the segregation error frequency after TEV-cleavage, as evidenced by the significant recovery in centromere distribution symmetry and the decrease in lagging centromeres (Figure 5C,D). Altogether, these results demonstrate that SAC inactivation rescues the chromosome segregation defects associated with premature loss of sister chromatid cohesion.

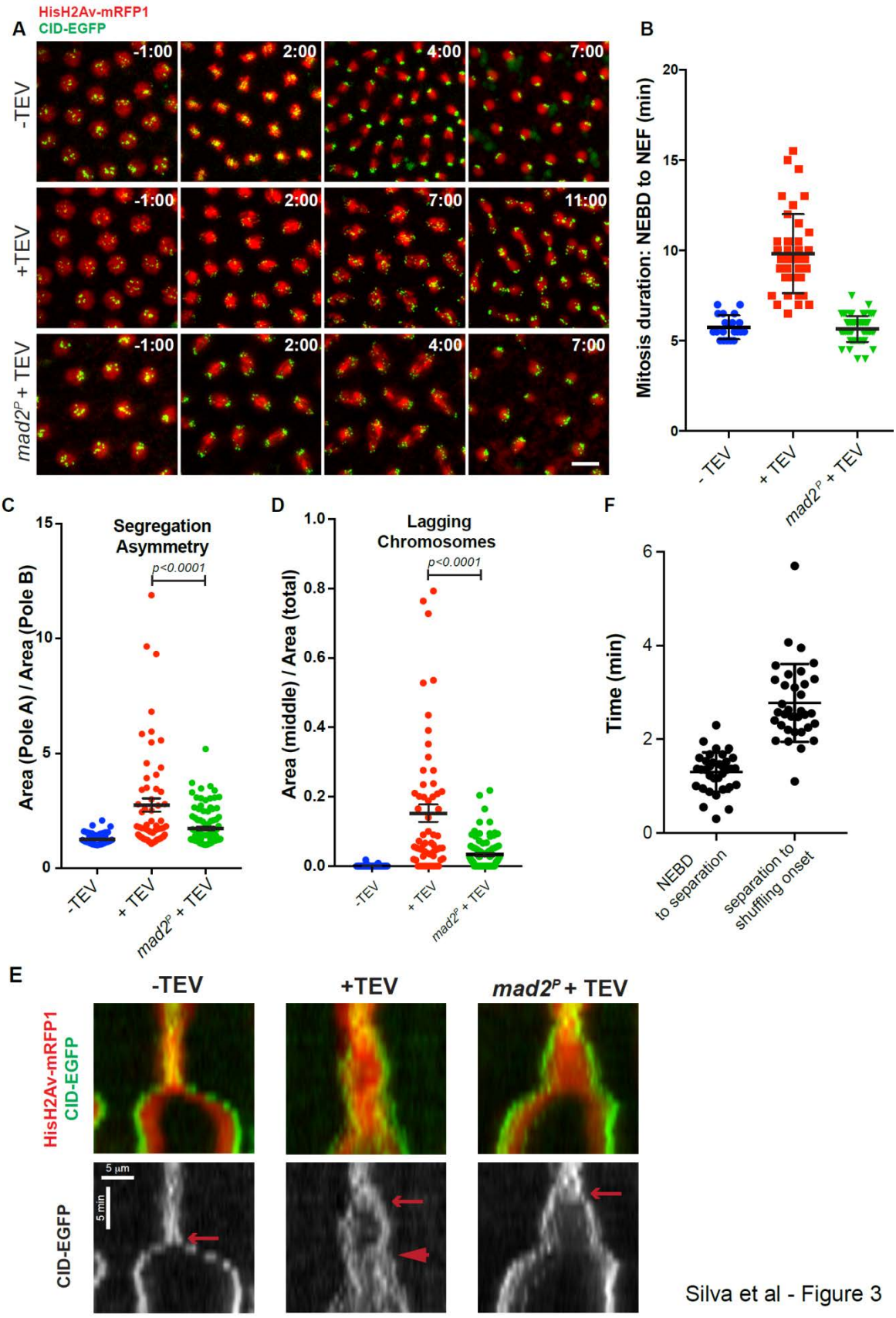

Silva et al - Figure 3

Figure 5. Inhibition of SAC in syncytial blastoderm embryos alleviates mitotic errors caused by premature loss of cohesin.

A) *Embryos surviving solely on Rad21TEV either non-injected (up) or injected with 5 mg/ml TEV protease (middle and bottom panels). Embryos are derived from females that are wild type or homozygous mutant for mad2 gene and express HisH2Av-RFP (red) and CID-EGFP (green). Images were taken every 30 seconds and times are relative to NEBD. Scale bar is 10 µm.* ***B)*** *Quantification of mitotic duration in un-injected embryos and embryos injected with TEV protease in strains containing solely Rad21TEV and wild type or mutant for mad2. The duration of mitosis was measured from nuclear envelope breakdown (NEBD) to nuclear envelope formation (NEF) using HisH2Av-RFP. Images were taken every 30 seconds. Each dot represents a single mitosis and lines represent mean ± SD (n= 20/4 for Rad21TEV no TEV, 40/8 for Rad21TEV + TEV and 55/11 for Rad21TEV+TEV in a mad2P background, n=number of mitosis/number of independent embryos).* ***C****) Quantification of segregation asymmetry in control, cohesin cleavage, and cohesin cleavage in mad2 mutant background. Each value was quantified by normalizing the area of pole A (with higher area) and the area of pole B (lower area) (n= 46/5 for Rad21TEV no TEV, 60/6 for Rad21TEV + TEV and 60/6 for Rad21TEV+TEV in a mad2P background, n=number of telophases/number of independent embryos)* ***D)*** *Relative area of lagging centromeres in control, RAD21TEV + TEV protease, and RAD21TEV + TEV protease in a mad2 mutant background; statistical analysis was performed using one-way ANOVA test.* ***E****) Kymographs of HisH2Av-RFP and CID-EGFP of cells entering mitosis in control, cohesin cleavage, and cohesin cleavage in mad2 mutant background. Arrow points to centromere separation and arrowhead to the shuffling onset. Scale bars are 5 min and 5 µm.* ***F****) Quantification of time for chromosome shuffling onset upon TEV-mediated cohesin cleavage, relative to NEBD. Each dot represents a single dividing nuclei from >10 independent embryos.*

II.3 SAC inactivation suppresses chromosome shuffling after loss of cohesion.

We demonstrated that loss of SAC enhanced mitotic fidelity upon cohesin impairment. The severity of the phenotypes associated with premature cohesion loss is associated with extensive genome randomization. Upon premature cohesin loss, single chromatids lack the opposing forces to ensure proper tension across and/or between kinetochores, leading to unstable microtubule-kinetochore interactions and error correction [8, 23, 24]. These reactions are mediated by Aurora-B kinase that destabilizes kinetochore-microtubule interactions that are not under tension [22-25]. Aurora B activity results in consequent cycles of chromosome attachment and de-attachment, leading to extensive shuffling of isolated sister chromatids between the spindle poles [22, 25]. Therefore, mitosis in absence of cohesion results in random chromosome segregation, with close to absolute probability of generating aneuploid cells.

We postulated that reduction of mitotic timing due to SAC loss limits the degree of chromosome shuffling and enhances mitotic fidelity. To evaluate this hypothesis we probed for genetic interactions between *san* RNAi and RNAi for genes whose depletion should prolong mitotic duration (Source data). In accordance with our hypothesis, RNAi for the APC subunit cdc23 and the cdc20 homologue (Fzy) aggravate the morphological defects in the wing associated with *san* RNAi (Figure 1E and Figure 2B).

The degree of aneuploidy should be proportional to number of events of isolated chromatids crossing the middle of the segregation plane. Therefore, we quantified the frequency of shuffling events, defined as each time one isolated chromatid close to one pole undergoes an erratic motion towards the opposite pole.

In embryos, the SAC-dependent mitotic delay observed upon cohesin cleavage, albeit short (~ 4 min) (Figure 5B), was long enough for a high degree of chromosome shuffling before mitotic exit (movie S3, Figure 6A, B). In the absence of a functional SAC, however, and despite the evident and full premature loss of cohesion, there was a decrease in chromosome shuffling events (Figure 6B and movie S3). Thus, SAC abolishment substantially decreases the amount of shuffling by shortening the mitotic duration.

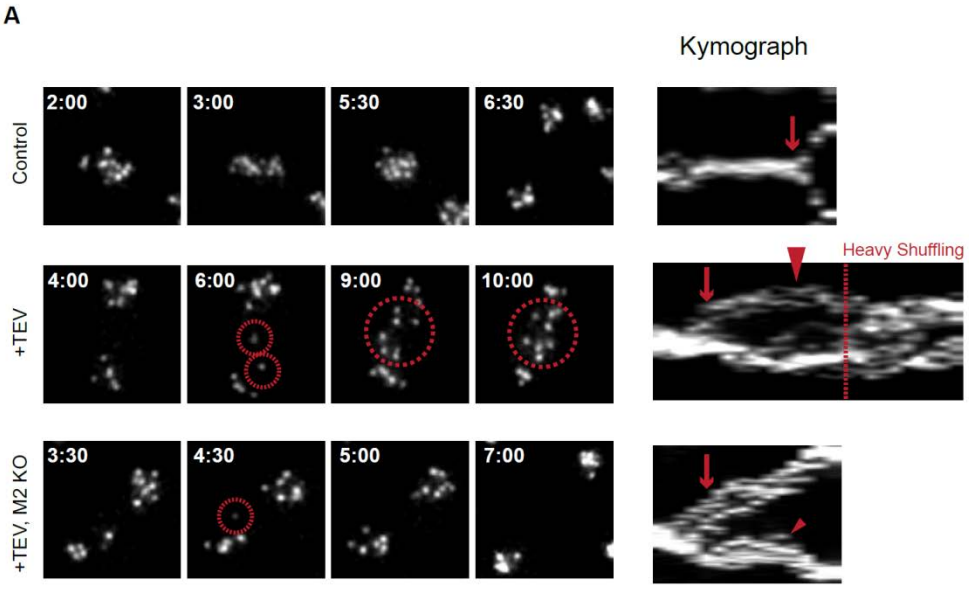

Figure 6A. Analysis of frequency and onset of chromosome shuffling events ***A****) Representative images centromere behaviour (Cid-EGFP) from embryos surviving solely on Rad21^{TEV} that were either non-injected (top), injected with TEV protease (+TEV) or injected with TEV protease in mad2^{P} embryos. Shuffling events were classified as each time centromeres were seen invading and/or crossing the middle of the segregation plane (dashed circles). Right panels depict the corresponding kymograph*

Altogether, these results suggest that despite cohesin loss, engaging into error-correction does not take place during early mitotic stages. To test this possibility, we sought out to measure the kinetics of chromosome shuffling onset upon full loss of sister chromatid cohesion. Analysis of chromosome configuration, both in embryos and wing disc cells, revealed that despite cohesin removal, chromosomes retain a pseudo-metaphase configuration for an extended period of time.

During this pseudo-metaphase stage, sister centromeres were found fully disjoined, confirming loss of sister chromatid cohesion. However, separation of chromatin itself was only initiated several minutes later. Even upon full sister chromatid separation, there was an evident delay in the initiation of chromosome shuffling, implying that sister chromatid separation does not trigger immediate error-correction. To confirm this possibility, the timing of error-correction engagement was analysed using kymographs that plot the positioning of centromeres along the segregation plane over time. The time of centromere separation can be easily detected by the split in centromere signals and the onset of chromosome shuffling by the time centromeres start crossing the middle of the segregation plane (Figure 5E arrow and arrow heads, respectively). This analysis revealed that upon cohesin cleavage, chromosome shuffling was only initiated 4.07±0.96 min after NEBD (1.3±0.4min for NEBD to centromere separation and 2.8±0.8min from centromere separation to initiation of shuffling) (Figure 5F).

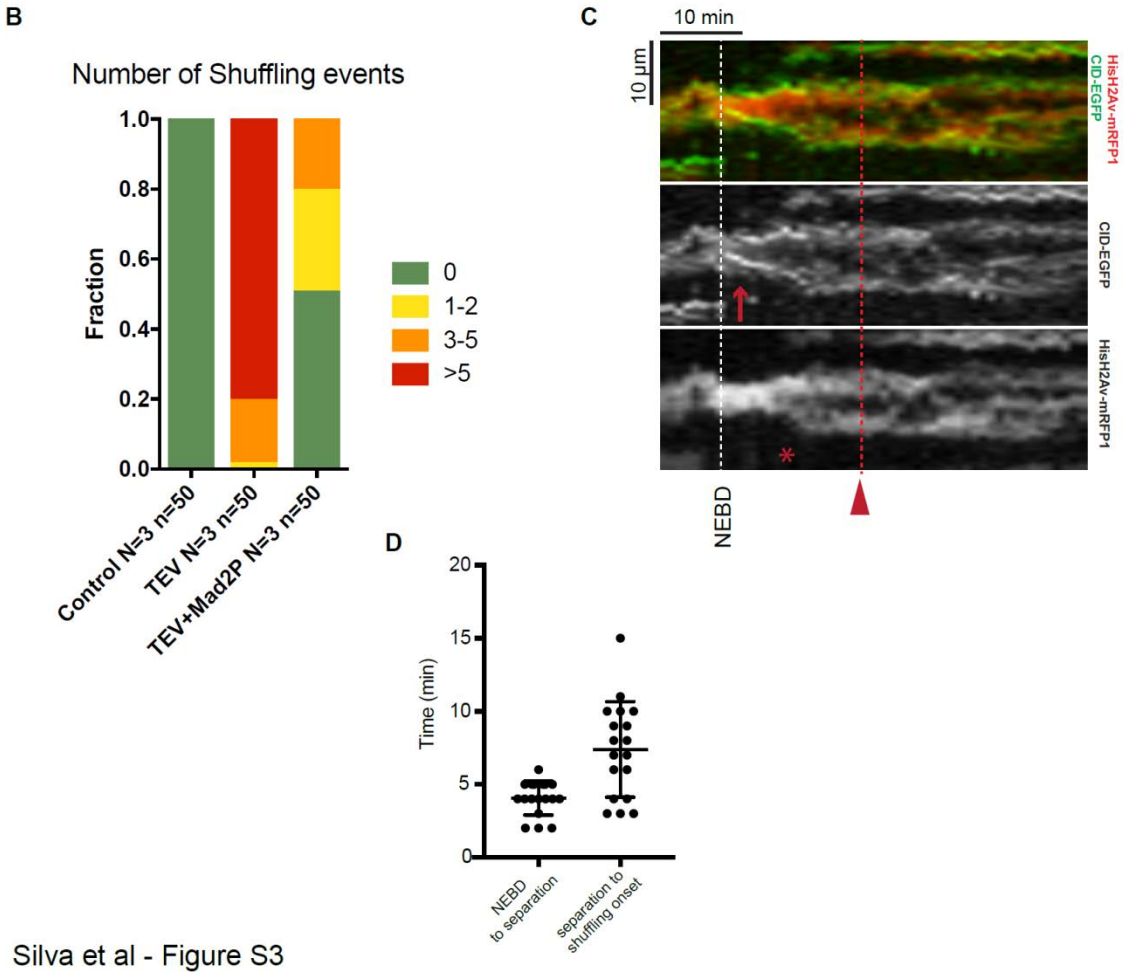

Figure 6B-D. Analysis of frequency and onset of chromosome shuffling events B) *Frequency of chromosome shuffling events quantified as in exemplified in A.* ***C****) Kymograph of HisH2AvD-mRFP1 and CID-EGFP of nuclei entering mitosis upon TEV-mediated cohesin cleavage in a SAC-competent wing disc cell. Scale bars are 10 min and 10 µm. Note that centromere separation (arrow) precedes chromosome individualization (*). Onset of chromosome shuffling is also indicated (arrowhead)* ***D****) Quantification of time between NEBD and centromere separation and centromere separation and the onset of chromosome shuffling in wing disc cells, upon TEV-mediated cohesin cleavage, relative to NEBD. Each dot represents a single cell derived from 4 independent wing discs.*

This analysis reveals a significant delay in the initiation of major error-correction events. A similar, yet extended behaviour was also observed in larvae wing disc cells. Upon NEBD, chromosomes retained a prolonged pseudo-metaphase configuration despite sister chromatid separation (as judged by centromere distances) and chromosome shuffling was only observed much later (11.4± 2.9min after NEBD, Figure 6C, D). The observed delay in extensive shuffling engagement is similar to the mitotic timing in the absence of a functional SAC (Figures 3B, D and 5B). Thus, SAC counteracts genome shuffling in the absence of cohesin by shortening mitosis duration and thereby preventing extensive error-correction.

A key prediction from this observation is that initial kinetochore-microtubule interactions are quite accurate, and that inhibition of error-correction, through modulation of Aurora B activity, should restore mitotic fidelity to a similar extent as SAC inactivation does. Knowing that Aurora B has multiple roles during mitosis [26], we first titrated the levels of Aurora B inhibitor, Binucleine 2, to a concentration that does not impair chromosome condensation, mitotic timing, SAC competency, or separation of daughter nuclei in dividing wing disc cells (Figure 7A-D). Using such concentration (5µM), we show that mild Aurora B inhibition shortened the mitotic delay induced by TEV-mediated Rad21 cleavage (Figure 7E).

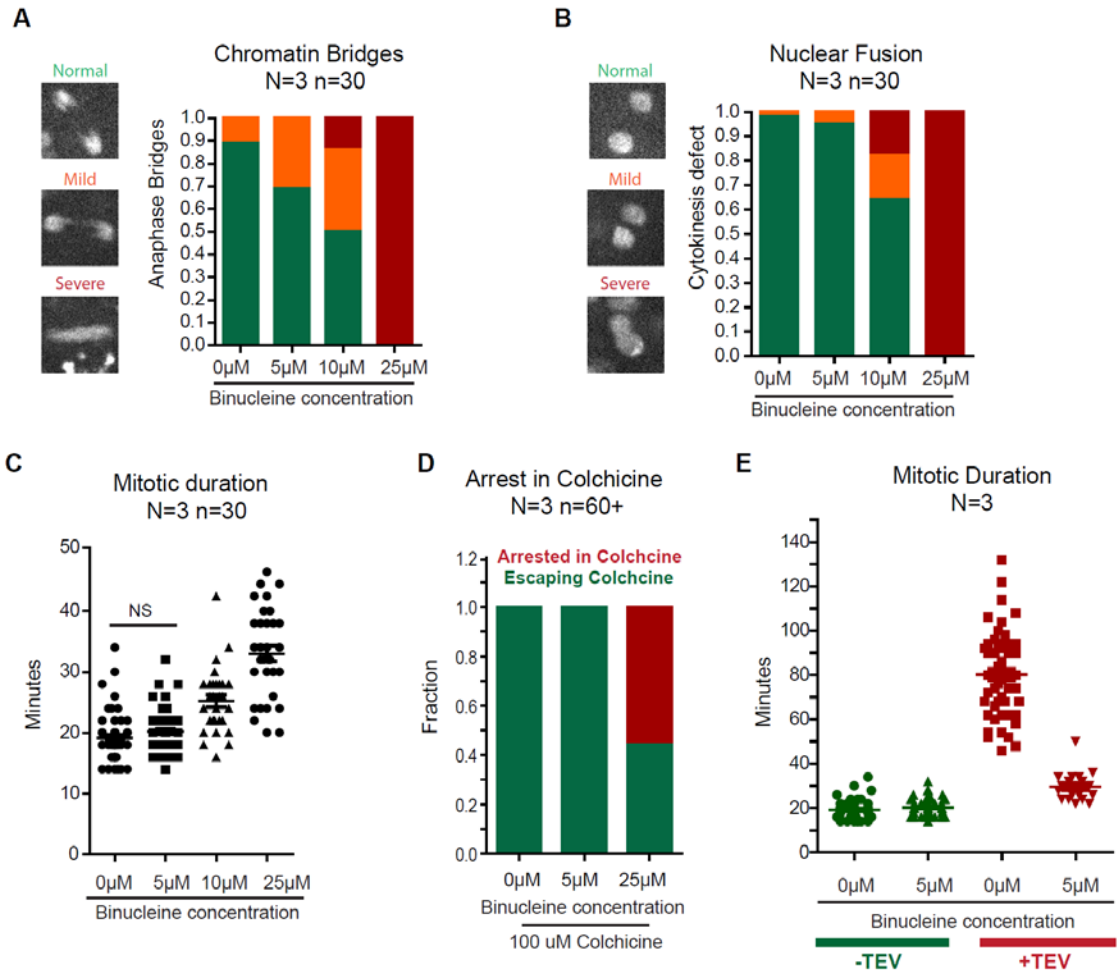

Figure 7A-E Binucleine 2 titration and effect on mitotic timing upon cohesin depletion by TEV

A-E) *Titration of Binucleine 2 concentration (0-25μm) to examine the inhibitor dose effect on chromosome condensation, nuclear separation, mitotic duration and SAC competency in control cells. Still images from live imaging of the wing disc pouch. Graphs depict frequencies or time (in minutes), N represents the number of independent wing discs and n the number of analysed cells.* ***E)*** *Mitotic duration of control, TEV cleavage and TEV+B2 incubated wing disc cells. N represents the number of independent wing discs and each dot corresponds to a single cell.*

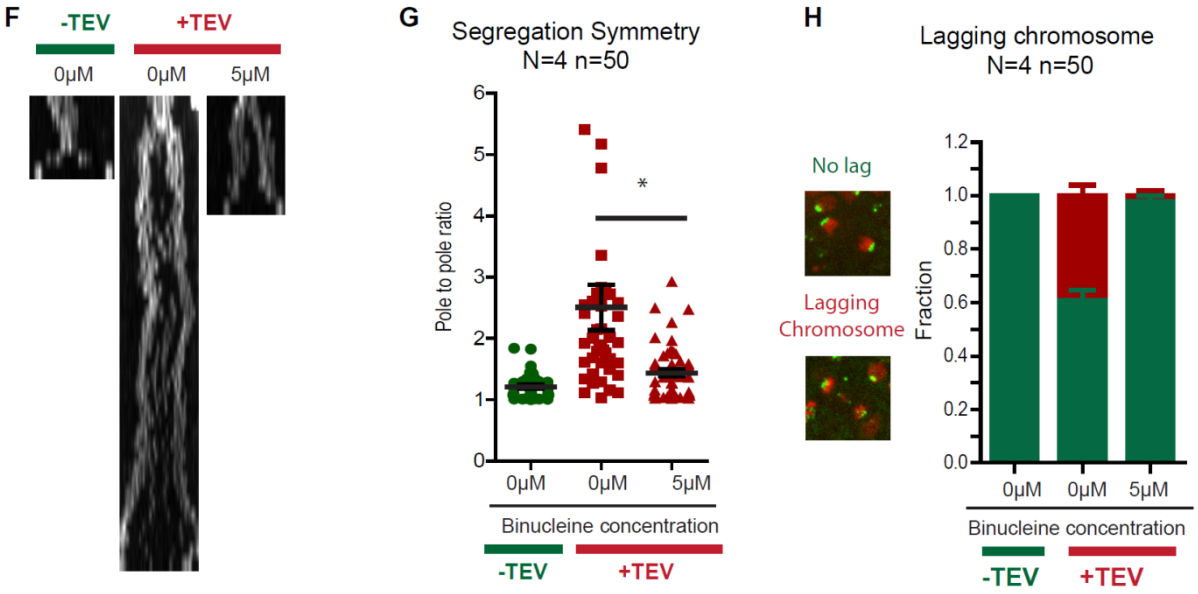

Figure 7. F-H Aurora B inhibition prevents chromosome shuffling and improves mitotic fidelity upon cohesin cleavage.

F) *A kymograph representing centromere positioning (Cid-EGFP) from Control, TEV cleavage, and TEV cleavage with 5μM Binucleine incubation.* ***G)*** *Segregation symmetry of control, TEV cleavage and TEV+ 5μM B2 incubated wing disc cells* ***H)*** *Lagging chromosome at anaphase frequency for control, TEV cleavage and TEV+B2 incubated wing disc cells*

Furthermore, this treatment completely abolished chromosome shuffling and motion after the initial separation of single chromatids to the poles (Figure 7F Movie S4). Importantly, such decrease in Aurora B activity is sufficient to restore centromere segregation symmetry upon premature cohesion loss, and eliminate the frequency of lagging chromosomes during mitotic exit (Figure 7G, H).

We therefore conclude that initial capture of kinetochores by the microtubules has a strong bias for symmetry, even in the complete absence of cohesin. Major asymmetry in chromosome distribution, in turn, depends on error correction events.

II.4 SAC inactivation restores cell survival after loss of cohesion.

Our results indicate that the mitotic defects upon loss of cohesion are less detrimental in the absence of SAC. If so, the degree of aneuploidy should follow a similar trend. Larvae wing discs are well known to eliminate cells with an erroneous DNA content by apoptosis [16, 17]. Therefore, SAC inactivation should reduce the levels of apoptosis after loss of cohesion. To evaluate the extent of apoptosis upon full cohesion loss, larvae carrying a TEV-sensitive Rad21 were heat-shocked to induce TEV protease expression and wing discs were dissected 24h after heat-shock. Virtually no apoptosis was detected (staining for cleaved caspase 3 (CC3)) within the control wing discs ($Rad21^{TEV}$ in the absence of TEV protease) (Figure 8A, B). In contrast, TEV-mediated cohesin cleavage induced high levels of apoptosis within 24hr, extending to over 15±2% (mean ± SD, n=7) of the entire wing disc area (Figure 8A, B). Remarkably, the levels of apoptosis were significantly reduced if cohesin loss was induced in the absence of a functional SAC (3±3%, mean ± SD, n=10) (Figure 8A, B). Similar results were obtained upon depletion of San (*san* RNAi), where apoptosis covered approximately 7±4% (mean ± SD, n=5) of the wing disc pouch area, compared to only approximately 0.9±0.6% (mean ± SD, n=6) of the pouch area after co-depletion of San and Mad2 (Figure 8C, D). These results show that inactivation of SAC in a

proliferating tissue significantly increases cell survival upon loss of cohesion.

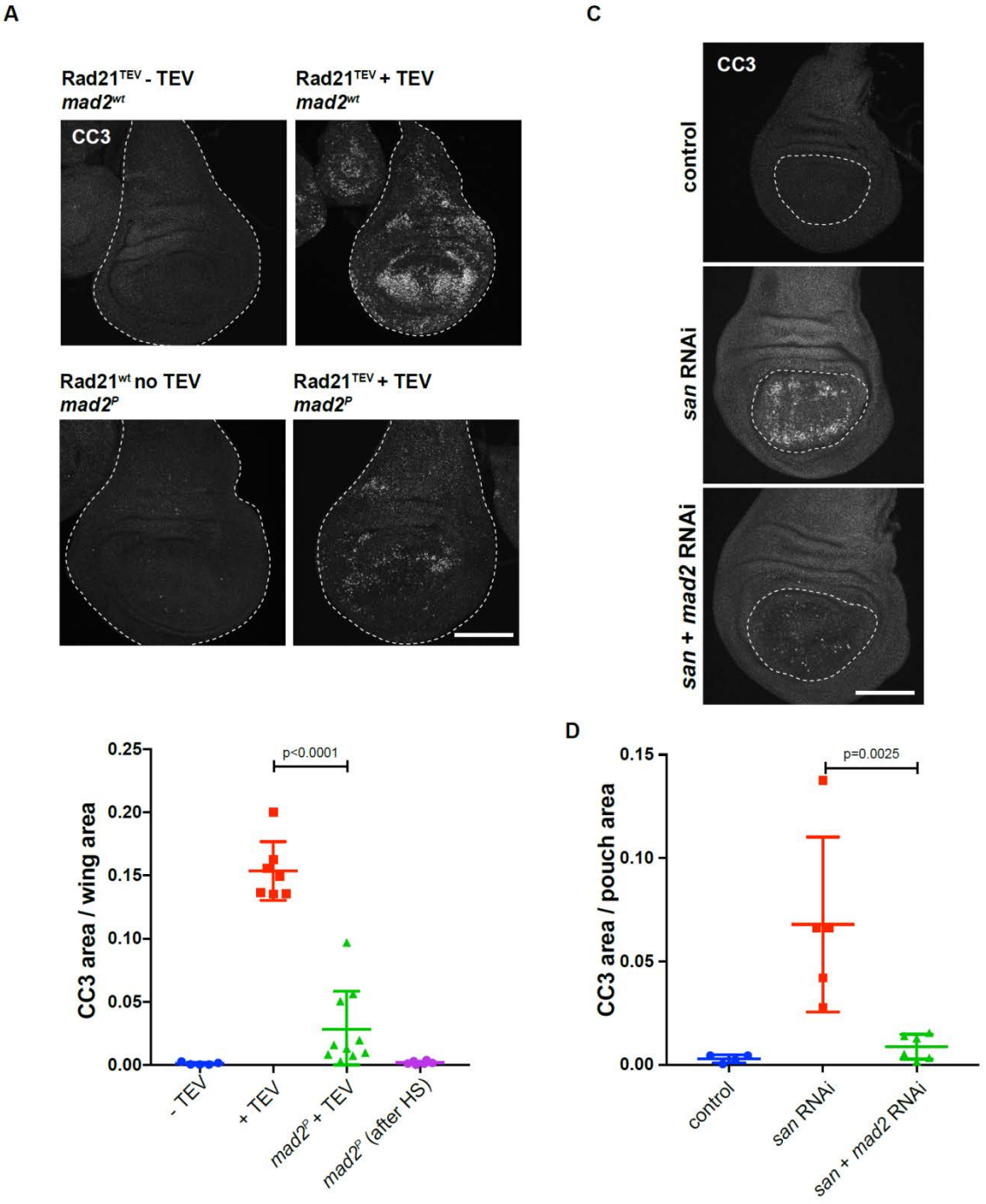

Figure 8. Inhibition of SAC suppresses imaginal wing disc apoptosis caused by premature loss of cohesin.

A) *Images of Cleaved Caspase 3 (CC3) immunofluorescence in controls (Rad21TEV without TEV and mad2P after heat-shock (HS)), RAD21TEV + TEV protease and RAD21TEV + TEV protease in mad2 mutant background after HS. Scale bar is 100 µm.* ***B)*** *Quantification of CC3 positive area of the entire wing disc, in the indicated experimental conditions; n≥ 5 independent discs per experimental condition; statistical analysis was performed using one-way ANOVA test.* ***C)*** *Representative images of CC3 immunofluorescence in control, san RNAi and san and mad2 double RNAi.* ***D)*** *Quantification of CC3 positive area of the wing disc pouch, in control, san, and san and mad2 RNAi; n≥ 4 independent discs per experimental condition; multiple comparison analysis was perform using a one-way ANOVA test.*

II.5 Discussion

In agreement with the "safeguard" function for the Spindle Assembly Checkpoint, mitotic errors are often exacerbated by impairment of the SAC. These include defects associated with multiple centrosomes, defective microtubule assembly or kinetochore structure [27-31]. Here we demonstrate that the opposite happens with regard to cohesion defects. Absence of the SAC alleviated mitotic errors and improved mitotic fidelity after cohesion loss. Cells with a functional SAC undergo extensive chromosome shuffling and consequent randomization of the genome, whereas virtually no shuffling could be observed in absence of the SAC. The detrimental nature of SAC in the presence of cohesion defects is likely related to the irreversibility of cohesion loss. Most mitotic defects can be corrected over time (e.g. SAC-mediated mitotic delay enables clustering of multiple

centrosomes [32]). In sharp contrast, premature cohesin loss is an irreversible error and prolonging mitosis duration further enhances genome randomization.

The improved mitotic fidelity after cohesion loss in the absence of SAC is likely a consequence of slow kinetics of error-correction engagement coupled with a bias for chromosome orientation towards a correct alignment. Several mechanisms are known to bias chromosome segregation towards the right orientation, including chromosome positioning [33], centromere geometry [34], bias on microtubule growth towards the kinetochores [35, 36] and/or kinetochore-mediated microtubule nucleation [37, 38]. Of these, chromosome geometry is believed to facilitate bipolar attachment by facing one kinetochore to the opposite pole upon attachment to a pole. If so, what ensures geometric arrangement during the initial mitotic stages, even in the absence of cohesin? A possible mechanism enabling a transient organization of sister chromatids towards opposing poles is incomplete resolution of sister chromatid intertwines. Yet, residual catenation present in metaphase chromosomes is unable to confer functional cohesion as removal of cohesin is sufficient to induce immediate sister chromatid separation [4, 22]. Additional mechanisms may thus impair prompt resolution of sister chromatids specifically during early mitosis, in contrast what is observed in metaphase chromosomes. Spindle forces were described to enhance decatenation [39-41] and thus resolution of several DNA-intertwines may only be achieved upon chromosome capture. Recent findings propose that efficient decatenation requires constant “guiding action” from condensin I [42]. Maximal levels of this complex are only observed on mitotic chromosomes once in

late-metaphase/anaphase [43, 44], which could also limit full decatenation to the later stages of mitosis. Residual catenation is unable to sustain cohesion and chromosome alignment in a SAC competent cell, yet it may be nevertheless sufficient to allow a transient pseudo-metaphase alignment that biases initial chromosome attachment to the right orientation. Although certainly error-prone, this process would be more accurate than the total genome randomization due to extensive chromosome shuffling.

Why separated single sisters are inefficient at triggering error-correction mechanisms during early mitosis remains to be addressed. This could be related to a partial tension state facilitated by pseudo-metaphase chromosomal configuration, precluding error-correction activation. Additionally, an intrinsic delayed action of error correction machinery may further account for observed late shuffling onset. Indeed, slow kinetics or a lag time of Aurora B-mediated chromosome detachment has been hypothesized in several theoretical studies [45-47] but so far little experimental observations support this claim. Such intrinsic delay would solve the “problem of initiation of biorientation” whereby initial interactions (necessarily under low tension) are able to survive such a tension-sensitive mechanism for chromosome detachment [24, 45].

Interestingly, the interplay between mitotic timing and sister chromatid cohesion has been previously reported in mammalian cells whereby extension of mitosis predisposes to sister chromatid cohesion defects. Cells arrested in mitosis for long periods were shown to display sister chromatid separation (referred as “cohesion fatigue”) [48]. Moreover, defective sister chromatid cohesion was

described to be synthetically lethal with impaired APC/C function in Warsaw breakage syndrome (WABS) patient-derived cells as well as several cancer cell lines with cohesion defects [49]. Our observations now demonstrate how reduction of mitotic timing is sufficient to rescue segregation defects associated with premature cohesin loss. Importantly, these experiments highlight the detrimental effect of the SAC upon cohesion defects. When sister chromatid cohesion is compromised, and thus mitotic fidelity irreversibly affected, the SAC exacerbates mitotic errors in contrast to its canonical protective function.

II.6 Materials and Methods

Drosophila strains and rearing conditions

Drosophila melanogaster flies were raised at 25ºC or 18ºC for hs-TEV containing crosses in polypropylene vials (51 mm diameter) containing enriched medium (cornmeal, molasses, yeast, soya flour and beetroot syrup). All RNAi lines used in the screen are from the Transgenic RNAi project (TRiP), are available in the Bloomington Drosophila Stock Center and are listed in the Source Data file. Other *Drosophila* stocks used in this study are also indicated in Source Data file (S5). To induce full cohesin cleavage in a temporally controlled manner, by TEV protease cleavage, *Drosophila* strains were used with TEV-cleavable Rad21 ($Rad21^{TEV}$) in a Rad21-null background (*rad21*^{ex15}*, Rad21*$^{271\text{-}3TEV}$*-myc* or *rad21*^{ex15}*, Rad21*$^{550\text{-}3TEV}$*-EGFP*) [19, 50], in strains mutant or wild type for the Mad2 gene [21, 51]. TEV expression was induced by heat-shocking 3rd instar larvae at 37ºC for 45 minutes. Larvae were then left to recover at room temperature. For live cell imaging,

fly strains also expressed *His2AvD-mRFP1* and *Cid-EGFP* [52] fluorescent markers.

Drosophila screen Details

In the screen we analysed 2955 RNAi lines that theoretically deplete 2920 proteins, corresponding to approximately 21% of all protein coding genes annotated in Flybase (Flybase versionFB2017_06). To select the lines to test we followed a list of available RNAi downloaded from the TRiP website. In this list, the lines are ordered alphabetically, according to gene name or CG number. However, our results do not strictly follow this list, since we mainly used lines constructed with Vallium20 or Valium22 vectors and some lines did not survive shipping. In the screen, females carrying the nubbin-Gal4, UAS-*san* RNAi were crossed with males of different RNAi lines from TRiP (see diagram in Figure S1A). The progeny of these flies were classified into different classes according to the adult wing phenotypes: class 1 - wild type wings; class 2 – flies with wings that present only mild morphological defects; class 3- flies whose wing morphological defects are intermediate (similar *san* RNAi); class 4 – flies whose wings show strong morphological defects; class 5 – flies without wings or vestigial wings (Figure 1C) [15]. The average adult wing class for each condition was always calculated using more than 50 adult flies ($n \geq 50$). If the average class for a given genetic interaction was equal or below 2.6 than the RNAi line tested was classified as suppressor, if the average class was equal or above 3.5 than the RNAi line was classified as enhancer (Figure S1A). To exclude RNAi lines whose expression by itself led to wing morphological defects, in otherwise wild type imaginal discs, we crossed all lines carrying RNAis identified in the first cross with

nubbin-Gal4 and discarded all RNAi lines that were enhancers and produced significant phenotypes by itself (Figure S1A).

Live imaging

For imaging of wing discs, larval imaginal wing discs were dissected in Schneider medium with 10% FBS. Dissected discs were placed and oriented in a 200µl drop of medium at the bottom of a glass-bottom petridish (MakTek). For Aurora B inhibition experiments (Figure S4), discs were incubated with Binuclein 2 (Sigma-Aldrich) at the indicated concentrations. Time lapse imaging analysis was performed on a spinning disc microscope using either a Revolution XD microscope (Andor, UK), equipped with immersion a 60x (water) and 100x (oil) objectives (Nikon, Japan) and a iXon +512 EMCCD camera (Andor, UK), or a Revolution XD microscope (Andor, UK) equipped with immersion a 60x glycerol-immersion 1.30 NA objective (Leica Microsystems, Germany) and a 100x oil-immersion 1.4 NA objective (Leica Microsystems, Germany) and a iXon Ultra 888 1024*1024 EMCCD (Andor, UK). Stacks of 20-30 frames 0,5 µm apart were taken every 1 to 3 minutes. For syncytial embryo imaging, embryos were aligned on coverslips and covered with Series 700 halocarbon oil (Sigma-Aldrich). Time-lapse microscopy was performed with an inverted wide-field DeltaVision microscope (Applied Precision Inc., Issaquah, WA) in a temperature-controlled room (18–20°C). One stack of 15 frames (0.8 mm apart) was acquired every 30 sec with a 100x 1.4 oil immersion objective (Olympus, Japan) and captured by an EMCCD camera (Roper Cascade 1024, Roper Technologies). Movies were assembled using FIJI software [53] and selected stills were processed with Photoshop CS6 (Adobe).

Microinjections

Microinjections were performed as previously described [22, 42]. 1-1.5 hr old embryos were collected and processed according to standard protocols, and were injected at the posterior pole. Injections were performed using a Burleigh Thorlabs Micromanipulator, a Femtojet microinjection system (Eppendorf, Germany), and pre-pulled Femtotip I needles (Eppendorf). TEV protease was injected at 5 mg/ml TEV protease in 20 mM Tris-HCl at pH 8.0, 1 mM EDTA, 50 mM NaCl and 2 mM DTT.

Immunofluorescence

Third instar wing imaginal disc fixation and staining was performed using standard procedures (Lee and Treisman, 2001). Briefly, third instar larvae wing disc tissue (still attached to the larva body) was fixed on ice for 30 min. The fixative consisted of 4% formaldehyde (Polysciences) in 1X PEM buffer solution. Following were washed by gentle agitation three times for 20 min in PBS-T (1x PBS + 0.1% Triton X-100). Primary antibodies incubation was performed overnight at 4 °C in PBS-T supplemented with 1% BSA and 1% donkey serum. The following day, the tissues were washed again and incubated for 2h at room temperature with the appropriate secondary antibodies diluted in PBS-T solution. Finally, after the wash of the secondary antibodies, wing discs were mounted in Vectashield (Vector Laboratories). Fluorescence images were acquired with a ×40 HCX PL APO CS oil immersion objective (numerical aperture: 1.25–0.75) on a Leica SP5 confocal microscope. Rabbit anti-cleaved caspase 3 at 1:300 (Cell

Signaling, 9661S) and anti-Rabbit Alexa Fluor 488 at 1:1000 (Molecular Probes).

Quantifications and statistics

Imaging analysis was performed using FIJI software [53]. Statistical analysis and graphic representations were performed using Prism 7 software. Multiple comparisons were performed using one-way ANOVA, using the Bonferroni's multiple comparison test. Graphs depict mean ± standard deviations (SD) or mean ± standard error of the mean (SEM), as indicated. Sample size details are included in the respective figure legends.

Acknowledgements

We thank S. Heidmann, C. Lehner, R. Karess and the Bloomington Stock Center for fly strains and antibodies, all the members of the Oliveira and Martinho laboratories for discussions, Ricardo Matos for assistance with graphic design and Bárbara Kellen for technical assistance in the pilot screen. We acknowledge the TRiP at Harvard Medical School (NIH/NIGMS R01-GM084947) for providing several transgenic RNAi fly stocks used in this study. The following authors were supported by Portuguese national funding (Fundação para a Ciência e Tecnologia, FCT), fellowships: Rui D. Silva (SFRH/BPD/87482/2012), Mihailo Mirkovic (SFRH /BD/52438/2013) and Om S. Rathore (PD/BD/52428/2013, within the scope of the ProRegeM PhD program Ref. PD/00117/2012, CRM:0027030). Rui Gonçalo Martinho is supported by funding from the Association for International Cancer Research [AICR 10–0553] and the following FCT grants: PTDC/BEX-BID/0395/2014 and UID/BIM/04773/2013 CBMR 1334. Raquel A Oliveira is supported by the following grants: FCT Investigator grant

(IF/00851/2012/CP0185/CT0004), EMBO Installation Grant (IG2778) and European Research Council Starting Grant (ERC-2014-STG-638917).

Authors Contributions

R.D.S.: Conceptualization, Investigation, Writing (review & editing). M.M.: Conceptualization, Investigation, Writing (review & editing). L.G.G.: Investigation. O.S.R.: Investigation. R.G.M: Conceptualization, Writing (original draft + review & editing), Funding acquisition. R.A.O.: Conceptualization, Investigation, Writing (original draft + review & editing), Funding acquisition.

Conflict of Interest Statement

The authors declare that they have no conflict of interest.

References

1. Michaelis, C., Ciosk, R., and Nasmyth, K. (1997). Cohesins: chromosomal proteins that prevent premature separation of sister chromatids. Cell *91*, 35-45.
2. Guacci, V., Koshland, D., and Strunnikov, A. (1997). A direct link between sister chromatid cohesion and chromosome condensation revealed through the analysis of MCD1 in S. cerevisiae. Cell *91*, 47-57.
3. Haering, C.H., Farcas, A.M., Arumugam, P., Metson, J., and Nasmyth, K. (2008). The cohesin ring concatenates sister DNA molecules. Nature *454*, 297-301.
4. Uhlmann, F., Wernic, D., Poupart, M.A., Koonin, E.V., and Nasmyth, K. (2000). Cleavage of cohesin by the CD clan protease separin triggers anaphase in yeast. Cell *103*, 375-386.
5. Uhlmann, F., Lottspeich, F., and Nasmyth, K. (1999). Sister-chromatid separation at anaphase onset is promoted by cleavage of the cohesin subunit Scc1. Nature *400*, 37-42.
6. Mirkovic, M., and Oliveira, R.A. (2017). Centromeric Cohesin: Molecular Glue and Much More. Prog Mol Subcell Biol *56*, 485-513.
7. Musacchio, A., and Salmon, E.D. (2007). The spindle-assembly checkpoint in space and time. Nature reviews. Molecular cell biology *8*, 379-393.
8. Foley, E.A., and Kapoor, T.M. (2013). Microtubule attachment and spindle assembly checkpoint signalling at the kinetochore. Nature reviews. Molecular cell biology *14*, 25-37.
9. Williams, B.C., Garrett-Engele, C.M., Li, Z., Williams, E.V., Rosenman, E.D., and Goldberg, M.L. (2003). Two putative acetyltransferases, san and deco, are required for establishing sister chromatid cohesion in Drosophila. Current biology : CB *13*, 2025-2036.

10. Ribeiro, A.L., Silva, R.D., Foyn, H., Tiago, M.N., Rathore, O.S., Arnesen, T., and Martinho, R.G. (2016). Naa50/San-dependent N-terminal acetylation of Scc1 is potentially important for sister chromatid cohesion. Sci Rep *6*, 39118.
11. Hou, F., Chu, C.W., Kong, X., Yokomori, K., and Zou, H. (2007). The acetyltransferase activity of San stabilizes the mitotic cohesin at the centromeres in a shugoshin-independent manner. The Journal of cell biology *177*, 587-597.
12. Rong, Z., Ouyang, Z., Magin, R.S., Marmorstein, R., and Yu, H. (2016). Opposing Functions of the N-terminal Acetyltransferases Naa50 and NatA in Sister-chromatid Cohesion. J Biol Chem *291*, 19079-19091.
13. Brand, A.H., and Perrimon, N. (1993). Targeted gene expression as a means of altering cell fates and generating dominant phenotypes. Development *118*, 401-415.
14. Ng, M., Diaz-Benjumea, F.J., Vincent, J.P., Wu, J., and Cohen, S.M. (1996). Specification of the wing by localized expression of wingless protein. Nature *381*, 316-318.
15. Wu, J., and Cohen, S.M. (2002). Repression of Teashirt marks the initiation of wing development. Development *129*, 2411-2418.
16. Poulton, J.S., Cuningham, J.C., and Peifer, M. (2014). Acentrosomal Drosophila epithelial cells exhibit abnormal cell division, leading to cell death and compensatory proliferation. Developmental cell *30*, 731-745.
17. Dekanty, A., Barrio, L., Muzzopappa, M., Auer, H., and Milan, M. (2012). Aneuploidy-induced delaminating cells drive tumorigenesis in Drosophila epithelia. Proceedings of the National Academy of Sciences of the United States of America *109*, 20549-20554.
18. Ryoo, H.D., Gorenc, T., and Steller, H. (2004). Apoptotic cells can induce compensatory cell proliferation through the JNK and the Wingless signaling pathways. Developmental cell *7*, 491-501.

19. Pauli, A., Althoff, F., Oliveira, R.A., Heidmann, S., Schuldiner, O., Lehner, C.F., Dickson, B.J., and Nasmyth, K. (2008). Cell-type-specific TEV protease cleavage reveals cohesin functions in Drosophila neurons. Developmental cell *14*, 239-251.
20. Liu, X., and Winey, M. (2012). The MPS1 family of protein kinases. Annu Rev Biochem *81*, 561-585.
21. Buffin, E., Emre, D., and Karess, R.E. (2007). Flies without a spindle checkpoint. Nature cell biology *9*, 565-572.
22. Oliveira, R.A., Hamilton, R.S., Pauli, A., Davis, I., and Nasmyth, K. (2010). Cohesin cleavage and Cdk inhibition trigger formation of daughter nuclei. Nature cell biology *12*, 185-192.
23. Nezi, L., and Musacchio, A. (2009). Sister chromatid tension and the spindle assembly checkpoint. Curr Opin Cell Biol *21*, 785-795.
24. Khodjakov, A., and Pines, J. (2010). Centromere tension: a divisive issue. Nature cell biology *12*, 919-923.
25. Mirkovic, M., Hutter, L.H., Novak, B., and Oliveira, R.A. (2015). Premature Sister Chromatid Separation Is Poorly Detected by the Spindle Assembly Checkpoint as a Result of System-Level Feedback. Cell reports *13*, 470-478.
26. Carmena, M., Wheelock, M., Funabiki, H., and Earnshaw, W.C. (2012). The chromosomal passenger complex (CPC): from easy rider to the godfather of mitosis. Nature reviews. Molecular cell biology *13*, 789-803.
27. Gogendeau, D., Siudeja, K., Gambarotto, D., Pennetier, C., Bardin, A.J., and Basto, R. (2015). Aneuploidy causes premature differentiation of neural and intestinal stem cells. Nature communications *6*, 8894.
28. Poulton, J.S., Cuningham, J.C., and Peifer, M. (2017). Centrosome and spindle assembly checkpoint loss leads to neural apoptosis and reduced brain size. The Journal of cell biology *216*, 1255-1265.
29. Lee, M.S., and Spencer, F.A. (2004). Bipolar orientation of chromosomes in Saccharomyces cerevisiae is monitored by

Mad1 and Mad2, but not by Mad3. Proceedings of the National Academy of Sciences of the United States of America *101*, 10655-10660.

30. Tarailo, M., Tarailo, S., and Rose, A.M. (2007). Synthetic lethal interactions identify phenotypic "interologs" of the spindle assembly checkpoint components. Genetics *177*, 2525-2530.
31. Daniel, J.A., Keyes, B.E., Ng, Y.P., Freeman, C.O., and Burke, D.J. (2006). Diverse functions of spindle assembly checkpoint genes in Saccharomyces cerevisiae. Genetics *172*, 53-65.
32. Basto, R., Brunk, K., Vinadogrova, T., Peel, N., Franz, A., Khodjakov, A., and Raff, J.W. (2008). Centrosome amplification can initiate tumorigenesis in flies. Cell *133*, 1032-1042.
33. Magidson, V., O'Connell, C.B., Loncarek, J., Paul, R., Mogilner, A., and Khodjakov, A. (2011). The spatial arrangement of chromosomes during prometaphase facilitates spindle assembly. Cell *146*, 555-567.
34. Tanaka, T., Fuchs, J., Loidl, J., and Nasmyth, K. (2000). Cohesin ensures bipolar attachment of microtubules to sister centromeres and resists their precocious separation. Nature cell biology *2*, 492-499.
35. Carazo-Salas, R.E., Guarguaglini, G., Gruss, O.J., Segref, A., Karsenti, E., and Mattaj, I.W. (1999). Generation of GTP-bound Ran by RCC1 is required for chromatin-induced mitotic spindle formation. Nature *400*, 178-181.
36. Wollman, R., Cytrynbaum, E.N., Jones, J.T., Meyer, T., Scholey, J.M., and Mogilner, A. (2005). Efficient chromosome capture requires a bias in the 'search-and-capture' process during mitotic-spindle assembly. Current biology : CB *15*, 828-832.
37. Maiato, H., Rieder, C.L., and Khodjakov, A. (2004). Kinetochore-driven formation of kinetochore fibers contributes to spindle assembly during animal mitosis. The Journal of cell biology *167*, 831-840.

38. Kitamura, E., Tanaka, K., Komoto, S., Kitamura, Y., Antony, C., and Tanaka, T.U. (2010). Kinetochores generate microtubules with distal plus ends: their roles and limited lifetime in mitosis. Developmental cell *18*, 248-259.
39. Baxter, J., Sen, N., Martinez, V.L., De Carandini, M.E., Schvartzman, J.B., Diffley, J.F., and Aragon, L. (2011). Positive supercoiling of mitotic DNA drives decatenation by topoisomerase II in eukaryotes. Science *331*, 1328-1332.
40. Charbin, A., Bouchoux, C., and Uhlmann, F. (2014). Condensin aids sister chromatid decatenation by topoisomerase II. Nucleic Acids Res *42*, 340-348.
41. Mariezcurrena, A., and Uhlmann, F. (2017). Observation of DNA intertwining along authentic budding yeast chromosomes. Genes Dev.
42. Piskadlo, E., Tavares, A., and Oliveira, R.A. (2017). Metaphase chromosome structure is dynamically maintained by condensin I-directed DNA (de)catenation. Elife *6*.
43. Gerlich, D., Hirota, T., Koch, B., Peters, J.M., and Ellenberg, J. (2006). Condensin I Stabilizes Chromosomes Mechanically through a Dynamic Interaction in Live Cells. Current biology : CB *16*, 333-344.
44. Oliveira, R.A., Heidmann, S., and Sunkel, C.E. (2007). Condensin I binds chromatin early in prophase and displays a highly dynamic association with Drosophila mitotic chromosomes. Chromosoma *116*, 259-274.
45. Tubman, E.S., Biggins, S., and Odde, D.J. (2017). Stochastic Modeling Yields a Mechanistic Framework for Spindle Attachment Error Correction in Budding Yeast Mitosis. Cell Syst *4*, 645-650 e645.
46. Zhang, T., Oliveira, R.A., Schmierer, B., and Novak, B. (2013). Dynamical scenarios for chromosome bi-orientation. Biophysical journal *104*, 2595-2606.

47. Kalantzaki, M., Kitamura, E., Zhang, T., Mino, A., Novak, B., and Tanaka, T.U. (2015). Kinetochore-microtubule error correction is driven by differentially regulated interaction modes. Nature cell biology *17*, 530.
48. Daum, J.R., Potapova, T.A., Sivakumar, S., Daniel, J.J., Flynn, J.N., Rankin, S., and Gorbsky, G.J. (2011). Cohesion fatigue induces chromatid separation in cells delayed at metaphase. Current biology : CB *21*, 1018-1024.
49. de Lange, J., Faramarz, A., Oostra, A.B., de Menezes, R.X., van der Meulen, I.H., Rooimans, M.A., Rockx, D.A., Brakenhoff, R.H., van Beusechem, V.W., King, R.W., et al. (2015). Defective sister chromatid cohesion is synthetically lethal with impaired APC/C function. Nature communications *6*, 8399.
50. Oliveira, R.A., Kotadia, S., Tavares, A., Mirkovic, M., Bowlin, K., Eichinger, C.S., Nasmyth, K., and Sullivan, W. (2014). Centromere-independent accumulation of cohesin at ectopic heterochromatin sites induces chromosome stretching during anaphase. PLoS biology *12*, e1001962.
51. Althoff, F., Karess, R.E., and Lehner, C.F. (2012). Spindle checkpoint-independent inhibition of mitotic chromosome segregation by Drosophila Mps1. Mol Biol Cell *23*, 2275-2291.
52. Schuh, M., Lehner, C.F., and Heidmann, S. (2007). Incorporation of Drosophila CID/CENP-A and CENP-C into Centromeres during Early Embryonic Anaphase. Current biology : CB *17*, 237-243.
53. Schindelin, J., Arganda-Carreras, I., Frise, E., Kaynig, V., Longair, M., Pietzsch, T., Preibisch, S., Rueden, C., Saalfeld, S., Schmid, B., et al. (2012). Fiji: an open-source platform for biological-image analysis. Nat Methods *9*, 676-682.

Chapter III:

Loss of cohesin in mitosis: Organismal consequences

Aneuploidy tolerance of neural stem cells impairs adult lifespan in flies (Adapted from)

Mihailo Mirkovic*, Leonardo G. Guilgur*, Diogo Santos, Raquel A. Oliveira

*These authors contributed equally

*Figures in this chapter where assembled by Leonardo G. Guilgur

Summary

Studying aneuploidy during organism development has strong limitations, as chronic mitotic perturbations used to generate aneuploidy result in lethality. We developed a genetic tool to induce aneuploidy in an acute and time controlled manner during *Drosophila* development. This is achieved by reversibly depleting cohesin, a key molecule controlling mitotic fidelity.

Larvae challenged with aneuploidy hatch into adults with severe motor defects shortening their lifespan. Despite being aneuploid, neural stem cells keep dividing, resulting in the quick appearance of chromosomal instability, complex array of karyotypes and cellular abnormalities. Notably, when cells are forced to do self-renewal, the aneuploidy-associated stress response is significantly delayed; indicating that stemness state confers resistance to aneuploidy. If only the brain is spared from induced aneuploidy, all motor defects are rescued as well as the adult lifespan, suggesting that neural tissue is the most ill-equipped to deal with developmental aneuploidy.

Highlights

- Reversible depletion of cohesin results in just a round or two of aberrant cell divisions, generating aneuploidy.
- Larvae challenged with aneuploidy during development hatch into impaired adults
- Few cell cycles are sufficient for chromosomal instability emerge from a previously stable aneuploid state.
- Neural stemness delays aneuploidy stress response.
- Protecting only the neural tissue from aneuploidy completely rescues adult lifespan.

Introduction

Aneuploidy, a state of chromosome imbalance, was observed over a century ago by Theodor Boveri. Since then, numerous studies have shown that aneuploidy is largely detrimental both at cellular and organism level. In multicellular organisms chromosome gain or loss results in lethality or developmental defects (Ambartsumyan and Clark, 2008; Holland and Cleveland, 2009). At the cellular level, studies in yeast and cell culture have demonstrated that aneuploidy has a high fitness cost for the cell, as unbalanced karyotypes lead to activation of multiple stress response pathways, resulting in reduced proliferation, cell cycle arrest, or cell death (Reviewed in (Santaguida and Amon, 2015). The aneuploidy stress response and consequential drop in fitness seems at odds with the

hypothesized role of aneuploidy in promoting malignancy, which is usually marked by over-proliferation (Sheltzer et al., 2017). Ninety percent of solid tumors harbor whole chromosome gains and/or losses (Gordon et al., 2012). Therefore, although usually detrimental to cell fitness, aneuploidy and its effects on cell proliferation can be context dependent, which emphasizes our need for a better understanding of the immediate and ultimate consequences of this abnormal cellular condition in a tissue context and through development.

However, study of aneuploidy *in vivo* is challenging since somatic aneuploidy is a rare event, difficult to capture and to trace in real time due to several constraints: i) Cells are equipped with surveillance mechanisms that prevent chromosome miss-segregation (e.g Spindle Assembly Checkpoint (SAC) (Reviewed in (Lara-Gonzalez et al., 2012) making naturally occurring aneuploidy events virtually impossible to evaluate; ii) experimentally-induced aneuploidy, by compromising mitotic fidelity, if often of low prevalence, as it has been demonstrated for several mammalian (Knouse et al., 2014) (Pfau et al., 2016) and *Drosophila* tissues (Dekanty et al., 2012; Poulton et al., 2017) and iii) induction of somatic or constitutional aneuploidy in metazoans relies on chronic mitotic perturbation (Listed in (Ly and Cleveland, 2017) which usually causes embryonic lethality (Reviewed in(Hassold and Hunt, 2001) as a result of progressive accumulation of damage in the developing organism. Thus, from these studies, it is impossible to disentangle short term and long term consequences of aneuploidy, or to examine kinetics of the response to aneuploid state during development. To circumvent these limitations, we generated a genetic system with the power to induce aneuploidy in an acute and time-controlled manner, in all the dividing tissues of the

developing *Drosophila*. The tool is based on reversible depletion of cohesin, a key molecule regulating mitotic fidelity (Guacci et al., 1993; Michaelis et al., 1997). Cohesin is a tripartite ring complex, composed by SMC1, SMC3 and the bridging kleisin subunit RAD21 (Mirkovic and Oliveira, 2017; Nasmyth and Haering, 2009). The primary mitotic role of cohesin is to mediate sister chromatid cohesion, by topologically entrapping DNA fibers from neighboring chromatids (Haering et al., 2008; Ivanov and Nasmyth, 2005). Cells entering mitosis with premature loss of cohesion and sister chromatid separation activate the Spindle Assembly Checkpoint (SAC) resulting in prolonged mitosis (Michaelis et al., 1997; Mirkovic et al., 2015). During this SAC-dependent mitotic delay, chromosomes are shuffled from one cell pole to the other by the mitotic spindle (Mirkovic et al., 2015). Consequently, chromosome shuffling induces genome randomization and aneuploidy upon mitotic exit with a theoretical rate of nearly 100%. Our engineered system enables a quick restoration of this complex shortly after its inactivation, thereby restricting mitotic abnormalities to a short time-frame, concomitantly with the generation of high levels of aneuploidy. Using such tool, we dissect the kinetics of aneuploidy response across various cell/tissue types and developmental timings.

Results

III.1 A genetic system for acute and time-controlled generation of aneuploidy in a developing organism

To induce aneuploidy in an acute and time-controlled manner, we developed a genetic system based on rapid removal of cohesin

complex, the molecular glue that holds sister chromatids together. To prevent a chronic cohesion depletion state and restrict mitotic failure to a single cell cycle, our genetic system is able to induce cohesin inactivation, followed by subsequent cohesion rescue. The system relies on the artificial cleavage of a modified version of the RAD21 cohesin subunit that contains TEV protease cleavage sites (RAD21-TEV). Cohesin is therefore quickly inactivated upon expression of the exogenous Tobacco Etch Virus (TEV) protease, induced by a heat-shock promoter (Oliveira et al., 2010; Pauli et al., 2008). After TEV-mediated inactivation, cohesin integrity is promptly rescued by inducing the expression of TEV-resistant RAD21 protein (RAD21-WT). For this purpose, RAD21-WT expression is under the control of UAS *promoter* (*UAS-Rad21-wt-myc*) that is induced by a Gal4 protein induced concomitantly with the TEV protease (also under a heat-shock promoter, *HSprom-GAL4*) (Figure 1A). Given that the TEV protease is under a direct control of heat-shock *promoter*, whereas RAD21-WT relies on a dual expression-system (*Gal4-UAS*); we anticipated that the temporal delay in RAD21-WT expression relative to the induction of TEV protease would lead to a short time window of cohesin inactivation (RAD21 cleavage) (Figure 1A).

To test this, we probed for the kinetics of TEV-mediated cleavage of RAD21-TEV and synthesis of RAD21-WT (Figures 1A´ and 1A´´) in different tissues of the developing larvae. After heat shock, both *Drosophila* larvae brains and wing discs, showed similar kinetics of the TEV-sensitive RAD21 disappearance followed by the appearance of RAD21-WT (Figures 1A´ and 1A´´). The timing of protein depletion/re-establishment differs slightly among different

tissues or developmental stages, but leads on average to a period of ~1 hour without cohesin (Figures 1A´; 1A´´).

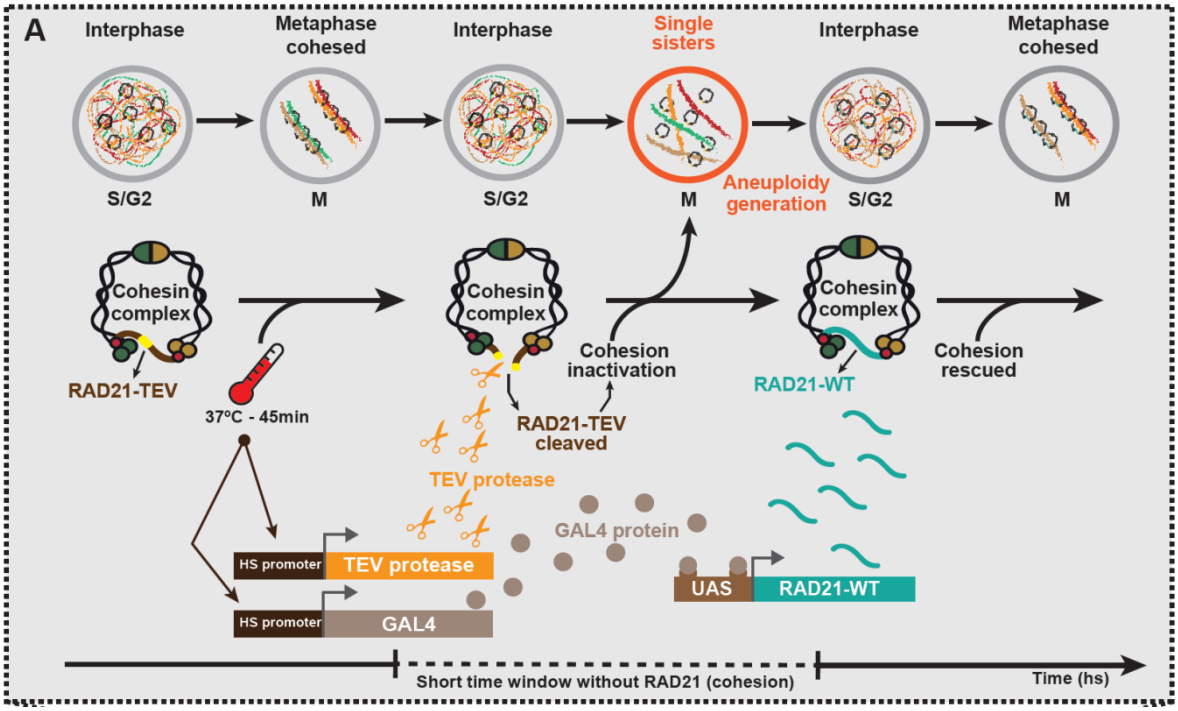

Figure 1A

Reversible system for acute cohesin depletion and generation of aneuploidy in the developing Drosophila

A genetic system for rapid cohesin cleavage relies on the expression of TEV protease from a heat shock promoter. This allows for complete Rad21 (TEV) removal in a Rad21WT excision background. To quickly rescue Rad21 and sister chromatid cohesion, we use the expression of UAS-Rad21WT from hs-Gal 4 promoter. The rescue should be slower than the cleavage to the one additional step of protein synthesis and binding in the Gal4-UAS system.

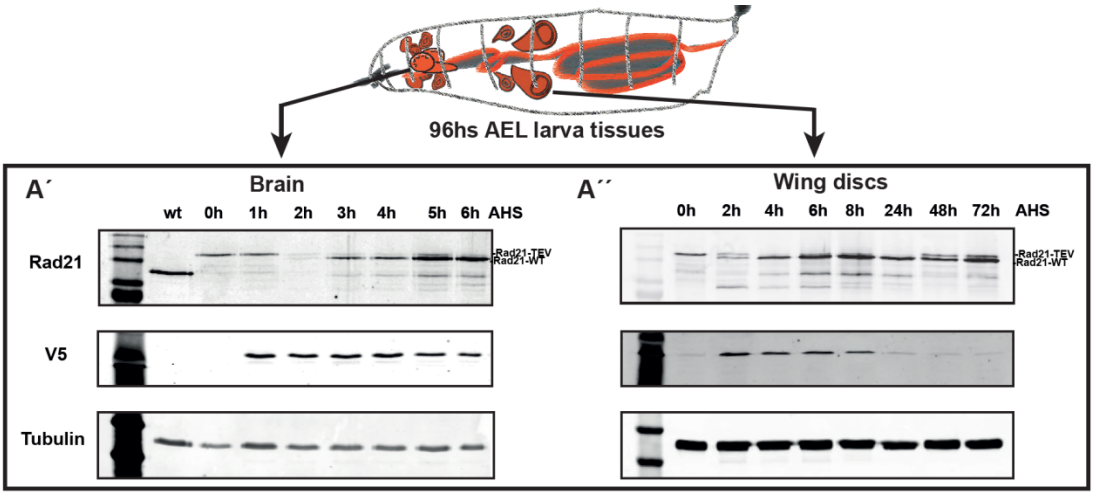

Figure 1A'-A''

Kinetics of Rad21 (TEV) depletion and Rad21-WT in the larval brain and wing disc

A'-A'') Time course of Rad21 (TEV) cleavage and expression of Rad2WT in the brain and wing disc, after the heat shock of the 3rd instar larvae. Rad21(TEV) cleavage takes place within two hours, followed by Rad21WT rescue.

III.2 Reversible removal of cohesin results in a single round of mitotic abnormalities and consequent aneuploidy.

The cohesive function of cohesin is established in S-phase, concomitantly with DNA replication. Once stabilized on the replicated genome, cohesin does not turn over (Gerlich et al., 2006). As such, loss of cohesin using our system will affect sister chromatid cohesion in all cells that are in S/G2/M phase during the short period between TEV protease expression and synthesis of

RAD21-WT (Figure 1A). In contrast to the cohesive pool, cohesin molecules involved in regulation of gene expression are known to be highly dynamic (Gerlich et al., 2006) and cohesin-mediated loops were recently reported “memorable” and quickly reformed upon cohesin re-establishment (Rao et al., 2017). We therefore anticipated that this function should not be severely affected by our system. In sharp contrast, mitotic errors induced upon cohesin cleavage are irreversible as there is no way to restore cellular ploidy after a compromised round of mitosis.

In contrast to canonical mitotic perturbations, that lead to several rounds of mitotic failures, our novel genetic system should lead to cohesion defects only in the first mitosis following the heat-shock, as the expression of RAD21-WT should be able to rescue cohesion in the subsequent cell cycle, if given enough time (see Figure 1A). To confirm that our genetic system works as anticipated, we focused our analysis on two different cycling tissues from the larva: the developing brain and the epithelial wing discs.

The developing brain of *Drosophila* is an excellent model to study the consequences of developmental aneuploidy. The well characterized cell lineages of the tissue in combination with our tractable system to induce miss-segregation of chromosomes offer a unique opportunity to trace the fate of aneuploid cells in real time and analyze their effect on the nervous system development. Through larval development ~100 large neural stem cells called Neuroblasts (Nbs) (Urbach et al., 2003) located in the central brain (CB) region divide asymmetrically to self-renew and generate distinct neuronal lineages via differentiating progeny (Homem and Knoblich, 2012)

We evaluated, by live cell imaging, mitotic fidelity using two independent criteria to estimate the state of sister chromatid cohesion: i) the presence of single sisters (a direct consequence of cohesion loss), as opposed to metaphase chromosome alignment and ii) the time cells spend in mitosis, given that premature loss of sister chromatid cohesion is known to activate the SAC and delay mitotic exit (Mirkovic et al., 2015).

As expected by our system, the first division after the heat shock results in full cohesin cleavage in Nbs, followed by cohesin rescue in subsequent divisions (see Sup Movie 1 and 2). The fast cell cycle of Nbs, coupled with continued proliferation of these cells despite their abnormal genome content (further discussed below), enables analysis of mitotic fidelity throughout several consecutive divisions in great detail. Consistently, in the first mitosis AHS, 95% of Nbs contain single sisters, and exhibit mitotic delay and chromosome shuffling (Figures 2A; 2B). In the subsequent mitosis, however, normal cohesion is observed in ~80% of the Nbs, with clear metaphases and a shorter mitotic delay (Figures 2A; 2B and 2C). Finally, during the third cell division AHS, the mitotic timing and the cohesive state of Nbs are comparable to heat-shocked controls (Figures 2A; 2B and 2C). Similar results were obtained for larvae heat-shocked at earlier stages of development (Figure 3A to A´´).

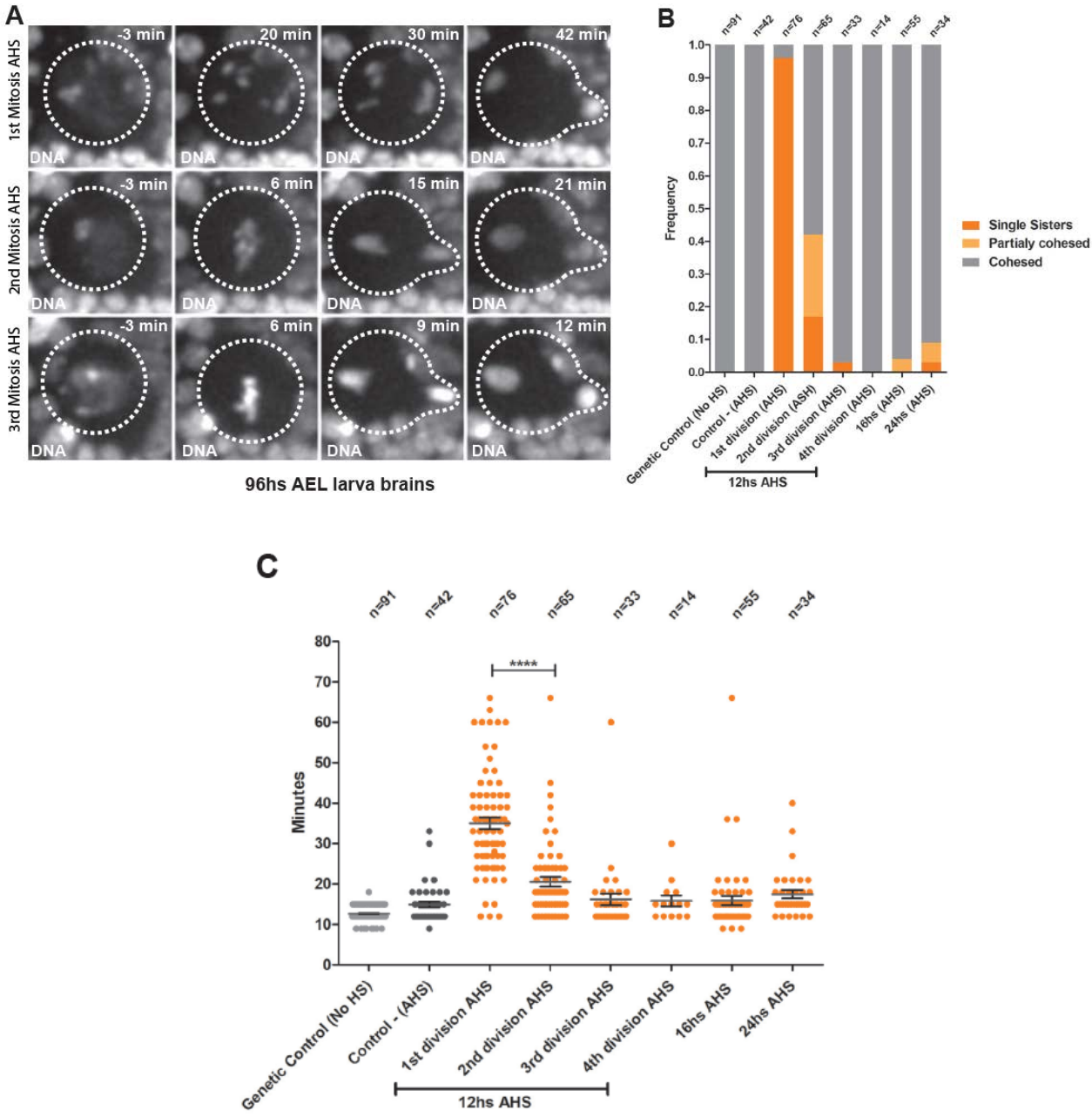

Figure 2A-C

Kinetics of reversible loss of cohesin in the 3rd instar brains

A- Stills from live imaging of Nbs after the heat-shock.Transient loss of cohesion results in a round of defective mitosis and genome shuffling (1st division AHS). After this round of division, the following mitosis (2nd and

3rd divisions AHS) shows the restoring of cohesion function and mitotic fidelity in larvae Nbs. B- Quantification of Cohesive states of 3rd instar larvae Nbs following RAD21-TEV cleavage and RAD21-WT restoring of cohesin function. More than 80% of the 2nd divisions AHS are already totally -or partially cohesed.

*C- Quantification of mitotic timing and delay caused by Spindle Assembly Checkpoint activation after RAD21-TEV cleavage and RAD21-WT rescue in the 3rd instar Nbs (2 to 24hs AHS). 2nd divisions AHS evidence a significant reduction in the mitotic timing as a consequence of the rescue of cohesin function. **** = P<0.0001.*

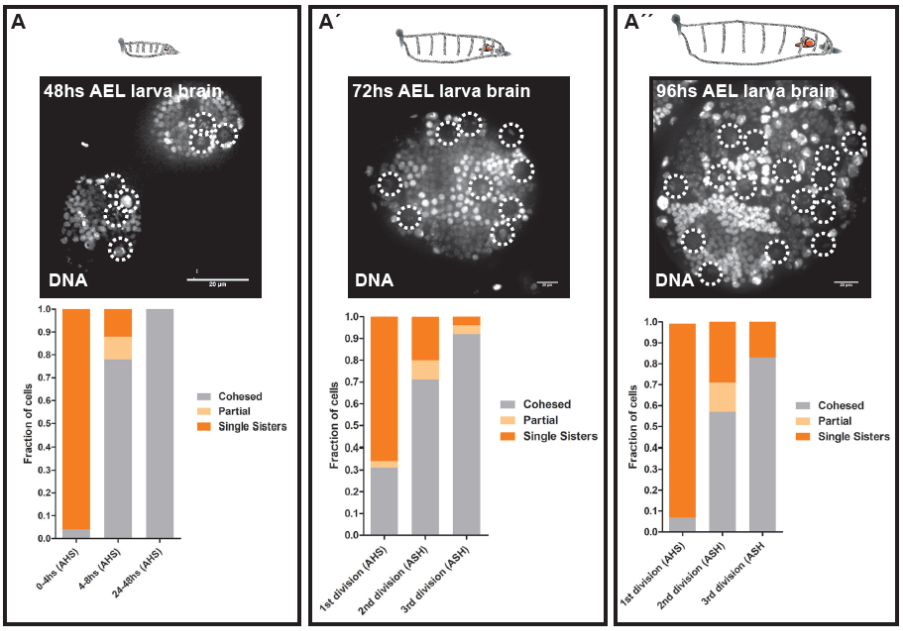

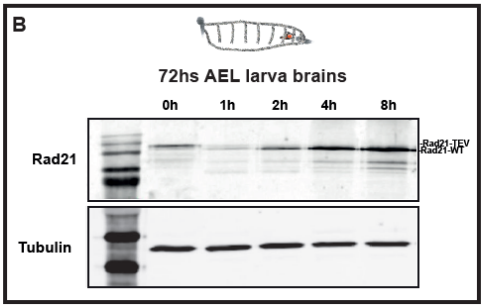

Figure 3

Heat-shock treatment induces brain aneuploidy at all stages of development.

A to A´´- *Stills from live imaging of lobe brains at different larvae stages (48, 72 and 96hs AEL); dashed circles are highlighting the Nbs in the lobes (N>3 brains per condition). The number of dividing Nbs increase with larvae development. Cohesive state of Nbs after the loss of cohesion and subsequent rescue in 48, 72 and 96hs AEL larvae were plotted.*
B- *Western blot of RAD21 cleavage and rescue dynamics in 72hs AEL larvae brains.*

In contrast to the Neuroblasts, in the epithelial cells of the wing disc, we observe the presence of single sisters and a mitotic delay even at 48hs AHS, despite the presence of high levels RAD21-WT (Figure 1A´´; 2D; 2E and 2F).These findings are consistent with the long cell cycle of the wing discs cells (Milan et al., 1996; Neufeld et al., 1998). The high incidence of cells affected by reversible-cohesin cleavage is also consistent with a high frequency of cells in S/G2 in this tissue, estimated using the fly FUCCI system (Zielke et al., 2014) (Figure 4B). To fully demonstrate the ability of our tool to induce aneuploidy in an acute manner in epithelial tissues we tested their regeneration capacity. In *Drosophila* epithelial cells, multiple cellular insults, including aneuploidy, can activate the Jun N-terminal kinase (JNK) signaling pathway, thus inducing the expression of pro-apoptotic genes and triggering the apoptotic cascade (Dekanty et al., 2012; Milan et al., 2014). In agreement with these studies, 24hs AHS in the wing disc, Cleaved Caspase 3 (CC3) staining reveals a large population of dying cells thus reinforcing the notion that cell death is mostly a consequence of the induced chromosome segregation errors and the resulting

aneuploidy (Figure 4A and 4A´). However, at 48hs AHS, the number of dying cells decreases significantly if cohesin activity is brought back, but not if the cohesion depletion by TEV is chronic (Figure 4A and 4A´).

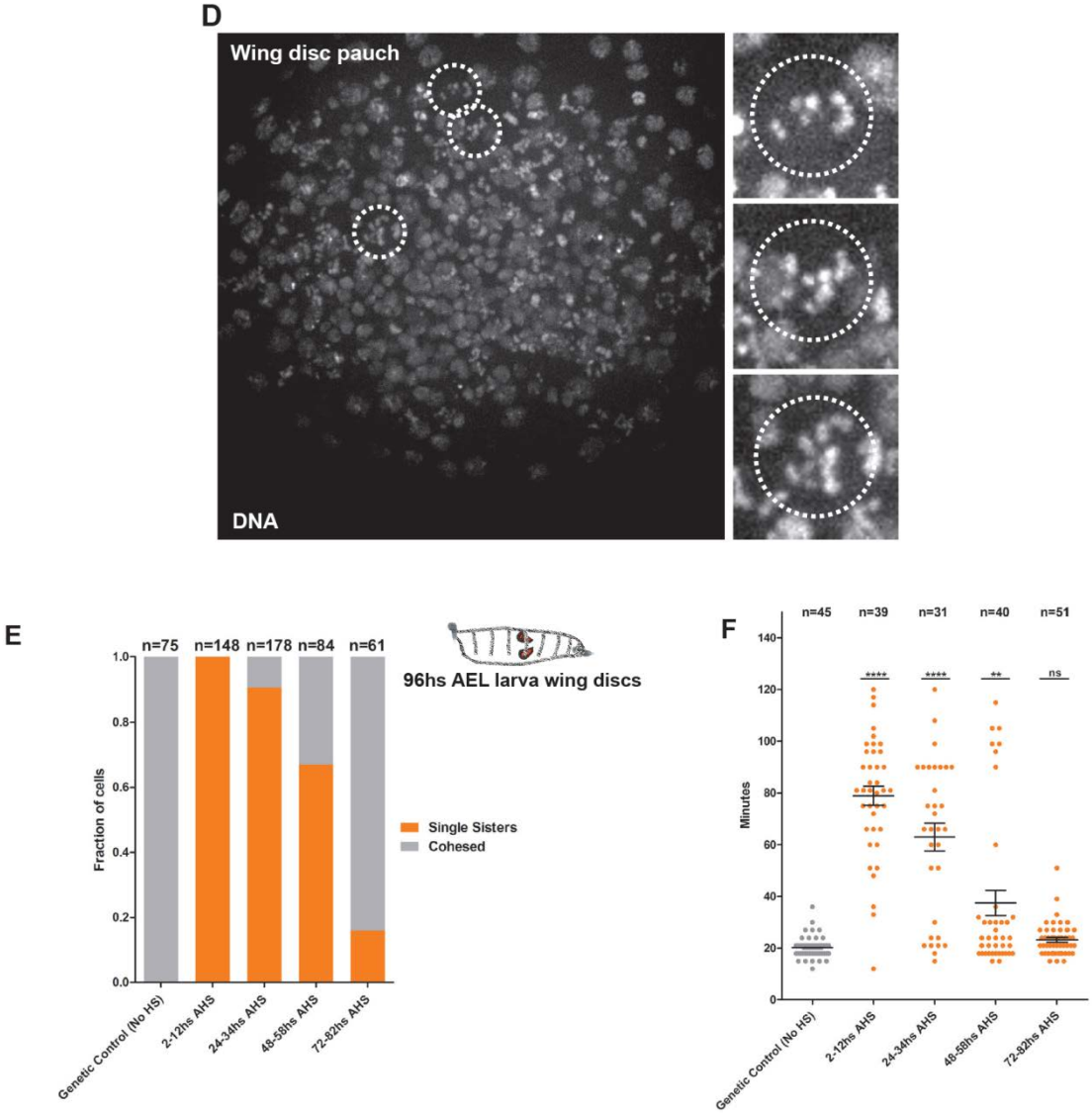

Figure 2D-F

Kinetics of reversible loss of cohesin in the 3rd instar wing disc

D- Cohesin cleavage in the Wing disc of 3rd instar larvae. Stills from live imaging showing single chromatids during mitosis.

E- Quantification of Cohesive states of divisions in the 3rd instar larvae wing disc following RAD21-TEV cleavage and Rad21-WT rescue from 2 to 80hs after heat-shock. Given the long cell cycle and the heterogeneous rate of division of cells in this tissue the presence of single sisters can be observed up to 72h after the heat-shock.

F- Quantification of mitotic timing and delay caused by Spindle Assembly Checkpoint activation after Rad21-TEV cleavage and Rad21-WT rescue in the 3rd instar wing discs from 2 to 80hs AHS.

*In all panels n= number of cells. **** = P<0.0001; ** = P<0.01.*

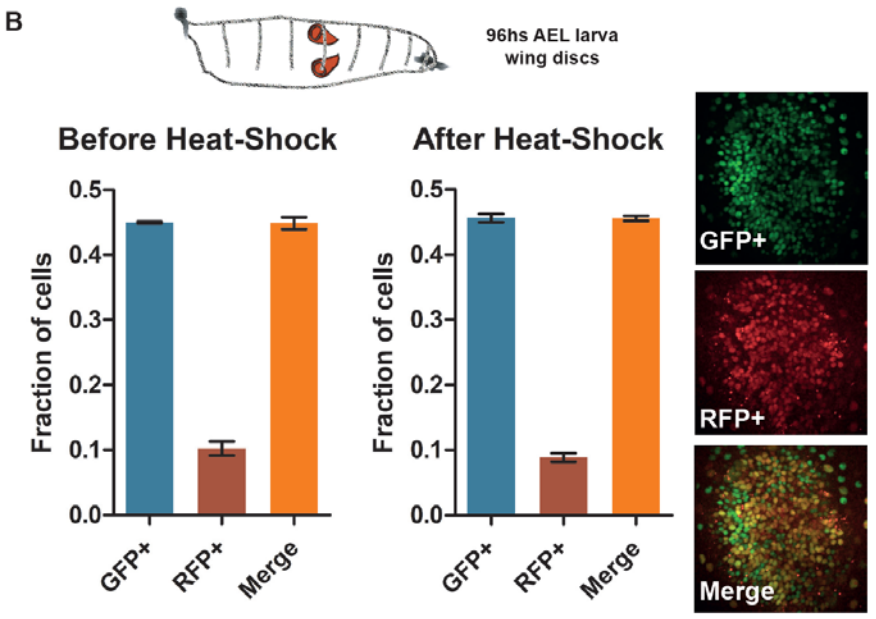

Figure 4B

Cell cycle profile evaluation of the 3rd instar wing disc, using the FLY-FUCCI system

The high incidence of cells affected by reversible cohesin cleavage is consistent with a high frequency of cells in G2/M in this tissue and slow cell cycle (see Merge). GFP: G1 cells; RFP: S phase cells; Merge: G2/M Cells.

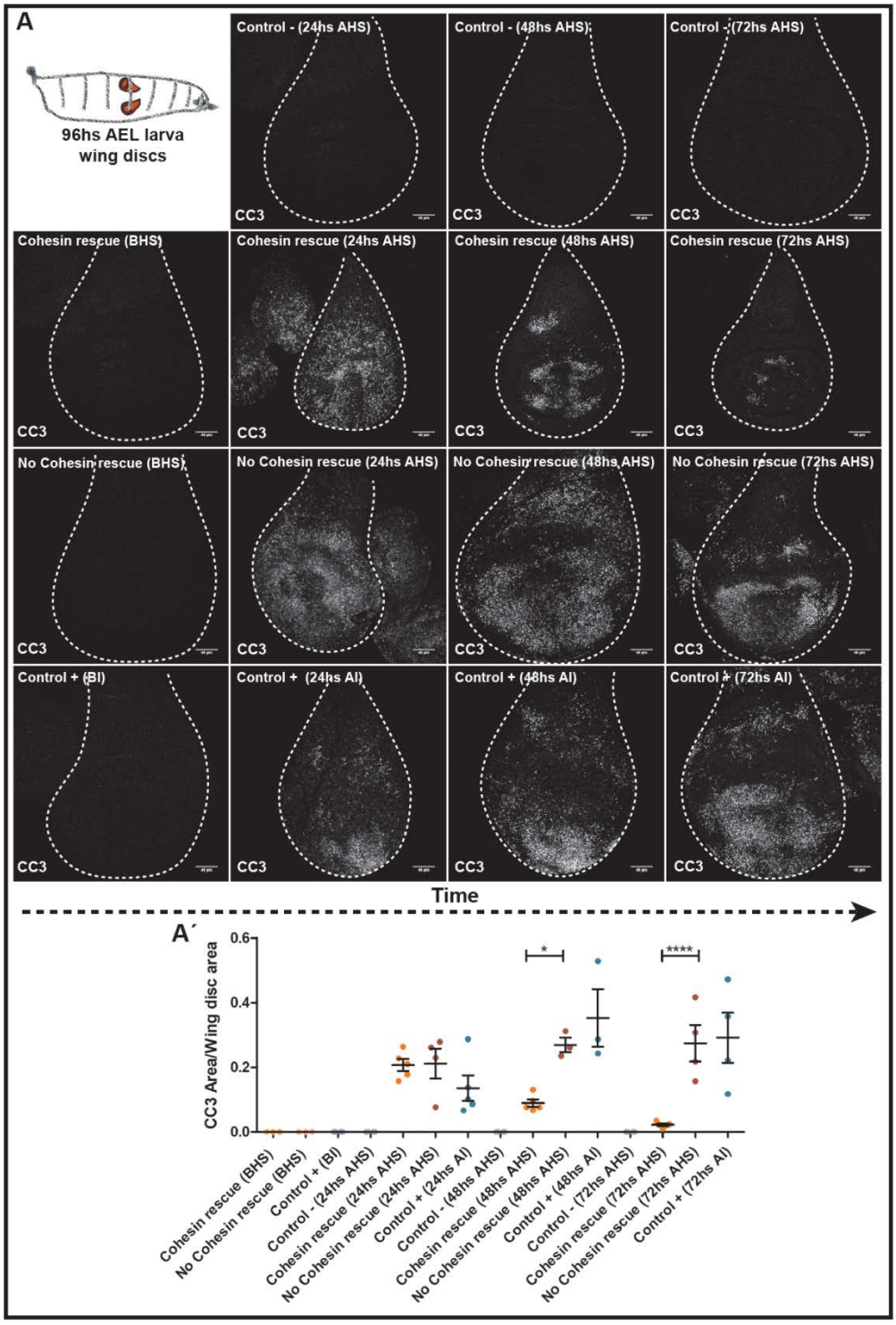
A
96hs AEL larva
wing discs
Control - (24hs AHS)
Control - (48hs AHS)
Control - (72hs AHS)
Cohesin rescue (BHS)
Cohesin rescue (24hs AHS)
Cohesin rescue (48hs AHS)
Cohesin rescue (72hs AHS)
No Cohesin rescue (BHS)
No Cohesin rescue (24hs AHS)
No Cohesin rescue (48hs AHS)
No Cohesin rescue (72hs AHS)
Control + (BI)
Control + (24hs AI)
Control + (48hs AI)
Control + (72hs AI)
CC3
Time
A´
CC3 Area/Wing disc area
0.6
0.4
0.2
0.0
*
****
Cohesin rescue (BHS)
No Cohesin rescue (BHS)
Control + (BI)
Control - (24hs AHS)
Cohesin rescue (24hs AHS)
No Cohesin rescue (24hs AHS)
Control + (24hs AI)
Control - (48hs AHS)
Cohesin rescue (48hs AHS)
No Cohesin rescue (48hs AHS)
Control + (48hs AI)
Control - (72hs AHS)
Cohesin rescue (72hs AHS)
No Cohesin rescue (72hs AHS)
Control + (72hs AI)

Figure 4

Epithelial tissues recover from high levels of aneuploidy by cell death and compensatory proliferation.

A to A´: A- *Reversible cohesin cleavage results in apoptosis in the 3rd instar wing discs (dashed shapes depict the wing disc areas). The amount of apoptosis per disc area was measured by cleaved caspase 3 (CC3) immunofluorescence at 24, 48 and 72hs AHS.* ***A´-*** *Rescue of cohesin function reduced significantly the amount of apoptosis 48hs after of the induced mitotic disruption. Contrastingly, a chronic inactivation of cohesin complex (No cohesin rescue) showed high levels of apoptosis through time. Control- (Control HS); Control+ (Irradiation: 4,000 rads); BHS (Before Heat-Shock, genetic control); AHS (After Heat-Shock, condition); BI (Before Irradiation); AI (After Irradiation). * = P<0.05; **** = P<0.0001. Scale bar = 40µm. z-proj (z projection).*

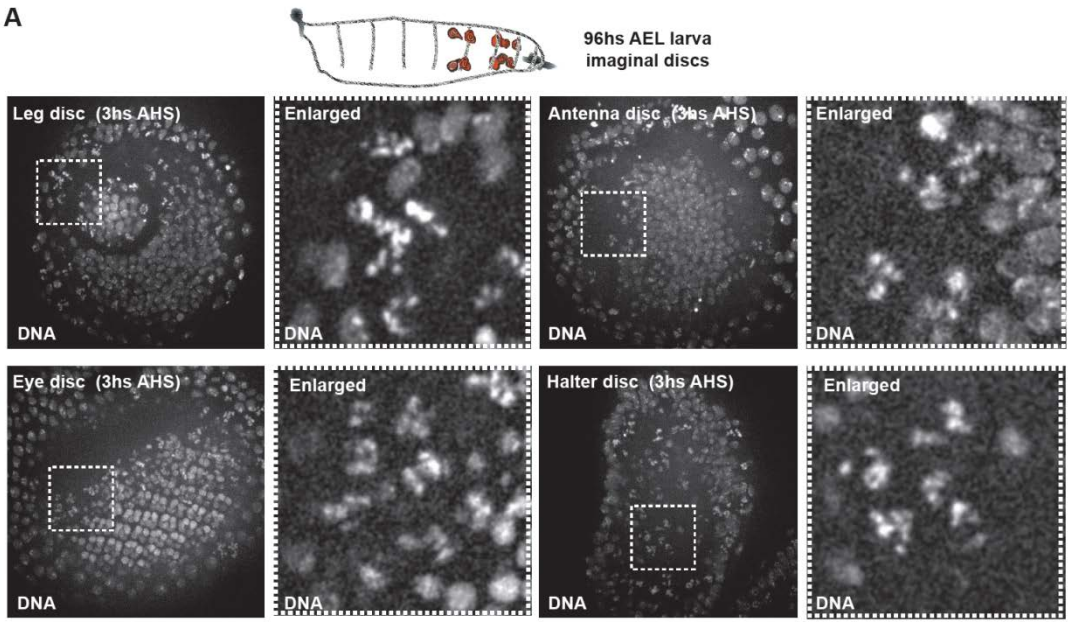

Figure 5A

RAD21 cleavage and rescue induces loss of cohesion in all examined dividing tissues

A- *Stills from live imaging of leg, eye, antennae and halter 3rd instar imaginal discs after induction of RAD21 cleavage. Dashed squares display epithelial cells from the imaginal discs undergoing mitosis with loss of cohesion and single chromatids (see enlarged picture).*

These results suggest that tissue recovery is limited and only possible if the mitotic disruption is restricted in time (or cell cycle), as achieved by our reversible genetic system. Although quantitative analysis was performed exclusively for wing discs epithelial cells and brain Nbs, analysis of other epithelial dividing tissues of the *Drosophila* larvae reveal a similar high incidence of single sisters 3hs AHS, implying that our system is able to induce a reversible-whole organism loss of cohesion (Figure 5A).

We therefore conclude that our novel genetic tools is able to induce a single round of aberrant cell division, followed by quick rescue of mitotic fidelity, across the entire organism, leading to tissue-specific responses.

III.3 Larvae challenged with aneuploidy during development hatch into impaired adults

To understand how the entire organism would respond to such high degree of induced chromosome segregation errors and consequent aneuploidy, we tracked the larvae through development after cohesin cleavage. For comparative analysis, we monitored eclosion rates for organisms with the “chronic” TEV-protease

cleavage system (inducing cohesin removal for ~48hs) and our newly developed system with reversible inactivation of cohesin. Both systems represent a strong insult for all the dividing tissues of the larva; therefore, we expected them to be lethal in the pupa to adult transition. However, in contrast to several studies using chronic mitotic perturbations (Gogendeau et al., 2015; Poulton et al., 2017) flies challenged with aneuploidy using a reversible mitotic perturbation ecloded into adult flies at high frequency, particularly if challenged up to 72hs after egg laying (AEL) (Figure 6A and Movie Sup 3). Eclosion rates of adults were dependent on the developmental stage at which cohesin was reversibly cleaved (Figure 3A). Early induction of aneuploidy, at 48hs AEL, resulted in eclosion both with and without cohesin rescue. However, with 72hs AEL heat-shock, there was almost no eclosion if the RAD21 protein subunit was not brought back (Figure 6A). If the larvae were heat-shocked 96hs AEL, no cohesin rescue resulted in dead pupae, while cohesin rescue resulted in flies trying to escape the pupa, but unable to do so ("Head-out pupae") (Figure 6A and 6B). These differences in developmental response to aneuploidy are likely due to increase of cell proliferation during larval development (Ito and Hotta, 1992; Poulton et al., 2017). Regardless of the developmental stage, all flies that were able to eclode into adults after the aneuploidy challenge were completely unable to fly or move normally even when showing serviceable wings and appendages (see Sup Movie 3, 4 and Figure 6B´). Consequently, these flies exhibited markedly shorter lifespans than their control counterparts (Figure 6B).

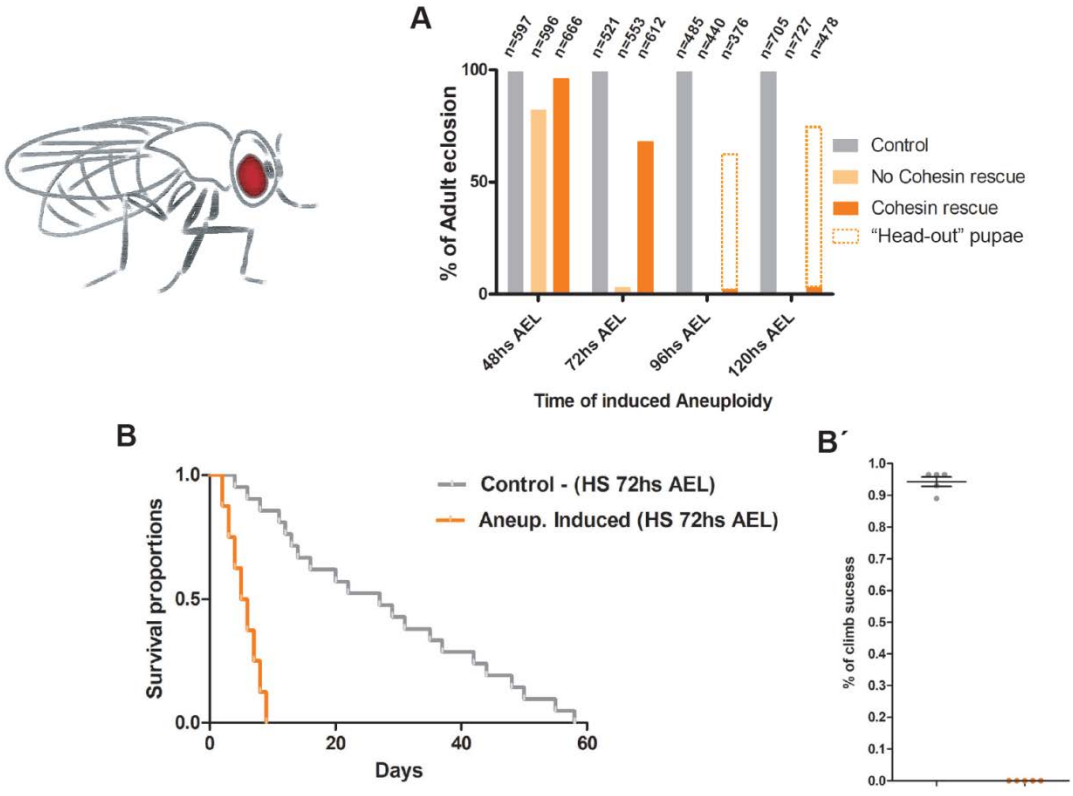

Figure 6

Larvae challenged with organism-wide mosaic aneuploidy hatch into adult flies with severe motor defects and reduced lifespan.

A- Percentages of adult eclosion according to the stage of development at which reversible loss of cohesin (aneuploidy) was inducted (48, 72, 96 and 120hs after egg laying, AEL). n= number of flies.

B to B´: B- Kaplan-Meier survival curves showing fractional survival as a function of time. Ecloded flies with 72hs AEL induced aneuploidy showed reduced lifespan when compared with control flies (only heat-shocked). B´- Climbing assay comparing adult flies with 72hs induced aneuploidy and control flies. Percentage of climb success was plotted over the halfway point (10cm). Ecloded flies with 72hs AEL induced aneuploidy showed impaired motor behavior

III.4 Few cell cycles are sufficient to induce chromosomal instability in aneuploid Neuroblasts.

We hypothesized that the severe motor defects in the newly hatched flies are a direct consequence of aneuploidy in the developing larva brain. Recently, it has been proposed that neural stem cells with unwanted karyotypes are eliminated (Gogendeau et al., 2015; Poulton et al., 2017). To measure the number of neural stem cells over time after aneuploidy induction, we used the Nb marker Deadpan (DPN) to quantify all the nuclei with Nb morphology (Nb-like cells), defined based on their size, and located at the central brain area (CB) per lobe. The analysis indicates that there is a gradual decline in the Nbs number after the induction of aneuploidy from 12hs AHS onwards, but never a complete loss of the neural stem cell population (Figure 7A and 7A´). The slow kinetics and incomplete elimination of the stem cell population was quite surprising given the high levels of aneuploidy generated upon cohesin loss (~100%).

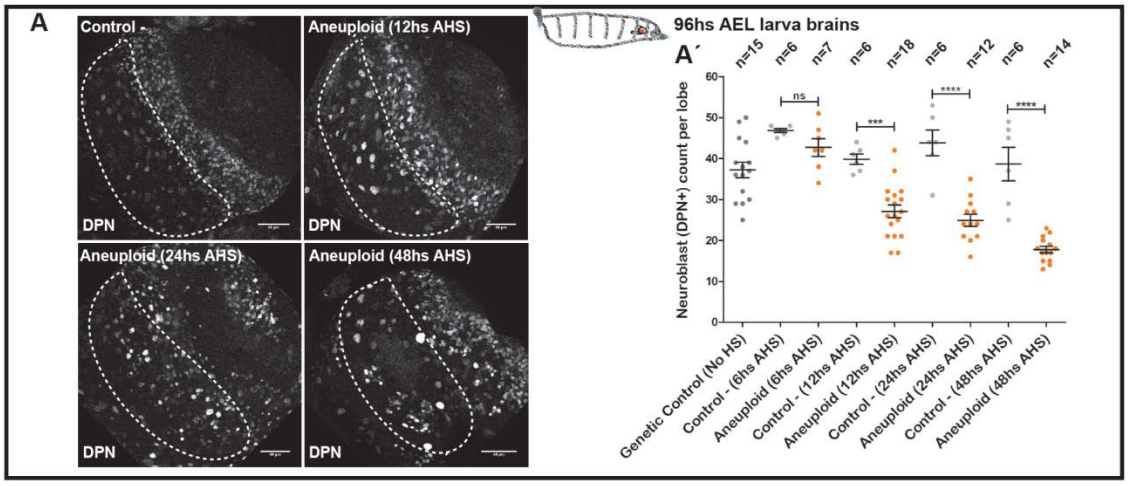

Figure 7A

Aneuploidy causes a gradual reduction in Neuroblasts numbers, but never a complete loss.

*A to A´: A- Nbs counts at the central brain (dashed shape) in 3rd instar lobe brains assessed by immunofluorescence with the Nbs marker Deadpan (DPN). A´- Nb numbers were quantified based on the correlation between morphology and positive signal for DPN at 12, 24 and 48hs AHS. Reversible loss of cohesion and aneuploidy are followed by a reduction in Nbs numbers, but not a complete loss of the neural stem cell pool. n= number of lobe brains. *** = P<0.001; **** = P<0.0001; ns= not significant. Scale bar = 40µm.*

Premature differentiation and apoptosis were suggested as the main mechanisms of aneuploid Nb elimination, reported in two recent studies (Gogendeau et al., 2015; Poulton et al., 2017). However, after acute aneuploidy induction in the entire Nb population, we found a very low frequency of cells undergoing premature differentiation or cell death (Figure 8). As a proxy for premature differentiation events, we quantified Nb-like cells that had either lost the DPN marker or abnormally exhibit the differentiation marker Prospero (Pros) with or without co-expression of DPN (Figure 8A and 8A´, arrowheads and dashed circles). Pros is the key factor acting as a switch for the transition from stem cell self-renewal to terminal differentiation (Choksi et al., 2006); therefore, should not be present in Nbs. We observed that upon acute aneuploidy induction in the entire Nb population, there is a very low frequency of cells indicative of premature differentiation (Figure 8). These findings suggest that premature differentiation, although still taking place, is unlikely to be the major form of stem cell elimination.

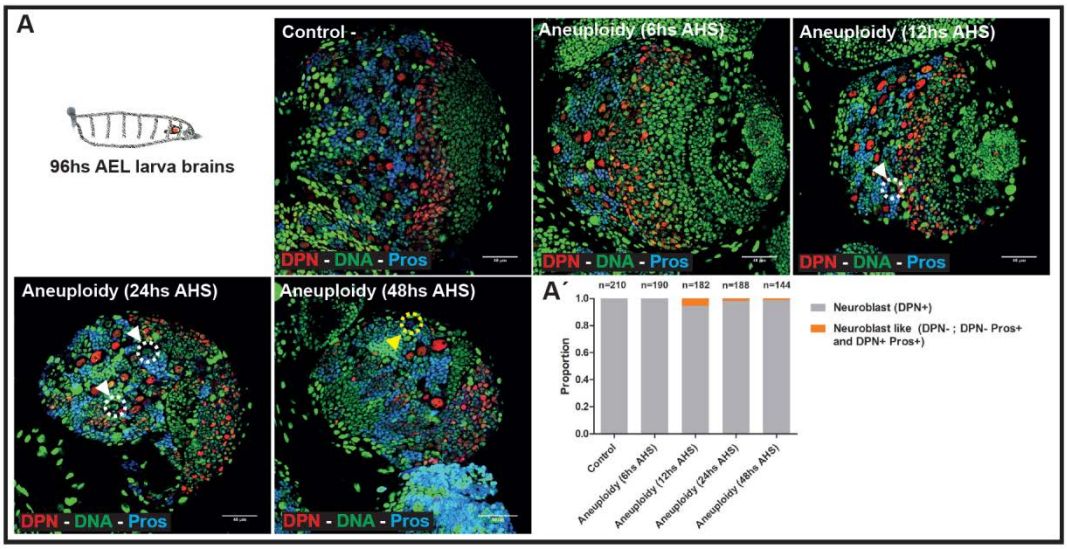

Figure 8

Aneuploidy promotes low frequency of loss of identity and/or premature differentiation in Neuroblasts

A to A´: A- *Pictures from fixed samples of 3rd instar larva brains stained with Deadpan (DPN), Prospero (Pros) and Histone RFP (DNA). Induction of aneuploidy results in the loss of stem cell identity measured by the absence of Deadpan (stem cell marker, white arrowhead with dashed circle), appearance of Prospero (differentiation marker, yellow arrowhead with dashed circle) or both markers together in cell nucleus with "Nbs shape like".* ***A´-*** *Percentage of loss of stem cell identity in the neural stem cell pool at different time points after the induction of aneuploidy. These events are observed at very low frequency. n= number of Nbs like cells. Scale bar = 40µm*

To estimate the levels of apoptosis, we also counted cells positive for cell death markers like CC3 and DCP1. We found a significant increase in CC3 and DCP1 positive cells in aneuploid brains (Figure 8B´ and 8B´´) indicating that induction of apoptosis may also contribute to the elimination of aneuploid cells, as recently proposed (Poulton et al., 2017). However, CC3 and DCP1 signals

rarely correspond to Nb-like cells (For CC3 staining: Control: N=4 lobes Nbs/CC3=157/0 (0%) and Aneuploidy induced 24hs AHS: N=9 lobes Nbs/CC3=159/6 (3,7%); for DCP1 staining Control: N=5 lobes Nbs/CC3=201/0 (0%) and Aneuploidy induced 24hs AHS: N=10 lobes Nbs/CC3=191/5 (2,6%) (Figure 8B, B´ and B´´, arrowheads and dashed circles), suggesting that apoptosis may not be the major cause for NB elimination. Thus, loss of stem-cell identity and/or cell death are more likely potential consequences of genome randomization, rather than a specific mechanism controlling aneuploidy in the neural stem cell population (see discussion). Supporting this idea, inhibition of apoptosis by over-expression of the baculovirus protein P35 does not rescue Nbs number per brain lobe 24hs after induction of aneuploidy (Figure 8C).

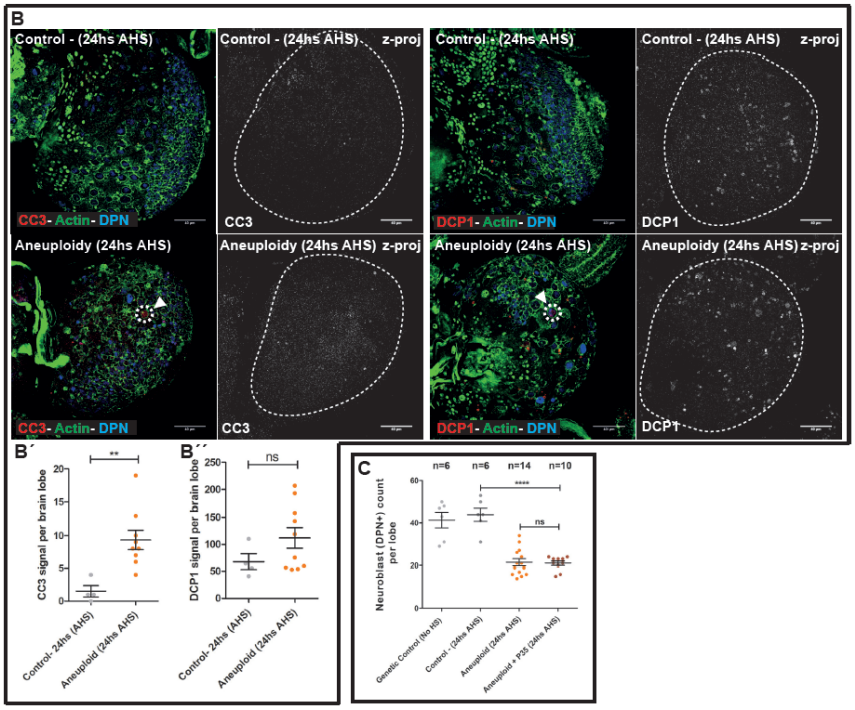

Figure 8B-C

Aneuploidy promotes low frequency of cell death in Neuroblasts.

B to B´´: ***B-*** *Pictures from fixed samples of 3rd instar larvae lobe brains stained with Deadpan (DPN), Cleaved Caspase 3 (CC3, death marker), DCP1 (death marker) and rhodamine phalloidin (Actin). Induction of aneuploidy results in cell death measured by the presence of CC3 or DCP1 signals (white arrowheads with dashed circles) in cells with "Nbs shape like".* ***B´ and B´´-*** *Quantification of cell death signals CC3 and DCP1 per larvae brain lobes at 24hs AHS. The presence of positive signal for the cell death markers in Nbs shape like cells is very low. ** = P<0.01. ns= not significant. Scale bar = 40µm. z-proj (z projection)*

C- *Quantification of Nbs at the central brain in 3rd instar lobe brains assessed by immunofluorescence with the Nbs marker DPN. Inhibition of apoptosis by over-expression of baculovirus P35 does not rescue Nbs number after 24hs induced aneuploidy. n= number of lobe brains. **** = P<0.0001. ns= not significant.*

To dissect the kinetics of the aneuploid response, we took advantage of the temporal resolution our system allowing for the tracking of aneuploid fate in real time. We restricted our analysis to 3rd *instar* wandering larvae as at this stage no new Nbs are generated from the neuro-epithelium (Homem and Knoblich, 2012). Induction of aneuploidy at this developmental stage, therefore, affects the entire Nbs population, which facilitates cell fate analysis. Consistently with our hypothesis, we observed a significant amount of Nbs proliferating for several days and displaying a tendency for chromosome accumulation over time (Figure 7B and 7B´). To analyze the number of chromosomes in each dividing Nbs we performed chromosome spreads and counted the number of centromeres per mitotic figure (each chromosome contains 2

centromere dots in mitosis). A single round of mitosis upon premature loss of sister chromatid cohesion should result in a maximum of 16 chromosomes per Nbs, in the rare cases of complete asymmetric segregation (the total set of chromosomes in the fly is 8). However, chromosome numbers can reach over 20 chromosomes per cell 24hs after loss of cohesion was induced (Figure 7B´).This analysis suggests that chromosome accumulation does not solely result from the initial perturbation.

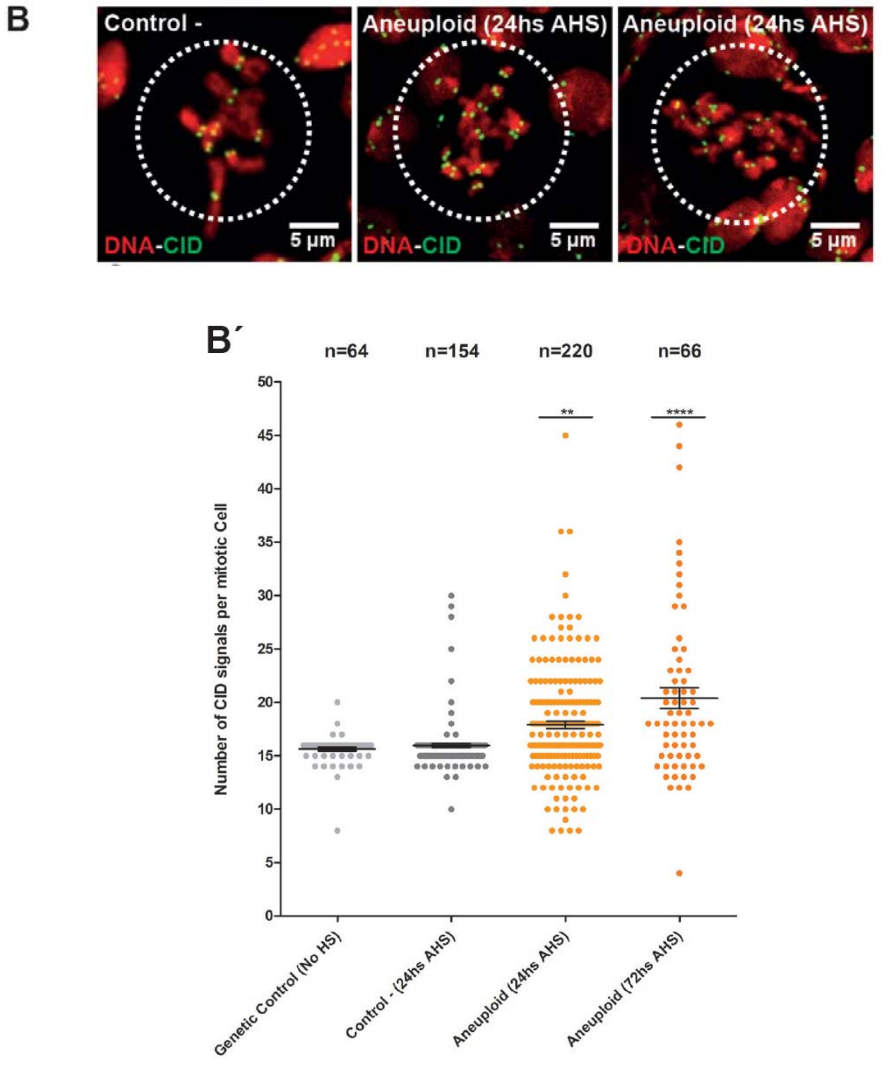

Figure 7B

Aneuploidy causes chromosome accumulation in proliferating Neuroblasts

*B to B´: B-Chromosome counts were assessed by CID immunofluorescence (Centromere counts) in 3rd instar Nbs arrested at metaphase with Colchicine (dashed circle) at 24 and 72hs AHS. B´- Aneuploid Nbs accumulate chromosomes through time. n= number of cells. **** = P<0.0001; ** = P<0.01. Scale bar = 5µm.*

To investigate this further, we characterized the mitotic fidelity of aneuploid Nbs. As described above, mitotic divisions that immediately follow the initial perturbation do not display significant mitotic errors and the low frequency of defects observed is cohesin-related (as expected from our experimental setup). However, 16hs AHS, aneuploid cells start changing their behavior and a variety of mitotic defects appear, becoming more frequent over time (Figure 7C). Detailed characterization of the mitotic defects arising 16hs after the induction of aneuploidy revealed that majority of them (~60%) are mild, consisting of either a prolonged metaphase or a lagging chromosome. However, the remaining ~40% consisted of cytokinesis defects, tri-polar spindles and sister chromatid cohesion defects, which are serious abnormalities that can drastically alter numerical ploidy (Figure 7D´ and 7D´´). Interestingly enough, this analysis shows that few hours are enough for the previously stable divisions of aneuploid karyotypes to become unstable, leading to further randomization of the genome. Furthermore, this chromosomal instability can also contribute to Nbs number decline, as catastrophic mitotic errors can result in complete loss of Nbs morphology and positioning (Figure 7E). All together, we conclude that neural stem cells exhibit

a complex array of abnormalities as consequence of their karyotype diversification, such as loss of identity, cell death, or chromosomal instability, contributing to their gradual loss over time.

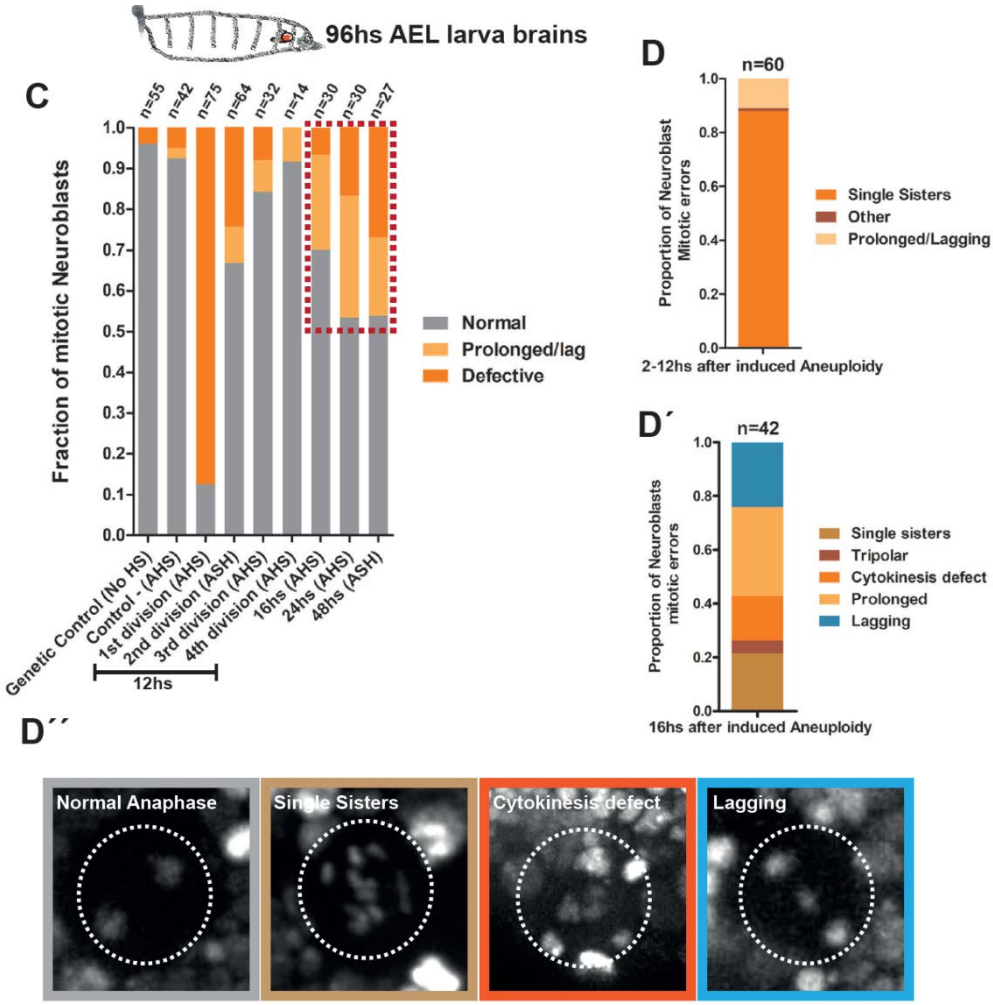

Figure 7C-E

Aneuploid Neuroblasts become chromosomally instable over time

C- Assessment of mitotic defects after aneuploidy induction from 2 to 48hs AHS. Chromosome instability arises shortly after aneuploidy induction (red dashed box). n= number of cells.

D to D´´: D and D´- Profile of mitotic errors as a consequence of reversible cohesin depletion and consequent aneuploidy from 2 to 12hs AHS and 16 to 48hs AHS. D´´- Stills from live imaging documenting mitotic abnormalities in aneuploid Nbs (dashed circles). n= number of cells.

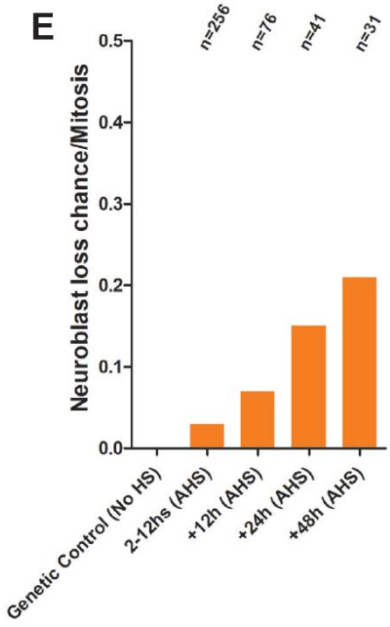

E- Graph displaying the frequency per mitosis of catastrophic mitotic events which result in Nbs loss from 2 to 48hs AHS. Chromosomal instability can result in complete loss of Nbs morphology. n= number of cells.

III.5 Karyotype restrictions in the proliferating aneuploid Neuroblast population

To test if there is a selection of specific karyotypes in the population of dividing aneuploid Nbs, we preformed FISH analysis at 8hs and 24hs after aneuploidy was induced. To estimate the predicted frequency of specific karyotypes we first modeled the probability of each karyotype, assuming full random chromosome segregation in a single round followed by a second round of random segregation in ~20% of the cases (this was based on our experimental observations, see Figure 2B). FISH profiles were then compared with the statistical predictions. The FISH profiles confirmed the propensity for chromosome accumulation over time (Figure 9A and 9B). Additionally, this analysis revealed that the karyotypes that can be tolerated by dividing Nbs are restricted to those containing at least one of the major three chromosomes, II III or X. The rate of complete loss of these chromosomes in the proliferating Nbs population was comparable to the control, and thus likely a consequence of experimental error of the FISH (Figure 9C; 9C´; 9D and 9D´). We concluded that, although dividing aneuploid Nbs can persist in the tissue, this also has boundaries, as complete loss of any of the big three chromosomes prevents their proliferation in the developing brain. In contrast, other aneuploid combinations are compatible with continued proliferation, particularly when cells gain chromosomes.

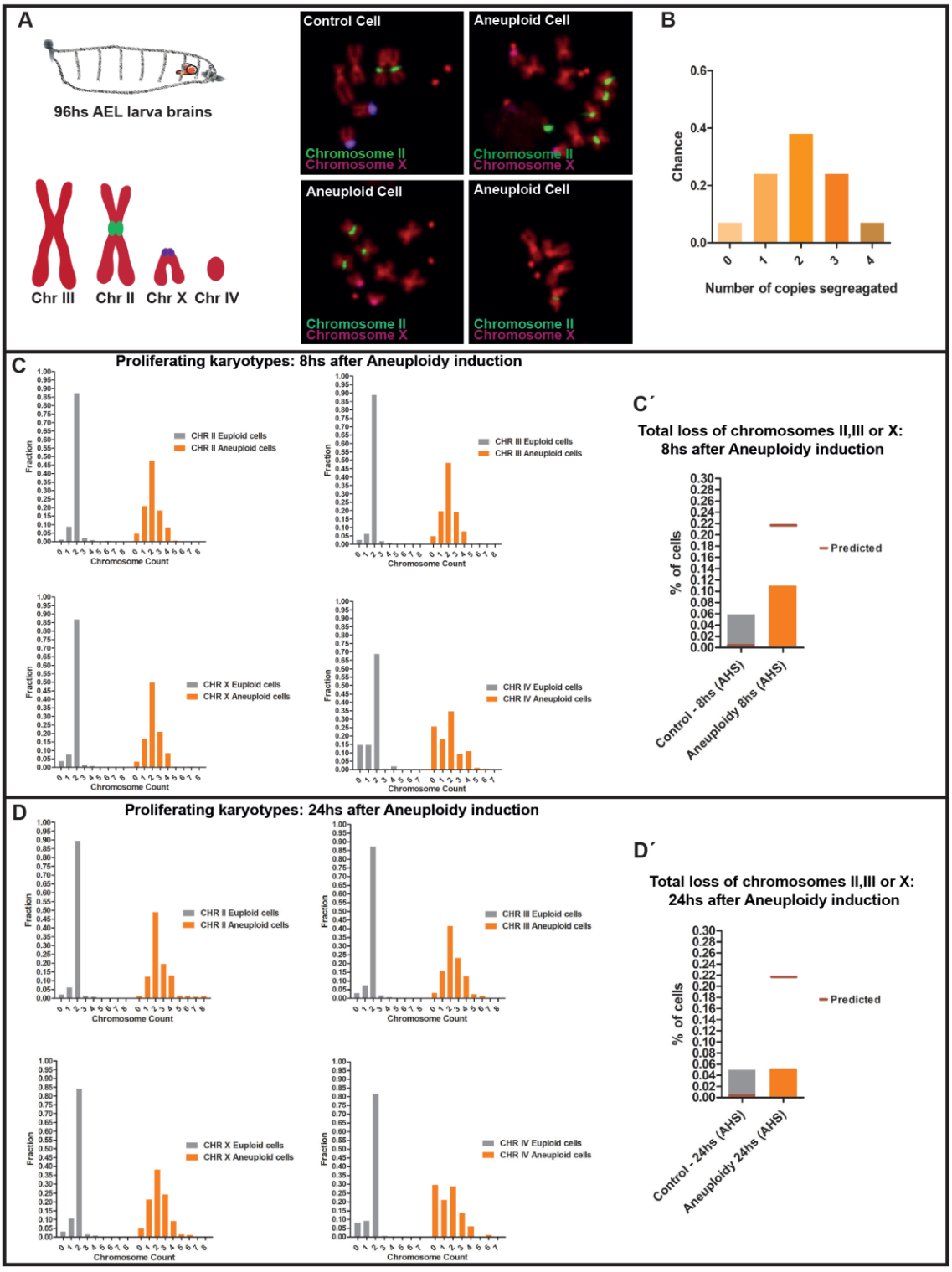
A
96hs AEL larva brains
Chr III
Chr II
Chr X
Chr IV
Control Cell
Aneuploid Cell
Aneuploid Cell
Aneuploid Cell
Chromosome II
Chromosome X
B
Chance
Number of copies segreagated
C
Proliferating karyotypes: 8hs after Aneuploidy induction
CHR II Euploid cells
CHR II Aneuploid cells
CHR III Euploid cells
CHR III Aneuploid cells
CHR X Euploid cells
CHR X Aneuploid cells
CHR IV Euploid cells
CHR IV Aneuploid cells
Fraction
Chromosome Count
C´
Total loss of chromosomes II,III or X:
8hs after Aneuploidy induction
% of cells
Predicted
Control - 8hs (AHS)
Aneuploidy 8hs (AHS)
D
Proliferating karyotypes: 24hs after Aneuploidy induction
D´
Total loss of chromosomes II,III or X:
24hs after Aneuploidy induction
Control - 24hs (AHS)
Aneuploidy 24hs (AHS)

Figure 9

Karyotype restrictions in the proliferating aneuploid Nbs population

A- *Panels of Fluorescent in situ Hybridization (FISH) of aneuploid Nbs and Control. Schematic of the FISH probe chromosome labeling.*
B- *Theoretical segregation of sister chromatids after cohesion loss, assuming segregation to be random. Full modeling data available.*
C to C´: C- *Frequency distribution of chromosome copy per Nbs, 8hs after aneuploidy induction.* ***C´-*** *Calculated theoretical loss rate for chromosome II, III or X, and the observed frequency of loss of any of these three chromosomes in the proliferating aneuploid Nbs.*
D to D´: D- *Frequency distribution of chromosome copy per Nbs, 24hs after aneuploidy induction.* ***D´-*** *Calculated theoretical loss rate for chromosome II, III or X, and the observed frequency of loss of any of these three chromosomes in the proliferating aneuploid Nbs*

III.6 Aneuploidy elicits a stress response in the brain tissue.

Our findings revealed that aneuploid cells are not promptly eliminated but instead continue to proliferate within certain karyotype restrictions. This should lead not only to the maintenance of aneuploid stem cells (due to Nb self-renewal) but also to the accumulation of differentiated aneuploid progeny (note that each Nb divides every ~2 hours (Ito and Hotta, 1992)). We therefore tested how such increase in aneuploid cells within the tissue could affect cellular physiology and influence normal tissue development.

Several aneuploidy-associated stresses that include oxidative, metabolic, and proteotoxic stress are likely to alter cellular homeostasis (Santaguida and Amon, 2015), which ultimately lead to p53 activation and a p53-dependent cell-cycle arrest (Kruiswijk

et al., 2015; Thompson and Compton, 2010). Interestingly, elevated levels of p53 have been observed in the Central Nervous System of Down syndrome patients (Liao et al., 2012). We decided to take advantage of our in vivo system to acutely induce aneuploidy to examine whether abnormal karyotypes trigger a stress response in the developing *Drosophila* brain and if so, what is the kinetics of such response. We assessed by immunohistochemistry the presence of P53 and the senescence marker Dacapo (DAP, a p21/p27 homologue (Lane et al., 1996)), after the loss of cohesin and consequent aneuploidy. We determined that both stress markers start to be evident at 12hs AHS in the tissue but only at 24hs AHS significant number of cells labeled with these markers are observed (Figure 10A; 10A´ and 10A´´). Furthermore, the large majority of the cells that appeared stress positive are not Nbs-like cells since the signal is limited to the small cells in the brain at that time (Figure 10A).

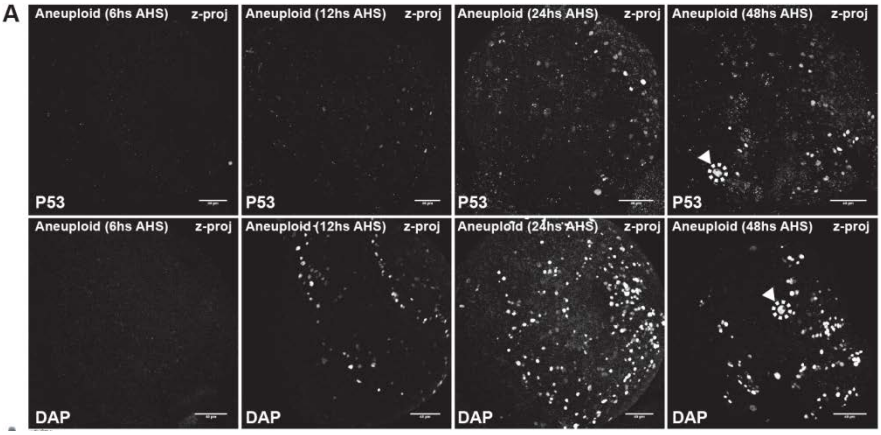

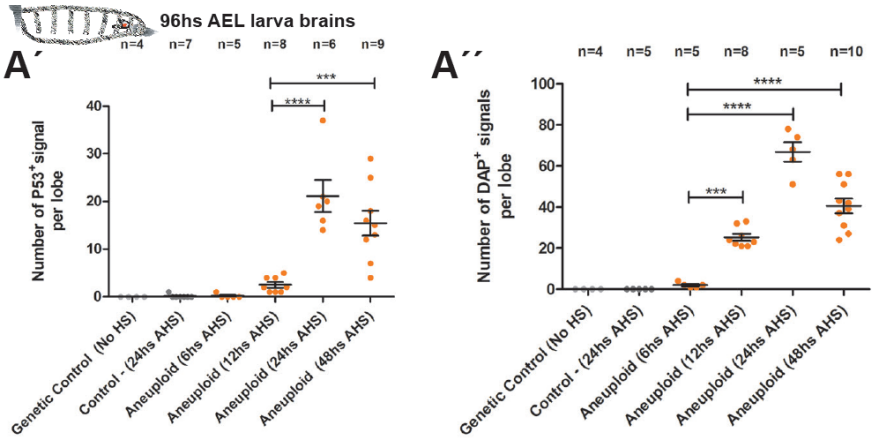

Figure 10A

Aneuploidy induced stress response is delayed in the neural tissue.

A to A´´: A- *Kinetics of the aneuploidy induced stress response at 6, 12, 24, and 48hs AHS; assessed by immunofluorescence of canonical markers P53 and Dacapo (DAP). Nbs show a delayed aneuploidy stress response at 48hs AHS (arrowheads with dashed circles).* ***A´ and A´´-*** *Counts of overall numbers of p53 and DAP signals per lobe, displaying a significant increase from 24hs AHS. ; *** = P<0.001; **** = P<0.0001. Scale bar = 40µm. z-proj (z projection).*

Nbs-like cells stained with the stress markers are noticeable only at 48hs AHS (Figure 10A, arrowheads and dashed circles), suggesting that despite their aneuploid state, neural stem cells are delayed at displaying an evident stress-response. We confirmed this observation by quantifying the appearance of cells co-stained with the stress markers and the Nb marker DPN through time (Figure 11). We concluded that even when being induced in a time controlled, acute manner, or very early in development, aneuploidy has a strong impact on the development of the *Drosophila* nervous

system. This is the case at it affects not only the dividing progenitors cells like Nbs and ganglia mother cells (GMC), but also their progeny, resulting in loss of tissue architecture.

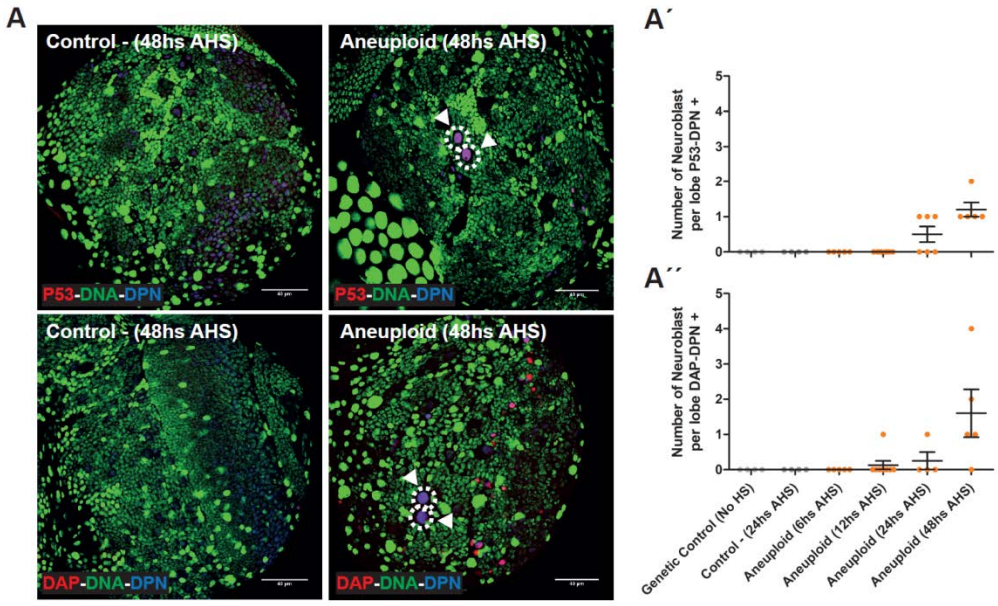

Figure 11

Aneuploidy stress response is delayed in Neuroblasts

A to A´´: *Pictures from fixed samples of 3rd instar larvae lobe brains showing the immunofluorescence of canonical stress response markers P53 and Dacapo (DAP) together with the Nbs marker (DPN) at 48hs AHS. Nbs display a delayed aneuploidy stress response at 48hs AHS (arrowheads with dashed circles).* ***A´ and A´´-*** *Quantification of the kinetics of the aneuploidy induced stress response at 6, 12, 24, and 48hs AHS in Nbs (DPN+). Scale bar = 40µm.*

III.7 Neural stemness delays aneuploidy stress response.

The delayed stress response (i.e. ~48hs after induction of aneuploidy) in the neural stem cell pool may imply selective stem cell tolerance for the aneuploid condition when compared to the other cell types of the developing brain. To test this idea we took advantage of the *brat* mutant condition (Arama et al., 2000). In *brat* mutant larvae brains each Nb divides into two daughter cells grow that retain Nbs properties, leading to the formation of a tumor-like neoplasm (Betschinger et al., 2006). We reasoned that cellular stemness confers tolerance to aneuploidy, the complete occupancy of the developing brain by Nbs-like cells observed in the *brat* mutant phenotype should be sufficient to prevent the stress response observed at 24hs AHS. To test this idea we combined our system for acute induction of aneuploidy with *brat* mutations to be able to induce aneuploidy in a *brat* mutant background and analyze the presence of stress markers at 24 and 48hs AHS. As predicted, DAP appearance was significantly delayed in aneuploid *brat* mutants when compared to aneuploid brains alone (Figure 10B and 10B´). The same result is observed for P53 staining (Figure 12). Note that the Nbs marker (DPN) stain almost all the cells in *brat* mutant brains, demonstrating the stem cell state of the entire tissue (Figure 10B and 10B´). This result strongly suggests that the neural stem cell identity confers extreme tolerance to aneuploidy-associated stresses.

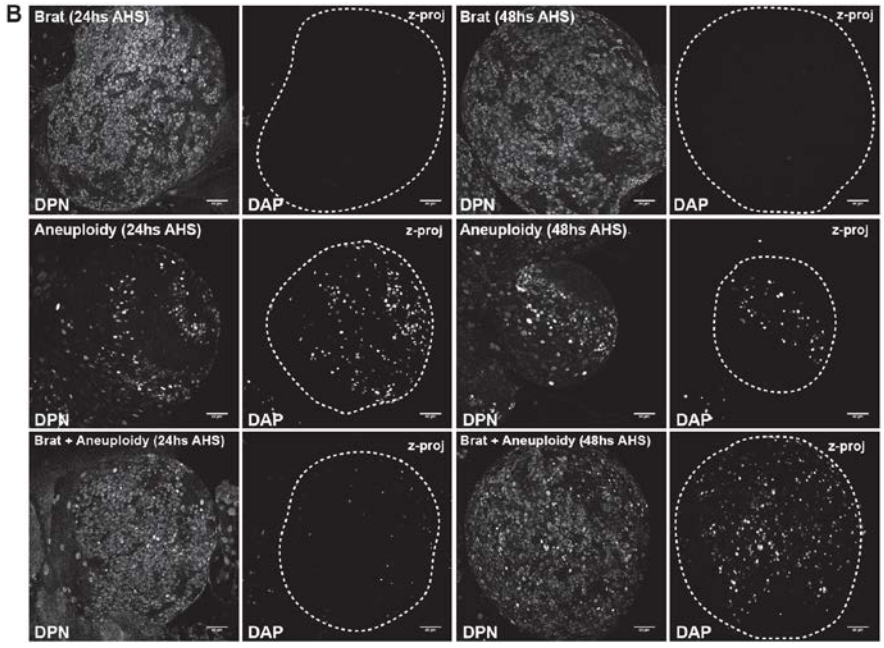
B
Brat (24hs AHS)
z-proj
DPN
DAP
Brat (48hs AHS)
Aneuploidy (24hs AHS)
Aneuploidy (48hs AHS)
Brat + Aneuploidy (24hs AHS)
Brat + Aneuploidy (48hs AHS)

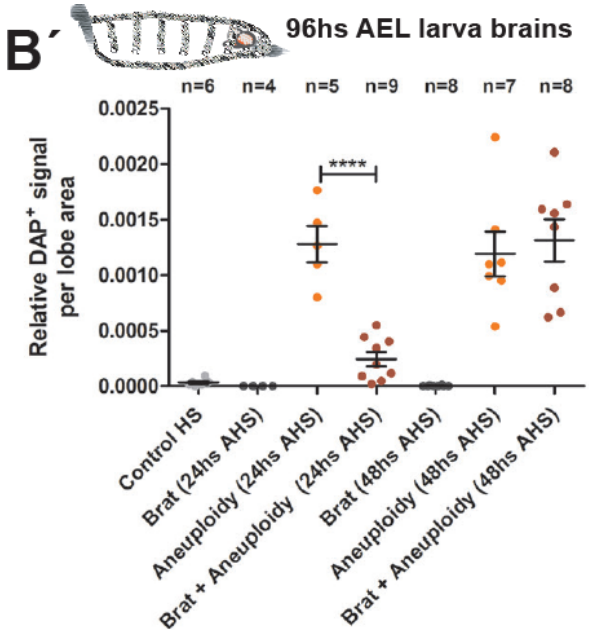
B´
96hs AEL larva brains
n=6
n=4
n=5
n=9
n=8
n=7
n=8
Relative DAP+ signal per lobe area
0.0025
0.0020
0.0015
0.0010
0.0005
0.0000
****
Control HS
Brat (24hs AHS)
Aneuploidy (24hs AHS)
Brat + Aneuploidy (24hs AHS)
Brat (48hs AHS)
Aneuploidy (48hs AHS)
Brat + Aneuploidy (48hs AHS)

Figure 10B

Stem cell state of the Neuroblast confers aneuploidy tolerance: B- *Pictures from fixed samples of 3rd instar larvae lobe brains showing the immunofluorescence of the stress marker DAP and the Nbs marker (DPN) at 24 and 48hs after induction of aneuploidy.* ***B´-*** *Quantification of relative DAP positive signal per lobe area from 24 to 48hs AHS tissues. Brat mutant lobe brains showed a clear reduction in the presence of the aneuploidy induced stress marker DAP at 24hs AHS. n= number of lobe brains. **** = P<0.0001. Scale bar = 40µm. z-proj (z projection).*

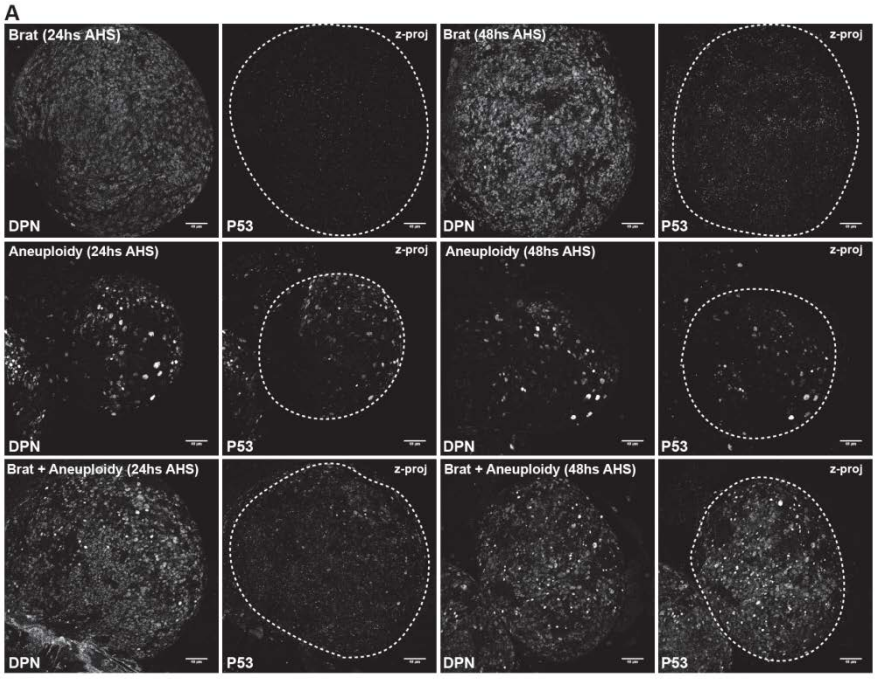

Figure 12

Aneuploidy induced P53 appearance is delayed in the neural stem cell pool.

A to A´: A- *Brat mutant lobe brains showed a clear reduction in the presence of the aneuploidy induced stress marker P53 at 24hs AHS.* ***A´-*** *Quantification of relative P53 positive signal per lobe area from 24 to 48hs AHS. n= number of lobe brains. **** = P<0.0001. Scale bar = 40µm. z-proj (z projection*

III.8 Acute induction of developmental aneuploidy does not significantly alter adult brain size.

All the flies that survive the developmental aneuploidy show severe motor defects suggesting an impaired central nervous system. Previously, it has been reported in a centrosome amplification models that the generation of aneuploid cells during brain development resulted in microcephaly (Marthiens et al., 2013; Poulton et al., 2017). Contrary to our expectations, size measurements of dissected brains from adult flies (i.e. 1-day old) both control and developmental aneuploidy-induced (72hs and 96hs AEL heat-shock) showed no major differences in the total length of the brain or diameter of the optic lobes (Figure 13; 13B´ and 13B´´). Moreover, no signs of neurodegenerative process (such as dramatic cortical cell loss and/or vacuolation) were detected (Figure 13B).These results indicate that understanding how aneuploidy in the developing brain influences the adult tissue homeostasis requires a more exhaustive analysis of the adult brain architecture.

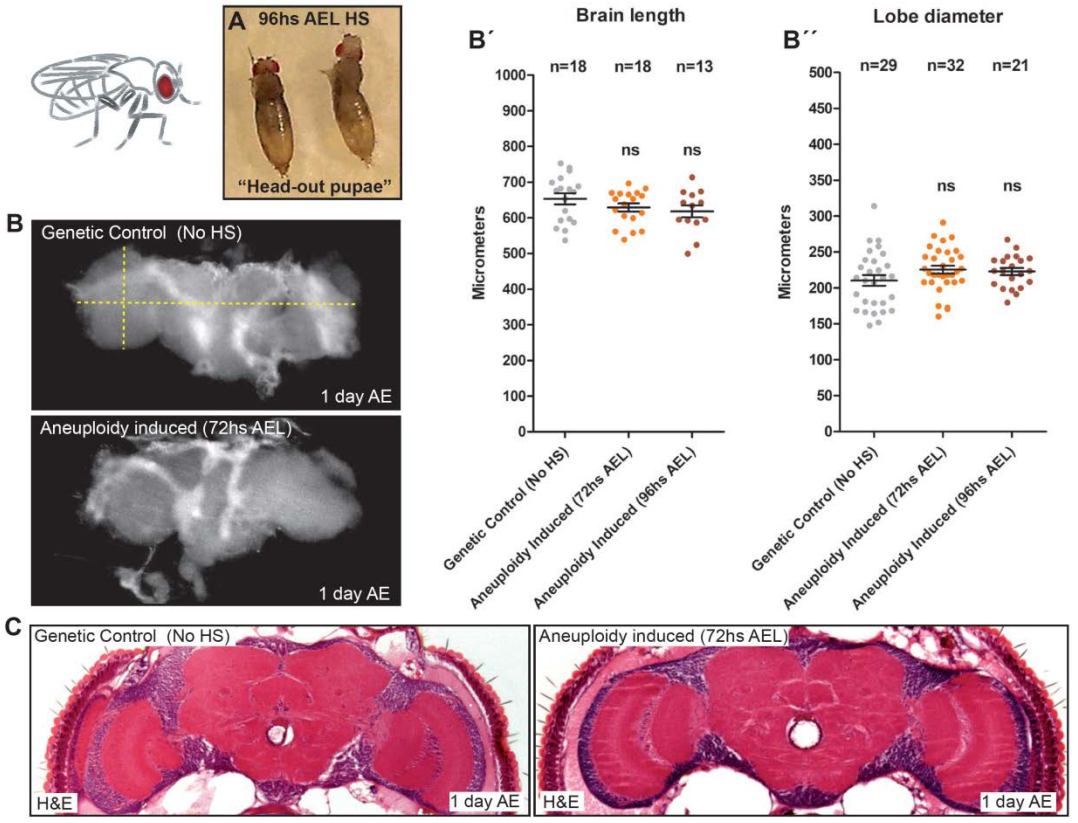

Figure 13

Adult brains do not show any significant alteration in shape and size after induction of aneuploidy during development.

A to A´´: A- *Dissected brains of adult flies from a control and a developmental aneuploidy-induced (72hs AEL heat-shock) organisms.* ***A´ and A´´-*** *Quantifications of lobe diameter and brain length in control and developmental aneuploidy-induced (72 and 96hs AEL heat-shock) adult flies showed no significant differences. n= number brains. ns= no significant*

B- *Histology analysis of brains from control and aneuploidy-induced during development (72hs AEL heat-shock) adult flies, one day after eclosion. Frontal sections at approximately midbrain showed no signal of neurodegenerative process (vacuolization). H&E= Hematoxylin and Eosin*

III.9 Protecting only the developing brain from induced aneuploidy rescues the lifespan of the ecloded flies.

Upon aneuploidy challenge, we observed a striking difference across analyzed *Drosophila* tissues: whereas epithelial tissues like wing discs are able to regenerate from this insult, neural stem cells are either irreversibly lost or become highly chromosomally unstable. These findings, together with the fact that most flies that survive the developmental aneuploidy induction show severe motor defects in otherwise healthy adult morphology, led us to hypothesize that the brain is the only limiting tissue in response to aneuploidy during development.

To test this hypothesis, we devised a system to selectively protect only the brain from cohesin removal and consequent aneuploidy. To achieve this, we complemented our reversible cohesin cleavage system with Brain-specific expression of RAD21-WT throughout the course of the experiment (Figure 14A). In this way, TEV expression should lead to cohesion loss in all larval tissues that survive solely on RAD21-TEV at the time of heat shock. In contrast, neural stem cells should be resistant to this challenge, as they express both RAD21-TEV and RAD21-WT (Figure 14B). Neuroblast-specific expression of RAD21-WT was achieved by the use of *inscuteable-Gal4* (*insc-Gal4*) or *worniu-Gal4* (*wor-Gal4*) drivers, to constitutively express *UAS-Rad21-wt-myc* in the developing brain (Figure 14B). As expected, constitutive presence of TEV-resistant RAD21 in the brain prevents any cohesion defects in 3rd *instar* larvae Nbs (Figure 14C). To confirm that the rescue of sister chromatid cohesion occurs exclusively in the brain; we performed parallel characterization of the first mitotic division after the heat shock in

the wing, derived from the same larvae. As anticipated, full cohesin cleavage was observed in all the dividing epithelial cells from the wing discs (Figure 14D).

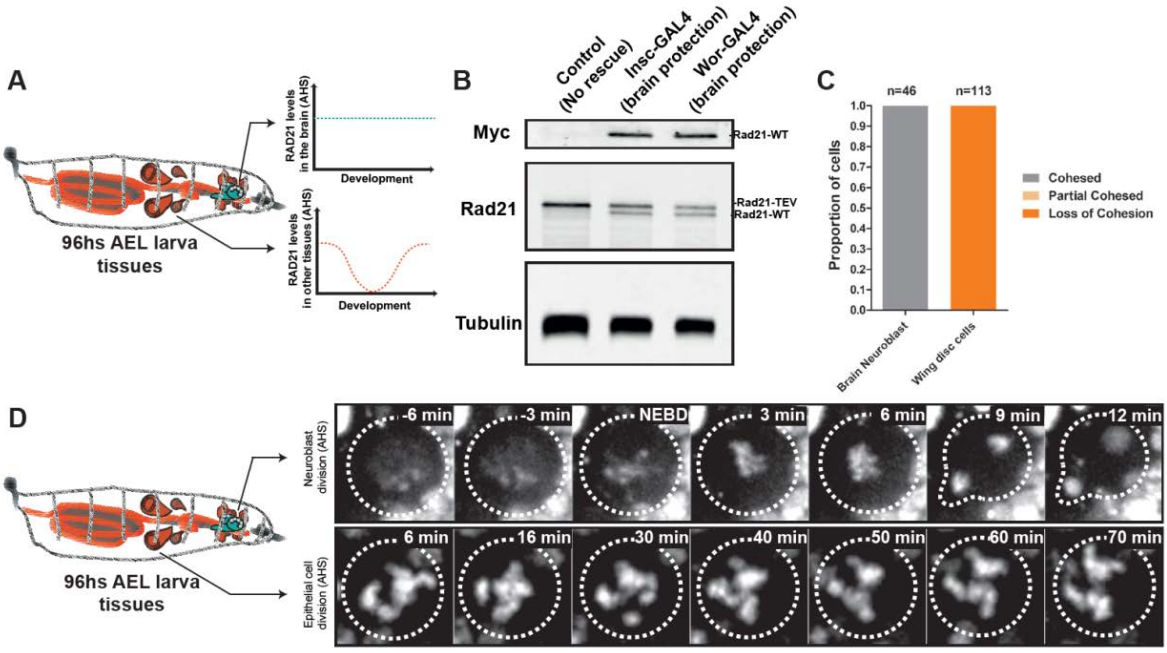

Figure 14A-B

Modifying the reversible cohesin cleavage system to protect only the developing Brain from aneuploidy

A*- Graphic scheme depicting how the developing brain is protected from the loss of cohesion and induction of aneuploidy upon the constitutive expression of the RAD21-WT driven by Nbs specific Gal4 (Insc-Gal4 or Wor-Gal4). In contrast, the rest of the dividing tissues from the larva experience the acute inactivation of cohesin complex (by TEV cleavage of RAD21-TEV) after the heat-shock.*

B*- Western blots showing the expression of both the cleavable (RAD21-TEV) and non-cleavable RAD21 (RAD21-WT) in 3rd instar brains. Insc-Gal4 and Wor-Gal4 drivers result in expression of RAD21-WT in the 3rd instar brain before the heat-shock.*

***C**- Quantification of Cohesive states of 3rd instar larvae Nbs and epithelial cells from wing discs following heat-shock. Insc-Gal4 protects the brain from cohesin loss, but has no effect in the wing disc.*

***D**- Live imaging cohesion profiles of Nbs and epithelial cells during mitotic divisions after the heat-shock. Insc-Gal4 prevents mitotic delay caused by cohesion loss in the Nbs.*

Notably, protecting only the brain from developmental aneuploidy fully rescued the severe motor defects of the ecloded flies from the 72hs AEL heat-shock, as demonstrated by mobility essays (Figure 14E´). Even more surprisingly, the brain protection was enough to rescue the lifespan of ~70% of the adult flies affected by organism-wide aneuploidy during development, demonstrating that the brain is indeed the most sensitive tissue when challenged with aneuploidy (Figure 14E).

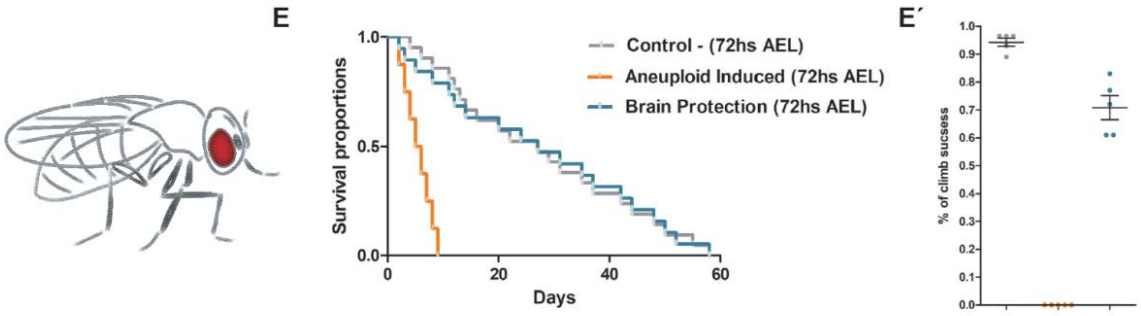

Figure 14E

Protecting only the developing brain from induced aneuploidy rescues the lifespan of the ecloded flies.

***E to E´: E**- Kaplan-Meier survival curves showing fractional survival as a function of time. Protection of the brain tissue from the induced aneuploidy rescues the adult lifespan of the ecloded flies with 72hs AEL heat-shock.*

***E´-** Climbing assay of adult flies. Percentage of climb success was plotted over the halfway point (10cm). Protection of the brain tissue from induced*

aneuploidy rescues motor defects of the ecloded flies with the 72hs AEL heat-shock.

III.10 Discussion

Acute disruption of mitotic fidelity enables tracing of aneuploidy *per se*.

We developed a novel genetic tool in *Drosophila* to study aneuploidy *in vivo*. This tool enables the induction of a controlled pulse of aneuploidy, at the developmental stage of choice. The outcomes using a reversible perturbation are significantly different to the ones resulted from a chronic disruption of mitotic fidelity. Whereas chronic mitotic perturbation is incompatible with organism viability, here we show a high survival rate upon controlled and acute organism-wide aneuploidy challenge. The long term survival after aneuploidy challenge coupled with the reversibility of the mitotic perturbation induced, overcomes one of the major limitations present in other metazoan models: We are able the study of the kinetics response to aneuploidy across different tissues/developmental stages, focusing solely on the effects aneuploidy and without the confounding variable the mitotic perturbation used to cause aneuploidy.

Cohesin loss and induction of aneuploidy is tolerated better by the organism if induced early in development, as observed comparing the rates of eclosion. The developing larvae are progressively scaling mitotic machines, with each consecutive stage containing more divisions than the previous one (Ito and Hotta, 1992). This implies that the heat-shock at the 1st and 3rd *instar* larvae are not the same, as they affect different number of dividing cells, thus

generating different numbers of aneuploid progeny, as demonstrated by our data. Although, the more parsimonious explanation for aneuploidy tolerance in early development would be a quantitative one, it is also important to mention that a developmental delay is observed after aneuploidy induction (e.g. delayed pupariation stage). It is well known that delayed development allows the organism to adjust their growth programs after disturbances (Gontijo and Garelli, 2018; Hackney and Cherbas, 2014). This induced delay is a development-stage dependent response, as some perturbations only appear to retard pupariation when induced at or before a certain stage in larval development as for example, beginning of the third *instar* (Garelli et al., 2012; Halme et al., 2010; Simpson et al., 1980). This clearly exposes the different tissue sensitivities, showing that the developing brain is extremely sensitive to any level of aneuploidy during development.

Chromosome mis-segregation in Neuroblast leads to a complex array of karyotypes and cellular abnormalities.

Neuroblasts have been used as a system to study aneuploidy in previous studies (Gogendeau et al., 2015; Poulton et al., 2017). These studies postulate two different but not mutually exclusive mechanisms of response to induced aneuploidy: premature differentiation (Gogendeau et al., 2015) and cell death by apoptosis (Poulton et al., 2017). We reasoned that if these are the major mechanisms of response to aneuploidy in neural stem cells, they should be detectable in high frequency after the aneuploidy induction by our acute approach. Contrary to that notion, after examined in detail the kinetics of the response, both premature

differentiation and cell death were detected at low frequency even days after cells became aneuploid. It is important to note that the degree of aneuploidy in the Nbs upon cohesin loss should be around 98% due to the extensive genome shuffling prior to mitotic exit. Therefore, the finding that aneuploidy does not eliminate the entire Nb population, strongly argues against the existence of specific, active mechanisms controlling the integrity of the neural stem cell genome. The more plausible explanation is that the Nb elimination due to aneuploidy stems from a wide spectrum of abnormalities due to a randomized genome. Supporting this idea, it has been shown in yeast cell-to-cell variability in cell-cycle progression and robustness of multiple cellular processes even among cells harboring the same aneuploidies (Beach et al., 2017)

Examination of Nbs in real time after aneuploidy induction further revealed that aneuploidy is sufficient to induce chromosomal instability within a short time-.period (~12h). The appearance of obvious chromosomal instability, characterized by a wide range of mitotic defects, takes several cell cycles after cohesin has been restored, which strongly supports the notion that chromosomal instability is consequence of the abnormal karyotype and not the mitotic disruption initially applied. Overall, we observe a selection towards the accumulation of chromosomes, generating huge Nbs, which keep proliferating despite their increased ploidy (Gogendeau et al., 2015).

Thus, our *in vivo* detailed examination of the aneuploid Nbs (immediately after aneuploidy was induced) and kinetics of events (through several hours) clearly demonstrates that just a single round of chromosome miss-segregation in these cells is enough to originate a complex array of karyotypes which can lead to a variability of mitotic abnormalities.

Neural stemness confers resistance to aneuploidy-associated stress response.

During the last years, studies from tissue cultured and yeast cells, have collected solid evidence on how abnormal karyotypes can remarkably alter physiology of eukaryotic cells (reviewed in (Santaguida et al., 2015). They can lead to a different aneuploidy-associated stresses that include oxidative, metabolic, and proteotoxic stress which likely contribute to p53 activation and cell senescence (Kruiswijk et al., 2015). However, our understanding about how the aneuploidy induced stress at cellular level influences development of disease-free tissues, is very limited.

Our time-course assessment of classical stress response markers (P53 and DAP) following chromosome mis-segregation in the brain tissue, clearly showed that aneuploidy response is not immediate and takes several hours for the cells to exhibit their up-regulation (12 to 24hs AHS). This delayed stress response is in agreement with recent observations in culture cells where it has been shown that chromosome miss-segregation did not lead to arrest in the following G1 in the vast majority of aneuploid daughter cells (Santaguida et al., 2017; Soto et al., 2017).

Interestingly, our results highlight that cell identity determines the kinetics of this stress response. Aneuploidy response is specifically delayed in the neural stem cell pool (displayed mainly at ~48hs AHS) compared to the rest of the tissue, which exhibits it considerably earlier. Forcing self-renewal is sufficient to delay stress response in the entire tissue, suggesting that cellular stemness alone makes cells less sensitive to aneuploidy-induced

stresses. Accordingly, unusual resistance to altered ploidy was observed in human and mouse embryonic stem cells (ESCs), mostly achieved by relaxing the cell cycle control and uncoupling the spindle checkpoint from apoptosis (Mantel et al., 2007). The ability of neural stem cells to continue dividing despite the aneuploid karyotype dubbed them as aneuploidy “tolerant” (Poulton et al., 2017). Yet, based on our findings it is clear that keeping these aneuploid cells is catastrophic is for normal tissue architecture and development. Thus, aneuploidy may be “tolerated” better in Nbs, but the tissue as a whole is unable to be functional. In contrast, the “sensitivity” of epithelial cells enables the tissue to clean up and regrow properly.

The developing brain restricts organism recovery after induced aneuploidy.

Chromosomal aberrations have been long associated with neurological disorders (Bushman and Chun, 2013). However, their impact on brain development and function remains complex and poorly understood, partially due to limitations of available experimental approaches. In almost all animal model system used to study aneuploidy and its consequences until now, the organisms die prematurely due to the chronic disruption of mitotic fidelity to generate chromosome imbalance. Therefore, it is only possible to address the short term effect of aneuploidy in nervous system development, but not to understand the ultimate consequences for brain function. Our acute system, reversibly affects chromosome segregation to induce just a pulse of aneuploidy, enabling to the organism recover from the insult and complete its development. The most noticeable phenotype observed in the adult was the

severe motor and behavioral defects that clearly affect the lifespan of the flies, evidencing the sensitiveness of the nervous system to aneuploidy. Previous studies in *Drosophila* have shown that the mitotic disruption in larvae Nbs generates a reduction of their brain size (Gogendeau et al., 2015; Poulton et al., 2017) reinforcing the idea about a link between aneuploidy and microcephaly. However, our results showed that induced acute aneuploidy has no significant impact in the size of the brain. These findings suggest that the continued proliferation of neuronal stem cells, caused by incomplete cell elimination and delayed aneuploidy-stress response, is sufficient to support the development of an apparently normal-sized organ. It is conceivable that the observed normal size reflects a sample selection, as this analysis was restricted to flies that survived the aneuploid challenge (~70%). Supporting this possibility, a screening performed to isolate anatomical brain mutants of *Drosophila* have shown that mutant strains showing altered brain shape and particularly small brains are very weak being mostly lethal at pupa stage (Heisenberg, 1979). Despite unaltered shape and size of the adult brains, we reasoned that the neural circuits are likely impaired in those brains giving rise to the adult phenotype observed in surviving flies.

In accordance with the notion of the brain as the tissue most sensitive to aneuploidy, we show that preventing aneuploidy exclusively in the brain is sufficient to rescue all the behavioral defects previously observed. This brain protection not only rescued motor defects but also the lifespan of the flies ecloded upon 72hs AEL heat-shock, suggesting that neural tissue is the most ill-equipped to deal with aneuploidy during development and impose a significant cost for the organism. Several pathophysiological chromosomal disorders in humans including trisomy 21, trisomy 18,

and trisomy 13, as well as the mosaic disorder MVA (mosaic variegated aneuploidy, characterized by the presence of a different number of chromosomes in some cells), are well-known to display intellectual disability (Bushman and Chun, 2013), yet the impact of the aneuploid condition on brain development is still unclear (Oromendia and Amon, 2014; Ricke and van Deursen, 2013). Therefore, it become evident the necessity of future studies in different animal model systems based on an acute induction of aneuploidy to properly investigate its consequences for tissue development and homeostasis. These approaches could help to elucidate the molecular mechanisms underlying the physiological changes in stem/somatic cells generated by aneuploidy and its implications on tissue development and homeostasis.

III.11 Materials and Methods

Fly husbandry and genetics

Flies were raised using standard techniques at room temperature (20-22 ºC). We stablished both the chronic and the acute inactivation of cohesin complex by crossing the following genotypes: *w; hspr-nlsV5TEV; Rad21(ex^{3})/TM6B* with *w;; tubpr-Rad21(550-3TEV)-EGFP, Rad21(ex^{15}), polyubiq-His-RFP,* and *w; hspr-nlsV5TEV; Rad21(ex^{3}), hspr-Gal4, UAS-Rad21(wt)-myc/TM6B* with *w;; tubpr-Rad21(550-3TEV)-EGFP, Rad21(ex^{15}), polyubiq-His-RFP*, respectively. The progeny was then heat shocked once at 37°C for 45min at the desired developmental stage. The correct genotype larvae were selected based on the absence of the "tubby" phenotype; the heat shocked "tubby" larvae were used as negative controls (control HS). As genetic control we used the same genotypes for the induction of aneuploidy but without performing the heat-shock.

To determine the proportion of adult eclosion, the crosses mentioned were raised in cages to monitor the time of egg collection. After 6hs collection, the plates were removed from the cages, the number of eggs counted and the plates were kept until larvae hatched. The plates were then heat-shocked at 37°C for 45min at different larvae developmental time (~48hs AEL, ~72hs AEL, ~96hs AEL and ~120hs AEL (± 6hs)) and placed in a new clean plastic cage. Once they reached pupae stage ("yellow body") the pupae were gently removed with a wet brush and separated in "tubby" (control HS) and "no tubby" phenotype (condition). The different batches of pupae were placed over agar plates covered with two layers of absorbent paper to maintain the humidity and

counted. The plates with the pupae were kept at room temperature until flies ecloded and the proportion of eclosion calculated.

To combine the induction of Aneuploidy (acute cohesion inactivation) and the *brat* mutant genetic background we generated the following stocks: *w; brat^{1}/CTG; Rad21(ex^{3}), hspr-Gal4, UAS-Rad21(wt)-myc/TM6B* and w*; hspr-nlsV5TEV,brat^{TS}/CTG; tubpr-Rad21(550-3TEV)-EGFP, Rad21(ex^{15}), polyubiq-His-RFP.* These stocks were crossed and the progeny was heat shocked once at 37°C for 45min at the developmental stage desired and the genotype *w; brat^{1}/hspr-nlsV5TEV, brat^{TS}; Rad21(ex^{3}), hspr-Gal4, UAS-Rad21(wt)-myc/tubpr-Rad21(550-3TEV)-EGFP, Rad21(ex^{15}), polyubiq-His-RFP*, was selected at larva stage based on the absent of both, GFP signal and "tubby" phenotype.

To inhibit apoptosis we induced the over-expression of the baculovirus p35 in the context of the genetic background for acute inactivation of cohesin complex. To achieve this purpose, we generated the following stock *w; UAS-P35; tubpr-Rad21(550-3TEV)-EGFP 3, Rad21(ex^{15}), polyubiq-His-RFP* to be crossed with *w; hspr-nlsV5TEV; Rad21(ex^{3}), hspr-Gal4, UAS-Rad21(wt)-myc/TM6B.* The progeny was then heat-shocked once at 37°C for 45min at the developmental stage desired.

Finally, for the "brain rescue" experimental setup, we generated the following stocks: *w; insc-Gal4; tubpr-Rad21(550-3TEV)-EGFP, Rad21(ex^{15}), polyubiqpr-His-RFP* and *w; wor-Gal4; tubpr-Rad21(550-3TEV)-EGFP, Rad21(ex^{15}), polyubiqpr-His-RFP*. These stocks were crossed with the *w; hspr-nlsV5TEV; Rad21(ex^{3}), hspr-Gal4, UAS-Rad21(wt)-myc/TM6B* stock. The crosses and the progeny were raised and treated as described above for the determination of the eclosion proportion.

Table with all stocks used in this study:

Stock genotype	Reference
w; hspr-nlsV5TEV; Rad21(ex^{3})/TM6B	*Pauli et al. 2008*
w;;tubpr-Rad21(550-3TEV)-EGFP, Rad21(ex^{15}), polyubiq-His-RFP	*Oliveira et al. 2010*
w; hspr-nlsV5TEV; Rad21(ex^{3}), hspr-Gal4, UAS-Rad21(wt)-myc/TM6B	*This study*
w; hspr-nlsV5TEV,brat^{TS}/CTG; tubpr-Rad21(550-3TEV)-EGFP, Rad21(ex^{15}), polyubiq-His-RFP	*This study*
w; brat^{1}/CTG; Rad21(ex^{3}), hspr-Gal4, UAS-Rad21(wt)-myc/TM6B	*This study*
w; UAS-P35;tubpr-Rad21(550-3TEV)-EGFP 3, Rad21(ex^{15}), polyubiq-His-RFP	*This study*
w; HisH2AvD mRFP1 II.2/CyO; 363, CGC III.1 (R26)/TM3,Ser	*Mirkovic et al. 2015*
brat^{ts1} rdo^{1} hook^{1} pr^{1}/CyO	*BDSC #3991*
brat^{1} rdo^{1} hook^{1} pr^{1}/CyO	*BDSC #3988*
w; P{wor.GAL4.A}2; Dr^{1}/TM3, P{Ubx-lacZ.w+}TM3, Sb^{1}*	*BDSC #56553*
w; P{GawB}^{inscMz1407}*	*BDSC #8751*

Lifespan analysis

Lifespan was measured at room temperature according to standard protocols. In brief, newly ecloded animals (0 to 3 days) were collected (50 per genotype: “control”, “Aneuploidy” and “Aneuploidy + brain rescue”), and then placed in vials (up to 10 per vial), and transferred to fresh vials every two days. Survival was recorded for each vial. Due to the reduced mobility of the aneuploidy genotypes, we scored flies stacked in the food as death events in all the vials analyzed. We created survival curves with Prism 5.00 for Windows (GraphPad Software, San Diego, CA, USA) using the method of Kaplan and Meier.aq

Climbing assay

For climbing assay flies were anesthetized with CO2, separated in groups of around twenty adults (3 replicas for each genotype) and allowed to recover for 2hs until to be subjected to a climbing assay. Briefly, the groups of over twenty flies were placed in an empty climbing vial and then tapped down to the bottom. They were allowed to climb past the halfway point from the bottom of the vial for 30 seconds (10cm). The number of flies above the 10 cm mark was recorded as a percentage of flies able to climb.

Histology

Briefly, flies were anesthetized with CO2 and then were placed gently in agarose blocks to immobilize them and prevent any damage to the head or eyes. The agarose blocks with the flies were immersed in Carnoy fixative overnight, at 4ºC. The next day the Carnoy solution was removed and three 70% ethanol washes

were performed. Immediately after, the flies were decapitated and the heads were oriented one by one in melted 2% agarose to guarantee similar orientation of the tissue sections. Agarose blocks were then processed, embedded, the whole head was sectioned into 5um-thick sequential sections and stained with Hematoxylin & Eosin. The histology was performed in the Histopathology unit at Instituto Gulbenkian de Ciência and the slides were analyzed by a pathologist with a DMLB2 microscope (Leica). Images were acquired with a DFC320 camera (Leica) and NanoZoomer-SQ Digital slide scanner (Hamamatsu).

Live-cell imaging

Larvae 3rd *instar* brains were dissected in Schneider medium supplemented with 10% FBS and intact brains were mounted on a glass-bottom dish (MakTek), covered with an oxygen-permeable membrane (YSI membrane kit), and sealed with Voltalef oil 10S (VWR). This procedure allowed long-term imaging of brains for periods up to 10 hours.

For imaging of imaginal discs and early *instar* larvae brains, tissues were dissected in Schneider medium with 10% FBS. Dissected discs were placed and oriented in a 200µl drop of medium at the bottom of a glass-bottom dish (MakTek).

Live imaging was performed on a spinning disc confocal using imaged on a Revolution XD microscope (Andor, UK) equipped with immersion a 60x glycerol-immersion 1.30 NA objective (Leica Microsystems) and a iXon Ultra 888 1024*1024 EMCCD (Andor, UK). 25-35 Z-series optical sections were acquired 0.5-1 µm apart.

Brain spreads and Immunofluorescence

For brain spreads and immunofluorescence, 3rd *instar* larvae brains were dissected in PBS, incubated with 100 µM colchicine for one hour, hypotonic shocked in 0.5% sodium citrate for 2–3 minutes, and fixed on a 5 µl drop of fixative (3.7% formaldehyde, 0.1% Triton-X100 in PBS) placed on top of a siliconized coverslip. After 30 seconds, the brains were squashed between the coverslip and a slide, allowed to fix for an additional 1 min and then placed in liquid nitrogen. Slides were further extracted with 0.1% Triton-X100 in PBS for 10 min, and used for immunofluorescence following standard protocols. Primary antibodies were rat anti-CID (gift from Claudio E. Sunkel) used at 1:2000 Cleaved *Drosophila* Dcp-1 (Asp216) Antibody (1:300) # 1679578S (Cell Signaling Technology), Cleaved Caspase-3 (Asp175) Antibody #9661 (1:300) (Cell Signaling Technology), Anti-Deadpan antibody #ab195173 (1:1500) (Abcam). Secondary antibodies conjugated with fluorescent dyes from Alexa series (Invitrogen) were used according to the manufacturer's instructions.

Third *instar* wing imaginal disc fixation and staining, as well as immunofluorescence of whole brains was performed using standard procedures (Lee and Treisman, 2001). Briefly, third *instar* larvae wing disc tissue (still attached to the larva body) was fixed on ice for 30 min. The fixative consisted of 4% formaldehyde (Polysciences) in 1X PEM buffer solution. Following were washed by gentle agitation three times for 20 min in PBS-T (1x PBS + 0.1% Triton X-100). Primary antibodies incubation was performed overnight at 4 °C in PBS-T supplemented with 1% BSA and 1% donkey serum. The following day, the tissues were washed again and incubated for 2h at room temperature with the appropriate secondary antibodies diluted in PBS-T solution. Finally, after the

wash of secondary antibodies, wing discs were mounted in Vectashield (Vector Laboratories). Fluorescence images were acquired with a ×40 HCX PL APO CS oil immersion objective (numerical aperture: 1.25–0.75) on a Leica SP5 confocal microscope.

Fluorescence In Situ Hybridization

Brains from 3rd instar larvae were dissected in PBS, incubated with 100 µM colchicine for one hour, and transferred to 0.5% sodium citrate solution for 3-4 minutes. Then, the brains were transferred to a fixative containing 11:11:2 Methanol: Acetic Acid: MQ Water, for 30 seconds before being placed in a droplet of 45% Acetic acid for 2 minutes, squashed and transferred to liquid Nitrogen. Then, the coverslip was removed and the slide incubated in absolute ethanol for 10 min at −20 °C (Freezer incubation). The slides were air dried at 4 °C. (20 minutes).The slides were dehydrated at room temperature in 70%, 90% and absolute ethanol for 3 minutes, prior to DNA denaturation in 70% formamide- 2xSCC solution for 2 minutes at 70 °C. This is done on the thermomixer set at 70 °C with a formamide solution heated to70 °.Then, the slides were transferred to cold 70% Ethanol (−20 °C) and dehydrated at room temperature in 90% and absolute ethanol for 3 min. FISH probes were denatured in the hybridization buffer at 92C for 3 min .Hybridization was done over-night at 37 °C using 30 ul of FISH hybridization buffer/probe mix per slide. Hybridization buffer: 20% dextran sulfate in 2x SCCT/50% Formamide/0,5mg/ml Salmon sperm DNA. Then, slides were washed 3 × 5 min in 50% formamide-2xSCC at 42 °C and 3 × 5 min in 0.1xSCC at 60 °C. These steps are done on the thermomixer, with the solutions previously heated to desired temperatures. Finally, the slides are

washed in PBS, and mounted in Vecta shield with DAPI. The probes were used in the final concentration of 70Nm in hybridization buffer. Probes used were: Chr_X (359 bp satellite DNA) A546-GGGATCGTTAGCACTGGTAATTAGCTGC, and Ch_3 (dodeca satellite DNA) Cy5-ACGGGACCAGTACGG DNA probes, Chr_2 A488-(AACAC).

Western-blot

To analyze RAD21 protein amounts, *Drosophila* tissues were dissected in PBS and homogenized with a pestle in Sample buffer. Samples were centrifuged, and boiled for 5 minutes in 2x Sample Buffer. Samples were loaded on a 13 % SDS-gel for electrophoresis and and then transferred to nitrocellulose membranes. Western-blot analysis was performed according to standard protocols using the following antibodies: anti-α-tubulin (1:50.000, DM1A, Sigma-Aldrich Cat# T9026), guinea pig anti-Rad21 (Heidmann et al., 2004) and V5 Tag Mouse Monoclonal Antibody (Novex®).

Image analysis

Imaging analysis was performed using FIJI software (Schindelin et al., 2012). For z-projections slices were stacked into maximum intensity (10 frames, 2µm each). Some pictures were rotated and/or flipped to orient them in the same way.

Statistical analysis

Statistical analysis and graphic representations were performed using Prism 5.00 for Windows (GraphPad Software, San Diego, CA, USA). Unpaired t test or one-way ANOVA (using the Bonferroni's multiple comparison) were applied depending the

measurements analyzed in the corresponding experiment. Sample size details are included in the respective plotted graphs.

Acknowledgments

We thank S. Heidmann and the Bloomington Stock Center for fly strains, the Advance Imaging Unit and Fly Facility, Histopathology of Instituto Gulbenkian de Ciencia for technical assistance, and C. Homem, F. Janody and M. Bettencourt-Dias, and all the members of the RAO laboratory for discussions and comments. MM was supported by a Fundação para a Ciência e Tecnologia, FCT, fellowship (SFRH /BD/52438/2013). This work was supported by the following grants awarded to RAO: FCT Investigator grant (IF/00851/2012/CP0185/CT0004), EMBO Installation Grant (IG2778) and European Research Council Starting Grant (ERC-2014-STG-638917).

References

Ambartsumyan, G., and Clark, A.T. (2008). Aneuploidy and early human embryo development. Hum Mol Genet *17*, R10-15.

Arama, E., Dickman, D., Kimchie, Z., Shearn, A., and Lev, Z. (2000). Mutations in the beta-propeller domain of the Drosophila brain tumor (brat) protein induce neoplasm in the larval brain. Oncogene *19*, 3706-3716.

Beach, R.R., Ricci-Tam, C., Brennan, C.M., Moomau, C.A., Hsu, P.H., Hua, B., Silberman, R.E., Springer, M., and Amon, A. (2017). Aneuploidy Causes Non-genetic Individuality. Cell *169*, 229-242 e221.

Betschinger, J., Mechtler, K., and Knoblich, J.A. (2006). Asymmetric segregation of the tumor suppressor brat regulates self-renewal in Drosophila neural stem cells. Cell *124*, 1241-1253.

Bushman, D.M., and Chun, J. (2013). The genomically mosaic brain: aneuploidy and more in neural diversity and disease. Semin Cell Dev Biol *24*, 357-369.

Choksi, S.P., Southall, T.D., Bossing, T., Edoff, K., de Wit, E., Fischer, B.E., van Steensel, B., Micklem, G., and Brand, A.H. (2006). Prospero acts as a binary switch between self-renewal and differentiation in Drosophila neural stem cells. Dev Cell *11*, 775-789.

Dekanty, A., Barrio, L., Muzzopappa, M., Auer, H., and Milan, M. (2012). Aneuploidy-induced delaminating cells drive tumorigenesis in Drosophila epithelia. Proc Natl Acad Sci U S A *109*, 20549-20554.

Eichinger, C.S., Kurze, A., Oliveira, R.A., and Nasmyth, K. (2013). Disengaging the Smc3/kleisin interface releases cohesin from Drosophila chromosomes during interphase and mitosis. EMBO J *32*, 656-665.

Garelli, A., Gontijo, A.M., Miguela, V., Caparros, E., and Dominguez, M. (2012). Imaginal discs secrete insulin-like peptide 8 to mediate plasticity of growth and maturation. Science *336*, 579-582.

Gerlich, D., Koch, B., Dupeux, F., Peters, J.M., and Ellenberg, J. (2006). Live-cell imaging reveals a stable cohesin-chromatin interaction after but not before DNA replication. Curr Biol *16*, 1571-1578.

Gogendeau, D., Siudeja, K., Gambarotto, D., Pennetier, C., Bardin, A.J., and Basto, R. (2015). Aneuploidy causes premature differentiation of neural and intestinal stem cells. Nat Commun *6*, 8894.

Gontijo, A.M., and Garelli, A. (2018). The biology and evolution of the Dilp8-Lgr3 pathway: A relaxin-like pathway coupling tissue growth and developmental timing control. Mech Dev.

Gordon, D.J., Resio, B., and Pellman, D. (2012). Causes and consequences of aneuploidy in cancer. Nat Rev Genet *13*, 189-203.

Guacci, V., Yamamoto, A., Strunnikov, A., Kingsbury, J., Hogan, E., Meluh, P., and Koshland, D. (1993). Structure and function of chromosomes in mitosis of budding yeast. Cold Spring Harb Symp Quant Biol *58*, 677-685.

Hackney, J.F., and Cherbas, P. (2014). Injury response checkpoint and developmental timing in insects. Fly (Austin) *8*, 226-231.

Haering, C.H., Farcas, A.M., Arumugam, P., Metson, J., and Nasmyth, K. (2008). The cohesin ring concatenates sister DNA molecules. Nature *454*, 297-301.
Halme, A., Cheng, M., and Hariharan, I.K. (2010). Retinoids regulate a developmental checkpoint for tissue regeneration in Drosophila. Curr Biol *20*, 458-463.
Hassold, T., and Hunt, P. (2001). To err (meiotically) is human: the genesis of human aneuploidy. Nat Rev Genet *2*, 280-291.
Heisenberg, B. (1979). Isolation of Anatomical Brain Mutants of Drosophila

by Histological Means. Z Naturforsch 34 c, 143 — 147 (1979)
Holland, A.J., and Cleveland, D.W. (2009). Boveri revisited: chromosomal instability, aneuploidy and tumorigenesis. Nat Rev Mol Cell Biol *10*, 478-487.
Homem, C.C., and Knoblich, J.A. (2012). Drosophila neuroblasts: a model for stem cell biology. Development *139*, 4297-4310.
Ito, K., and Hotta, Y. (1992). Proliferation pattern of postembryonic neuroblasts in the brain of Drosophila melanogaster. Dev Biol *149*, 134-148.
Ivanov, D., and Nasmyth, K. (2005). A topological interaction between cohesin rings and a circular minichromosome. Cell *122*, 849-860.
Knouse, K.A., Wu, J., Whittaker, C.A., and Amon, A. (2014). Single cell sequencing reveals low levels of aneuploidy across mammalian tissues. Proc Natl Acad Sci U S A *111*, 13409-13414.
Kruiswijk, F., Labuschagne, C.F., and Vousden, K.H. (2015). p53 in survival, death and metabolic health: a lifeguard with a licence to kill. Nat Rev Mol Cell Biol *16*, 393-405.
Lane, M.E., Sauer, K., Wallace, K., Jan, Y.N., Lehner, C.F., and Vaessin, H. (1996). Dacapo, a cyclin-dependent kinase inhibitor, stops cell proliferation during Drosophila development. Cell *87*, 1225-1235.
Lara-Gonzalez, P., Westhorpe, F.G., and Taylor, S.S. (2012). The spindle assembly checkpoint. Curr Biol *22*, R966-980.
Liao, J.M., Zhou, X., Zhang, Y., and Lu, H. (2012). MiR-1246: a new link of the p53 family with cancer and Down syndrome. Cell Cycle *11*, 2624-2630.
Ly, P., and Cleveland, D.W. (2017). Interrogating cell division errors using random and chromosome-specific missegregation approaches. Cell Cycle, 1-7.
Mantel, C., Guo, Y., Lee, M.R., Kim, M.K., Han, M.K., Shibayama, H., Fukuda, S., Yoder, M.C., Pelus, L.M., Kim, K.S.*, et al.* (2007). Checkpoint-apoptosis uncoupling in human and mouse embryonic stem cells: a source of karyotpic instability. Blood *109*, 4518-4527.
Michaelis, C., Ciosk, R., and Nasmyth, K. (1997). Cohesins: chromosomal proteins that prevent premature separation of sister chromatids. Cell *91*, 35-45.
Milan, M., Campuzano, S., and Garcia-Bellido, A. (1996). Cell cycling and patterned cell proliferation in the wing primordium of Drosophila. Proc Natl Acad Sci U S A *93*, 640-645.

Milan, M., Clemente-Ruiz, M., Dekanty, A., and Muzzopappa, M. (2014). Aneuploidy and tumorigenesis in Drosophila. Semin Cell Dev Biol *28*, 110-115.
Mirkovic, M., Hutter, L.H., Novak, B., and Oliveira, R.A. (2015). Premature Sister Chromatid Separation Is Poorly Detected by the Spindle Assembly Checkpoint as a Result of System-Level Feedback. Cell Rep *13*, 470-478.
Mirkovic, M., and Oliveira, R.A. (2017). Centromeric Cohesin: Molecular Glue and Much More. Prog Mol Subcell Biol *56*, 485-513.
Nasmyth, K., and Haering, C.H. (2009). Cohesin: its roles and mechanisms. Annu Rev Genet *43*, 525-558.
Neufeld, T.P., de la Cruz, A.F., Johnston, L.A., and Edgar, B.A. (1998). Coordination of growth and cell division in the Drosophila wing. Cell *93*, 1183-1193.
Oromendia, A.B., and Amon, A. (2014). Aneuploidy: implications for protein homeostasis and disease. Dis Model Mech *7*, 15-20.
Pauli, A., Althoff, F., Oliveira, R.A., Heidmann, S., Schuldiner, O., Lehner, C.F., Dickson, B.J., and Nasmyth, K. (2008). Cell-type-specific TEV protease cleavage reveals cohesin functions in Drosophila neurons. Dev Cell *14*, 239-251.
Pfau, S.J., Silberman, R.E., Knouse, K.A., and Amon, A. (2016). Aneuploidy impairs hematopoietic stem cell fitness and is selected against in regenerating tissues in vivo. Genes Dev *30*, 1395-1408.
Poulton, J.S., Cuningham, J.C., and Peifer, M. (2017). Centrosome and spindle assembly checkpoint loss leads to neural apoptosis and reduced brain size. J Cell Biol *216*, 1255-1265.
Rao, S.S.P., Huang, S.C., Glenn St Hilaire, B., Engreitz, J.M., Perez, E.M., Kieffer-Kwon, K.R., Sanborn, A.L., Johnstone, S.E., Bascom, G.D., Bochkov, I.D.*, et al.* (2017). Cohesin Loss Eliminates All Loop Domains. Cell *171*, 305-320 e324.
Ricke, R.M., and van Deursen, J.M. (2013). Aneuploidy in health, disease, and aging. J Cell Biol *201*, 11-21.
Santaguida, S., and Amon, A. (2015). Short- and long-term effects of chromosome mis-segregation and aneuploidy. Nat Rev Mol Cell Biol *16*, 473-485.
Santaguida, S., Richardson, A., Iyer, D.R., M'Saad, O., Zasadil, L., Knouse, K.A., Wong, Y.L., Rhind, N., Desai, A., and Amon, A. (2017). Chromosome Mis-segregation Generates Cell-Cycle-Arrested Cells with Complex Karyotypes that Are Eliminated by the Immune System. Dev Cell *41*, 638-651 e635.
Santaguida, S., Vasile, E., White, E., and Amon, A. (2015). Aneuploidy-induced cellular stresses limit autophagic degradation. Genes Dev *29*, 2010-2021.
Sheltzer, J.M., Ko, J.H., Replogle, J.M., Habibe Burgos, N.C., Chung, E.S., Meehl, C.M., Sayles, N.M., Passerini, V., Storchova, Z., and Amon, A. (2017). Single-chromosome Gains Commonly Function as Tumor Suppressors. Cancer Cell *31*, 240-255.
Simpson, P., Berreur, P., and Berreur-Bonnenfant, J. (1980). The initiation of pupariation in Drosophila: dependence on growth of the imaginal discs. J Embryol Exp Morphol *57*, 155-165.

Soto, M., Raaijmakers, J.A., Bakker, B., Spierings, D.C.J., Lansdorp, P.M., Foijer, F., and Medema, R.H. (2017). p53 Prohibits Propagation of Chromosome Segregation Errors that Produce Structural Aneuploidies. Cell Rep *19*, 2423-2431.
Thompson, S.L., and Compton, D.A. (2010). Proliferation of aneuploid human cells is limited by a p53-dependent mechanism. J Cell Biol *188*, 369-381.
Urbach, R., Technau, G.M., and Breidbach, O. (2003). Spatial and temporal pattern of neuroblasts, proliferation, and Engrailed expression during early brain development in Tenebrio molitor L. (Coleoptera). Arthropod Struct Dev *32*, 125-140.
van Ruiten, M.S., and Rowland, B.D. (2018). SMC Complexes: Universal DNA Looping Machines with Distinct Regulators. Trends Genet *34*, 477-487.
Zielke, N., Korzelius, J., van Straaten, M., Bender, K., Schuhknecht, G.F., Dutta, D., Xiang, J., and Edgar, B.A. (2014). Fly-FUCCI: A versatile tool for studying cell proliferation in complex tissues. Cell Rep *7*, 588-598.

General discussion:

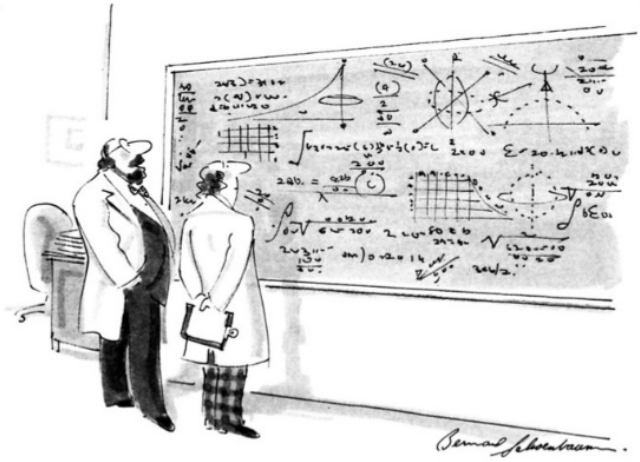

"Oh, if only it were so simple."

In modern Science, the process of discussion happens in the group meetings, hallways, conferences, but almost never within the scientific publication itself. The reason behind this is that today's scientists are pigeonholed into making "stories", matching pieces of data into a smooth narrative, packaging it nicely, and almost forcing the reader to take it at face value (Katz, 2013). This kind of packaging is required by all the major journals in order to have a chance of publishing in the first place. Pointing to the downsides of the study or the scientific approach is left to the reviewers during the revision process, and the general public after the paper is accepted. If done by the author himself, within a publication, it is usually perceived as a weakness in the scientific argument.

Everyone who has ever set a foot in the laboratory knows that this is fundamentally wrong approach, and that every biological story, no matter how sound or smoothly packaged, has gaping holes, either conceptual or experimental. And more often than not, the

author of the study knows very well what they are. Overlooking them for the sake coherence and storytelling is a scientific crime, the one which the entire community is guilty of, as authors will almost never criticize or point to caveats of their own experiments in scientific publications. It is unfortunate that within these gaps, many interesting topics and potential new avenues of research lay unexplored.

Therefore, I will use most of this general discussion to examine the caveats of our research as well as some interesting possibilities that we have not explored or have overlooked. In addition to this unorthodox general discussion, every one of the three chapters has a more conventional discussion section

(See *Discussion* in Chapter I, II, and III).

Chapter I

In Chapter I (*Mirkovic et al 2015*, *Cell Reports*), we discussed the interplay between cohesin loss and the machinery in charge of mitotic fidelity. The complexity of the SAC response, and the numerous feedback loops involved in the process are immense, and doing clean experiments in this kind of system is amazingly difficult.

In order to study the mitotic response to cohesin loss, we utilized the previously developed TEV protease system. Such a system presents great advantage over any other means of protein depletion, apart from maybe the Auxin-Degron inducible system. The TEV is rapidly expressed, and all cohesin is cleaved within two hours, just in time when Neuroblasts start entering mitosis after the heat shock. This has really worked in our favor, as we are sure that

there is no partial cohesin depletion that would make our analyses more difficult. The mitotic phenotype observed was very dynamic, with chromosomes oscillating from one pole to another. They displayed an oscillating, relatively weak Mad2 signal, which declined as the cells progressed through the mitotic delay. One thing that our analyses were unable to trace is the motion and signaling of individual kinetochores on single sisters. Due to photo-toxicity limitations, one must compromise when imaging a tissue, either limiting the depth, intensity, or time resolution of the imaging. In order to image and trace single kinetochores reliably, one should image at least 0.5 micrometer thick z stacks, which is quite incompatible with the long term imaging of the thick live tissue. To trace the motion of individual kinetochores, 5-10 second imaging intervals are needed, which is completely incompatible with our laser exposure conditions.

The reason why single kinetochore tracing and imaging could be very interesting is because we could identify the possible preferential locations where error correction takes place, as well as the possible Mad2 signaling by “attached” chromosomes. During chromosome shuffling, we can clearly observe Mad2 positive signals in the mid-zone between the two poles where the chromosomes initially segregate after entering mitosis with no cohesin. This could mean three different things: 1) chromosomes engage in Mad2 signaling while being attached and yanked between the two poles 2) chromosomes are in the process of losing attachments midway through the motion (not likely, as they seem to usually complete the pole to pole motion) 3) chromosomes need some time to silence Mad2 attachment by RZZ dependent

stripping, after the attachment occurs, thus the residual Mad2 occupancy on the moving chromosomes.

For me, the most interesting out of these three is the possibility that chromosomes can engage in SAC signaling even when “attached” to the spindle. When we discuss kinetochore attachment, we tend to do it in the same way as we discussed the SAC twenty years ago. Either the chromosome is attached, or it is not, a false binary dilemma. However, the kinetochore has multiple microtubule attachment sites. The *Drosophila* kinetochore for instance, has eleven microtubule attachment sites (Maiato et al., 2006). Therefore, it is not likely that a single attached microtubule would silence the SAC same with the same efficiency as a fully occupied kinetochore would. Indeed, if viewed like this, SAC and chromosome attachment might not be mutually exclusive, as partial kinetochore occupancy might still lead to SAC signaling. This is a plausible conclusion, as it is mathematically impossible for the attachment to be synchronous on all sites across the large kinetochore. Therefore, a model in which the binding of initial microtubules provides some tension and allows for more efficient further binding might be a more accurate one. At the same time, these partial attachments would still generate the MCC at the unoccupied binding sites, signaling to the cell that the attachment process is not complete.

The decay in the MAD2 signaling activity and chromosome motion led us to postulate that this is due to the declining activity of the error correction mechanisms, resulting in the decline of the SAC signaling and Cyclin B levels. While this is likely to be true, these three are almost impossible to disentangle in our experimental setup. Our hypothesis was that the declining rate or error correction

occurs due to inevitably declining Cyclin B levels. To test this, we used Roscovitine addition, which negatively affects all three modules: Cyclin B, Aurora B, and the SAC. The roscovitine concentration we used resulted in no mitotic acceleration in the control cells, and no mitotic exit in colchicine incubated cells, however, it resulted in 50% shortening of the mitotic delay when cohesin was cleaved. This result shows that the cohesin dependent mitotic delay is very Cdk1 inhibition sensitive, yet which of the three main components is the most sensitive one is impossible to determine. Cohesin cleaved cells will generate fewer Mad2 signaling kinetochores and a weaker Mad2 signal than the colchicine will, so it is logical that the Cdk1 inhibition will have a stronger result on the weaker SAC signaling. Furthermore, the decay in error correction activity, which is also Cyclin B dependent, accelerates the process of SAC inhibition. Therefore, it is impossible to disentangle what happens first: The weak SAC inhibition by Roscovitine or the error correction inhibition by Roscovitine. Our feedback model accounts for this however, as decay in any of the three main players (Cyclin B, SAC, and Aurora B) will lead to the decay of others.

A better experiment to test these dependencies would be the following: stabilize the Cyclin B levels and see if the checkpoint signaling and error correction activity stay high throughout the arrest. Unfortunately, it is hard to inhibit the APC/C in *Drosophila* tissues as Ubch10, MG132, Protame, Apcin and other proteasome inhibitory drugs have no effect, and non-degradable Cyclin B has mosaic expression in Neuroblasts, making these experiments technically difficult.

Another interesting caveat of our study of cohesin defects during Neuroblast mitosis is that we were unsure if Aurora B activity is lower in cohesin depleted cells. We noticed that Aurora B gets delocalized if cohesin is cleaved, shifting its distribution from a sharp signal at the inner centromere region, to a smear of about 50% lower mean fluorescence, in a wide chromatin region. However, we had no assay to assess the amount of functional Aurora B at the kinetochore, as phosphorylation antibodies for Aurora B activation did not work, and FRET sensor development and optimization were too time-consuming for the purpose of this study. It would be very interesting to see if cohesin depletion directly impairs error correction before the cascade of mitotic events takes place. The proper experiment for this would be a comparison of single sisters with cohesin depletion and delocalized Aurora B versus the single sisters with normal cohesion and Aurora B levels, which seems quite biologically impossible, without a very artificial experimental setup, such as Aurora B tethering.

In the same publication, we demonstrated that the duration of mitotic arrest and chromosome shuffling upon cohesin depletion is Aurora B dependent. We did so by addition of 25µM Binucleine 2, which is a specific Aurora B kinase inhibitor. Addition of Binucleine 2 resulted in a halt of chromosome motion and abrupt mitotic exit (*3-5min after addition)*. However, this concentration of Binucleine caused mitotic exit after some time colchicine as well, which is a positive control for SAC activation in the Neuroblast. When using such high Binucleine concentration in our system, it is impossible to dissect if we preferentially inhibit the weak checkpoint mounted by cohesin cleavage, or the error correction mechanism. However, in our more recent study (*Silva et al 2018*) we have used a 5µM

concentration of Binucleine in the wing disc. This Binucleine concentration does not cause mitotic exit in colchicine, but completely prevents chromosome motion and shuffling for the duration of mitotic delay if cohesin is cleaved. This occurs in the Neuroblast as well (not shown), validating our hypothesis from the previous study *(Mirkovic et al 2015)*.

An ideal experiment for testing Aurora B involvement in chromosome motion and shuffling would be the usage of Binucleine 2 in a situation where Cyclin B degradation is prohibited, allowing us to separate the Cyclin B effect on error correction activity from the error correction activity itself. This is important, as Cyclin B and Cyclin A levels have been implicated in microtubule dynamics.

However, situations in which the 5µM Binucleine is used resulted in no shuffling motion in both the Neuroblasts and the wing disc, even at the beginning of mitosis when Cyclin B-Cdk activity is still high. Taken in sum, these observations would point out that the shuffling of chromosomes which occurs when cohesin is depleted indeed relies on the error correction activity of the CPC complex, and that the likely order of events after Binucleine addition is error correction inhibition, followed by SAC silencing, resulting in mitotic exit.

Chapter II

In the Chapter II *(Silva et al 2018)* of the thesis we investigated conditions that might alleviate the consequences of cohesin loss during mitosis. This was a product of an interesting collaboration with a group that performed a modulator screen for RNAi against a cohesin regulator, San, probing for genes that might rescue/enhance cohesion defects in the wing disc. The discovery

of SAC genes (Mps, Mad1, Mad2, and BubR1) as modulators of the cohesin loss phenotype was quite surprising and unexpected. What we noticed in our previous study (Mirkovic et al., 2015) is that the shuffling motion of chromosomes from pole to pole took some time to initiate. This lead to the hypothesis that the rescue of cohesion defects by SAC impairment came from mitotic shortening which did not allow for the chromosome content to be randomized.

This hypothesis was validated by the measures of segregation efficiency in cohesive defective wing discs and embryos, with and without the SAC.

A validating result came when we tested if error correction inhibition produces the same rescue of symmetry in the absence of cohesin. To our surprise, it did, showing that initial attachments made by the spindle are quite close to the ones you want to be having in the first place, even in complete absence of cohesin. However, we had to titrate Binucleine 2 in order to avoid the side effects of Aurora B inhibition. This likely means that the inhibition we enforced on the error correction is partial. An interesting thing would be to see if mutants for Ndc80/Hec1, which would be unable to engage in error correction, would be viable in flies. This would point to the immense efficiency of initial microtubule capture in *Drosophila*. Another observation arising from this work is that the initial microtubule capture is quite accurate, even in complete absence of cohesin. Previous studies in mammals showed that the kinetochore geometry biases their orientation for bipolar microtubule capture and congression. In *Drosophila*, this seems to be the case even in the absence of cohesin. Cohesin is thought of as the major modulator of elasticity and kinetochore architecture, so the fact that the flies can segregate their genome quite fine

without any cohesion, as long as mitosis is shortened, is quite surprising.

Probably contributing to this phenomenon is the fact that complete absence of cohesion does not result in complete chromosome separation at the very beginning of the mitosis. After the nuclear envelope breakdown, it takes a few minutes for chromosomes to segregate to the poles. This is likely due to the fact that the processes of condensation and catenation are not complete, and still confer some cohesive forces between the chromosomes. What is possible here is that the attachments that occur in this state, are still under some tension, and therefore, quite accurate. Indeed, it is known that Topoisomerase II inhibition can rescue cohesion defects via enforcing catenation, generating “cohesion” which is cohesin independent. We also observed this with our experimental system, using low doses of Topo II inhibitor, ICRF-193, which can rescue cohesin defects (data not shown). It would be interesting to dissect the temporal resolution of cohesive forces during mitosis in the cell. While it is clear that in late mitosis, with a fully active spindle and condensed chromosomes, cohesin is the only force strong enough to resist the spindle; in early mitosis, this might not be the case.

Chapter III

In the last part of the thesis, Chapter III (*Mirkovic, Guilgur et al*), we started off by designing a tool for reversible loss of cohesin, in hope of generating aneuploid karyotypes in order to follow their evolution and selection. What we did not count on is the rise of chromosomal instability in previously stable aneuploid cells, as well as the fact that the flies would actually eclode into adults when challenged with

aneuploidy. This enticed us to switch to the more holistic approach of studying an entire organism instead of focusing on a cell line, which was quite a challenge.

For starters we were amazed with the ability of Neuroblasts to tolerate aneuploidy. I have seen thousands of aneuploid divisions and karyotypes, and there is something about these cells that makes them uniquely resistant to aneuploidy and cell death. It goes to say that in two years of reading papers on Neuroblasts and aneuploidy, I am yet to see a convincing panel showing apoptosis of a larval Neuroblast using conventional apoptosis markers.

This amazing aneuploidy tolerance should be a target of a directed genetic screen, challenging selected mutations with DNA damage or mitotic perturbations and observing if they induce apoptosis in the Neuroblast. Furthermore, aneuploid Neuroblasts which persisted after the challenge, accumulated chromosomes in absurd numbers, likely due to chromosomal instability. In introduction 1.3 about Aneuploidy, it was mentioned that aneuploidy results in a severe strain for the proteasome machinery of the dividing cell due to imbalances in genomic content, coupled to protein overexpression. Therefore, it is fascinating how a Neuroblast can cope with this kind of stress for so long.

Furthermore, the aneuploid stress inflicted on the brain resulted in no detectable reduction of brain size or shape in the adult. Previous studies reported that aneuploid larval brains are smaller. This is likely a difference between the acute mode of aneuploidy induction and the chronic mode that earlier studies utilized. If the system is challenged with aneuploidy for the entirety of its lifespan, the kinetics of aneuploid response are impossible to dissect. Therefore,

microcephaly observed in Plk4 overexpression and SAC larva mutants is likely due to this tissue succumbing to aneuploidy after days of aneuploid proliferation. In our system however, it is clear that while aneuploidy results in appearance of stress markers, Neuroblast loss and chromosomal instability, the tissue still holds a great proliferative potential for several days. This is likely enough to achieve the proper size of the tissue, when morphogenesis can take over and mold it into a “normal”-looking brain. Still, the tolerance of the tissue to aneuploidy is simply remarkable, and although it might be an insect-specific phenomenon, it needs to be investigated further.

One of the reasons for developing a genetic system for reversible mitotic perturbation is the lack of the tools to induce controlled aneuploidy in metazoans. The concept of removing the source of aneuploidy (Cohesin cleavage, in this case), and then studying aneuploidy alone is the only way to study this very complex phenomenon in a somewhat clean manner. Otherwise, the effects of perturbation and aneuploidy might both be contributing to the phenotype. In retrospect, an ideal protein for perturbation would be a purely mitotic one, with no other characterized interphase roles, which cohesin has plenty (Such for example, would be a CenpC-TEV system).

The acuteness of our approach resulted in a full metazoan development cycle, after a severe aneuploidy challenge. As our expertise is far from development, developmental regulation, and *drosophila* tissue biology, we are very excited to make this acute tool for aneuploidy induction available for the community, as there is a dearth of good tools to study aneuploidy in metazoans,

especially ones resulting in the entire developmental cycle after perturbation.

The amazing power Drosophila compensatory proliferation response has been well characterized and studied for decades. Therefore, it is not surprising that a transient insult for the epithelium can result in almost full recovery. What is more interesting is what happens in the aneuploid brain. The possible mechanisms of regeneration are not well studied in the drosophila brain. Therefore, in light of our current knowledge, there are two options when brain is faced with severe aneuploidy: the aneuploid cells persist throughout adulthood, or they are eliminated.

The problem with the elimination hypothesis is that this should severely alter brain size or shape in the absence of compensation mechanisms. However, when we dissected adult brains from flies that were induced to aneuploidy 72 or 96 hours after egg laying, we observe no drastic difference. We know that in our system, heat shock at 96 hours after egg laying results in aneuploidy in every single dividing Neuroblast. Coupled to the continued proliferation of these cells, as well as cohesin cleavage in other cells of the larval brains, this would mean that the massive part of the brain is aneuploid. If indeed these cells were eliminated, and there was no compensation, there should be a clear size difference between a brain challenged with aneuploidy and a control.

This leaves the other option: the aneuploid Neuroblasts and their progeny remain, and become a part of an adult, aneuploid brain. We tried assessing the ploidy state of the neurons in the adult brain through multiple means: FISH, FACS, protein fluorescence, DNA content, just to name a few. However, this is a very difficult task, as

each one of these methods has profound flaws which preclude any definitive conclusion on the state of ploidy. The optimal thing to do would be to separate the neurons in the adult brain challenged by aneuploidy and the control, and compare DNA content by single cell sequencing.

Inducing aneuploidy in the entire organism, studying and tracking its consequences in tissues is too big of a task for any single scientific group. Therefore, I think one of the strongest parts of this work is the tool for the entire drosophila community, which can be used to study aneuploidy in metazoans in a controlled and acute manner, *in vivo*.

References

Katz, Y. (2013). Against storytelling of scientific results. Nat Methods *10*, 1045.

Maiato, H., Hergert, P.J., Moutinho-Pereira, S., Dong, Y., Vandenbeldt, K.J., Rieder, C.L., and McEwen, B.F. (2006). The ultrastructure of the kinetochore and kinetochore fiber in Drosophila somatic cells. Chromosoma *115*, 469-480.

Mirkovic, M., Hutter, L.H., Novak, B., and Oliveira, R.A. (2015). Premature Sister Chromatid Separation Is Poorly Detected by the Spindle Assembly Checkpoint as a Result of System-Level Feedback. Cell Rep *13*, 470-478.